ANALYTICAL STUDIES OF SOME ACOUSTIC PROBLEMS

OF JET ENGINES

Thesis by

Sebastien M. Candel

In Partial Fulfillment of the Requirements

For the Degree of

Doctor of Philosophy

California Institute of Technology

Pasadena, California

1972

(Submitted November 18, 1971)

To My Parents.

ACKNOWLEDGMENTS

ABSTRACT

This thesis presents analytical studies of internal noise generation and transmission in jet engines and its radiation from the duct ends.

The propagation and generation of acoustic waves in a choked nozzle is considered first. Pressure and entropy fluctuations caused by gas stream non-uniformities like "hot spots," are incident on the nozzle entrance. A novel noise-generation mechanism is uncovered where acoustic waves are produced by a distribution of sources of strength proportional to the entrance entropy fluctuation and local gradient of the mean flow velocity.

The propagation of acoustic waves in a moving medium in the presence of semi-infinite or finite boundaries is then considered. A transformation is introduced which relates the solutions of such problems to the solutions of associated problems in a stationary medium. The method is described by discussing the Sommerfeld problem of diffraction of a plane wave by a half plane immersed in a subsonically moving medium. When the plane has a trailing edge, it is shown that both reflection and shadow regions expand; while the opposite occurs for a leading edge, in which circumstance an additional diffracted wave also appears.

In the supersonic case, all the diffraction problems are related to a single reference problem, solved by Fourier transform methods. A decomposition of the pressure field in a "geometrical optics" field and a diffracted field is given, showing some remark-

able similarities with the subsonic case solution.

The radiation of acoustic modes from a duct immersed in a subsonically moving medium is treated by a similar transform method. The presence of the uniform flow has roughly the same effect as an increase in frequency of the incident wave, at constant mode number. The effect of acoustical lining on the radiation pattern is examined, and side radiation is shown to be greatly reduced for the lower order modes.

The transmission and reflection of acoustic waves incident on a blade row is analyzed by the transform method, and the transmission and reflection coefficients for the blade row immersed in a moving medium are expressed in terms of the basic acoustic characteristics of the blade row in a stationary medium.

TABLE OF CONTENTS

1. GENERAL INTRODUCTION --
BACKGROUND TO THE ENGINE NOISE PROBLEM

In recent years noise has become a major consideration in the design of jet propulsion systems for aircraft. Development programs of new engines include acoustical constraints in the first stages of conception. Some programs, like the NASA Quiet Engine or the SNECMA M56, seek to include all available features which would result in noise reduction. The goal for the NASA Quiet Engine is to attain a noise reduction of 15 to 20 PNDB below the sound level of current turbofan engines like the Pratt and Whitney JT3D. The development of short- or vertical-takeoff and landing aircraft (S/VTOL) also depends heavily on our future capacity to design quiet engines.

The noise of jet propulsion systems may be classified in two categories: the internal noise generated by the turbomachinery combustor and other internal processes, the external noise associated with the turbulent exhaust jet and the related turbulent shear layer, and in the supersonic case with the external shock pattern.

The relative magnitude of these noise sources depends on the engine type and characteristics and on the phase of operation (takeoff, flyby, landing). In the Pratt and Whitney JT3D (bypass ratio 1.43), at takeoff the jet noise dominates the inlet noise and is almost as loud as the fan noise radiated from the discharge duct. During the landing phases the noise radiated by the jet is greatly reduced and the fan noise radiated by the inlet determines the noise level on the ground [1.1]. For the current high bypass fan engines like the Pratt and Whitney JT9D, the General Electric CF6 or the

Rolls Royce RB211, the noise relation is modified. At takeoff and landing the fan noise dominates the external jet noise. Moreover, at low jet speeds (approach) another internal noise different from the fan noise and depending on the sixth power of the exhaust velocity (V^6) becomes more important than the jet noise (V^8). For the Concorde powerplant, the Olympus 593, at maximum thrust regime the main noise is that produced by the turbulent jet and shear layer; all other sources are in comparison unimportant. At lower thrust regimes, the compressor and turbine noise become significant and another internal noise appears [1.2].

As can be seen from these examples, internal noise is the major noise for the present-day high-bypass engines and is important during the landing phases for aircraft with more conventional turbofans or turbojets.

This thesis is mainly concerned with internal noise generation, propagation and radiation. A first problem of interest is the noise generation and transmission in a region of non-homogeneous flow velocity and non-homogeneous sound speed like the nozzle. This problem is treated for the particular case when the nozzle is choked.

A common situation in jet engines is when acoustic waves propagate in a moving medium in the presence of finite boundaries. The radiation of noise from the nacelle end sections, the reflection and transmission at a blade row, are two examples considered in this thesis. Before treating these cases, a more fundamental problem is discussed: the Sommerfeld problem of diffraction of a plane

wave by a semi-infinite plane immersed in a uniform flow.

It is here worthwhile to review briefly the history of research on noise in jet engines, to provide a context to the problems treated in the present thesis.

The initial research on jet noise suppression considered almost exclusively the turbulence-generated noise. The fundamental work by Lighthill [1.3, 1.4] set a theoretical basis for the analysis of this noise. Lighthill explained the sound field induced by the jet as resulting from a quadrupolar source distribution of strength equal to the local fluctuation of the Reynolds stress tensor. This theory was extended by Curle [1.5] to include the influence of solid boundaries and Ffowcs-Williams [1.6] to high-speed jets. A different approach was followed by Ribner, who introduced a pseudo-sound pressure field induced by the fluid dilatations. The two theories lead to the same far-field expressions and are summarized by Ribner [1.7] in a comprehensive survey of the jet noise research. Ribner and his co-workers at UTIAS were also able to explain how the basic radiation pattern of self- and shear-noise is modified by convection and refraction to produce the actual radiation pattern. Their work is summarized in reference [1.8]. At present, the basic qualitative features of noise from the subsonic jets are well understood, while quantitative estimation from measured flow parameters is still beyond reach. The noise from supersonic jets is less well understood; other mechanisms like shock-shear layer, shock-turbulence interactions become important in this case.

With the introduction of the bypass engines, research efforts

focused on the internal noise produced by the rotating machinery, and in particular the fan. The discrete tone noise was described by Tyler and Soffrin [1.9] as resulting from rotor-stator interaction producing acoustic modes at blade passage frequency and its harmonics. Reference [1.9] gives also a clear and simple discussion of the duct transmission and radiation in free space of the spinning acoustic modes. The fan also produces broadband and multiple-tone noise. The multiple tones are generally associated with the existence of shock patterns attached to the rotor blades. This noise is important in the new high-bypass engines where the tone generation has been reduced, but has not received until now much attention.

The broadband noise is generally thought to be a result of flow turbulence and blade row interaction [1.1], or of blade lift fluctuations [1.10]. Recently, Mather and Savidge [1.11] performed a detailed spectral analysis of this noise and identified a series of discrete tones around the harmonics of the shaft frequency corresponding to the stator vane number. According to Mather and Savidge, the so-called broadband noise is in fact a discrete tonal noise produced by interaction of the almost axisymmetric rotor pressure field with the stator guide vanes.

Some attempts have been made to estimate the noise production by fans as, for instance, by Lowson in reference [1.12] where Lighthill's theory is applied to study four separate mechanisms.

At present, the identification and quantitative estimation of the noise sources in fans and compressors is far from complete. While the duct transmission of discrete tones has been studied exten-

sively and is well understood, the radiation from the duct ends has received little attention despite its importance in the determination of the sound pressure level at various positions with respect to the aircraft. Similarly, the attenuation properties of acoustic lining set in the engine nacelle have been studied in detail, while its influence on the radiation pattern has not been examined.

Very little is known on the internal noise not related to the turbomachinery. This noise becomes important in the approach and landing phases when the main jet velocity is reduced. The noise sources have been tentatively associated with the combustion process and various turbulence and solid boundary interactions. The transmission of this noise through the nozzle and the noise-generating mechanisms which might occur in the nozzle were not previously considered.

Chapter 2 of this thesis deals with this problem; the nozzle is supposed choked, and at the nozzle entrance both pressure and entropy fluctuations are considered. The entropy fluctuations conveniently represent gas stream non-uniformities which might be produced in the upstream region by some mechanism like inhomogeneous combustion or rotation of shock patterns. The incoming entropy fluctuations are shown to be partly converted into pressure fluctuations by the non-homogeneous velocity field in the nozzle. This mechanism constitutes a novel noise source.

In Chapter 3 we introduce an algebraic transformation which greatly simplifies the analysis of the interaction of acoustic waves with edges immersed in a moving medium. The transformation is

first applied to the diffraction problem of a plane wave by a semi-infinite hard plane in a subsonic moving medium.

The transformation does not apply in the supersonic case, and other methods are developed in Chapter 4 to treat this case.

A method similar to that of Chapter 3 is then used in Chapter 5 to study the radiation from a duct immersed in a uniform flow. The radiation of acoustically-lined ducts is also discussed.

In Chapter 6 we study the reflection and transmission of acoustic waves at a blade row, using methods similar to those of Chapters 3 and 5. The transmission and reflection coefficients for the blade row immersed in a moving medium are deduced from the acoustical characteristics of the blade row in a stationary medium. A better understanding of the effect of the moving medium is thus obtained.

REFERENCES

1.1 Kramer, J. J., Chestnutt, D., Kresja, E. A., Lucas, J. G., and Rice, E. J., "Noise Reduction," Aircraft Propulsion Conference, Lewis Research Center, November 1970. NASA SP-259 (1971).

1.2 Hawkins, R., and Hoch, R., "Recherches sur l'emission et la reduction del bruit des propulseurs de Concorde," 10e Congrès International Aeronautique, Paris (1971).

1.3 Lighthill, M. J., "On sound generated aerodynamically, I. General theory," Proc. Roy. Soc., Ser. A, 211 (1952), pp. 564-587.

1.4 Lighthill, M. J., "On sound generated aerodynamically, II. Turbulence as a source of sound," Proc. Roy. Soc., Ser. A, 222 (1954), pp. 1-32.

1.5 Curle, N., "The Influence of Solid Boundaries upon Aerodynamic Sound," Proc. Roy. Soc., Ser. A, 231 (1955), pp. 505-514.

1.6 Ffowcs-Williams, J. E., "The noise from turbulence convected at high speed," Proc. Roy. Soc., Ser. A, 255 (1963), pp. 469-503.

1.7 Ribner, H. S., "The Generation of Sound by Turbulent Jets," Advances in Applied Mechanics, Academic Press, New York (1964), Vol. 8.

1.8 Ribner, H. S., "Jets and Noise," Proceedings of AFOSR-UTIAS Symposium on Aerodynamic Noise, Toronto, 1968, University of Toronto Press (1969).

1.9 Tyler, J. M., and Soffrin, T. G., "Axial Flow Compressor Noise Studies," SAE Trans., 70 (1962), p. 309.

1.10 Large, J. B., Wilby, J. F., Grande, E., and Anderson, A.O., "The Development of Engineering Practices in Jet, Compressor, and Boundary Layer Noise," Proceedings of AFOSR-UTIAS Symposium on Aerodynamic Noise, Toronto, 1968, University of Toronto Press (1969).

1.11 Mather, J. S. B., and Savidge, J., "New Observations on Tone Generation in Fans," J. Sound Vib., 16 (1971), pp. 407-418.

1.12 Lowson, M. V., "Theoretical Studies of Compressor Noise," NASA CR-1287 (March 1969).

CHAPTER II

EXTERNAL NOISE LEVEL INDUCED BY ACOUSTIC

OSCILLATIONS AND GAS STREAM NON-UNIFORMITY

AHEAD OF A SUPERCRITICAL NOZZLE

2.1 INTRODUCTION

A great amount of research has been devoted in recent years to study of the noise generating mechanisms in turbojets/turbofans. The early formulations by Lighthill, Ribner, Ffowcs-Williams, and twenty years of research have led to a reasonable understanding of turbulence noise from high-speed subsonic jets (V^8 noise). The noise of supersonic jets (V^3) is less well understood; probably the non-stationary shock pattern is also important. The recent development of high bypass ratio turbofans has triggered extensive research on fan/compressor noise. The duct propagation of the discrete tones generated at rotor blade passage frequency has been intensively studied (Tyler and Soffrin, Morfey), while the noise sources have not been completely identified.

A noise source which has received little attention is that due to events ahead of the nozzle: (a) the acoustic fields caused by combustion noise or by turbine noise ahead of the nozzle; (b) the entropy non-uniformities in the stream, generated by the combustion processes or by rotating shock patterns attached to the turbine rotor and which tend to cause mass fluctuations and hence induce pressure fluctuations.

Experimental observations on low speed jets from high bypass ratio turbofans have shown that rough flow conditions upstream of the nozzle generate an acoustic power which varies like V^6 and is not affected by the noise suppressors designed for the V^8 noise of higher speed jets. The noise sources in this case were tentatively identified as combustion noise, broadband turbine noise, and dipole

radiation from the nozzle end section (Large, et al. [2.1]).

It is our aim in this chapter to study this novel noise source utilizing a one-dimensional model employed by Tsien [2.2] and Crocco [2.3] to study internal oscillations of rocket motors. At the nozzle entrance we shall consider both pressure and entropy fluctuations. The nozzle will be assumed choked when in steady state operation. This case is considered because the noise source under study might be important for turbojets with supersonic exhaust jets, especially in the case where the nozzle is preceded by an afterburner. The acoustical problem is also greatly simplified when the nozzle is choked because only outgoing waves may then propagate after the sonic section and thus the acoustic radiation from the end section does not influence the propagation in the nozzle. In other words, the radiation impedance of the end section is irrelevant to the present problem; the nozzle may be viewed as a 'black box' with as input the entrance pressure and entropy fluctuations and a transfer function independent of the output conditions. We shall see that the sonic section also plays a key role in imposing an impedance relation in the throat.

The mathematical model is one-dimensional (i.e., it involves averaged quantities in each nozzle section) and uses the basic assumptions of theoretical acoustics (non-viscous, non-conducting fluid, linearized perturbations), but the isentropic condition is relaxed to allow for entropy fluctuations at the nozzle entrance. Because the viscosity and heat conductivity are set equal to zero, the entropy non-uniformities or "hot spots" do not diffuse but are only convected by the flow.

The present model was developed by Tsien [2.2] and Crocco [2.3] to study the behavior of a nozzle under unsteady entrance conditions in relation to combustion instability in rocket engines. Tsien and Crocco were principally interested in the boundary condition imposed by a choked nozzle on the chamber oscillations. They did not consider the transmission through the nozzle and only studied special entrance conditions, isothermal fluctuations by Tsien [2.2] and isentropic fluctuations by Crocco [2.3], with only a few remarks on non-isentropic conditions.

The present problem is formulated in section 2.2, a system of two first-order ordinary differential equations is obtained, and the suitable set of boundary conditions is discussed in detail.

Asymptotic solutions in the form of series expansions are derived in section 2.3. Because the system of differential equations is singular in the throat section, some care is necessary to obtain a regular (bounded) solution of this system by numerical methods: one procedure is described in section 2.4.

2.2 FORMULATION OF THE PROBLEM

The nozzle has an area profile $A(x)$, the entrance section is at x_e, the throat at x^*, the length of the subsonic section is $\ell = x^* - x_e$. The flow in the nozzle channel of an ideal non-viscous, non-conducting perfect gas may be described by writing the equations of continuity, momentum, energy, and state

$$\frac{\partial}{\partial t}(\tilde{\rho} A) + \frac{\partial}{\partial x}(\tilde{\rho}\tilde{u} A) = 0 \tag{2.1}$$

$$\frac{\partial \tilde{u}}{\partial t} + \tilde{u}\frac{\partial \tilde{u}}{\partial x} + \frac{1}{\tilde{\rho}}\frac{\partial \tilde{p}}{\partial x} = 0 \tag{2.2}$$

$$\left(\frac{\partial}{\partial t} + \tilde{u}\frac{\partial}{\partial x}\right)\tilde{s} = 0 \tag{2.3}$$

$$\tilde{s} = c_v \ln(\tilde{p}/\tilde{\rho}^\gamma) \tag{2.4}$$

This is a system of four nonlinear equations for the four unknowns $\tilde{p}, \tilde{\rho}, \tilde{u}, \tilde{s}$, respectively pressure, density, velocity, and entropy.

We assume that the fluctuations at the nozzle entrance are small so that the stationary flow in the nozzle is only slightly perturbed. It is then convenient to write

$$\tilde{p} = p + p' \tag{2.5}$$

$$\tilde{\rho} = \rho + \rho' \tag{2.6}$$

$$\tilde{u} = u + u' \tag{2.7}$$

$$\tilde{s} = s + s' \tag{2.8}$$

where p, ρ, u, s pertain to the stationary flow in the nozzle, and p', ρ', u', s' are small unsteady perturbations. By substituting equations (2.5) to (2.8) in the system (2.1) to (2.4) and separating the terms of same order, we obtain the following zeroth order system:

$$\frac{d}{dx} (\rho u A) = 0 \qquad (2.9)$$

$$\rho u \frac{du}{dx} + \frac{dp}{dx} = 0 \qquad (2.10)$$

$$s = c_v \ln (p/\rho^\gamma) = cst. \qquad (2.11)$$

and the first order system:

$$\frac{\partial}{\partial t} \left(\frac{\rho'}{\rho}\right) + u \frac{\partial}{\partial x} \left(\frac{\rho'}{\rho} + \frac{u'}{u}\right) = 0 \qquad (2.12)$$

$$\frac{\partial}{\partial t} \left(\frac{u'}{u}\right) + \left(\frac{\rho'}{\rho} + 2 \frac{u'}{u}\right) \frac{du}{dx} + u \frac{\partial}{\partial x} \left(\frac{u'}{u}\right)$$
$$= \frac{p'}{p} \frac{du}{dx} - \left(\frac{p}{\rho u}\right) \frac{\partial}{\partial x} \left(\frac{p'}{p}\right) \qquad (2.13)$$

$$\left(\frac{\partial}{\partial t} + u \frac{\partial}{\partial x}\right) \frac{s'}{c_v} = \left(\frac{\partial}{\partial t} + u \frac{\partial}{\partial x}\right) \left(\frac{p'}{p} - \gamma \frac{\rho'}{\rho}\right) = 0 \qquad (2.14)$$

The zeroth order system is the classical set of equations describing the isentropic flow of a perfect gas in a channel: its solution is well known.

The first order system for the unsteady perturbations has been

written in the form (2.12), (2.13), (2.14) so that the nozzle profile $A(x)$ would not appear explicitly. This system is linear, of first order, with variable coefficients. We are not interested in this chapter in the transient behavior of the nozzle: it is therefore natural to perform a harmonic analysis of this system.

All the perturbations have a time factor $\exp(-i\omega t)$ and we define $\varphi, \delta, \nu, \sigma, \theta$ by

$$\frac{p'}{p} = \varphi(x) \, e^{-i\omega t} \tag{2.15}$$

$$\frac{\rho'}{\rho} = \delta(x) \, e^{-i\omega t} \tag{2.16}$$

$$\frac{s'}{c_v} = \sigma(x) \, e^{-i\omega t} \tag{2.17}$$

$$\frac{u'}{u} = \nu(x) \, e^{-i\omega t} \tag{2.18}$$

$$\frac{T'}{T} = \theta(x) \, e^{-i\omega t} \tag{2.19}$$

At the nozzle entrance the index e will be used to designate the fluctuations

$$\varphi(x_e) = \varphi_e \,, \quad \delta(x_e) = \delta_e \,, \quad \nu(x_e) = \nu_e$$

$$\sigma(x_e) = \sigma_e \,, \quad \theta(x_e) = \theta_e \tag{2.20}$$

The energy equation (2.14) is immediately integrable

$$\frac{s'}{c_v} = \frac{p'}{p} - \gamma \frac{\rho'}{\rho} = f\left(t - \int_{x_e}^{x} \frac{dx}{u}\right) \tag{2.21}$$

and as s'/c_v is harmonic in t

$$\sigma = \varphi - \gamma \delta = \sigma_e \exp\left(i\omega \int_{x_e}^{x} \frac{dx}{u} \right) \qquad (2.22)$$

We introduce the definitions (2.15) to (2.17) into (2.12) and (2.13) and rearrange (2.22) to get

$$-i\omega \delta + u\frac{d\nu}{dx} + u\frac{d\delta}{dx} = 0 \qquad (2.23)$$

$$-i\omega \nu + (\delta + 2\nu)\frac{du}{dx} + u\frac{d\nu}{dx} =$$

$$\varphi\frac{du}{dx} - \frac{u}{\gamma}\frac{c^2}{u^2}\frac{d\varphi}{dx} \qquad (2.24)$$

$$\delta = \frac{1}{\gamma}\varphi - \frac{\sigma_e}{\gamma} \exp\left(i\omega \int_{x_e}^{x} \frac{dx}{u} \right) \qquad (2.25)$$

Then δ may be easily eliminated to obtain

$$\gamma u\frac{d\nu}{dx} + u\frac{d\varphi}{dx} - i\omega\varphi = 0 \qquad (2.26)$$

$$\left(\frac{c^2}{u^2} - 1\right)u\frac{d\varphi}{dx} - \left[(\gamma-1)\frac{du}{dx} - i\omega\right]\varphi$$

$$+ \gamma\left(2\frac{du}{dx} - i\omega\right)\nu = \sigma_e\frac{du}{dx} \exp\left(i\omega \int_{x_e}^{x} \frac{dx}{u}\right) \qquad (2.27)$$

This is a system of two first-order ordinary differential equations for the pressure and velocity fluctuations, φ and ν. The non-homogeneous term in (2.27) results from the entrance entropy fluctuations. This source term is proportional to the entrance entropy fluctuation σ_e and to the local derivative of the mean velocity du/dx. We shall see that this term is responsible for the conversion of entropy fluctuations into pressure fluctuations. This conversion only occurs in a non-homogeneous velocity field (i.e., $du/dx \neq 0$).

The system (2.26), (2.27) may be solved numerically for any velocity profile $u(x)$ corresponding to a given nozzle profile $A(x)$. However, it is difficult to obtain analytical information in this general case. It is therefore convenient at this point to suppose that the nozzle profile is such that the velocity distribution $u(x)$ is linear. This does not suppress any essential feature of the system, and is in fact a good approximation of the situation in actual nozzles. We write

$$\frac{du}{dx} = \frac{u}{x} = \frac{a^*}{x^*} = \frac{a^* - u_e}{\ell} \tag{2.28}$$

where a^* is the sound speed in the throat.

It is also convenient to introduce, following Tsien [2.2] and Crocco [2.3], the new variable γ, defined by

$$\gamma = \left(\frac{x}{x^*}\right)^2 = \left(\frac{u}{a^*}\right)^2 \tag{2.29}$$

The Mach number and γ are related by

$$M^2 = 2\gamma / \left[(\gamma+1) - (\gamma-1)\gamma\right] \tag{2.30}$$

We also define the dimensionless angular frequency, or reduced frequency

$$\beta = \omega x^*/a^* = \omega \ell/(a^* - u_e) \qquad (2.31)$$

The system (2.26), (2.27) becomes

$$\frac{d\nu}{d\zeta} = -\frac{1}{\gamma}\frac{d\varphi}{d\zeta} + \frac{i\beta}{2\gamma\zeta}\varphi \qquad (2.32)$$

$$\frac{d\varphi}{d\zeta} = \frac{\sigma_e}{(\gamma+1)(1-\zeta)}\left(\frac{\zeta}{\zeta_e}\right)^{i\beta/2} + \frac{\gamma-1-i\beta}{(\gamma+1)(1-\zeta)}\varphi$$
$$- \frac{\gamma(2-i\beta)}{(\gamma+1)(1-\zeta)}\nu \qquad (2.33)$$

By eliminating ν between (2.32) and (2.33), a second order equation for φ only is obtained

$$(1-\zeta)\zeta\frac{d^2\varphi}{d\zeta^2} - \left(2 - \frac{2i\beta}{\gamma+1}\right)\zeta\frac{d\varphi}{d\zeta} + \frac{i\beta}{2}\frac{2-i\beta}{\gamma+1}\varphi =$$
$$\frac{i\beta}{2(\gamma+1)}\sigma_e\left(\frac{\zeta}{\zeta_e}\right)^{i\beta/2} \qquad (2.34)$$

This is a hypergeometric equation with singularities at $\zeta = 0$, $\zeta = 1$, $\zeta = \infty$, of which only $\zeta = 1$ lies in the range of interest for ζ. At $\zeta = 1$, the Mach number is unity and the mean flow becomes supersonic for $\zeta > 1$. In this region the characteristic lines of the system (2.12), (2.13), (2.14) all have positive slopes

$$\frac{dx}{dt} = u \pm c \qquad \text{on} \quad C_{\pm} \qquad (2.35)$$

(Mach lines)

$$\frac{dx}{dt} = u \qquad \text{on} \quad C_s \qquad (2.36)$$

(path lines)

They point in the positive X direction and only propagate signals in the flow direction. The singularity $\gamma = 1$ corresponds to the change in direction of the characteristic C_- at the sonic section. This singularity plays a key role in the present problem by providing one of the boundary conditions.

Generally we are guided by the principle that an acceptable physical relation must be regular at the critical point. We define the velocity of propagation of pressure disturbances $U(x)$ by

$$\frac{\partial}{\partial t}\left(\frac{p'}{p}\right) + U(x) \frac{\partial}{\partial x}\left(\frac{p'}{p}\right) = 0 \qquad (2.37)$$

which for the time harmonic perturbation (2.15) gives

$$U(x) = i\omega \, \varphi / (d\varphi / dx) \qquad (2.38)$$

Since the supersonic section only propagates signals in the forward direction, the velocity $U(x)$ should keep the same sign and remain finite across the throat section. This in turn requires that $d\varphi/dx$ and φ be finite and that φ be different from zero at the throat. The same argument is applicable to the other perturbations. The boundary condition to be satisfied at the nozzle throat is that all the perturbations be regular in that section.

To obtain a second condition, we consider the nozzle entrance. The main idea here is that in the subsonic region it is not possible to

uncouple the nozzle from the elements situated upstream. When the noise generating process depends on the nozzle dynamics, it is convenient to suppose that the complete (incident and reflected) pressure and entropy fluctuations are prescribed at the nozzle entrance

$$\varphi(x_e) = \varphi_e \tag{2.39}$$

$$\sigma(x_e) = \sigma_e \tag{2.40}$$

This artificially uncouples the nozzle from the upstream elements, and allows a simple analysis of the nozzle dynamics.

Another situation of interest is when the complete fluctuations (2.39), (2.40) are not known, but only the incident fluctuations, generated by some upstream mechanism, are given. The case when the incident pressure fluctuation $\varphi_{ie} = 0$, while only entropy fluctuations σ_e are present at the nozzle entrance, is of particular importance because it singles out the effects of gas non-uniformities. The condition $\varphi_{ie} = 0$ reduces to an impedance relation at the nozzle entrance. To see this we have to consider the wave propagation in the upstream region. We suppose that this region contains a uniform flow with a mean velocity u_e, the pressure perturbation is solution of the convective wave equation

$$\frac{1}{c^2}\left(\frac{\partial}{\partial t} + u_e \frac{\partial}{\partial x}\right)^2 p' = \frac{\partial^2 p'}{\partial x^2} \tag{2.41}$$

and the velocity perturbation u' is related to p' by the momentum equation in the x direction

$$\rho\left(\frac{\partial}{\partial t} + u_e \frac{\partial}{\partial x}\right) u' = -\frac{\partial p'}{\partial x} \tag{2.42}$$

In terms of φ and ν these two equations may be written as

$$\frac{1}{c^2}\left(\frac{\partial}{\partial t} + u_e \frac{\partial}{\partial x}\right)^2 \varphi = \frac{\partial^2 \varphi}{\partial x^2} \tag{2.43}$$

and

$$\rho u_e \left(\frac{\partial}{\partial t} + u_e \frac{\partial}{\partial x}\right) \nu = -p \frac{\partial \varphi}{\partial x} \tag{2.44}$$

The time harmonic waves propagating in this region are plane waves with wavenumbers

$$k_+ = \omega / (c + u_e) \tag{2.45}$$

$$k_- = \omega / (c - u_e) \tag{2.46}$$

and

$$\varphi = \varphi_i e^{i(k_+ x - \omega t)} + \varphi_r e^{-i(k_- x + \omega t)} \tag{2.47}$$

$$\nu = \nu_i e^{i(k_+ x - \omega t)} + \nu_r e^{-i(k_- x + \omega t)} \tag{2.48}$$

and from (2.44)

$$\nu_i = \varphi_i / \gamma M_e \tag{2.49}$$

$$\nu_r = -\varphi_r / \gamma M_e \tag{2.50}$$

Thus

$$\frac{\varphi}{\nu} = \gamma M_e \frac{\varphi_i e^{ik_+ x} + \varphi_r e^{-ik_- x}}{\varphi_i e^{ik_+ x} - \varphi_r e^{-ik_- x}} \tag{2.51}$$

The specific acoustic impedance ζ defined by

$$\mathfrak{Z} = (\rho c)^{-1} (p'/w')$$ (2.52)

is related to φ/ν by

$$\varphi/\nu = \gamma M \mathfrak{Z}$$ (2.53)

Hence,

$$\mathfrak{Z}(x) = \frac{\varphi_i e^{ik_+ x} + \varphi_r e^{-ik_- x}}{\varphi_i e^{ik_+ x} - \varphi_r e^{-ik_- x}}$$ (2.54)

If the specific acoustic impedance $\mathfrak{Z}$ is given in some upstream section, then

$$\mathfrak{Z}_e = (\gamma M_e)^{-1} \varphi_e / \nu_e$$ (2.55)

at the nozzle entrance is known through expression (2.54), and constitutes the second boundary condition. When $\varphi_i = 0$, then $\mathfrak{Z} = -1$ in every upstream section, and in particular at the nozzle entrance

$$\varphi_e / \nu_e = - \gamma M_e$$ (2.56)

It is now possible to write the solution of system (2.32), (2.33) in a general form. If $(\varphi^!, \nu^!)$ designates a regular solution of the homogeneous system ($\sigma_e = 0$) and (φ^*, ν^*) is a regular solution of the non-homogeneous system ($\sigma_e = 1$), then the general solution of the system (2.32), (2.33) is of the form

$$\varphi = \lambda \varphi^! + \sigma_e \varphi^*$$ (2.57)

$$\nu = \lambda \nu^! + \sigma_e \nu^*$$ (2.58)

The entrance condition then determines the constant λ. For condition (2.39)

$$\lambda = (\varphi_e - \sigma_e \varphi_e^*) / \varphi_e' \qquad (2.59)$$

For condition (2.55)

$$\lambda = -\sigma_e (\varphi_e^* - \mathcal{J} \gamma M_e \nu_e^*) / (\varphi_e' - \mathcal{J} \gamma M_e \nu_e') \qquad (2.60)$$

and in the special case when $\mathcal{J} = -1$ corresponding to $\varphi_{ie} = 0$

$$\lambda = -\sigma_e (\varphi_e^* + \gamma M_e \nu_e^*) / (\varphi_e' + \gamma M_e \nu_e') \qquad (2.61)$$

2.3 ASYMPTOTIC BEHAVIOR OF SOLUTIONS

For low frequencies we expand $\varphi(z)$ in powers of $i\beta$

$$\varphi(z,\beta) = \varphi_0(z) + i\beta\varphi_1(z) + (i\beta)^2\varphi_2(z) + \ldots \tag{2.62}$$

and introduce (2.62) in (2.34) to get the hierarchy of equations

$$(1-z)z\frac{d^2\varphi_0}{dz^2} - 2z\frac{d\varphi_0}{dz} = 0 \tag{2.63}$$

$$(1-z)z\frac{d^2\varphi_1}{dz^2} - 2z\frac{d\varphi_1}{dz} =$$
$$-\frac{2z}{\gamma+1}\frac{d\varphi_0}{dz} - \frac{1}{\gamma+1}\varphi_0 + \frac{\sigma_e}{2(\gamma+1)} \tag{2.64}$$

$\bullet\ \bullet\ \bullet$

When these equations are integrated, all singular solutions must be discarded. The velocity fluctuation ν is obtained by using expression (2.33). This procedure yields a solution of the homogeneous system $(\sigma_e = 0)$

$$\varphi' = \varphi_e - \frac{i\beta}{\gamma+1}\varphi_e\left[f_0(z) - f_0(z_e)\right] + O(\beta^2) \tag{2.65}$$

$$\nu' = \frac{\gamma-1}{2\gamma}\varphi_e + O(i\beta) \tag{2.66}$$

and a solution for the non-homogeneous system $(\sigma_e = 1)$

$$\varphi^* = \frac{i\beta}{2(\gamma+1)}\left[f_0(z) - f_0(z_e)\right] + O(\beta^2) \tag{2.67}$$

$$\nu^* = \frac{1}{2\gamma} + O(i\beta) \tag{2.68}$$

where the function $f_0(\gamma)$ is regular at $\gamma = 1$ and defined by

$$f_0(\gamma) = \gamma \ln \gamma / (1-\gamma) \tag{2.69}$$

On the other hand, for high frequencies we look for φ^1 in the form

$$\varphi^1 = \exp\left(-i\beta \int y \, d\gamma\right) \tag{2.70}$$

where y is solution of the first order equation

$$(1-\gamma)\gamma y' = \frac{2-i\beta}{2(\gamma+1)} + 2\left(1 - \frac{i\beta}{\gamma+1}\right)\gamma y$$
$$+ i\beta \gamma (1-\gamma) y^2 \tag{2.71}$$

We then expand y in inverse powers of $i\beta$

$$y = y_0(\gamma) + \frac{1}{i\beta} y_1(\gamma) + \frac{1}{(i\beta)^2} y_2(\gamma) + \dots \tag{2.72}$$

After some algebra and use of relation (2.30), the following solution is obtained

$$\varphi^1 = \varphi_e \frac{f_1(M)}{f_1(M_e)} \exp(-i\beta \alpha_0) + O(1/i\beta) \tag{2.73}$$

$$\nu^1 = \frac{1}{\gamma M} \varphi^1 + O(1/i\beta) \tag{2.74}$$

where

$$f_1(M) = \left[1 + (\gamma-1)M^2/2\right]^{1/2} M^{1/2} / (1+M) \tag{2.75}$$

and α_0 is a real function so that $\exp(-i\beta\alpha_0)$ is only a phase factor.

For the inhomogeneous system $(\sigma_e = 1)$ we seek a solution of the form

$$\varphi^* = \widetilde{\varphi}(\mathfrak{z})(\mathfrak{z}/\mathfrak{z}e)^{i\beta/2} \tag{2.76}$$

The function $\widetilde{\varphi}(\mathfrak{z})$ is solution of

$$(1-\mathfrak{z})\mathfrak{z}\,\widetilde{\varphi}'' - \left[i\beta\left(\frac{\gamma-1}{\gamma+1}\mathfrak{z} - 1\right) + 2\mathfrak{z}\right]\widetilde{\varphi}'$$

$$+\left[\frac{(i\beta)^2}{4}\left(\frac{1}{\mathfrak{z}} - \frac{\gamma-1}{\gamma+1}\right) - \frac{i\beta}{2}\left(\frac{1}{\mathfrak{z}} + \frac{\gamma-1}{\gamma+1}\right)\right]\widetilde{\varphi} = i\beta\,\frac{1}{2(\gamma+1)} \tag{2.77}$$

$\widetilde{\varphi}(\mathfrak{z})$ is then expanded in inverse powers of $i\beta$ to get

$$\varphi^* = \frac{M^2}{i\beta}\left(\frac{\mathfrak{z}}{\mathfrak{z}e}\right)^{i\beta/2} + O(1/\beta^2) \tag{2.78}$$

$$\nu^* = \frac{1}{i\beta\gamma}\left(\frac{\mathfrak{z}}{\mathfrak{z}e}\right)^{i\beta/2} + O(1/\beta^2) \tag{2.79}$$

Using the foregoing results, we can now compute the transmission coefficient $T = |\varphi/\varphi_e|$ and the ratio φ/ν for isentropic entrance condition $(\sigma_e = 0)$.

For low frequencies (2.65) yields

$$T = |\varphi/\varphi_e| = 1 + O(\beta^2) \tag{2.80}$$

and from (2.65) and (2.66)

$$|\varphi/\nu| = 2\gamma/(\gamma-1) + O(\beta^2)$$ (2.81)

The transmission coefficient is close to one; thus,

$$p'/p = p'_e/p_e \qquad :$$ (2.82)

the pressure disturbances decrease in the same ratio as the mean

flow pressure along the nozzle. At low frequencies, the nozzle re-

sponse is quasisteady.

For high frequencies,

$$T = |\varphi/\varphi_e| = f_1(M)/f_1(M_e) + O(1/\beta^2)$$ (2.83)

and

$$|\varphi/\nu| = \gamma M + O(1/\beta^2)$$ (2.84)

The transmission coefficient T is greater than one and depends

on entrance and exhaust Mach numbers. The ratio φ/ν, related

to the specific acoustic impedance by expression (2.53), is seen to

have a modulus almost equal to γM, which is the value taken

by $|\varphi/\nu|$ for a plane wave propagating in a medium moving with

a uniform Mach number M. Because of their high frequency, the

disturbances are able to "adjust" their impedance in each particular

nozzle section.

When the upstream flow contains entropy non-uniformities but

no incident pressure wave $(\varphi_{ie} = 0)$, the solution has the form

(2.57), (2.58) with λ determined by (2.61). Using the foregoing

results, we get for low frequencies

$$\varphi = -\sigma_e \frac{M_e}{2\gamma + (\gamma-1)M_e} + O(i\beta) \qquad (2.85)$$

while for high frequencies

$$\varphi_e = \sigma_e \; M_e(1-M_e)/2i\beta + O(1/i\beta) \qquad (2.86)$$

For low frequencies, expression (2.85) shows that the pressure fluctuations resulting from the entrance entropy fluctuations depend only on the entrance Mach number M_e .

For high frequencies, the evaluation of φ in the exhaust section requires a large amount of algebra and was not carried out. Instead, the expression for the entrance fluctuation φ_e is given (2.86). As $\varphi_{ie} = 0$ in this case, φ_e is also the reflected pressure fluctuation due to the incident entropy non-uniformities.

The preceding asymptotic expansions give only partial information; a numerical solution was therefore developed and is described below.

2.4 NUMERICAL SOLUTION

We consider first the homogeneous system $(\sigma_e = 0)$. We need a basic solution (φ^1, ν^1) which is regular at the throat $\zeta = 1$. If the integration of system (2.32), (2.33) is started from the nozzle entrance $\zeta = \zeta_e$, the solution produced will most probably be singular (unbounded) at the throat. This drives us to start the integration from the singular point $\zeta = 1$ towards higher and lower ζ . To obtain an initial value problem we use the regularity conditions as follows. In the neighborhood of $\zeta = 1$, φ and ν may be expanded in Taylor series

$$\varphi = \varphi(1) + (\zeta - 1) \frac{d\varphi(1)}{d\zeta} + \frac{1}{2}(\zeta - 1)^2 \frac{d^2\varphi(1)}{d\zeta^2} + \ldots \quad (2.87)$$

$$\nu = \nu(1) + (\zeta - 1) \frac{d\nu(1)}{d\zeta} + \frac{1}{2}(\zeta - 1)^2 \frac{d^2\nu(1)}{d\zeta^2} + \ldots \quad (2.88)$$

Then we insert (2.87), (2.88) in (2.32), (2.33) and equate coefficients of $(\zeta - 1)^{-1}$ and $(\zeta - 1)^0$ to produce

$$\nu(1) = \frac{\gamma - 1 - i\beta}{\gamma(2 - i\beta)} \varphi(1) \quad (2.89)$$

$$\frac{d\varphi(1)}{d\zeta} = \frac{i\beta}{4} \frac{2 - i\beta}{\gamma + 1 - i\beta} \varphi(1) \quad (2.90)$$

$$\frac{d\nu(1)}{d\zeta} = \frac{i\beta}{4} \frac{2\gamma - i\beta}{\gamma + 1 - i\beta} \varphi(1) \quad (2.91)$$

We assign an arbitrary value to $\varphi(1)$, say 1. Then expressions (2.89), (2.90), (2.91) may be used to begin a fourth-order Runge-Kutta integration procedure from $\zeta = 1$ towards lower and

higher ζ .

To solve the inhomogeneous system $(\sigma_e = 1)$, we consider a solution in the form

$$\varphi^* = \tilde{\varphi} \, (\zeta / \zeta e)^{i\beta/2} \tag{2.92}$$

$$\mathcal{V}^* = \tilde{\mathcal{V}} \, (\zeta / \zeta e)^{i\beta/2} \tag{2.93}$$

and $\tilde{\varphi}, \tilde{\mathcal{V}}$ is a solution of the system

$$\frac{d\tilde{\mathcal{V}}}{d\zeta} = -\frac{1}{\gamma} \frac{d\tilde{\varphi}}{d\zeta} - \frac{i\beta}{2\zeta} \tilde{\mathcal{V}} \tag{2.94}$$

$$\frac{d\tilde{\varphi}}{d\zeta} = \frac{1}{(\gamma+1)(1-\zeta)} + \frac{(\gamma-1-i\beta)}{(\gamma+1)(1-\zeta)} \tilde{\varphi} - \frac{i\beta}{2\zeta} \tilde{\varphi}$$

$$- \frac{\gamma(2-i\beta)}{(\gamma+1)(1-\zeta)} \tilde{\mathcal{V}} \tag{2.95}$$

The same method may be used to obtain the initial values at $\zeta = 1$. They are

$$\tilde{\varphi}(1) = 1. \tag{2.96}$$

$$\tilde{\mathcal{V}}(1) = \frac{\gamma - i\beta}{\gamma(2 - i\beta)} \tag{2.97}$$

$$\frac{d\tilde{\varphi}(1)}{d\zeta} = -\frac{i\beta}{4} \frac{2\gamma+1-i\beta}{\gamma+1-i\beta} \tag{2.98}$$

$$\frac{d\tilde{\nu}(1)}{d\zeta} = -\frac{1}{\gamma}\frac{d\tilde{\varphi}(1)}{d\zeta} - \frac{i\beta}{2}\tilde{\nu}(1) \qquad (2.99)$$

These values are then used to start a fourth-order Runge-Kutta integration procedure.

Before we discuss the results of the numerical integration, it is interesting to estimate the reduced frequencies β corresponding to the various pressure and entropy fluctuations which may be present at the nozzle entrance.

The turbine produces various discrete tones at the frequency of the rotor blade passage and its harmonics and multiple tones associated with the shaft frequency and the stator guide vane number, and spanning the range from 800 to 3000 Hz. The corresponding reduced frequencies β are between 8 and 20.

The acoustic frequencies found in combustion instability are situated in the interval 100 to 400 Hz, generally close to the natural modes of oscillation of the combustion chamber. For longitudinal modes

$$f = n \frac{c_{co}}{2 L_{co}} \qquad (2.100)$$

where c_{co} is the speed of sound in the combustion chamber of length L_{co}. The corresponding β are

$$\beta = n\pi \left(\frac{\ell}{L_{co}}\right) \left(\frac{c_{co}}{a^* - u_e}\right) \qquad (2.101)$$

the fundamental β is of order 3.

Another type of disturbance found in combustors is an oscillation associated with the unstable shear region generated by the flame

in the duct and whose frequency depends on the flow velocity u_{co} and the combustor width W_{co} (see, for instance, Blackshear and Rayle [2.4])

$$f \simeq 2 u_{co} / W_{co} \qquad (2.102)$$

The reduced frequency β is again around 3.

The entropy non-uniformities which arise from the rotation of the shock pattern attached to the turbine rotor have their frequency in the same range as the pressure fluctuations generated by the turbine. The entropy non-uniformities produced by the combustion processes (hot spots) probably do not exceed the size of the approach duct diameter and are convected with a velocity u_e . Their frequency is therefore

$$f \gtrsim u_e / 2 D_e \qquad (2.103)$$

and

$$\beta \gtrsim \pi \frac{u_e}{(a^* - u_e)} \frac{\ell}{D_e} \simeq \pi M_e \frac{\ell}{D_e} \qquad (2.104)$$

Thus, β would be in this case of order one.

2.5 RESULTS AND DISCUSSION

The numerical integration was performed for a range of frequencies β between 0 and 16, for a gas with a specific heat ratio γ = 1.4 . We first generated the basic solutions (φ', ν') for the homogeneous system $(\sigma_e = 0 , \varphi'(1) = 1)$ and $(\tilde{\varphi}, \tilde{\nu})$ for the non-homogeneous system $(\sigma_e = \quad , \tilde{\varphi}(1) = 1)$. A typical solution φ' is represented on fig. 2-1 for a reduced frequency β = 5. Figure 2-2 shows a typical solution $\tilde{\varphi}$ for the same reduced frequency. From these basic solutions, any solution corresponding to particular entrance conditions may be constructed using expressions (2.57) and (2.58).

Isentropic Case $(\sigma_e = 0)$

From the basic solution φ' , the pressure transmission coefficient

$$T = |\varphi / \varphi_e| = |(p'/p)/(p'_e/p_e)|$$

may be computed. T is shown graphically on figs. 2-3 and 2-4. The transmission coefficient is seen to remain above one and below its limit for large frequencies. This limit was computed in section 2.3 and was found to be

$$T_\infty = \lim_{\beta \to \infty} T = f_1(M)/f_1(M_e) \tag{2.105}$$

A decrease in the entrance Mach number M_e or a larger frequency β results in a larger transmission coefficient. The numerical data for T may be compressed by using the reduced ratio

$$\tau = (T-1)/(T_\infty - 1) \tag{2.106}$$

which is represented on fig. 2-5.

Another important quantity is the ratio of pressure fluctuation to velocity fluctuation,

$$\varphi/\nu = |\varphi/\nu| \, e^{-i\Phi}$$

This ratio is related to the specific acoustic impedance ζ by formula (2.53). The modulus $|\varphi/\nu|$ is represented on fig. 2-6 and the phase Φ is shown on fig. 2-7. A full analytical expression for φ/ν is available for the throat section (2.89) and may be rearranged as

$$\frac{\varphi(1)}{\nu(1)} = \frac{2\gamma}{\gamma-1} \; \frac{1-i\beta/2}{1-i\beta/(\gamma-1)} \tag{2.107}$$

In other nozzle sections φ/ν behaves very much like $\varphi(1)/\nu(1)$ and may be represented by the approximate expression

$$\frac{\varphi}{\nu} = \frac{2\gamma}{\gamma-1} \; \frac{1-i\beta M/2}{1-i\beta/(\gamma-1)} \tag{2.108}$$

This expression is exact for the limits $\beta \to 0$ and $\beta \to \infty$. For low β, φ/ν is the same in all nozzle sections and has the value $2\gamma/(\gamma-1)$ imposed by the presence of the sonic throat. When $\beta > 1$, the modulus $|\varphi/\nu|$ rapidly approaches its limit for large β: γM. This is also the value of $|\varphi/\nu|$ for a plane wave propagating in a medium of uniform Mach number M.

It is also interesting to compare the mass fluctuation

$$\mu = \nu + \delta \tag{2.109}$$

to the associated pressure fluctuation φ. The ratio μ/φ was therefore represented on fig. 2-8. For the exhaust sections $M \geqslant 1$,

the mass fluctuation is seen to have approximately the same magnitude as the pressure fluctuation, with a slight phase lead on the pressure fluctuation. For very low frequencies the ratio μ/φ does not depend on the section Mach number:

$$\mu/\varphi = (\gamma+1)/2\gamma \tag{2.110}$$

No Incident Pressure Is Present $\quad (\varphi_{ie} = 0)$

A typical solution φ for $\sigma_e = 1$ and $\varphi_{ie} = 0$ is shown on fig. 2-9. This solution was obtained by combining the basic solutions φ_1 and $\tilde{\varphi}$ represented on figs. 2-1 and 2-2 and using λ given by expression (2.61). In this case, the entrance Mach number was $M_e = 0.29$. At the nozzle entrance φ represents the reflected pressure wave and is seen to be a small quantity. Along the nozzle φ increases rapidly as the entropy fluctuations present at the nozzle entrance are converted into pressure fluctuations.

Figure 2-10a, b, c, shows the ratio $|\varphi/\sigma_e|$ of conversion of entropy fluctuations into pressure fluctuations for several entrance and exhaust Mach numbers. This conversion factor generally shows a maximum for reduced frequencies β around 3. For low β the factor $|\varphi/\sigma_e|$ depends only on the entrance Mach number and may be found from expression (2.85)

$$|\varphi/\sigma_e| = \frac{M_e}{2\gamma + (\gamma-1)M_e} \tag{2.111}$$

It is worth applying the last results to a specific example and estimating the radiated pressure at some distance from the nozzle exhaust, when only entropy non-uniformities are present at the nozzle

entrance. An approximate expression for the far-field radiated pressure has been developed in Appendix 2-A, (2A.21), (2A.22); the maximum radiated pressure is given by

$$|p'_{max}| \simeq \frac{A\,x_0}{2\pi b}\,G_M\left(\frac{b}{R}\right) \tag{2.112}$$

where A is the pressure fluctuation amplitude in the exhaust section, b is the exhaust radius, x_0 is some effective radiation length of the order of a nozzle diameter, G_M is a factor defined in Appendix 2-A.

We consider a nozzle operating under the following conditions. at the nozzle entrance,

$$T_e = 2000°k \quad, \quad p_e = 3.46\,bars \quad, \quad M_e = 0.29$$

at the nozzle exhaust,

$$p = 1\,bar \quad, \quad M = 1.5$$

At the nozzle entrance we suppose that no incident pressure fluctuation is present, $\varphi_{ie} = 0$. The pressure fluctuation at the entrance is only the reflected pressure fluctuation, and was seen to be small compared to the entropy fluctuation. The following relations between the entrance fluctuations may be written

$$\varphi_e - \delta_e = \theta_e \tag{2.113}$$

$$\varphi_e - \gamma\delta_e = \sigma_e \tag{2.114}$$

then

$$\varphi_e = \frac{\gamma\theta_e - \sigma_e}{\gamma - 1} \tag{2.115}$$

and $\varphi_e \simeq 0$ implies that $\sigma_e \simeq \gamma \theta_e$. The entropy fluctuation σ_e is proportional to the temperature fluctuation θ_e .

The amplitude of the pressure fluctuation in the exhaust section may be found by using the factor $|\varphi/\sigma_e|$

$$A \simeq \gamma \theta_e |\varphi/\sigma_e| \tag{2.116}$$

If the temperature oscillation at the entrance $T'_e = 100°K$ and the frequency $\beta = 3$, then expressions (2.112) and (2.116) yield a maximum radiated pressure at a hundred nozzle radii of

$$|P'_{MAX}| \text{ at } R=100b = 21 \text{ Newtons}/m^2$$

and the corresponding sound pressure level is

$$SPL \text{ at } R=100b = 120 \text{ db} \quad , \quad P_{ref} = 2.10^{-5} N/m^2$$

This example shows that entropy non-uniformities in the stream ahead of the nozzle may produce large external noise levels.

REFERENCES

2.1   Large, J.B., Wilby, J.F., Grande, E., and Anderson, A.O., "The Development of Engineering Practices in Jet, Compressor and Boundary Layer Noise," AFOSR-UTIAS Symposium on Aerodynamic Noise, Toronto (1968), University of Toronto Press.

2.2   Tsien, H.S., "The Transfer Functions of Rocket Nozzles," J. Am. Rocket Soc., 22 (1952), 139.

2.3   Crocco, L., "Supercritical Gaseous Discharge with High Frequency Oscillations," L'Aeronautica, 33 (1953), 46-53.

2.4   Blackshear, P.L. Jr., and Rayle, W.D., "Oscillations in Combustors," Basic Considerations in the Combustion of Hydrocarbon Fuels with Air, NASA Rep. 1300, Chapter VIII (1957).

2.5   Kramer, H.P., "Note on the Emission of Noise by Supersonic Jets," J. Acoust. Soc. Am., 27 (1955), 789.

APPENDIX 2-A

Acoustic Radiation from a Supercritical Nozzle.

It is difficult to obtain an exact solution for the problem of acoustic radiation from a supercritical nozzle in a stationary medium, principally because of the complex structures of the jet and shear layer. Even if the jet is represented by an infinite cylindrical region of uniform supersonic flow with the shear layer reduced to the cylinder surface, the radiation problem remains complex.

A simple model is therefore developed here and will provide an approximate solution and an order of magnitude for the sound pressure level at a distance from the nozzle. The model is based on the assumption that the pressure fluctuations which reach the nozzle end section are propagated along the jet on some effective length X_0 after which they disappear by breaking in smaller turbulent eddies. Only the radiation from the region of length X_0 will be calculated: it should be noted at this point that the value of X_0 is not known but is of the order of a few nozzle radii. Similar assumptions were used in a note by Kramer [2.5] to compute the noise emitted by supersonic jets.

For convenience we choose the origin of the x axis so that the nozzle end section is at $x = -X_0/2$. The pressure fluctuation in this section is

$$p'(r, -X_0/2, t) = A e^{-i\omega t} \qquad (2A-1)$$

where A is the amplitude of the pressure fluctuation. The pressure pulsation at the nozzle discharge section produces a pressure wave

along the jet surface, convected by the jet with a velocity u_1

$$p'(b, x, t) = A e^{i(k_x x - \omega t)} \qquad -x_0/2 < x < x_0/2$$

$$= 0 \qquad +x_0/2 < x \text{ or } x < -x_0/2 \qquad (2A-2)$$

and the wave number in the x direction is

$$k_x = \omega/(c_1 + u_1) \qquad (2A-3)$$

where c_1 and u_1 are the sound speed and velocity of the jet in the neighborhood of the exhaust section. Outside the jet $(r > b)$ the pressure perturbation is solution of the Helmholtz equation

$$\nabla^2 p'_\omega + (\omega^2/c_2^2) p'_\omega = 0 \qquad (2A-4)$$

and satisfies Sommerfeld's radiation condition at infinity

$$\lim_{R \to \infty} R \left(\frac{\partial p}{\partial n} - i k_2 p \right) = 0 \qquad (2A-5)$$

where $R = (x^2 + r^2)^{1/2}$ and $k_2 = \omega/c_2$. The solution of the boundary value problem (2A-2), (2A-4), (2A-5) may be easily obtained by Fourier transform methods and only the main steps are given here. We define the Fourier transform of the pressure fluctuation by

$$\tilde{p}'_\omega (r, \alpha) = \frac{1}{(2\pi)^{1/2}} \int_{-\infty}^{+\infty} p'_\omega (r, x) e^{i\alpha x} dx \qquad (2A-6)$$

where

$$\alpha = \sigma + i \tau \qquad (2A-7)$$

Then $\tilde{p}'_\omega$ is solution of the ordinary differential equation obtained

by transforming (2A-4)

$$\frac{d^2 \tilde{p}'_\omega}{dr^2} + \frac{1}{r} \frac{d\tilde{p}'_\omega}{dr} + (k_2^2 - \alpha^2) \tilde{p}'_\omega = 0 \qquad (2A-8)$$

As usual, k_2 is assigned a small positive imaginary part, which will help to settle questions about the position of the branch points, path of integration, and behavior at infinity

$$k_2 = k_{2r} + i k_{2i} \qquad , \qquad k_{2i} > 0 \qquad (2A-9)$$

Then we define

$$\kappa = (k_2^2 - \alpha^2)^{1/2} \qquad (2A-10)$$

and use the branch of κ such that $\text{Im}(\kappa) > 0$ for $-k_{2i} < \sigma < k_{2i}$

Transforming the boundary condition (2A-2)

$$\tilde{p}'_\omega (b, \alpha) = \frac{A x_0}{(2\pi)^{1/2}} \frac{\sin[(k_x + \alpha) x_0 / 2]}{[(k_x + \alpha) x_0 / 2]} \qquad (2A-11)$$

Then the solution of (2A-8) satisfying (2A-11) and bounded when $r \rightarrow \infty$ for α in the strip $-k_{2i} < \sigma < k_{2i}$ is

$$\tilde{p}'_\omega (r, \alpha) = \frac{A x_0}{(2\pi)^{1/2}} \frac{\sin[(k_x + \alpha) x_0 / 2]}{[(k_x + \alpha) x_0 / 2]} \frac{H_0'(\kappa r)}{H_0'(\kappa b)} \qquad (2A-12)$$

The inverse of $\tilde{p}'_\omega$ is given by

$$p'_\omega (r,x) = \frac{1}{(2\pi)^{1/2}} \int_{-\infty+ia}^{+\infty+ia} e^{-i\alpha x} \tilde{p}'_\omega(r,\alpha) \, d\alpha \qquad (2A\text{-}13)$$

where the path of integration is situated in the strip

$$-k_{2i} < a < k_{2i}$$

To evaluate (2A-13) in the far field we first require $Kr \gg 1$ so that the following asymptotic expression for H'_0 may be used:

$$H'_0 (Kr) \sim \left(\frac{2}{\pi Kr}\right)^{1/2} e^{iKr - i\pi/4} \qquad (2A\text{-}14)$$

Then the saddle point of the integrand in (2A-13) is $\alpha_0 = -k_2 \cos\theta$ where θ designates the polar angle of the propagation direction with respect to the X axis

$$\theta = \tan^{-1}(r/x) \qquad (2A\text{-}15)$$

A straightforward application of the saddle point method to (2A-13) yields

$$p'(R,\theta,t) \simeq \frac{Ax_0}{2\pi b} \frac{\sin[(k_x - k_2\cos\theta)x_0/2]}{[(k_x - k_2\cos\theta)x_0/2]} \frac{1}{H'_0(k_2 b \sin\theta)}$$

$$e^{i(k_2 R - \omega t)} (b/R) \qquad (2A\text{-}16)$$

for

$$k_2 R \sin\theta \gg 1$$

where

$$R = \left(x^2 + r^2\right)^{1/2} \qquad (2A\text{-}17)$$

It is then convenient to define the following quantities:

$$G(\theta) = \frac{\sin\left[(k_x - k_2\cos\theta)x_0/2\right]}{\left[(k_x - k_2\cos\theta)x_0/2\right]} \; \frac{1}{|H_0'(k_2 b \sin\theta)|} \qquad (2A\text{-}18)$$

$$G_M = \operatorname*{Max}_{\theta} \; G(\theta) \qquad (2A\text{-}19)$$

the normalized angular distribution

$$g(\theta) = G(\theta)/G_M \qquad (2A\text{-}20)$$

and the amplitude

$$Q = \frac{A x_0}{2\pi b} \; G_M \qquad (2A\text{-}21)$$

Then

$$|p'| \simeq Q \; g(\theta) \; (b/R) \qquad (2A\text{-}22)$$

The pressure amplitude is given as a product of three factors: the third factor is the usual R^{-1} decay of the acoustic field at infinity; the second factor is an angular distribution function which, because of its definition, is of order one; the first factor Q contains the essential information about the radiated pressure. The factor Q is proportional to x_0/b and G_M. Thus, the radiation efficiency for the present model increases with the effective length x_0. For numerical applications we shall assume that $x_0 \simeq 2b$. The value of G_M depends on the reduced frequency $\beta = \omega x^*/a^*$, the ratio of the nozzle radius to the length of the subsonic section

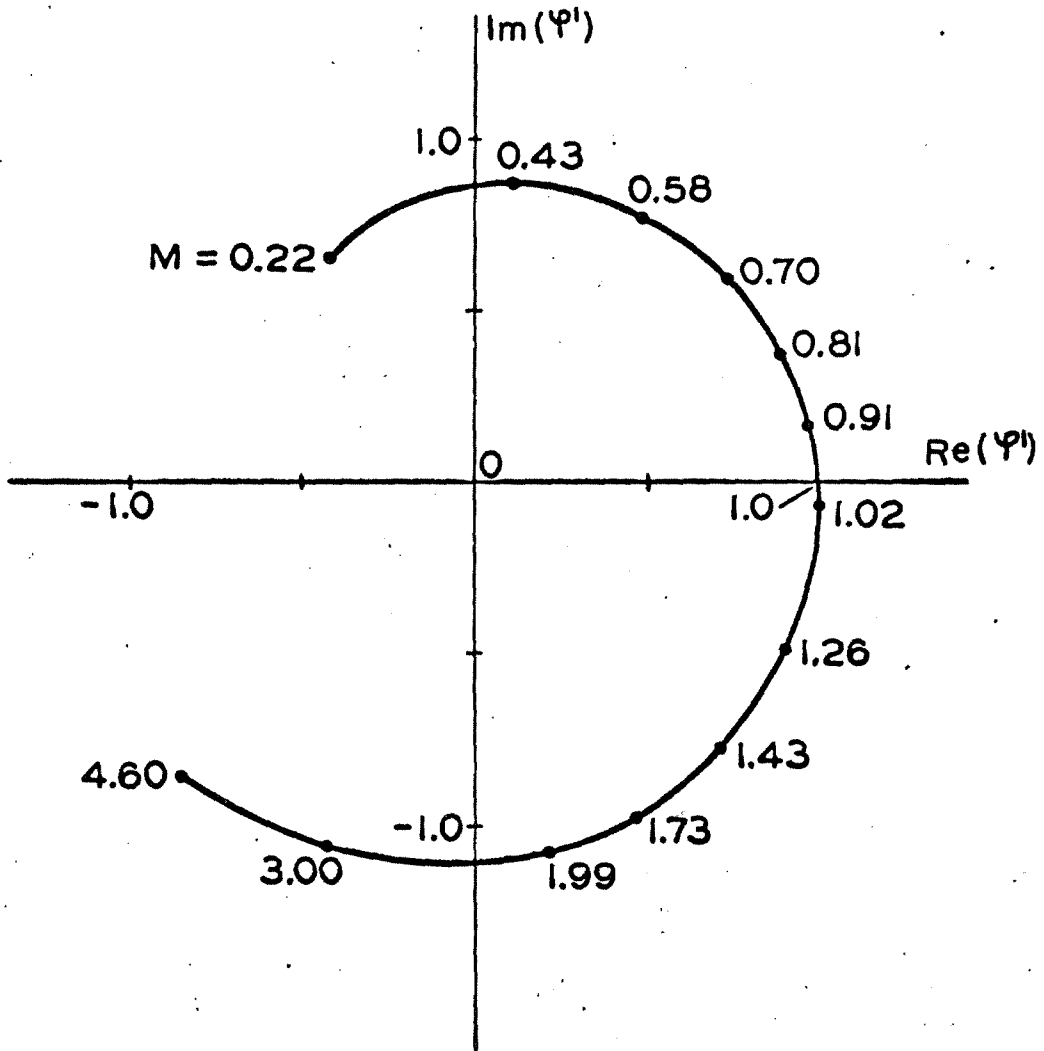b/x^* and only weakly on x_0/x^*. For a nozzle with $b/x^* = 2$ and $\beta = 3$ the value of $G_M = 3$, then $Q \simeq A$.

Fig. 2-1. Dimensionless pressure fluctuation φ' for isentropic condition at the nozzle entrance ($\sigma_e = 0.$). At the throat $\varphi'(1)$ is assigned the value one. Reduced frequency $\beta = \omega x^*/a^* = 5.0$
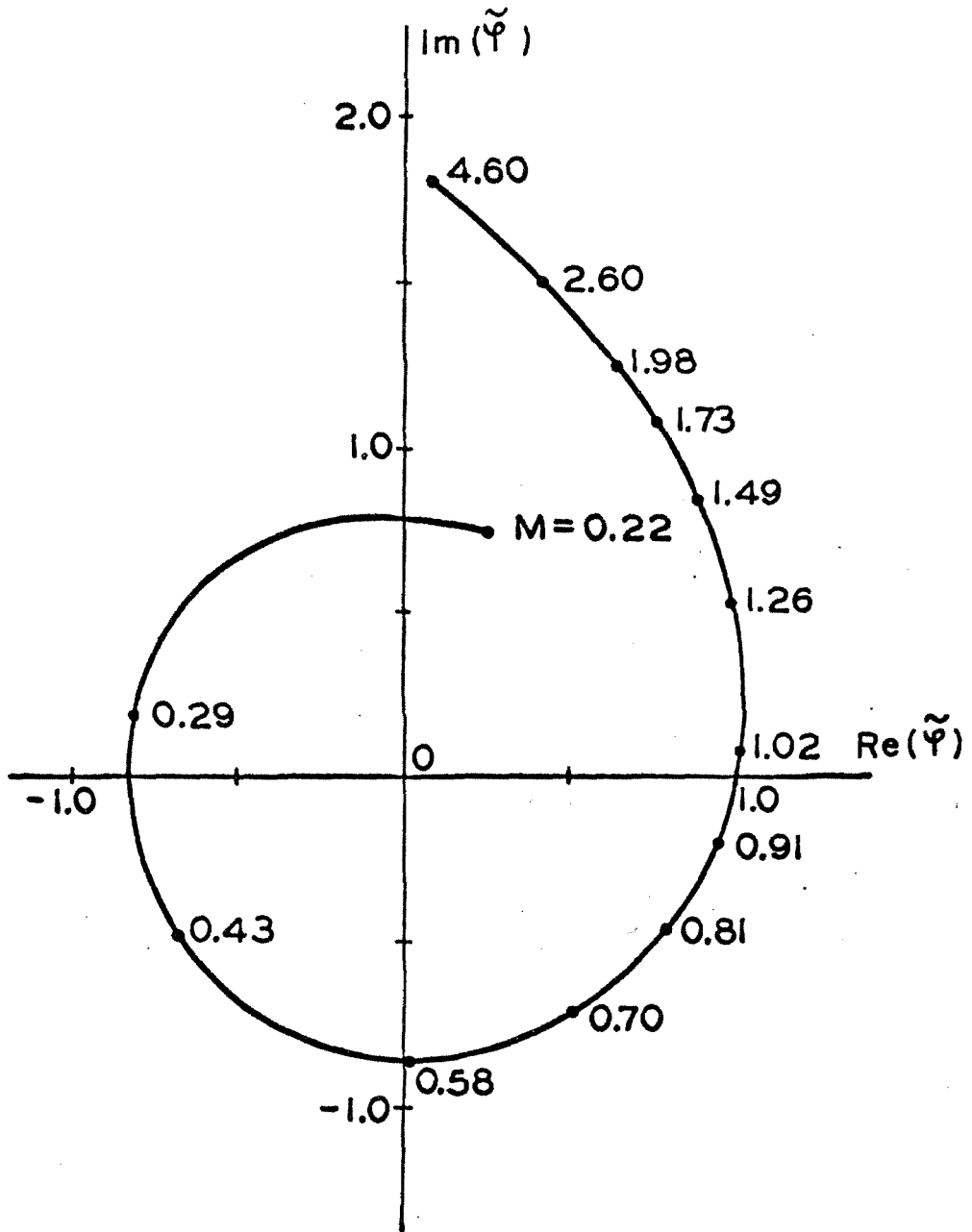
Fig. 2-2. Dimensionless pressure fluctuation $\tilde{\varphi}$ for an entropy fluctuation at the nozzle entrance $\sigma_e = 1$. At the throat $\tilde{\varphi}(1)$ is assigned the value one.
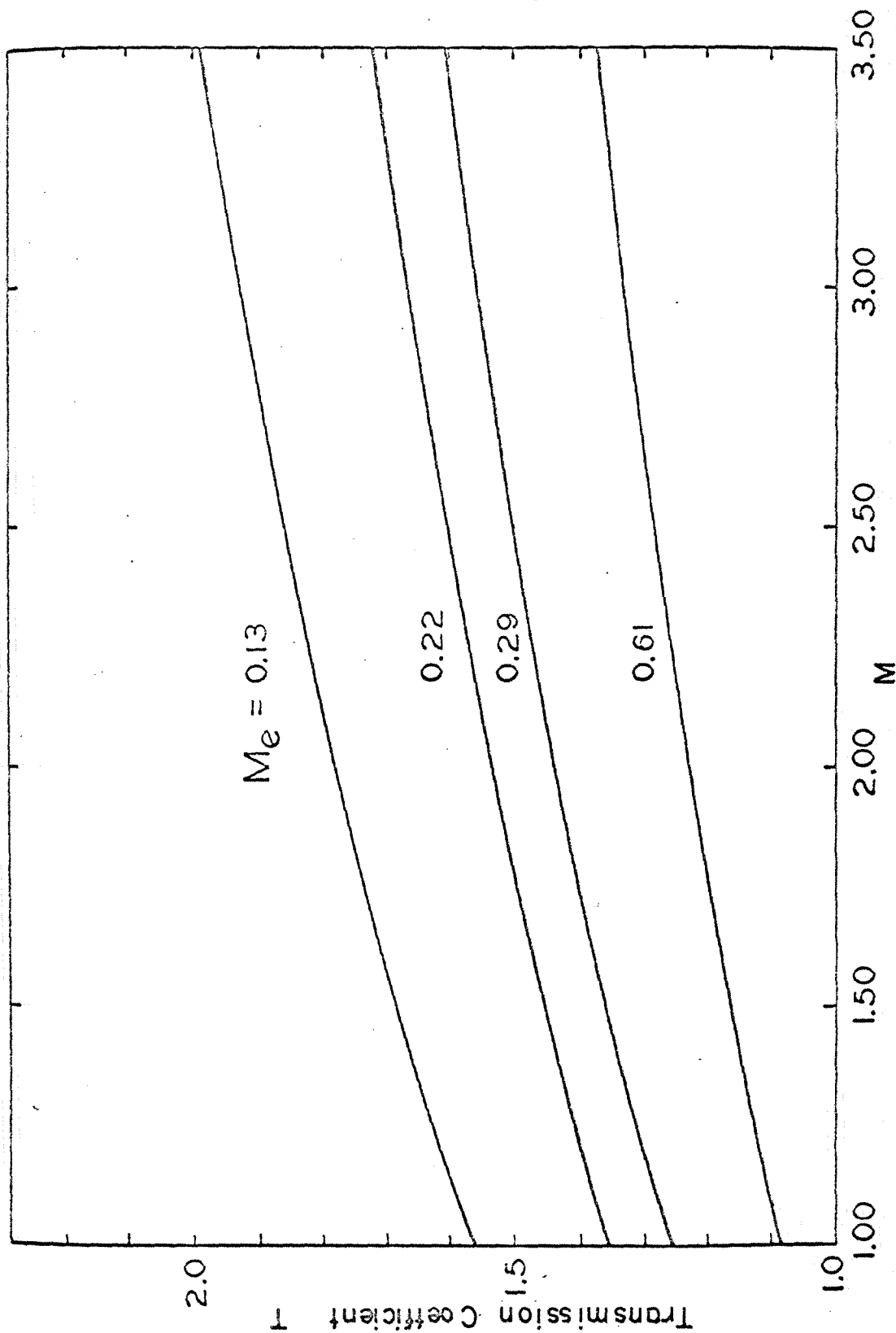Reduced frequency $\beta = \omega x'/a^* = 5.0$

Fig. 2-3. Pressure transmission coefficient $T = (\tilde{p}'/p)/(\tilde{p}'_e/p_e)$ for isentropic condition at the nozzle entrance ($\sigma_e = 0$). Reduced frequency $\beta = \omega x^*/a^* = 5.0$
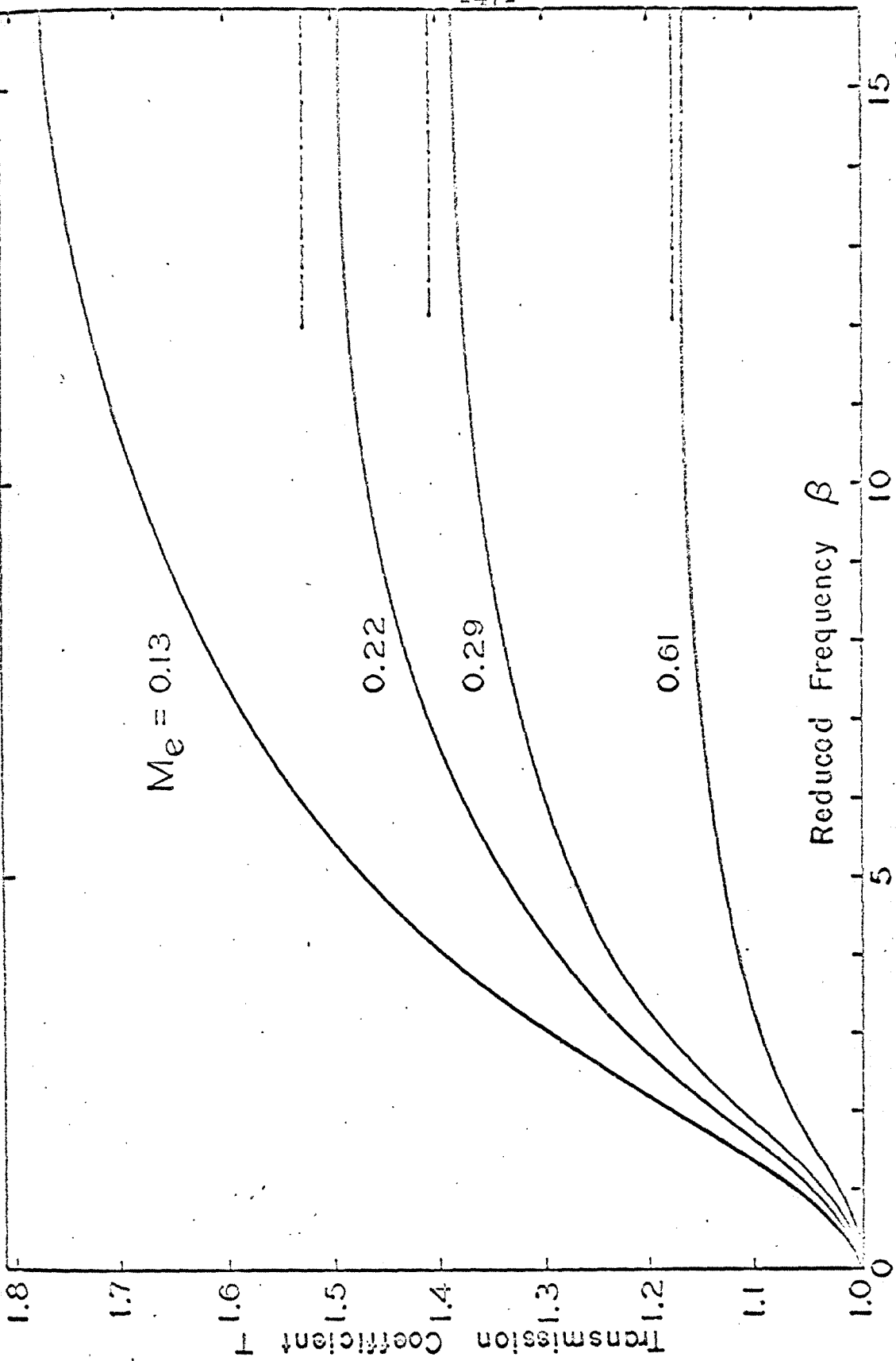
Fig. 2-4. Pressure transmission coefficient T for isentropic conditions at the nozzle entrance ($\sigma_e = 0$). The interrupted lines are the asymptotic values T_∞ for large frequencies β. $M = 1.52$.
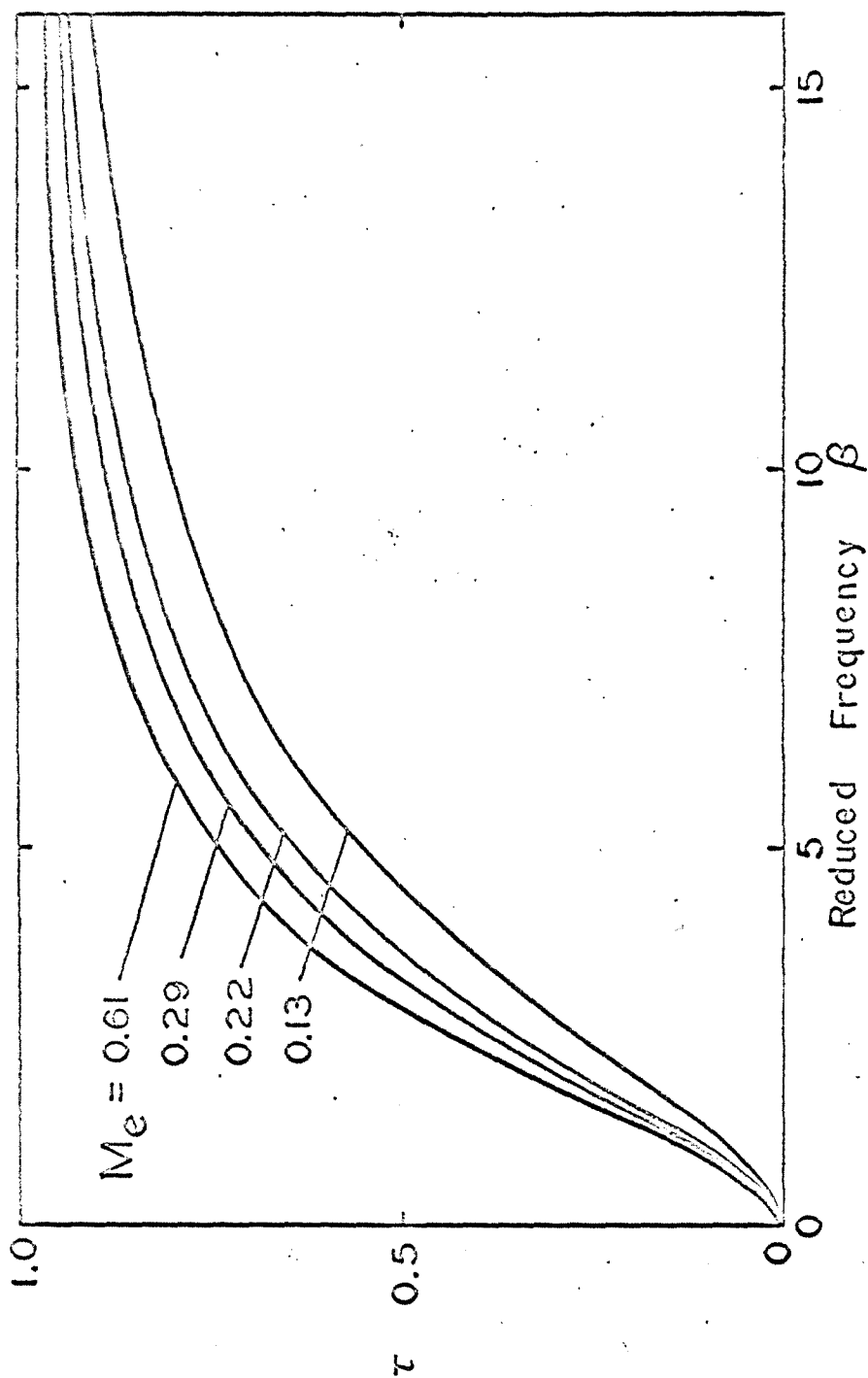
Fig. 2-5. Reduced transmission ratio for isentropic conditions at the nozzle entrance ($\sigma_e = 0$)

$$\tau = (T-1)/(T_{\infty}-1)$$

$$T_{\infty} = f_1(M)/f_1(M_c)$$

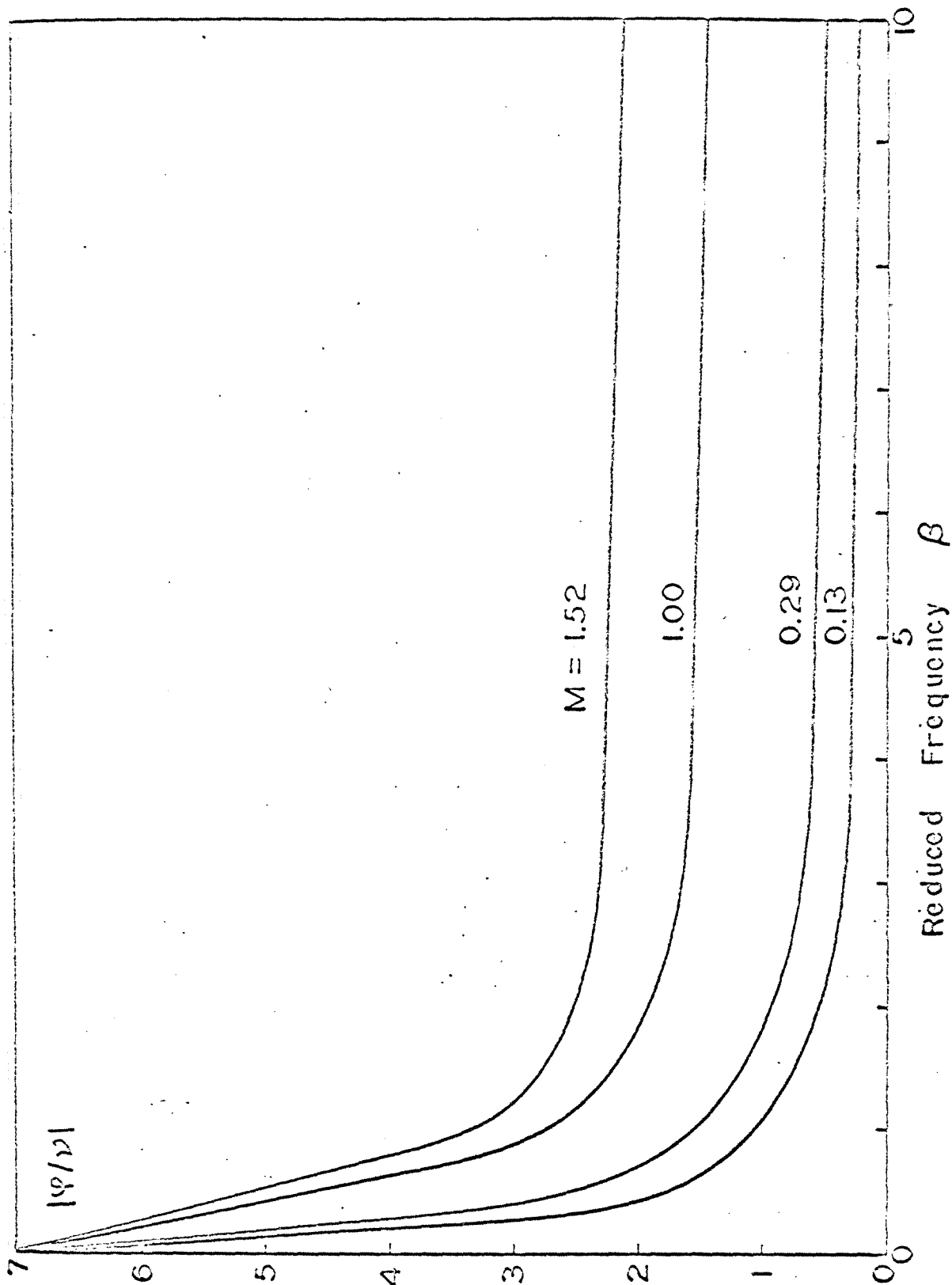$$f_1(M) = [1 + (\gamma-1)M^2/2]^{1/2} \, M^{1/2}/(1+M)$$

Fig. 2-6. Modulus of the pressure to velocity ratio, $|\wp/\nu|$, for isentropic conditions at the nozzle entrance ($\sigma_\wp = 0$).
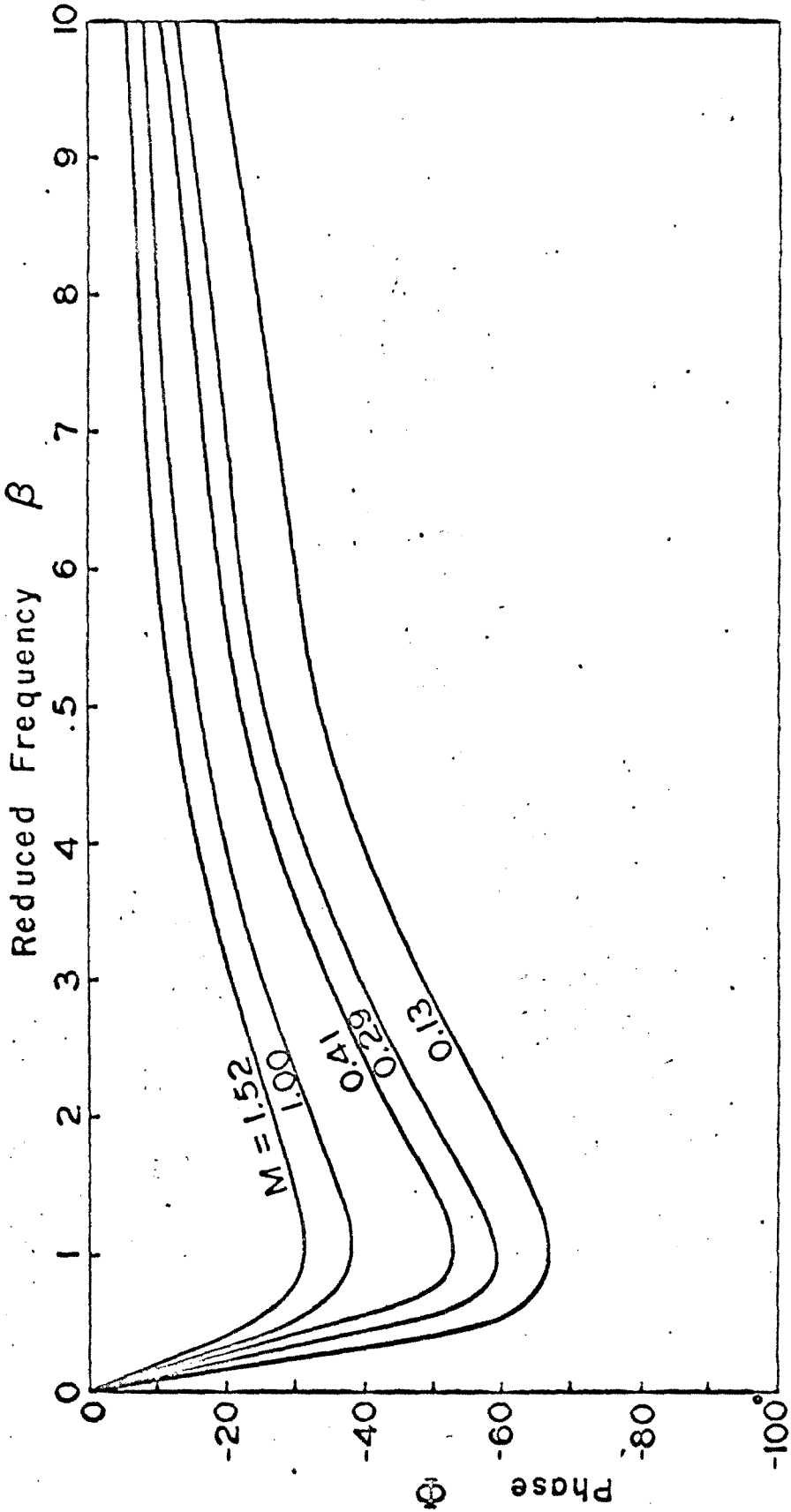
Fig. 2-7. Phase of the pressure to velocity ratio, $\varphi/v = |\varphi/v|e^{-i\Phi}$, for isentropic condition at the nozzle entrance ($\sigma_c = 0$). The specific acoustic impedance ζ is related to φ/v by $\zeta = (\gamma M)^{-1} \varphi/v$.
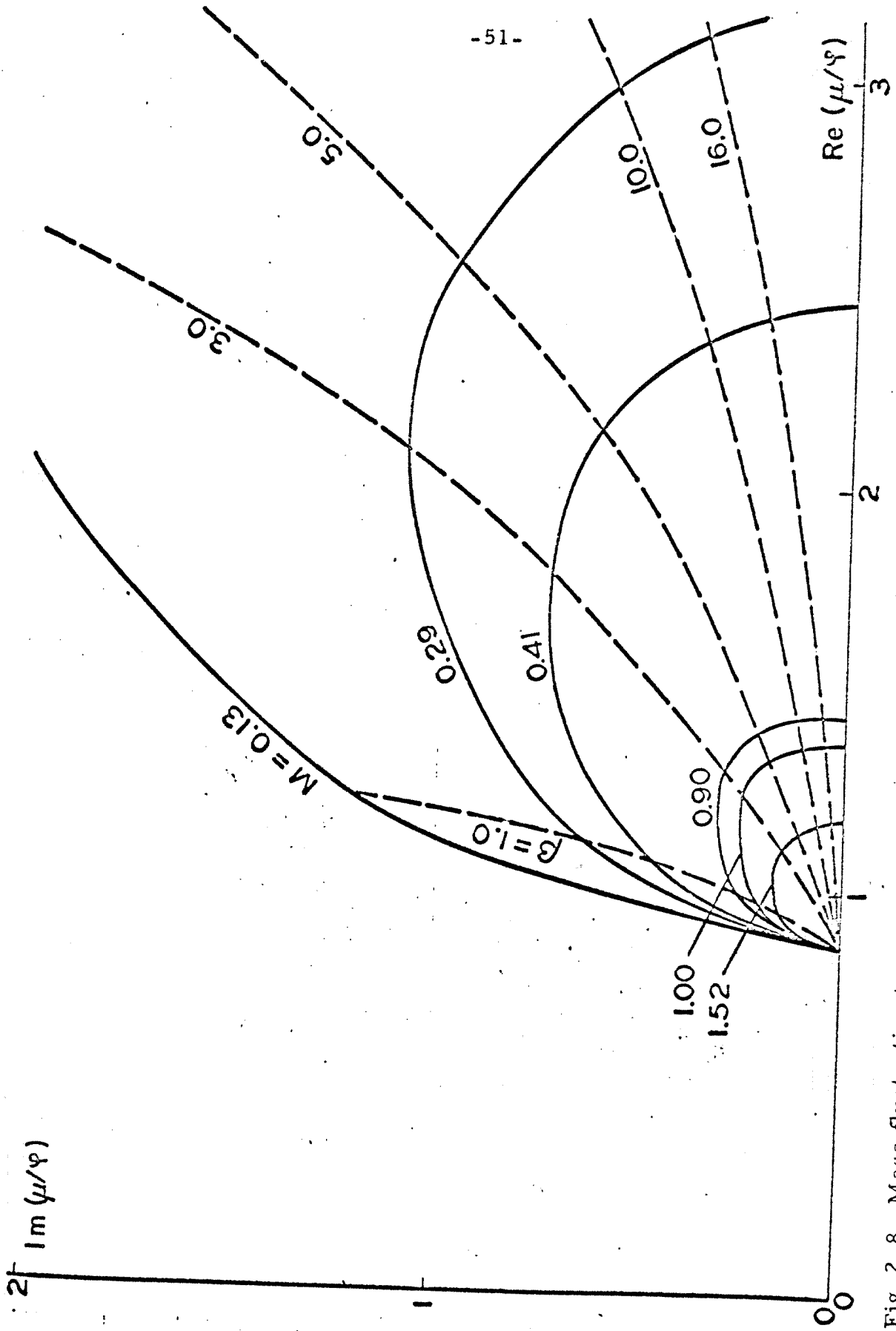
Fig. 2-8. Mass fluctuation to pressure fluctuation ratio μ/φ, for isentropic condition at the nozzle entrance ($\sigma_e = 0$).
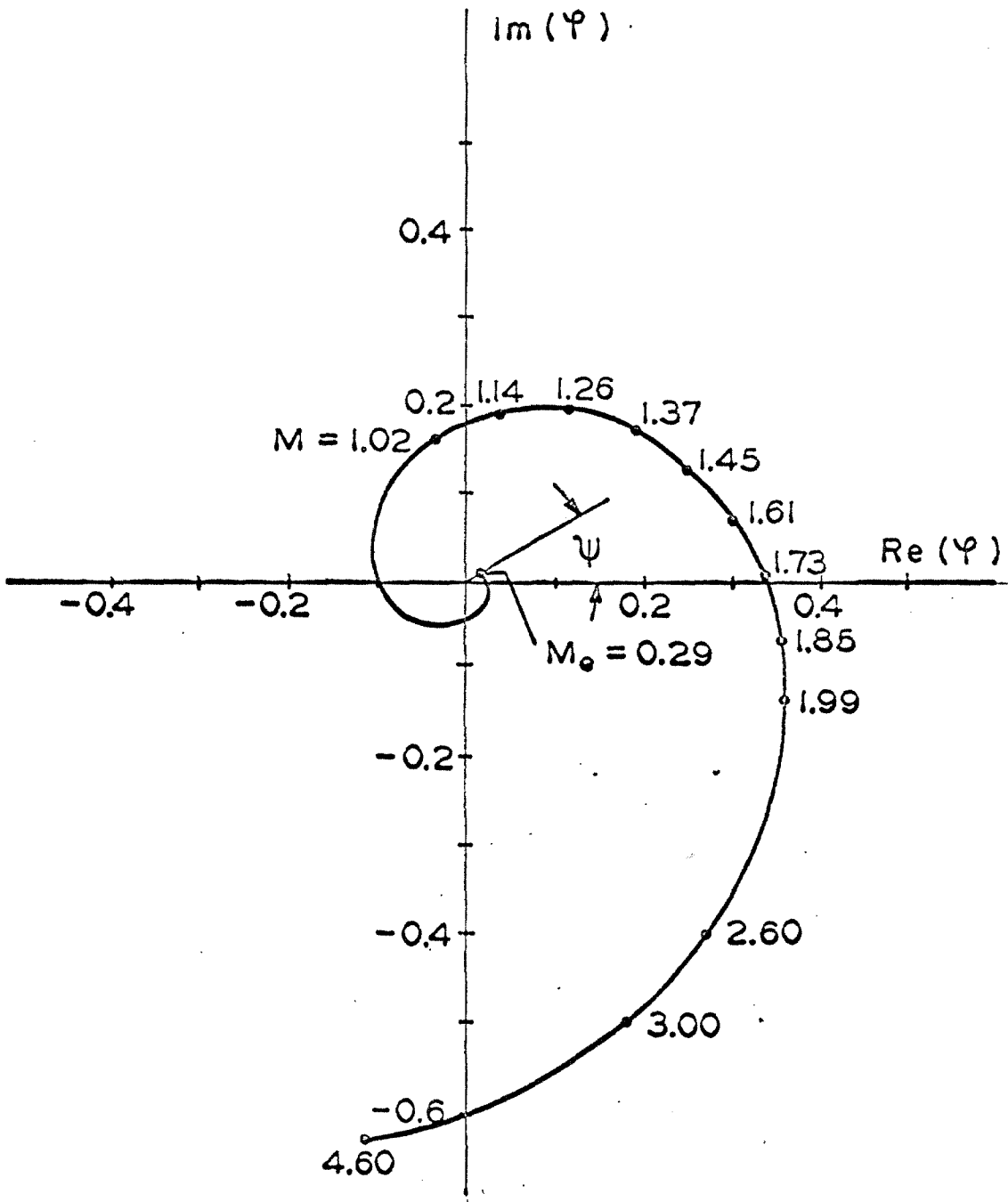
Fig. 2-9. Dimensionless pressure fluctuation φ for an entropy
fluctuation $\sigma_e = 1$, and no incident pressure wave
$\varphi_{ie} = 0$ at the nozzle entrance. Reduced frequency
$\beta = \omega x^* / a^* = 5.0$.

Fig. 2.10a. Ratio of the pressure fluctuation to the entrance entropy fluctuation $|\varphi/\alpha_e|$ when no incident pressure wave is present at the entrance $\varphi_{ie} = 0$. Exhaust Mach number $M = 1.02$.

Fig. 2.10b. Ratio of the pressure fluctuation to the entrance entropy fluctuation $|\mathcal{P}/\sigma_e|$ when no incident pressure wave is present at the entrance $\mathcal{P}_{ie} = 0$. Exhaust Mach number $M = 1.49$.
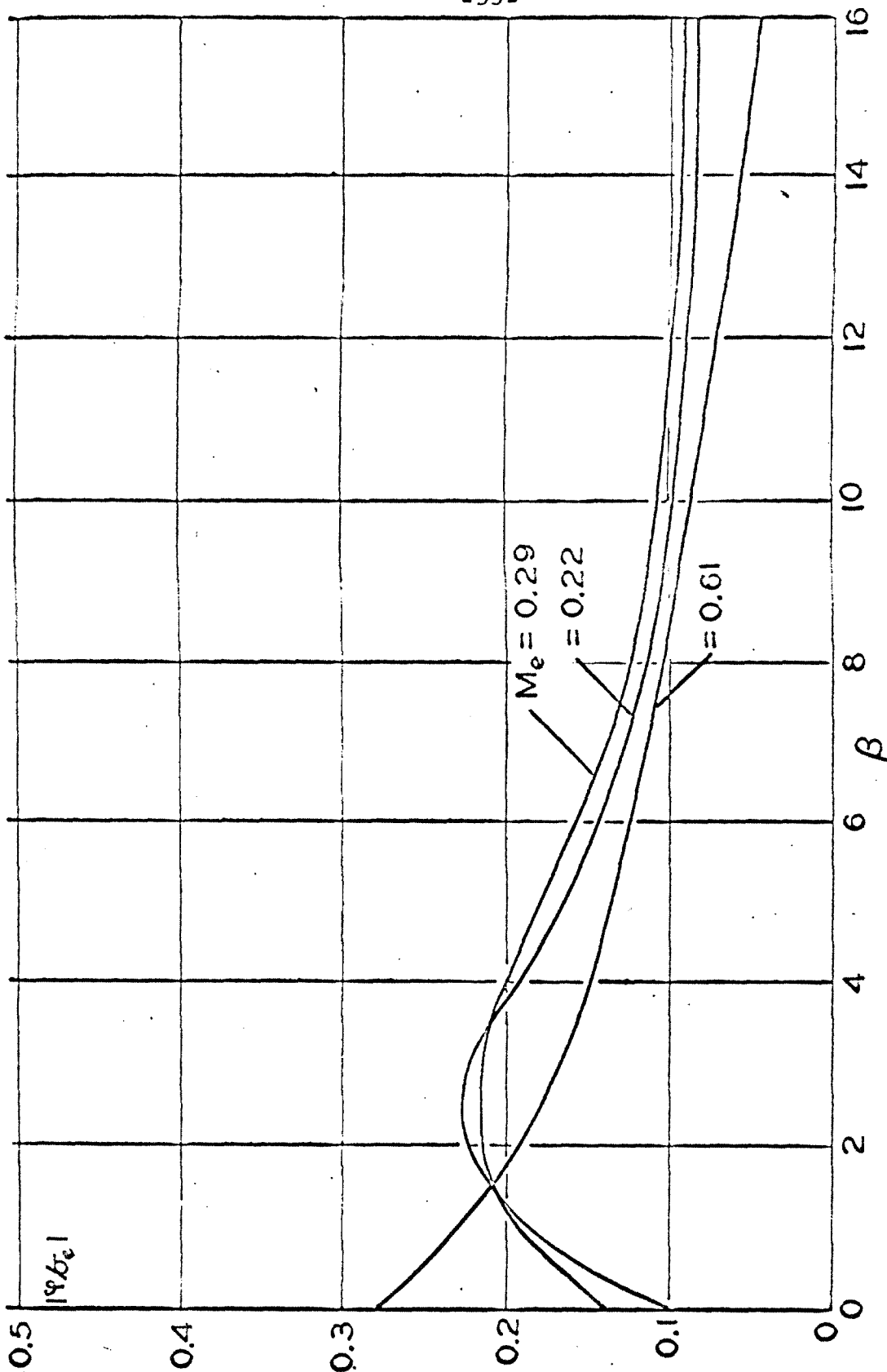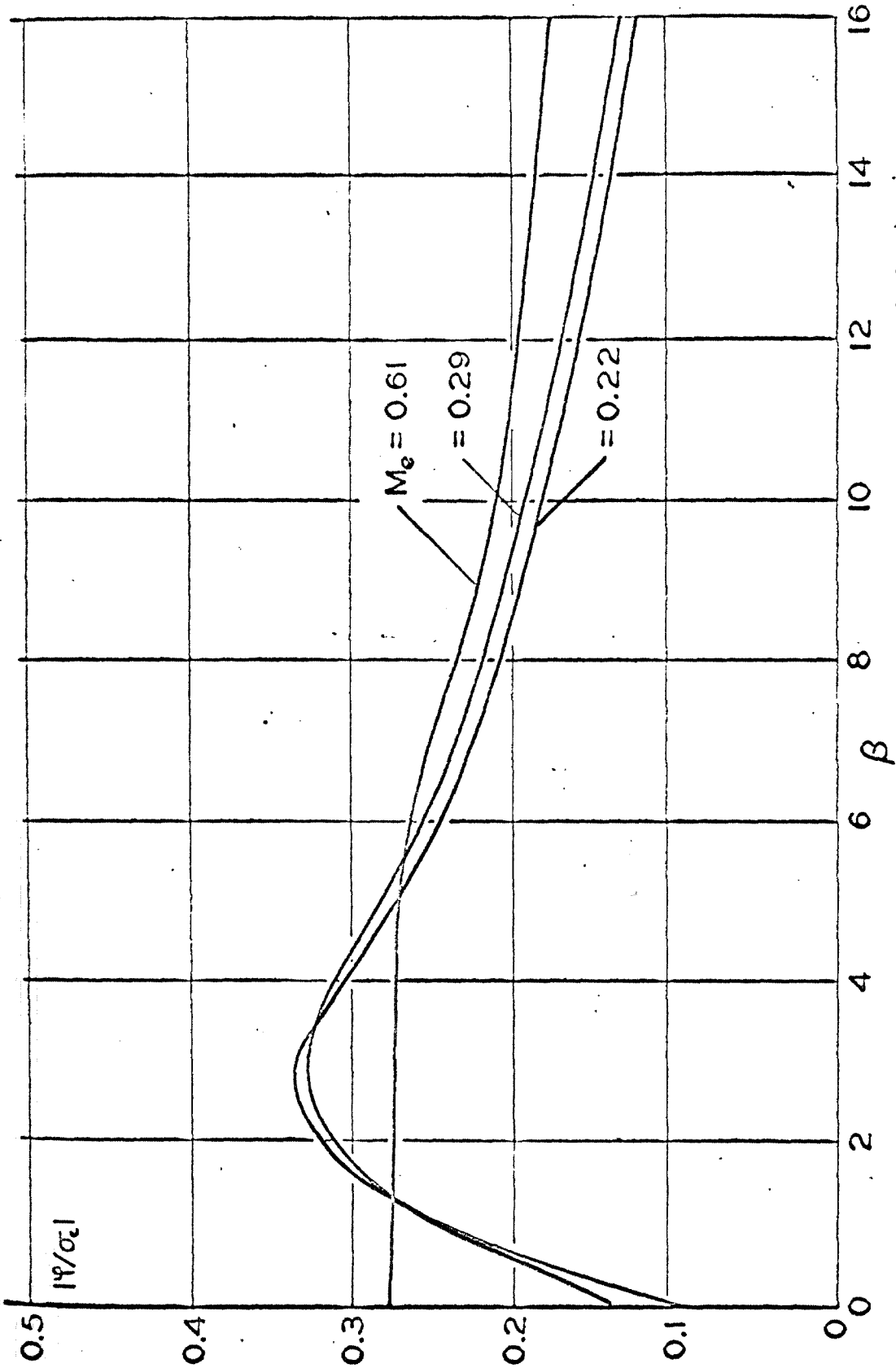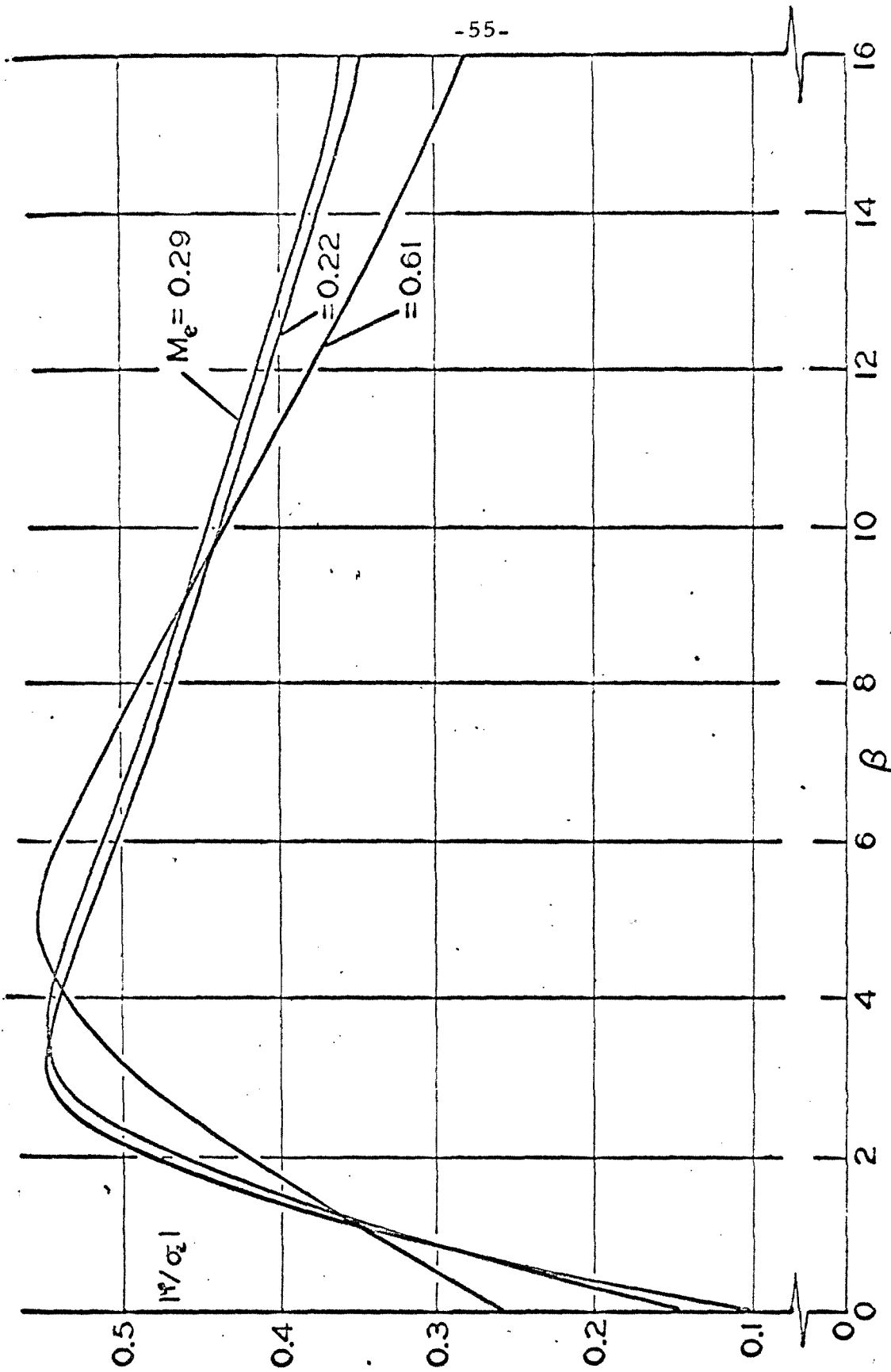
Fig. 2.10c. Ratio of the pressure fluctuation to the entrance entropy fluctuation $|\mathcal{P}/\sigma_{\ell}|$ when no incident pressure wave is present at the entrance $\mathcal{P}_{i\ell} = 0$. Exhaust Mach number $M = 2.00$.

CHAPTER III

A TECHNIQUE FOR TRANSFORMING CERTAIN ACOUSTICAL

BOUNDARY VALUE PROBLEMS IN A SUBSONIC MOVING MEDIUM

TO A PROBLEM INVOLVING A STATIONARY MEDIUM

3.1 INTRODUCTION

In numerous situations of current interest acoustical propagation occurs in a moving medium with fixed boundaries. Because this feature changes the acoustic problem in an essential manner, such problems have been discussed more extensively in non-steady aerodynamics than in acoustics.

The early work by Blokhintsev [3.1] which discusses acoustic fields in a moving inhomogeneous medium considers boundaries only in relation to sound excitation problems (vortex sound). In recent years interest in turbofan noise abatement has stimulated a number of studies of acoustic propagation in a moving fluid contained in an infinite cylindrical boundary.

Morfey [3.2, 3.3] discusses the change in cutoff frequency, the energy propagation and sound generation in an infinite duct containing a uniform flow.

The cutoff frequency of duct modes has been studied experimentally by Mason [3.4]. The change in the acoustical lining properties is examined by Rice [3.5], Eversman [3.6], Kurze and Allen [3.7]. Some refinements have been introduced by Pridmore-Brown [3.8], who considers a nonuniform mean flow and by Munger and Gladwell [3.9] and Munger and Plumblee [3.10] who in addition take the viscous effects into account.

References [3.2] to [3.10] all study problems involving a moving medium and an infinite boundary. Acoustical propagation in a moving medium in the presence of boundaries with end edges (finite and semi-infinite boundaries) are rarely discussed.

Carrier [3. 11] studies the reflection coefficient of a plane wave at the end of a duct immersed in a uniform flow. He shows that the reflection coefficient R when the medium flows uniformly may be obtained from the reflection coefficient R_0 corresponding to a stationary medium. Carrier does not evaluate the pressure radiated outside the duct and also limits his discussion to plane wave propagation.

Kaji and Okazaki [3. 12, 3. 13], Mani and Horvay [3. 14], Amiet [3. 15] study the reflection and transmission coefficients of a plane wave incident on a blade row set in a uniform flow. References [3. 12, 3. 13, 3. 14] use specialized methods and fail to single out the effect of the uniform flow from the basic transmission and reflection characteristics of the blade row in a stationary medium. The method of matched asymptotic expansions used in [3. 15] seems to provide only the flow induced acoustical field.

The present work is concerned with a class of acoustical problems involving finite or semi-infinite boundaries and a moving medium. When the flow is subsonic we show that such problems may be treated by simply transforming the known solution of an associated problem in a stationary medium. The simplicity of the results obtained by Carrier [3. 11] suggested the present method.

The ideas leading to this transformation are most easily introduced by considering a specific problem. It is convenient to start with the Sommerfeld problem of diffraction of a plane wave by a semi-infinite hard plane. This problem in a stationary medium is formulated by Section 3. 2. The solution ϕ^0 representing the pressure or

the velocity potential is given in several forms. The problem for the half plane immersed in a uniform flow is then described. There is an essential difference between positive and negative directions of flow. In the positive direction ($M > 0$) the plane has a trailing edge, the velocity potential is discontinuous, but the pressure p is continuous and is used to describe this case.

When the flow occurs in the negative x direction ($M < 0$), the plane has a leading edge, the velocity potential φ is continuous and is best suited to describe this case.

In Section 3.3 these two problems are then expressed as a unique boundary value problem for a function ϕ replacing the pressure (when $M > 0$) or the velocity potential (when $M < 0$). A solution is then obtained by transforming the solution ϕ^0 of the diffraction problem in a stationary medium.

The results are discussed in Section 3.4.

3.2 ANALYSIS OF THE PROBLEM

Stationary Medium

The problem of diffraction of a plane wave by a hard plane originally solved by Sommerfeld [3.16] has been treated by numerous techniques; a particularly relevant presentation utilizing the Wiener Hopt technique is given by Noble in [3.17]. We shall use this text as a constant reference and we adopt most of its notations.

A plane wave propagating in the direction $\odot$ is incident on a half plane $-\infty < x \leq 0, y = 0$. The incident wave has a potential of the form

$$\phi_i^o = \exp(-ikx\cos\odot - iky\sin\odot) \qquad (3.1)$$

where

$$0 < \odot < \pi$$
$$k = \omega/c \qquad (3.2)$$

The complete potential may be written as the sum of the incident wave potential and an induced potential

$$\phi_t^o = \phi_i^o + \phi^o \qquad (3.3)$$

where ϕ^o is a solution of the Helmholtz equation

$$\phi_{xx}^o + \phi_{yy}^o + k^2\phi^o = 0 \qquad (3.4)$$

Equation (3.3) must satisfy the following conditions.

On the rigid wall there is no displacement:

$$\frac{\partial \phi_t^o}{\partial y} = 0$$

or

$$\frac{\partial \phi^0}{\partial y} = ik \sin \Theta \, \exp(-ikx \cos \Theta) \tag{3.5}$$

$\partial \phi_t^0 / \partial y$ and hence $\partial \phi^0 / \partial y$ are continuous on

$$-\infty < x < +\infty \quad , \quad y = 0 \tag{3.6}$$

ϕ_t^0, ϕ^0 are continuous on

$$0 \leqslant x < +\infty \quad , \quad y = 0 \tag{3.7}$$

ϕ^0 satisfies one of the following edge conditions:

$$\text{(a)} \quad \phi^0(x, 0_+) - \phi^0(x, 0_-) \sim x^{1/2} \tag{3.8}$$

when $x \longrightarrow 0_-$ on $y = 0$

$$\text{(b)} \quad \partial \phi^0 / \partial y \sim x^{-1/2} \tag{3.9}$$

when $x \longrightarrow 0_+$ on $y = 0$.

We shall discuss the physical meaning of these edge conditions when we state the moving medium problems. It can be shown that the solution of the boundary value problems (3.4 - 3.7) with either (3.8) or (3.9) is unique. For this, consider equation (2.29) of reference [3.17] and use (3.8) and then (3.9) to find that they lead to the same conclusion concerning the behavior of $J(\alpha)$ at infinity, namely that $J(\alpha) \sim \alpha^{-1}$ when $|\alpha| \longrightarrow \infty$. As $J(\alpha)$ is analytic in the whole plane, by Liouville theorem we have $J(\alpha) \equiv 0$, and thus the solution of (2.29) is unique.

This unique solution $\phi_t^0(x, y; k, \Theta)$ can be expressed as

$$\varphi_t^o(r, \theta; k, \odot) = \pi^{-1/2} e^{-i\pi/4} \Big\{$$

$$e^{-ikr\cos(\theta - \odot)} F\left[-(2kr)^{1/2}\cos\frac{1}{2}(\theta - \odot)\right]$$

$$+ e^{-ikr\cos(\theta + \odot)} F\left[(2kr)^{1/2}\cos\frac{1}{2}(\theta + \odot)\right]\Big\} \qquad (3.10)$$

for
$$-\pi \leqslant \theta \leqslant \pi$$
$$0 < \odot < \pi$$

where $F(v)$ is the complex Fresnel integral defined by

$$\bar{F}(v) = \int_v^{+\infty} e^{iu^2} du \qquad (3.11)$$

Expression (3.10) is very well suited for numerical computation but does not allow an easy physical interpretation. To facilitate the discussion of our results we give below the very useful description of φ_t^o as a sum of a geometrical optics field and a diffracted wave. Other expressions and details may be found in Morse and Inyard [3.18], Bowman and Senior [3.19], Noble [3.17].

The complete field may be decomposed as follows:

$$\varphi_t^o = \phi_i^o + \phi_r^o + \phi_d^o \qquad \pi - \odot < \theta < \pi \qquad (3.12)$$

$$\varphi_t^o = \phi_i^o \qquad\qquad + \phi_d^o \qquad \odot - \pi < \theta < \pi - \odot \qquad (3.13)$$

$$\phi_t^o = \qquad\qquad\qquad \phi_d^o \qquad -\pi < \theta < \odot - \pi \qquad (3.14)$$

where Φ_i^o is the incident wave

$$\Phi_i^o = \exp\left(-ikr\cos(\theta - \Theta)\right) \tag{3.15}$$

Φ_r^o is the reflected wave

$$\Phi_r^o = \exp\left(-ikr\cos(\theta + \Theta)\right) \tag{3.16}$$

Φ_d^o is the diffracted field which may be expressed, for instance, as

$$\Phi_d^o = \frac{1}{\pi} \sin\frac{\Theta}{2} \int_{-\infty}^{+\infty} \frac{\sin\frac{1}{2}(\theta + it)\, e^{ikr\cosh t}}{\cos(\theta + it) + \cos\Theta}\, dt \tag{3.17}$$

When θ is sufficiently far from $\Theta - \pi$ and $\pi - \Theta$ the integral (3.17) may be expanded asymptotically for $kr \gg 1$, to give

$$\Phi_d^o \sim (2\pi kr)^{-1/2} \frac{2\sin\frac{1}{2}\theta \sin\frac{1}{2}\Theta}{\cos\theta + \cos\Theta} e^{ikr + i\pi/4} \tag{3.18}$$

The complete field can be recast as a sum of a "geometrical optics" $\Phi_{g.o.}^o$ field and the diffracted field Φ_d^o :

$$\Phi_t^o = \Phi_{g.o.}^o + \Phi_d^o \tag{3.19}$$

where

$$\Phi_{g.o.}^o = \Phi_i^o\, h(\theta - \Theta + \pi) + \Phi_r^o\, h(\theta - \pi + \Theta) \tag{3.20}$$

$h(x)$ is the Heaviside step function

$$
\begin{aligned}
h(x) &= 1 \qquad \text{when} \qquad x > 0 \\
h(x) &= 0 \qquad \text{when} \qquad x < 0
\end{aligned}
\tag{3.21}
$$

The diffracted field ϕ_d^o is given by (3.17) or by the asymptotic expression (3.18) and compensates for the discontinuities of the "geometrical optics" field at $\theta = \Theta - \pi$ and $\pi - \Theta$.

After this brief exposition of the classical Sommerfeld diffraction problem we may start to examine the diffraction problem in the presence of flow.

Moving Medium $1 > M \geqslant 0$

Consider the similar problem, but where the medium flows in the positive x direction with subsonic velocity. The half plane then has a trailing edge. The problem is most conveniently expressed in terms of the perturbation pressure p in order to avoid treating in detail the vortex sheet which extends over $0 \leqslant x < +\infty, y = 0$

The conditions to be satisfied by p are:

no displacement at the rigid wall

$$\frac{\partial p}{\partial y}(x, 0) = 0 \qquad \text{for} \quad -\infty < x \leqslant 0 \qquad (3.22)$$

Across the vortex sheet $0 \leqslant x < +\infty, y = 0$ the pressure and displacement are continuous

$$p(x, 0_+) = p(x, 0_-) \qquad (3.23)$$

$$\frac{\partial p}{\partial y}(x, 0_+) = \frac{\partial p}{\partial y}(x, 0_-) \qquad (3.24)$$

Near the edge, at a distance much smaller than a wavelength, the flow is similar to the potential flow of an incompressible flow past a trailing edge. The Kutta-Joukowski condition applies, the potential func-

tion may be found easily [3.20], and the associated pressure jump

across the wall behaves like:

$$p(x, 0_+) \; - \; p(x, 0_-) \; \sim \; x^{1/2} \tag{3.25}$$

as $\quad x \longrightarrow 0_-$ on $\quad y = 0$.

Moving Medium, $\quad -1 < M \leqslant 0$

Similarly, the problem may be formulated for the case where

the medium flows in the negative $\quad x \quad$ direction with subsonic veloci-

ty. Now the half plane has a leading edge and the problem may be

written in terms of the velocity potential. The conditions to be satis-

fied by the velocity potential are:

at the rigid wall there is no displacement

$$\frac{\partial \varphi}{\partial y}(x, 0) = 0 \qquad\qquad \text{for} \quad -\infty < x \leqslant 0 \, , \; y = 0 \tag{3.26}$$

on the wall continuation the velocity potential and the velocity

are continuous across the $\quad x - \quad$ axis.

$$\varphi(x, 0_+) \; = \; \varphi(x, 0_-) \tag{3.27}$$

$$\frac{\partial \varphi}{\partial y}(x, 0_+) \; = \; \frac{\partial \varphi}{\partial y}(x, 0_-) \tag{3.28}$$

The edge condition is obtained now by considering the potential

flow of an incompressible fluid near a leading edge, with a stagnation

point

$$\frac{\partial \varphi}{\partial y}(x, 0) \; \sim \; x^{1/2} \tag{3.29}$$

as $\quad x \longrightarrow 0_+ \quad$ on $\quad y = 0$.

The similarity of conditions (3.22 - 3.24) and (3.26 - 3.28) is evident. The two edge conditions (3.25) and (3.28) differ, but as was remarked above, they yield a unique solution.

We can therefore write a unique boundary value problem for a function ϕ representing the pressure perturbation P (when $M > O$) or the perturbation velocity potential φ (when $M < O$).

3.3 SOLUTION OF THE GENERAL HALF PLANE PROBLEM
IN A MOVING MEDIUM

A plane wave with a normal direction $\odot$ is incident on the half plane. The incident wave has the potential

$$\Phi_i = \exp\left(-\frac{ikx\cos\odot}{1-M\cos\odot} - \frac{iky\sin\odot}{1-M\cos\odot}\right) \qquad (3.30)$$

$$0 < \odot < \pi$$

$$k = \omega/c$$

The total potential is $\Phi_t = \Phi_i + \Phi$ where Φ is solution of the convective wave equation

$$\Phi_{xx}(1-M^2) + \Phi_{yy} + 2Mik\,\Phi_x + k^2\Phi = 0 \qquad (3.31)$$

On the rigid wall, $-\infty < x \leq 0, y = 0$

$$\frac{\partial \Phi_t}{\partial y} = 0$$

or

$$\frac{\partial \Phi}{\partial y} = \frac{ik\sin\odot}{1-M\cos\odot} \exp\left(-\frac{ikx\cos\odot}{1-M\cos\odot}\right) \qquad (3.32)$$

Conditions (3.6), (3.7), and either (3.8) or (3.9) given for Φ^0 also apply to the present general potential Φ.

If an attempt is made to solve the above problem by a transform method similar to the one used by Noble [3.17, pp. 49-57], it is found that much work can be spared by introducing the following transformed quantities:

$$x_1 = x / (1 - M^2)^{1/2} \tag{3.33}$$

$$k_1 = k / (1 - M^2)^{1/2} \tag{3.34}$$

$$\cos \Theta_1 = (\cos \Theta - M)/(1 - M \cos \Theta) \tag{3.35}$$

$$\phi = e^{-ik_1 M x_1} \Psi(x_1, y; k_1, \Theta_1) \tag{3.36}$$

The function Ψ is then the solution of the following boundary value problem:

$$\Psi_{x_1 x_1} + \Psi_{yy} + k_1^2 \Psi = 0 \tag{3.37}$$

$$\frac{\partial \Psi}{\partial y} = ik_1 \sin \Theta_1 \exp(-ik_1 x_1 \cos \Theta_1) \tag{3.38}$$

on $\quad -\infty < x \leqslant 0, \quad y = 0$

The four other conditions (3.6), (3.7), (3.8), or (3.9) remain unchanged. The boundary value problem for Ψ is identical to the problem for Φ^o. Thus,

$$\Psi \equiv \Phi^o(x_1, y; k_1, \Theta_1) \tag{3.39}$$

and then from (3.36)

$$\Phi_t(x, y; k, \Theta, M) = e^{-ik_1 M x_1} \Phi_t^o(x_1, y; k_1, \Theta_1) \tag{3.40}$$

Thus, to solve the diffraction problem in a subsonically moving medium for a plane wave (k, Θ) one associates the solution for the

diffraction problem for a plane wave (k_1, Θ_1) in a stationary medium. The solutions of these two problems are related by (3.40).

3.4 RESULTS

By using the transformation procedure described above, the pressure field and diffraction patterns may be obtained for the moving medium quite easily.

When $1 > M \geqslant 0$ the function ϕ represents the pressure p and therefore:

$$p_t(x, y; k, \Theta, M) = e^{-ik_1 M x_1} \phi_t^o(x_1, y; k_1, \Theta_1) \quad (3.41)$$

where ϕ^o represents the corresponding solution for a stationary medium.

When $0 \geqslant M > -1$ the function ϕ represents the velocity potential φ. The pressure may be deduced from φ as

$$p_t = -\bar{\rho}\left(-i\omega \varphi_t + u \frac{\partial \varphi}{\partial x} t\right) \quad (3.42)$$

which becomes, by introducing (3.36),

$$p_t = \frac{\bar{\rho} c i k_1}{(1-M^2)^{1/2}}\left(\phi_t^o + \frac{iM}{k_1}\frac{\partial \phi_t^o}{\partial x_1}\right) e^{-ik_1 M x_1} \quad (3.43)$$

This is the complete pressure field for an incident velocity potential wave of amplitude unity

$$\varphi_i = e^{-ik_1 M x_1} \exp\left(-ik_1 x_1 \cos\Theta_1 - ik_1 y \sin\Theta_1\right) \quad (3.44)$$

The corresponding incident pressure wave is

$$p_i = \frac{\bar{\rho} c i k_1}{(1-M^2)^{1/2}}(1 + M\cos\Theta_1)\varphi_i \quad (3.45)$$

To obtain the complete pressure field for a unit pressure
wave we divide (3.43) by the amplitude of p_i in (3.45):

$$p_t = \frac{1}{1 + M\cos\Theta_1}\left(\phi_t^0 + \frac{iM}{k_1}\frac{\partial\phi_t^0}{\partial x_1}\right)e^{-ik_1 M x_1} \tag{3.46}$$

Using expression (3.10) for ϕ_t^0 and (3.46) we get

$$p_t = e^{-ik_1 M x_1}\phi_t^0(r_1, \Theta_1; k_1, \Theta_1)$$
$$+ e^{-ik_1 M x_1}e^{ik_1 r_1 + i\pi/4}(2\pi k_1 r_1)^{-1/2}\frac{2M\sin\frac{1}{2}\Theta_1\sin\frac{1}{2}\Theta_1}{1 + M\cos\Theta_1} \tag{3.47}$$

Comparing expressions (3.41) and (3.47) we observe that an
additional diffracted wave appears when the medium flows in the
negative X direction.

$$p_{d.a.} = e^{-ik_1 M x_1}e^{ik_1 r_1 + i\pi/4}$$
$$(2\pi k_1 r_1)^{-1/2}\frac{2M\sin\frac{1}{2}\Theta_1\sin\frac{1}{2}\Theta_1}{1 + M\cos\Theta_1} \tag{3.48}$$

This expression is valid for the whole space. (Actually, $p_{d.a.}$ is
proportional to a well-known solution of the Helmholtz equation

$$e^{ikr}(kr)^{-1/2}\sin\frac{1}{2}\theta \tag{3.49}$$

which has a jump discontinuity across the wall, $\theta = \pm\pi$). The
source strength of the additional diffracted wave is

$$\frac{M\sin\frac{1}{2}\Theta_1\sin\frac{1}{2}\Theta_1}{1 + M\cos\Theta_1} \tag{3.50}$$

and vanishes for $M = 0$.

The usual diffracted wave appears for both flow directions; its asymptotic expansion for $k_1 r_1 \gg 1$ and Θ_1 far from $\pi - \Theta_1$ and $\Theta_1 - \pi$ may be obtained by transforming (3.18):

$$p_d \sim e^{-ik_1 M x_1} e^{ik_1 r_1 + i\pi/4}$$

$$(2\pi k_1 r_1)^{-1/2} \frac{2\sin\frac{1}{2}\Theta_1 \sin\frac{1}{2}\Theta_1}{\cos\Theta_1 + \cos\Theta_1} \tag{3.51}$$

Its source strength is

$$\frac{\sin\frac{1}{2}\Theta_1 \sin\frac{1}{2}\Theta_1}{\cos\Theta_1 + \cos\Theta_1} \tag{3.52}$$

A trailing edge and an edge in a stationary medium behave in essentially the same way when impinged by a plane wave, while at the leading edge the flow induces additional sources. A typical diffraction diagram is shown on fig. 3-1. The amplitude (in decibels) of the pressure field is represented for a constant value of kr . The incidence angle Θ and the apparent incidence angle Θ_1 are shown. The diagram may be decomposed in three angular regions corresponding to the decomposition of the complete field given by (3.12), (3.13), (3.14).

Region 1, $\pi - \Theta_1 < \Theta_1 < \pi$, is a reflection region where incident, reflected, and diffracted waves coexist. In Region 2, $\Theta_1 - \pi < \Theta_1 < \pi - \Theta_1$, the incident wave and the diffracted field are present. Region 3 is in the shadow with only the diffracted wave propagating.

The boundaries between the three regions correspond to polar angles $\delta_{1+} = \pi - \Theta_1$ and $\delta_{1-} = \Theta_1 - \pi$. The angles δ_1 and δ are related by

$$\tan \delta = \frac{\tan \delta_1}{(1 - M^2)^{1/2}} \tag{3.53}$$

From (3.35) and (3.53) it is easy to obtain

$$\tan \delta_{\pm} = \pm \frac{\sin \Theta}{M - \cos \Theta} \tag{3.54}$$

This relation gives the actual polar angles for the boundary Δ_+ between the direct propagation and reflection zones, and Δ_- between direct propagation and shadow zones. Figure 3-2 is a graphical representation of (3.54) for several values of the Mach number.

It is possible to justify (3.54) by a simple geometrical argument. Figure 3-3a shows a plane wave propagating in the Θ direction in a stationary medium. The wavefront IJ travels with speed c to $I'J'$ and the information from Q is carried to R in the same Θ direction.

The information received by the half plane edge is transmitted in a direction parallel to QR. A shadow region therefore appears for angles beyond $\delta_- = \Theta - \pi$. Consider now fig. 3-3b which shows the same plane wave propagating now in a medium moving in the x direction with velocity $u = cM$. The motion brings the wave front IJ to $I''J''$, while the information from Q is carried to S. The angle of QS with the x direction is Θ', given by

$$\tan \Theta' = c \sin \Theta / (c \cos \Theta - cM) \tag{3.55}$$

The information arriving at the edge will propagate parallel to QS thus defining the new polar angle δ_- for the shadow boundary:

$$\tan \delta_- = \tan(\Theta' - \pi) = -\frac{\sin \Theta}{M - \cos \Theta}$$

A similar argument may be given to obtain the value of δ_+. The propagation features of the "geometrical optics" field are thus simply explained.

To be complete, we have shown graphically on fig. 3-4 the relation (3.35) between Θ_1 and Θ. When M is positive, the angle Θ_1 is superior to Θ, while the opposite is true when M is negative.

Additional diffraction patterns are shown on figs. 3-5a, b, c, d for several constant values of kr and three values of the free stream Mach number. It can be seen that the flow acts on the acoustical field roughly like an increase in frequency and a change in the wave impingement angle Θ. When M is positive, the shadow 3 broadens, while the opposite occurs when M is negative.

3.5 CONCLUSION

The half plane diffraction problem was solved when the plane is immersed in a uniform subsonic flow $|M| < 1$. The solution was obtained without effort from the well known solution of the $M = 0$ diffraction problem, by a simple transformation. The framework of acoustical theory was used (inviscid non-conducting flow, small perturbations). The boundary layer effect on the edge condition was thus not considered. This might be justified when the wavelength is sufficiently large compared to the boundary layer thickness. The convected wave equation was also used, and this implies that the term $(1 - M^2) \, \phi_{xx}$ is not of second order.

REFERENCES

3.1   Blokhintsev, D. I., "Acoustics of a Nonhomogeneous Moving Medium," NACA TM 1399 (February 1956).

3.2   Morfey, C. L., "Sound Transmission and Generation in Ducts with Flow," J. Sound Vib., 14 (1971), pp. 37-55.

3.3   Morfey, C. L., "A Review of the Sound Generating Mechanisms in Aircraft Engine Fans and Compressors," AFOSR-UTIAS Symposium on Aerodynamic Noise, Toronto (May 1968).

3.4   Mason, V., "Some Experiments on the Propagation of Sound Along a Cylindrical Duct Containing Flowing Air," J. Sound Vib., 10 (1969), pp. 208-226.

3.5   Rice, E. J., "Propagation of Waves in an Acoustical Lined Duct with a Mean Flow," NASA SP-207, Basic Aerodynamic Noise Research (July 1969).

3.6   Eversman, W., "The Effect of Mach Number of an Acoustic Lining in a Flow," J. Acoust. Soc. Am., 48 (1970), pp. 425-428.

3.7   Kurze, U. J., and Allen, C. H., "Influence of Flow and High Sound Level on the Attenuation in a Lined Duct," J. Acoust. Soc. Am., 49 (1971), pp. 1643-1654.

3.8   Pridmore-Brown, D. C., "Sound Propagation in a Fluid Flowing through an Attenuating Duct," J. Fluid Mech., 4 (1958), p. 393.

3.9   Munger, P., and Gladwell, C. M. L., "Acoustic Wave Propagation in a Sheared Fluid Contained in a Duct," J. Sound Vib., 9 (1969), pp. 28-48.

3.10   Munger, P., and Plumblee, H. E., "Propagation and Attenuation of Sound in a Soft Walled Annular Duct Containing a Sheared Flow," NASA SP-207, Basic Aerodynamic Noise Research (July 1969).

3.11   Carrier, G. F., "Sound Transmission from a Tube with Flow," Quart. Appl. Math., 13 (1956), pp. 457-461.

3.12   Kaji, S., and Okazaki, T., "Propagation of Sound Waves through a Blade Row, I. Analysis Based on the Semi-Actuator Disk Theory," J. Sound Vib., 11 (1970), pp. 339-353.

3.13   Kaji, S., and Okazaki, T., "Propagation of Sound Waves through a Blade Row, II. Analysis Based on the Accleration Potential Method," J. Sound Vib., 11 (1970), pp. 355-375.

3.14   Mani, R., and Horvay, G., "Sound Transmission through Blade Rows," J. Sound Vib., 12 (1970), pp. 83-107.

3.15   Amiet, R.K., "Aerodynamic Sound Production and the Method of Matched Asymptotic Expansions," Ph. D. Thesis (June 1969), Cornell University.

3.16   Sommerfeld, A., Optics, Lectures on Theoretical Physics, Vol. IV, Academic Press, New York (1964).

3.17   Noble, B., Methods Based on the Wiener Hopf Technique, Pergamon Press, New York (1958).

3.18   Morse, P.M., and Ingard, K.U., Theoretical Acoustics, McGraw-Hill, New York (1968), pp. 450-453.

3.19   Bowman, J. J., and Senior, T.B.A., "The Half Plane," Electromagnetic and Acoustic Scattering by Simple Shapes, J. J. Bowman, T.B.A. Senior, and P.L.E. Uslignhi, Eds. North Holland Publishing Co., Wiley Interscience Division, Amsterdam and New York (1969), pp. 308, 345.

3.20   Jones, R.T., and Cohen, D., "Aerodynamics of Wings at High Speeds," Aerodynamic Components of Aircraft at High Speeds, A. F. Donovan and H. R. Lawrence, Eds., Princeton University Press, Princeton (1957).
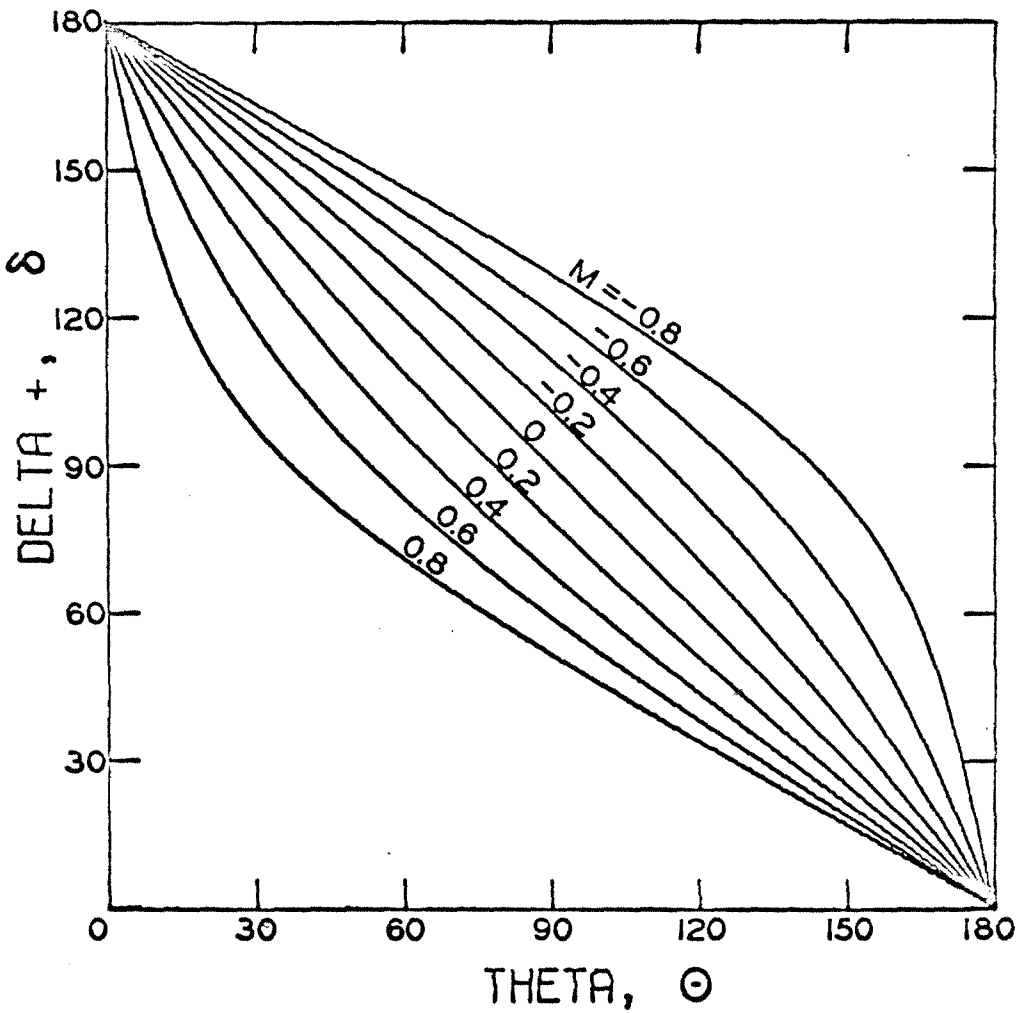
Fig. 3-1. Diffraction of a plane wave by a semi-infinite hard plane.
Incident, reflected, and diffracted waves in region 1. In-
cident and diffracted waves in region 2. Diffracted wave
only in region 3. kr = 20., Θ = 90°, M = 0.8.

Fig. 3-2. Polar angle δ+ defining the boundary of the reflection region. The boundary of the shadow region is at δ- = - δ+.
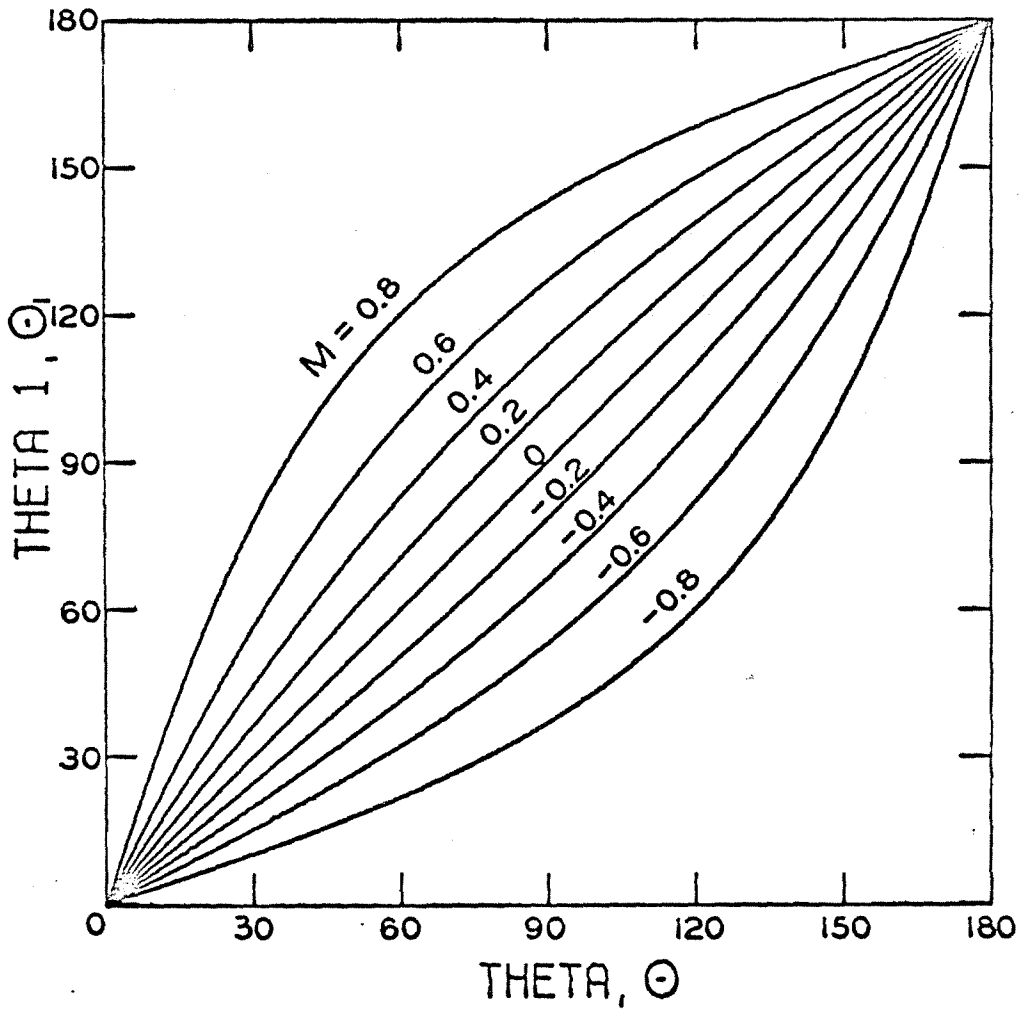
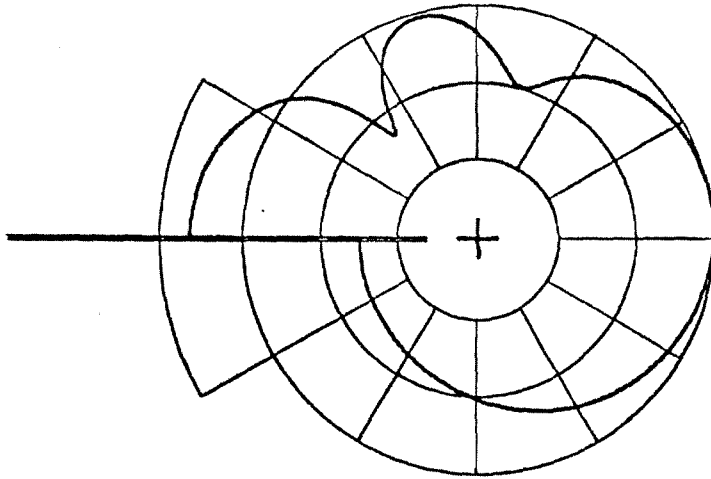Fig. 3-3a. Plane wave impinging on a half plane in a stationary medium.

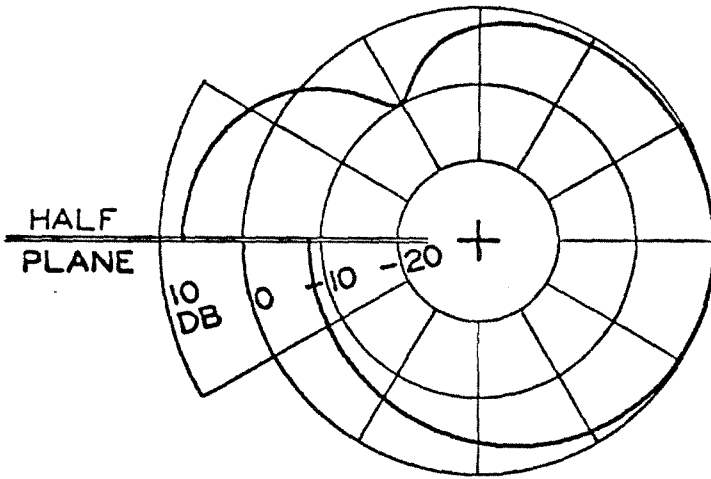Fig. 3-3b. Plane wave impinging on a half plane in a medium moving in the x-direction with velocity u = cM.
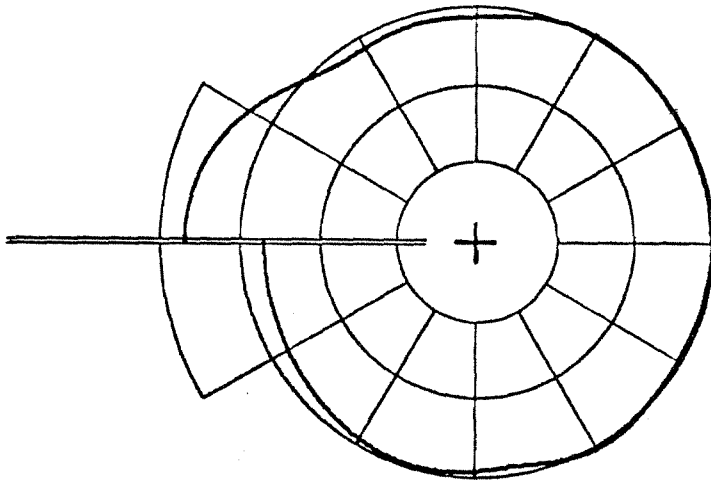
Fig. 3-4. Relation between the actual ($M \neq 0$) incidence angle Θ and the transformed angle Θ_1 of the associated $M = 0$ problem. $\cos \Theta_1 = (\cos \Theta - M)/(1 - M \cos \Theta)$.

Fig. 3 5a. Diffraction patterns of a plane wave by a semi-infinite hard plane. The plane wave incidence angle is $\Theta = 90°$; $kr = 2$.
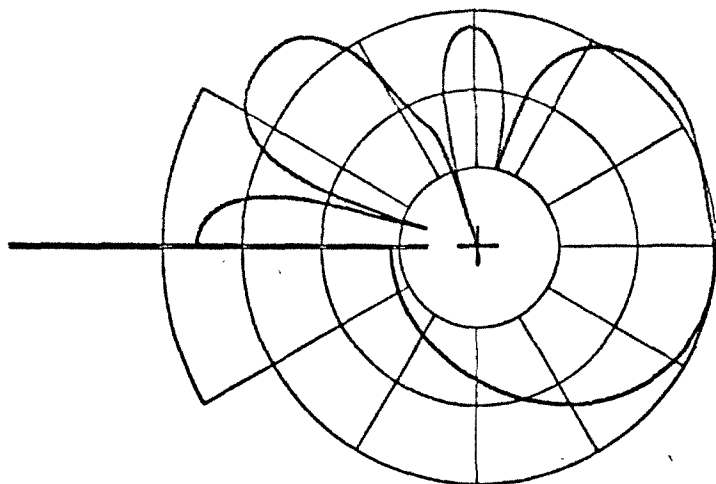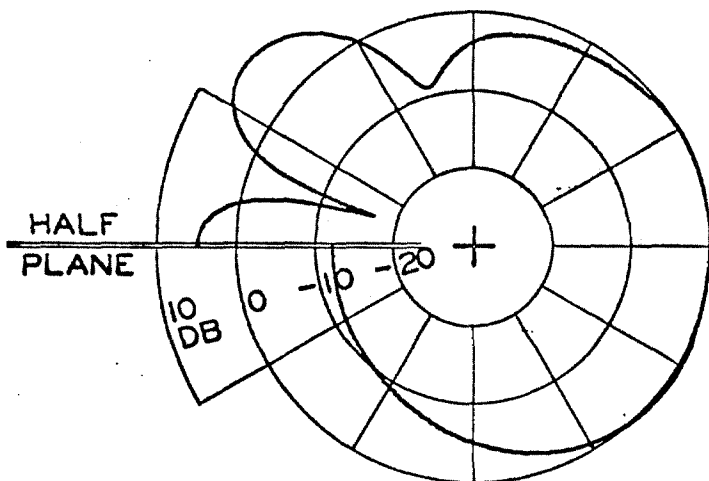
M = 0.8

HALF
PLANE

10
DB   0 -10 -20

M = 0

M = -0.8

Fig. 3-5b. Diffraction patterns of a plane wave by a semi-infinite
hard plane.   The plane wave incidence angle is $\Theta = 90^{\circ}$;
kr = 5.

M = 0.8

HALF
PLANE

10
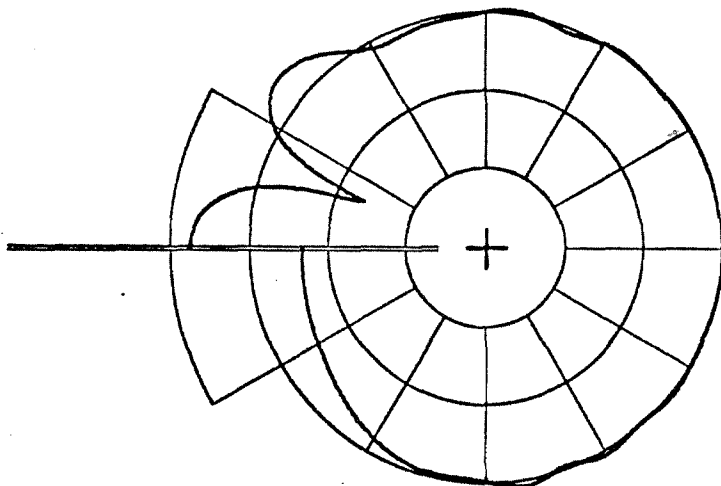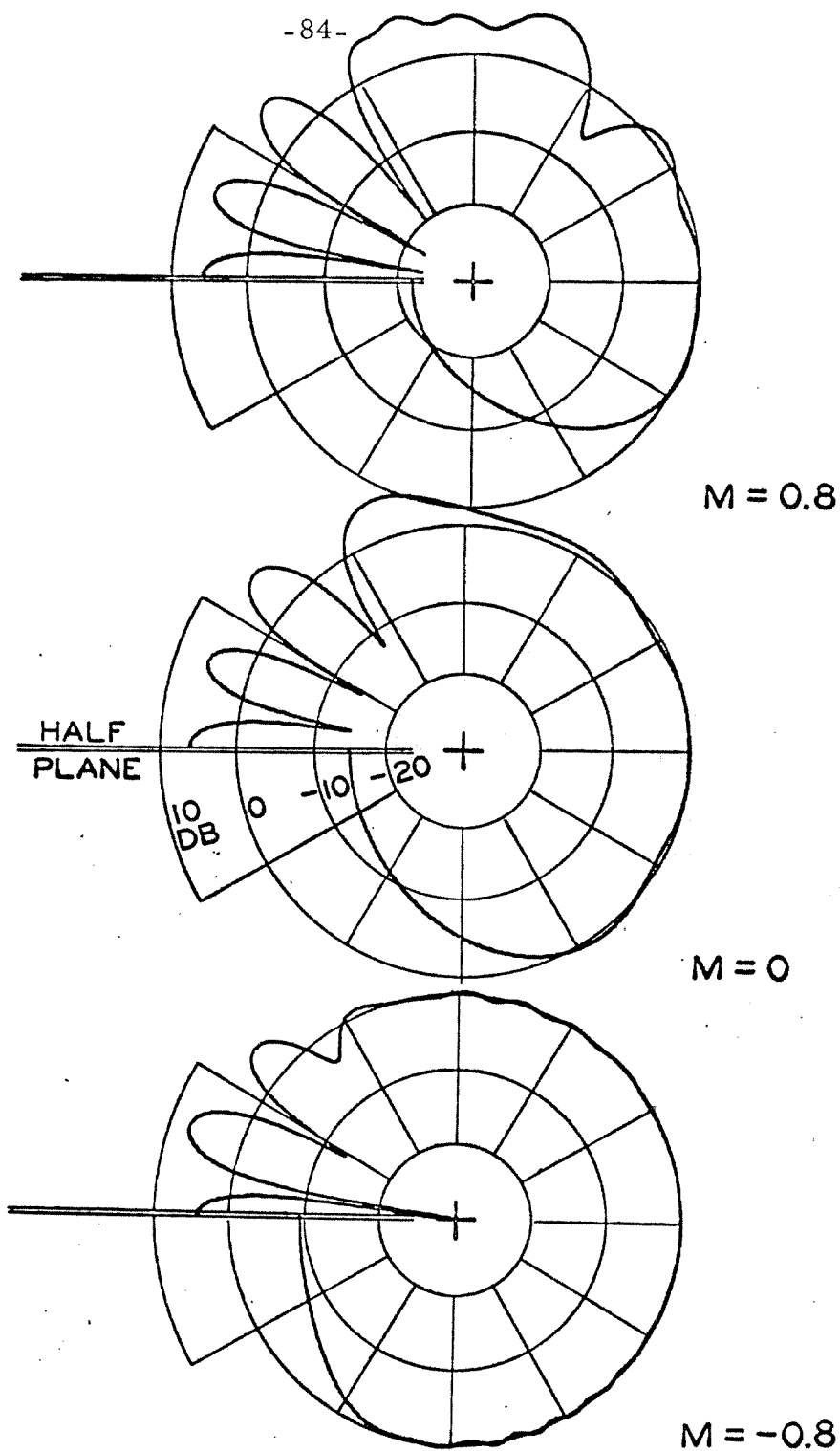DB

0 -10 -20

M = 0

M = -0.8

Fig. 3-5c. Diffraction patterns of a plane wave by a semi-infinite
hard plane. The plane wave incidence angle is $\Theta = 90^{\circ}$;
$kr = 10$.
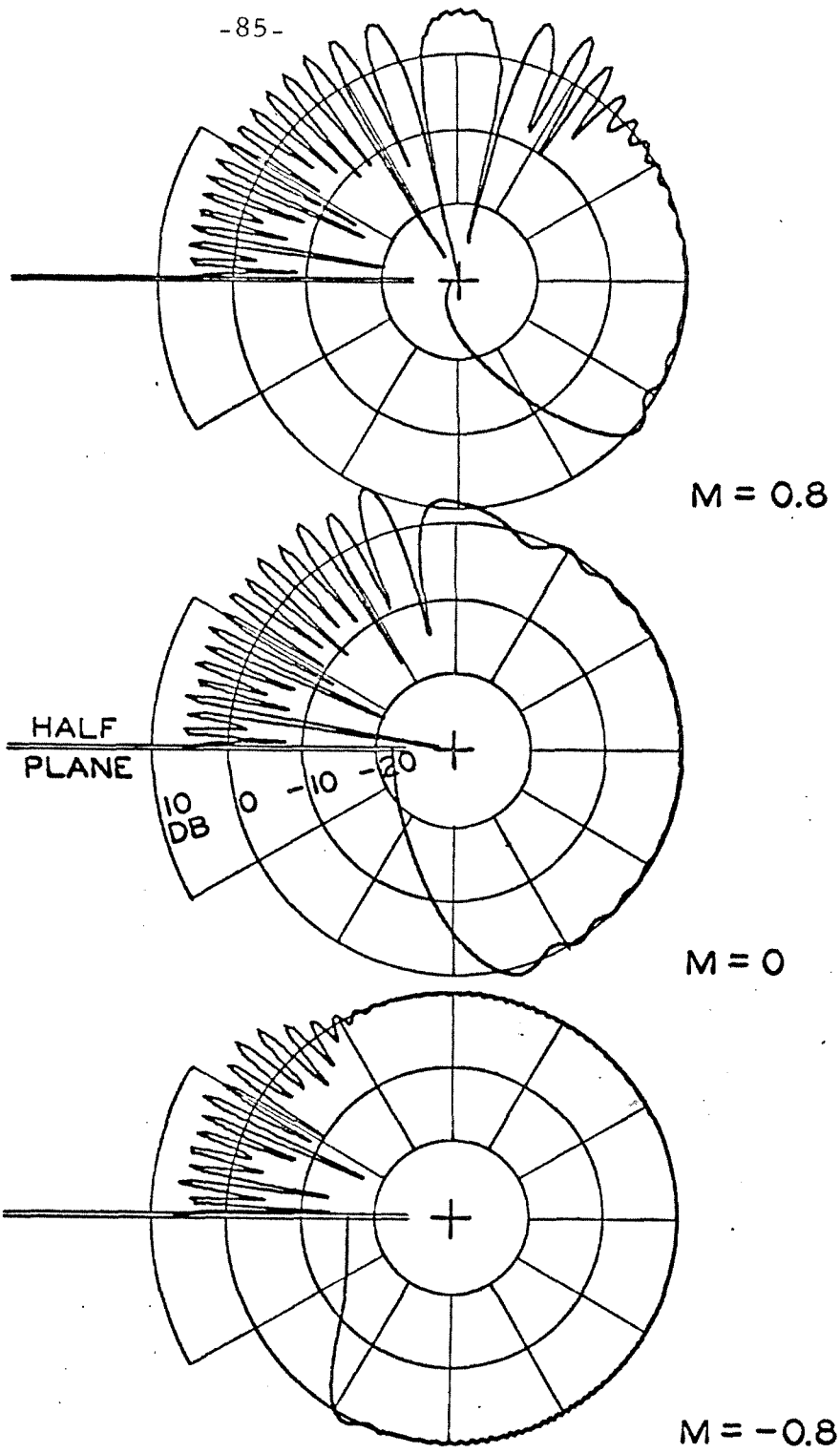
M = 0.8

HALF
PLANE

10
DB   0 -10 -20

M = 0

M = -0.8

Fig. 3-5d. Diffraction patterns of a plane wave by a semi-infinite
hard plane. The plane wave incidence angle is Θ = 90°;
kr = 50.

CHAPTER IV

DIFFRACTION OF A PLANE WAVE BY A HALF PLANE

IN A SUPERSONICALLY MOVING MEDIUM

4.1 INTRODUCTION

We treated in Chapter 3 the diffraction of a plane wave by a half plane in a subsonic stream. The solution was obtained by transforming the solution of an associated diffraction problem in a stationary medium. In the present chapter we study the diffraction of a plane wave by a half plane immersed in a supersonic stream. The nature of the diffraction problem changes strongly when the medium flows supersonically; the associated boundary value problem, of elliptic type in the subsonic case, becomes hyperbolic in the supersonic situation. As a consequence, characteristic lines appear, discontinuities may occur along these lines, zones of silence (undisturbed) or of pure reflection are possible.

Because of this essential change we were not able to find a simple transformation between the diffraction problem in a stationary medium and the present supersonic situation. However, applying the same ideas as those of Chapter 3 we were able to relate all the supersonic diffraction problems to a unique reference problem. The solution of this problem once developed may be simply transformed to provide the solution for a specific Mach number.

We analyze separately the negative (section 4.2) and positive (section 4.3) flow directions, because the physical situations and the corresponding boundary value problems are different. Our procedure remains the same in both cases. We first write the boundary value problem for a given Mach number. By a suitable transformation we obtain the reference problem. This problem is then solved by Fourier transform methods. The inversion of the transformed solution may be

performed in various ways. We give first the solution obtained by the
convolution theorem. This solution does not contain much informa-
tion on the physics of the problem and, moreover, it is not very suit-
able for numerical computation. We then give an expression obtained
by a change in integration contour in the complex plane. This pro-
vides a solution in the form of a sum of a geometrical optics field and
a diffracted wave. This solution has more physical meaning and per-
mits a partition of space in regions of different propagation character.
Remarkably, the diffracted wave may be expressed for both flow direc-
tions by using the same function $G(\lambda, \eta)$. Because of its
central role, the properties of G are studied in some detail in
Appendix 4-B and summarized at the end of section 4.2.

4.2 THE MEDIUM FLOWS IN THE NEGATIVE DIRECTION, $M < -1$

Formulation of the Problem

A plane wave propagating in the $\odot$ direction impinges on the half plane $-\infty < x \leqslant 0, y = 0$. The wave has a potential of the form

$$\Phi_i = \exp\left(\frac{-ikx\cos\odot}{1-M\cos\odot} - \frac{iky\sin\odot}{1-M\cos\odot}\right) \qquad (4.1)$$

$$k \equiv \omega/c$$

It is convenient to assume that k has an arbitrary, small, positive imaginary part

$$k = k_r + ik_i \qquad , \qquad k_i > 0 \qquad (4.2)$$

This is equivalent to introducing a small damping term in the partial differential equation which governs the problem and thus will help us settle questions concerning the position of branch points, branch cuts, choice of integration path, and behavior at infinity.

The wave (4.1) will reach the half plane if

$$1 - M\cos\odot > 0 \qquad (4.3)$$

We define the angle $\theta_M = \cos^{-1}(1/M)$ and require that

$$0 < \odot < \theta_M \qquad (4.4)$$

to satisfy condition (4.3).

Because the medium flows supersonically, the half plane will only influence the region D where $x \leqslant -(M^2-1)^{1/2}|y|$, limited by the two characteristic lines originating from the leading edge of the half plane (fig. 4-1a).

Outside D in the region R where $x > -(M^2-1)^{1/2}|y|$, the only disturbance is the incident wave ϕ_i .

We may now formulate the boundary value problem to determine the field in region D . As usual, we write the complete potential as a sum of the incident wave potential and an induced potential

$$\phi_t = \phi_i + \phi \tag{4.5}$$

The potential ϕ is solution of the convective wave equation

$$-\phi_{xx}(M^2-1) + \phi_{yy} + 2Mik\phi_x + k^2\phi = 0 \tag{4.6}$$

Equation (4.5) satisfies the following conditions:

no displacement at the hard wall

$$\frac{\partial \phi_t}{\partial y} = 0 \qquad \text{on} \quad -\infty < x \leqslant 0, y = 0$$

or

$$\frac{\partial \phi}{\partial y} = \frac{ik\sin\Theta}{1-M\cos\Theta} \exp \frac{-ikx\cos\Theta}{1-M\cos\Theta} \tag{4.7}$$

$\partial \phi_t / \partial y$ and hence $\partial \phi / \partial y$ are continuous across

$$-\infty < x < \infty, \quad y = 0 \tag{4.8}$$

$$\phi(x, 0) = 0 \qquad \text{on} \quad 0 \leqslant x < \infty, y = 0 \tag{4.9}$$

We shall not solve this problem as stated above, but first seek a reference problem. For this we define the transformed quantities

$$\Psi(x_1, y; k_1, \mu) = e^{-ik_1 Mx_1} \phi \tag{4.10}$$

$$x_1 = x / (M^2-1)^{1/2} \tag{4.11}$$

$$k_1 = k / (M^2 - 1)^{1/2} \qquad (4.12)$$

Equation (4.6) becomes

$$\Psi_{yy} - \Psi_{x_1 x_1} - k_1^2 \Psi = 0 \qquad (4.13)$$

and (4.5) yields

$$\frac{\partial \Psi}{\partial y} = \frac{i k_1 (M^2 - 1)^{1/2} \sin \Theta}{1 - M \cos \Theta} \exp\left(- i k_1 x_1 \frac{M - \cos \Theta}{1 - M \cos \Theta}\right)$$

on

$$-\infty < x_1 \leqslant 0 \quad , \quad y = 0 \qquad (4.14)$$

As a consequence of condition (4.3) and of $M < -1$

$$\frac{M - \cos \Theta}{1 - M \cos \Theta} \leqslant -1 \qquad (4.15)$$

It is natural then to define the real hyperbolic angle μ such that

$$ch \, \mu = - \frac{M - \cos \Theta}{1 - M \cos \Theta} \quad , \quad \mu \geqslant 0 \qquad (4.16)$$

(In the subsonic case, at this point we introduced a new angle Θ_1 defined by $\cos \Theta_1 = (\cos \Theta - M)/(1 - M \cos \Theta)$.) The definition (4.16) allows us to write (4.14) as

$$\frac{\partial \Psi}{\partial y} = i k_1 \, sh \, \mu \, \exp(i k_1 x_1 \, ch \, \mu) \qquad (4.17)$$

on

$$-\infty < x_1 \leqslant 0 \quad , \quad y = 0$$

The two conditions (4.8) and (4.9) set on ϕ apply also to Ψ . To solve the above boundary value problem we are going to use complex Fourier transform methods. We shall need, in the course of this solution, some information on the behavior of $\Psi(x_1, y)$ at

infinity.

In region R_1 the only disturbance is Ψ_i, and thus

$$\Psi(x_1, y) = 0 \qquad \text{for} \qquad x_1 > -|y| \qquad (4.18)$$

In region D_{1+} where $x_1 < -|y|$ and $y > 0$ (the part of region D_1 above the half plane), Ψ consists of a diffracted wave and a reflected wave.

In region D_{1-} where $x_1 < -|y|$, $y > 0$, below the half plane, a diffracted wave and the opposite of the incident wave will constitute Ψ. Let

$$\eta = (x_1^2 - y^2)^{1/2} \qquad (4.19)$$

From results in the theory of nonsteady aerodynamics in supersonic flow (see, for instance, Miles [4.1]), we infer that the diffracted wave behaves like

$$\Psi_d \sim c_1 J_0(k_1 \eta) \qquad \text{as} \qquad \eta \longrightarrow \infty \qquad (4.20)$$

$$\Psi_d \sim 0 \qquad \text{as} \qquad \eta \longrightarrow 0 \qquad (4.21)$$

The reflected wave in D_{1+} is

$$\Psi_r = \exp(i k_1 x_1 ch\mu + i k_1 y sh\mu) \qquad (4.22)$$

From the above discussion we finally deduce

$$|\Psi| < c_2 \exp(- k_{1i} x_1 ch\mu - k_{1i}|y| sh\mu)$$

$$\text{for} \qquad -\infty < x < -|y| \qquad (4.23)$$

$$|\Psi| = 0 \qquad \text{for} \qquad -|y| < x < +\infty \qquad (4.24)$$

Solution by Fourier Transform Methods

We seek a solution to the boundary value problem for Ψ :

we delete the index 1 , but keep in mind that x, k are transformed
quantities. We adopt Noble's [4.2] definitions for the complex Fourier
transforms.

The Fourier variable α is complex and has a real part σ
and an imaginary part τ

$$\alpha = \sigma + i\tau \tag{4.25}$$

Then

$$\widetilde{\Psi}_+ (\alpha, y) = \frac{1}{(2\pi)^{1/2}} \int_0^\infty \Psi(x,y) e^{i\alpha x} dx \tag{4.26}$$

$$\widetilde{\Psi}_- (\alpha, y) = \frac{1}{(2\pi)^{1/2}} \int_{-\infty}^0 \Psi(x,y) e^{i\alpha x} dx \tag{4.27}$$

$$\widetilde{\Psi}(\alpha, y) = \widetilde{\Psi}_+ (\alpha, y) + \widetilde{\Psi}_- (\alpha, y) \tag{4.28}$$

or

$$\widetilde{\Psi}(\alpha, y) = \frac{1}{(2\pi)^{1/2}} \int_{-\infty}^{+\infty} \Psi(x,y) e^{i\alpha x} dx \tag{4.29}$$

We know that $\Psi(x,y) = 0$ for $x > -|y|$; therefore,
$\widetilde{\Psi}_+ (\alpha, y) \equiv 0$. If we suppose that Ψ is sufficiently

smooth (i. e., Ψ satisfies the conditions of theorem A, p. 11, in Noble [4.2]), then we can deduce from conditions (4.23) and (4.24) that $\widetilde{\Psi}_-(\alpha, y)$ is analytic for

$$Im(\alpha) < -Im(k\,ch\,\mu)$$

or

$$\sigma < -k_i\,ch\,\mu \qquad (4.30)$$

We can also deduce the behavior of $\widetilde{\Psi}(\alpha, y)$ when $|y|$ tends to infinity:

$$|\widetilde{\Psi}(\alpha, y)| \leqslant \frac{1}{(2\pi)^{1/2}} \int_{-\infty}^{+\infty} |\Psi\, e^{-\sigma x}|\, dx$$

$$\leqslant C_3 \int_{-\infty}^{-|y|} dx\, \exp\left[-(\sigma + k_i\,ch\,\mu)x - k_i|y|\,sh\,\mu\right] \qquad (4.31)$$

This shows that $|\widetilde{\Psi}(\alpha, y)|$ is bounded as $|y|$ tends to infinity when α is in the region of analyticity for $\widetilde{\Psi}(\alpha, y)$. We now apply the Fourier transform to the partial differential equation (4.13) and obtain

$$\widetilde{\Psi}_{yy}(\alpha, y) - \gamma^2 \widetilde{\Psi}(\alpha, y) = 0 \qquad (4.32)$$

with

$$\gamma = (k^2 - \alpha^2)^{1/2} \qquad (4.33)$$

and we use the branch of γ such that $Re(\gamma) < 0$ for

$$Im(\alpha) < -Im(k) \quad \text{or} \quad \sigma < -k_i \ .$$

A solution of (4.32) bounded when $|y|$ tends to infinity has the form

$$\tilde{\Psi}(\alpha, y) = A_1(\alpha)\, e^{\gamma y} \qquad , \; y \geq 0 \qquad\qquad (4.34)$$

$$= A_2(\alpha)\, e^{-\gamma y} \qquad , \; y < 0 \qquad\qquad (4.35)$$

The continuity of $d\tilde{\Psi}(\alpha, y)/dy$ across $y = 0$ requires

$$A_1(\alpha) = -A_2(\alpha) = A(\alpha) \qquad\qquad (4.36)$$

and we can write

$$\frac{d\tilde{\Psi}(\alpha, y)}{dy} = \frac{d\tilde{\Psi}(\alpha, y)}{dy} = \gamma A(\alpha) \qquad\qquad (4.37)$$

From (4.17) we get (under the condition $\sigma < -k_i\, ch\mu$)

$$\frac{d\tilde{\Psi}(\alpha, y)}{dy} = \frac{1}{(2\pi)^{1/2}} \frac{k\, sh\mu}{\alpha + k\, ch\mu} \qquad\qquad (4.38)$$

and then (4.37) yields

$$A(\alpha) = \frac{1}{(2\pi)^{1/2}} \frac{k\, sh\mu}{\gamma(\alpha + k\, ch\mu)} \qquad\qquad (4.39)$$

The inverse Fourier transform is

$$\Psi(x, y) = sgn(y) \frac{1}{(2\pi)^{1/2}} \int_{-\infty + ia}^{+\infty + ia} A(\alpha)\, e^{\gamma|y| - i\alpha x}\, d\alpha \qquad\qquad (4.40)$$

$sgn(y)$ represents the sign of y ; the path of integration is chosen so that

$$a < -k_i\, ch\mu < -k_i \qquad\qquad (4.41)$$

Only the absolute value of y appears in the integrand of (4.40). From here on, we shall consider the region $y > 0$ only. To obtain

the field for $y < 0$, we take the opposite of $\Psi(x, |y|)$.

Consider now the region D_+ where $x < -|y|, y > 0$: we close the path of integration by a big semi-circle Γ_R in the upper half plane (fig. 4-2). The contribution of this path integral can be easily estimated:

$$\left| \int_{\Gamma_R} A(\alpha) e^{\gamma y - i\alpha x} d\alpha \right| \leqslant \int_{\Gamma_R} |A(\alpha)| |e^{-i\alpha(x+y)}| |d\alpha|$$

$$\leqslant \underset{\Gamma_R}{Max} |A(\alpha)| \int_{\Gamma_R} e^{\sigma(x+y)} |d\alpha| \qquad (4.42)$$

A classical estimation of the integral in (4.42) yields

$$\left| \int_{\Gamma_R} A(\alpha) e^{\gamma y - i\alpha x} d\alpha \right| \leqslant \frac{\pi}{|x+y|} \underset{\Gamma_R}{Max} |A(\alpha)| \qquad (4.43)$$

As $\underset{\Gamma_R}{Max} |A(\alpha)|$ tends to zero as $|\alpha|$ goes to infinity, the contribution of Γ_R vanishes as the radius R tends to infinity, and we can write for the region D_+

$$\Psi(x, y) = \frac{1}{(2\pi)^{1/2}} \int_{\frown} A(\alpha) e^{\gamma y - i\alpha x} d\alpha \qquad (4.44)$$

In the same way, we can write for the region R_+ where $x > -y$, $y > 0$,

$$\Psi(x,y) = \frac{1}{(2\pi)^{1/2}} \int_{\curvearrowleft} A(\alpha) e^{\gamma y - i\alpha x} d\alpha \qquad (4.45)$$

The integrand in (4.45) is analytic inside the integration contour. Cauchy's theorem yields $\Psi(x,y) \equiv 0$ in the region R_+, which was to be expected.

Inversion by the Convolution Theorem

We start from (4.39) and (4.40) and suppose y positive

$$\Psi(x,y) = \frac{1}{2\pi} \int_{-\infty+ia}^{+\infty+ia} \frac{k\,sh\mu}{(\alpha+kch\mu)\gamma} e^{\gamma y - i\alpha x} d\alpha \qquad (4.46)$$

From Appendix 4-A,

$$f_1(x,y) = \frac{1}{2\pi} \int_{-\infty+ia}^{+\infty+ia} \gamma^{-1} e^{\gamma y - i\alpha x} d\alpha$$

$$= -J_0\left[k(x^2-y^2)^{1/2}\right] \quad , \quad x < -y$$

$$= 0 \qquad\qquad\qquad , \quad x > -y \qquad (4.47)$$

and we have, by the residue theorem,

$$f_2(x,y) = \frac{1}{2\pi} \int_{-\infty+ia}^{+\infty+ia} \frac{k\,sh\mu}{\alpha + kch\mu}\, e^{-i\alpha x} d\alpha$$

$$= ik\,sh\mu\,\exp(ikx\,ch\mu)\ ,\ x < 0$$

$$= 0 \qquad\qquad\qquad , x > 0 \qquad (4.48)$$

Then the convolution theorem yields

$$\Psi(x,y) = -\int_{x}^{-y} d\sigma\, ik\,sh\mu\, e^{ik(x-\sigma)ch\mu} J_0\!\left[k(\sigma^2 - y^2)^{1/2}\right]$$

$$\text{for}\quad x < -y,\quad y > 0$$

$$= 0 \qquad \text{for}\quad x > -y,\quad y > 0 \qquad (4.49)$$

Inversion by Change of Integration Contour

We now start from (4.39) and (4.44), which expresses Ψ as a contour integral. We work in the region D_+ ($x < -y$, $y > 0$) where we can define the following set of polar hyperbolic coordinates

$$x = -\rho\,ch\,\xi \qquad\qquad (4.50)$$

$$y = \rho\,sh\,\xi \qquad\qquad (4.51)$$

with

$$0 \leqslant \eta < + \infty$$
$$0 \leqslant \zeta < + \infty$$

The form of the exponent in the integrand of expression (4.44) drives us to replace the integration contour ⌒ by the elliptical contour E defined in the α -plane by

$$\alpha = k \, ch (\zeta - it) \qquad (4.52)$$

where $-\pi < t < \pi$.

When $\zeta > 0$ (as in the present case) the ellipse E is described in the clockwise direction. The ellipse E has its focuses at the two branch points $\pm k$ of the integrand of expression (4.44).

When $\infty > \zeta > \mu$, all the singularities of the integrand of (4.44) which are situated inside ⌒ are also contained inside E (figure 4-2). Then

$$\Psi = -\frac{1}{(2\pi)^{1/2}} \int_{E\zeta} A(\alpha) \, e^{\gamma y - i\alpha x} d\alpha \qquad (4.53)$$

When $\mu > \zeta > 0$ the pole $\alpha = -kch\mu$, which is inside ⌒ , is outside E (fig. 4-2) and thus its contribution must be added

$$\Psi = -\frac{1}{(2\pi)^{1/2}} \int_{E\zeta} A(\alpha) \, e^{\gamma y - i\alpha x} d\alpha$$
$$+ \frac{1}{(2\pi)^{1/2}} \int_{C\zeta} A(\alpha) \, e^{\gamma y - i\alpha x} d\alpha \qquad (4.54)$$

where C is a small contour around the pole $\alpha = -k\,ch\mu$. Then

$$\Psi = -\frac{1}{(2\pi)^{1/2}} \int_{E\}} A(\alpha)\, e^{\gamma y - i\alpha x}\, d\alpha$$

$$+ e^{ikxch\mu + ikysh\mu} \tag{4.55}$$

We now evaluate the contribution Ψ_E of the integration on contour E :

$$\gamma = -ik\,sh(\mathcal{G} - it) \tag{4.56}$$

$$\gamma y - i\alpha x = iky\cos t \tag{4.57}$$

Thus

$$\Psi_E = -\frac{sh\mu}{2\pi} \int_{-\pi}^{\pi} \frac{e^{iky\cos t}\,dt}{ch(\mathcal{G} - it) + ch\mu} \tag{4.58}$$

Consider now

$$B = \frac{sh\mu}{ch(\mathcal{G} - it) + ch\mu} \tag{4.59}$$

The imaginary part of B is odd and thus does not contribute to the integral in (4.58). The real part of B can be written after some algebra

$$Re(B) = \frac{(1/2)sh(\mathcal{G} + \mu)}{\cos t + ch(\mathcal{G} + \mu)} - \frac{(1/2)sh(\mathcal{G} - \mu)}{\cos t + ch(\mathcal{G} - \mu)} \tag{4.60}$$

We then define the function

$$G(\lambda, \eta) = \frac{1}{2\pi} \int_0^\pi e^{ik\eta \cos t} \frac{sh\lambda}{\cos t + ch\lambda} \, dt \qquad (4.61)$$

which enables us to write (4.58) as

$$\Psi_E = -G(\xi + \mu, \eta) + G(\xi - \mu, \eta) \qquad (4.62)$$

Assembling results (4.53), (4.55), and (4.62) we have, in the region D_+ ,

$$\Psi = e^{ikx \, ch\mu + iky \, sh\mu} h(\mu - \xi)$$

$$- G(\xi + \mu, \eta) + G(\xi - \mu, \eta) \qquad (4.63)$$

where $h(x)$ is the Heaviside step function

$$h(x) = \begin{cases} 1 & x > 0 \\ 0 & x < 0 \end{cases} \qquad (4.64)$$

Before we discuss the physical significance of expression (4.63), it is useful to study the function $G(\lambda, \eta)$ in some detail.

Properties of $G(\lambda, \eta)$

The integrand in expression (4.61) defining the function G has a singularity at $\lambda = 0$. Apart from the neighborhood of $\lambda = 0$, the function $G(\lambda, \eta)$ may be easily computed. The modulus of G is shown on fig. 4-3, while the real and imaginary parts of G are represented on fig. 4-4.

Some properties of G are summarized below; the proofs

are given in Appendix 4-B.

<u>Lemma 1</u>

$$G(\lambda, \eta) \quad \text{is an odd function of } \lambda$$

$$G(-\lambda, \eta) = -G(\lambda, \eta) \tag{4.65}$$

<u>Lemma 2</u>

The function $G(\lambda, \eta)$ converges uniformly for λ belonging to $[\lambda_0, +\infty)$ and η belonging to $[\eta_0, +\infty)$ where λ_0 and η_0 are arbitrarily small but different from 0

$$\tag{4.66}$$

<u>Lemma 3</u>

The function $G(\lambda, \eta)$ converges uniformly to $(1/2) J_0(k\eta)$ when λ tends to infinity

$$\lim_{\lambda \to \infty} G(\lambda, \eta) = (1/2) J_0(k\eta) \tag{4.67}$$

<u>Lemma 4</u>

The function $G(\lambda, \eta)$ converges to $1/2$ when η tends to 0 and λ tends to infinity

$$\lim_{\lambda \to \infty, \eta \to 0} G(\lambda, \eta) = 1/2 \tag{4.68}$$

<u>Lemma 5</u>

The function $G(\lambda, \eta)$ has a jump discontinuity at $\lambda = 0$. When λ tends to 0 by superior values

$$\lim_{\lambda \to 0_+} G(\lambda, \eta) = (1/2) e^{-ik\eta} \qquad \text{uniformly} \tag{4.69}$$

<u>Lemma 6</u>

When $k\eta (ch\lambda - 1) \gg 1$, then $G(\lambda, \eta)$ has

an asymptotic expansion of the form

$$G(\lambda,\eta) \sim \frac{1}{(8\pi k\eta)^{1/2}} \left[\coth\frac{\lambda}{2}\, e^{-ik\eta + i\pi/4} \right.$$

$$\left. + \operatorname{th}\frac{\lambda}{2}\, e^{ik\eta - i\pi/4} \right] + O\left[\frac{1}{k\eta\,(\operatorname{ch}\lambda - 1)}\right] \qquad (4.70)$$

The modulus of G given by the previous asymptotic expression is shown on fig. 4-5; the real and imaginary parts of G are represented on fig. 4-6.

A comparison of figs. 4-3 and 4-5 and of figs. 4-4 and 4-6 shows that the function $G(\lambda,\eta)$ is closely approximated by expression (4.7) when $k\eta > 20$ and $\lambda > 0.2$.

Lemma 7

When $k\eta(\operatorname{ch}\lambda - 1) \ll 1$ and $k\eta \gg 1$, an asymptotic expansion for $G(\lambda,\eta)$ is

$$G(\lambda,\eta) \sim \operatorname{sgn}(\lambda)\,(1/2)\, e^{-ik\eta}$$

$$+ O\left\{[k\eta(\operatorname{ch}\lambda - 1)]^{1/2}\right\} + O\left[(k\eta)^{-1/2}\right]$$

The consequences of these lemmas follow. We consider the field in the region D_+ .

From Lemma 4 we obtain immediately

$$\lim_{x \to -y} \Psi_\epsilon (x,y) = 0 \qquad (4.72)$$

Using Lemma 5 it is easy to show that the field expression (4.63)

has no discontinuity across the line $\xi = \mu$. The jump introduced by the Heaviside function is compensated by an opposite jump in Ψ_E :

$$\Psi(\xi_+, \eta) = -G(2\mu, \eta) + \frac{1}{2} e^{-ik\eta} \qquad (4.72)$$

$$\Psi(\xi_-, \eta) = e^{-ik\eta} - G(2\mu, \eta) - \frac{1}{2} e^{-ik\eta} \qquad (4.73)$$

and thus

$$\Psi(\xi_+, \eta) = \Psi(\xi_-, \eta) \qquad (4.75)$$

Lemma 6 yields an asymptotic expression for Ψ_E in the region $k\eta [ch(\xi - \mu) - 1] \gg 1$ (i.e., sufficiently far from the line $\xi = \mu$). In this region Ψ_E is of order $(k\eta)^{-1/2}$ and has the form

$$\Psi_E \sim \frac{sh\mu}{(2\pi k\eta)^{1/2}} \left[\frac{e^{-ik\eta + i\pi/4}}{ch\xi - ch\mu} - \frac{e^{ik\eta - i\pi/4}}{ch\xi + ch\mu} \right]$$

$$+ O\left\{ 1/[k\eta (ch(\xi - \mu) - 1)] \right\} \qquad (4.75)$$

In the transition region around the lines $\xi = \mu$, for $k\eta (ch(\xi - \mu) - 1) \ll 1$ while $k\eta \gg 1$, Lemmas 6 and 7 yield the following asymptotic expansion for :

$$\Psi_E \sim sgn(\xi - \mu) (1/2) e^{-ik\eta}$$

$$- \frac{1}{(8\pi k\eta)^{1/2}} \left[coth\mu \, e^{-ik\eta + i\pi/4} + th\mu \, e^{ik\eta - i\pi/4} \right]$$

$$+ O\left\{ [k\eta(ch(\xi - \mu) - 1)]^{1/2} \right\} + O(1/k\eta) \qquad (4.77)$$

Results

Using expression (4.63) the complete field in D_+ may be written as a sum of a "geometrical optics" field

$$\Psi_{g.o.} = \Psi_i + h(\mu - \xi)\Psi_r \tag{4.78}$$

and the field Ψ_E given by (4.62)

$$\Psi_t = \Psi_{g.o.} + \Psi_E \tag{4.79}$$

The asymptotic expression (4.76), the fact that Ψ_E compensates for the discontinuity in the geometrical optics field at $\xi = \mu$, and the form of (4.79) leads us to consider Ψ_E as a diffracted wave. We write in D_+

$$\Psi_d = \Psi_E(\xi, \mu) \tag{4.80}$$

$$\Psi_t = \Psi_{g.o.} + \Psi_d \tag{4.81}$$

and in D_-

$$\Psi_{g.o.} = \Psi_i \, h(|\xi| - \mu) \tag{4.82}$$

$$\Psi_d = -\Psi_E(|\xi|, \mu) \tag{4.83}$$

The total field takes the form (4.81).

Expressions (4.78) and (4.82) for the geometrical optics field show that the line $\xi = +\mu$ is the boundary of the reflection region in D_+, while $\xi = -\mu$ is the boundary of the shadow region in D_-. It is interesting at this point to seek the polar angles $\delta_\pm$ corresponding to these lines. We have

$$th\, \xi = -y/x_1 = -(M^2-1)^{1/2} y/x \tag{4.84}$$

$$= -(M^2-1)^{1/2} \tan \delta \tag{4.85}$$

Consider, for instance, $\varsigma = \mu$

$$th \, \varsigma \; = \; th \, \mu \; = \; - \; \frac{(M^2-1)^{1/2} \sin \Theta}{M - \cos \Theta} \tag{4.86}$$

and then from (4.85)

$$\tan \delta_+ \; = \; \frac{\sin \Theta}{M - \cos \Theta} \tag{4.87}$$

This expression was encountered in Chapter 3, and a simple kinematical explanation was given. The polar angle δ_+ is represented on fig. 4-7 for subsonic and supersonic Mach numbers. It is now evident that the "geometrical optics" part of the field in the supersonic case behaves essentially in the same way as in the subsonic case, while the diffracted wave contains the main differences. All the characteristics discussed above may be found in the diffraction patterns of fig. 4-8a, b. Their general appearance is substantially different from the subsonic diffraction patterns.

4.3 THE MEDIUM FLOWS IN THE POSITIVE DIRECTION, $M > 1$

Formulation of the Problem

We consider a plane wave having a potential of the form (4.1). This wave reaches the half plane if (4.3) is satisfied. We define again the angle $\Theta_M = \cos^{-1}(1/M)$, but now to satisfy (4.3) we require

$$\Theta_M < \Theta < \pi \tag{4.88}$$

The medium flows now in the positive X -direction and the half plane edge will only influence the region D where $X \geqslant (M^2-1)^{1/2}|y|$; the region D is bounded by the two characteristic lines originating from the edge (fig. 4-1b). In the region R_+ where $X < (M^2-1)^{1/2}y$ and $y > 0$, the incident and reflected waves ϕ_i and ϕ_r propagate , while R_- where $X < (M^2-1)^{1/2}y$ and $y < 0$ remains unperturbed.

The preceding results will come out from the solution of the boundary value problem which we now formulate.

As usual, we write the complete potential in the form (4.5), ϕ is the solution of the convective wave equation (4.6) and satisfies (4.7) and (4.8), but now (4.9) is replaced by : ϕ_t and thus ϕ are continuous across

$$0 \leqslant X < \infty \quad, \quad y = 0 \tag{4.89}$$

As in section 4.2, we define the transformed quantities Ψ, X_1, k_1 but now the condition $\Theta_M < \Theta < \pi$ and $M > 1$ lead to

$$\frac{M - \cos\Theta}{1 - M\cos\Theta} \geqslant 1 \tag{4.90}$$

and we have to replace the definition (4.16) of μ by

$$ch\mu = \frac{M - \cos\Theta}{1 - M\cos\Theta} \tag{4.91}$$

Then expression (4.14) becomes

$$\frac{\partial\Psi}{\partial y} = i k_1 sh\mu \, exp(-ik_1 x_1 \, ch\mu)$$

for

$$-\infty < x \leqslant 0, \quad y = 0 \tag{4.92}$$

The function Ψ is solution of equation (4.13) and satisfies the conditions (4.7), (4.8), (4.89) given for Φ.

We also need some information on the behavior of Ψ at infinity. This will help us to determine the transformed solution, the regions of analyticity of this solution, the integration path for the inversion formula.

In region R_{1+}, the complete field Ψ_t consists of an incident and a reflected wave

$$\Psi_i = exp(-ik_1 x_1 ch\mu - ik_1 y \, sh\mu) \tag{4.93}$$

$$\Psi_r = exp(-ik_1 x_1 ch\mu + ik_1 y \, sh\mu) \tag{4.94}$$

In region R_{1-} there is no disturbance $\Psi_t \equiv 0$, and thus Ψ is the opposite of the incident wave

$$\Psi = -exp(-ik_1 x_1 ch\mu - ik_1 y \, sh\mu) \tag{4.95}$$

From (4.94) and (4.95) we deduce

$$\Psi < exp(k_1 i x_1 ch\mu - k_1 i |y| \, sh\mu) \tag{4.96}$$

for $x_1 < |y|$

In region D_1, Ψ reduces to a diffracted wave when x_1 tends

to infinity; the results of section 4.2 and various results in nonsteady aerodynamics of supersonic flow suggest that

$$\Psi_d \sim c_3 J_0(k_1 \eta) \tag{4.97}$$

with $\quad \eta = (x_1^2 - y^2)^{1/2}$

Then

$$|\Psi| < c_4 \exp\left[k_{1i}(x_1^2 - y^2)^{1/2}\right] \tag{4.98}$$

for $\quad x_1 > |y|$

The behavior of Ψ near the half plane edge will also be used and may be found very easily from the discussion at the beginning of the present section,

$$\Psi(x_1, 0_+) - \Psi(x_1, 0_-) \longrightarrow c_5 = 2 \tag{4.99}$$

and $x_1 \longrightarrow 0_-$ on $y = 0$.

Solution by Fourier Transform Methods

While the solution Ψ may be obtained in other ways, it is convenient to use the framework of the Wiener-Hopf technique, more specifically using D. S. Jones' approach as treated by Noble [4.2]. In this method the Fourier transform is applied directly to the partial differential equation to obtain a complex variable equation which is then solved by analytic continuation.

We delete the index 1 and use the definitions (4.25) through (4.29). We suppose that Ψ is sufficiently smooth, in the sense of theorem A, p. 11 in Noble [4.2], then we deduce from condition (4.96) that $\widetilde{\Psi}_-(\alpha, y)$ is analytic in the half plane $\tau < k_i ch \mu$ while condition (4.98) shows that $\widetilde{\Psi}_+(\alpha, y)$ is analytic in the half plane $k_i < \tau$.

The behavior of $\widetilde{\Psi}(\alpha, y)$ as $|y|$ tends to infinity can be deduced from (4.96) and (4.98) as follows:

$$|\widetilde{\Psi}(\alpha, y)| \leqslant \frac{1}{(2\pi)^{1/2}} \int_{-\infty}^{+\infty} |\Psi e^{-\sigma x}| \, dx$$

$$\leqslant \frac{1}{(2\pi)^{1/2}} \int_{-\infty}^{|y|} |\Psi e^{-\sigma x}| \, dx + \frac{1}{(2\pi)^{1/2}} \int_{|y|}^{+\infty} |\Psi e^{-\sigma x}| \, dx$$

$$\leqslant |\Psi_1| + |\Psi_2| \tag{4.100}$$

with

$$|\Psi_1| < c_6 \int_{-\infty}^{|y|} \exp[(k_i \, ch\mu - \sigma)x - k_i |y| sh\mu] \, dx \tag{4.101}$$

$$|\Psi_2| < c_7 \int_{|y|}^{+\infty} \exp[k_i (x^2 - y^2)^{1/2} - \sigma x] \, dx \tag{4.102}$$

Expressions (4.100), (4.101), (4.102) show that $|\widetilde{\Psi}(\alpha, y)|$ is bounded when $|y|$ tends to infinity with

$$k_i < \sigma < k_i \, ch\mu \tag{4.103}$$

Hence, $\widetilde{\Psi}(\alpha, y)$ is analytic and bounded in the strip (4.103).

The Fourier transformed differential equation for $\widetilde{\Psi}(\alpha, y)$ is (4.32) with γ defined by (4.33), and we use the same branch of

γ as in section 4.2. This branch is such that $Re(\gamma) > 0$ in the region $k_i < \tau$.

A solution of (4.32), bounded when $|y|$ tends to infinity and having a continuous derivative with respect to y across the line $y = 0$, is

$$\widetilde{\Psi}(\alpha, y) = A(\alpha) e^{-\gamma y} \qquad , \quad y > 0$$

$$= -A(\alpha) e^{\gamma y} \qquad , \quad y < 0 \qquad (4.104)$$

To find $A(\alpha)$ we use D. S. Jones' method and write the following identities:

$$\widetilde{\Psi}_+(\alpha, 0) + \widetilde{\Psi}_-(\alpha, 0_+) = A(\alpha) \qquad (4.105)$$

$$\widetilde{\Psi}_+(\alpha, 0) + \widetilde{\Psi}_-(\alpha, 0_-) = -A(\alpha) \qquad (4.106)$$

$$\frac{d\widetilde{\Psi}_+(\alpha, 0)}{dy} + \frac{d\widetilde{\Psi}_-(\alpha, 0)}{dy} = -\gamma A(\alpha) \qquad (4.107)$$

From (4.105) and (4.106)

$$2A(\alpha) = \widetilde{\Psi}_-(\alpha, 0_+) - \widetilde{\Psi}_-(\alpha, 0_-) \qquad (4.108)$$

The right hand side of (4.108) is analytic in the half plane $\tau < k_i ch\mu$ and will therefore be called $2D_-(\alpha)$. $d\widetilde{\Psi}_-(\alpha, 0)/dy$ is known from (4.92),

$$\frac{d\widetilde{\Psi}_-(\alpha, 0)}{dy} = \frac{k\, sh\mu}{(2\pi)^{1/2}\,(\alpha - kch\mu)} \qquad (4.109)$$

for $\tau < k_i ch\mu$.

Expression (4.107) may then be written as

$$\gamma^{-1}\frac{d\tilde{\Psi}_+(\alpha,0)}{dy} + \frac{k\,sh\mu}{(2\pi)^{1/2}\gamma(\alpha - kch\mu)} = -D_-(\alpha) \qquad (4.110)$$

This equation holds in the skip $\quad k_i < \sigma < k_i\,ch\mu$.

The first term of this equation is analytic in the upper half plane

$\sigma > k_i$, while the third term in analytic in the lower half plane

$\sigma < k_i\,ch\mu$. The second term may be decomposed as follows:

$$\frac{k\,sh\mu}{(2\pi)^{1/2}\gamma(\alpha - kch\mu)} = \frac{k\,sh\mu}{(2\pi)^{1/2}(\alpha - kch\mu)}\left[\frac{1}{(k^2-\alpha^2)^{1/2}} - \frac{1}{(k^2 - k^2ch^2\mu)^{1/2}}\right]$$

$$+ \frac{k\,sh\mu}{(2\pi)^{1/2}(\alpha - kch\mu)(k^2 - k^2ch^2\mu)^{1/2}}$$

$$= H_+(\alpha) + H_-(\alpha) \qquad (4.111)$$

It is easy to see that $\quad H_+(\alpha) \quad$ does not have a pole at

$\alpha = kch\mu \quad$ and is therefore analytic in the upper half plane.

$H_-(\alpha)$ is analytic in the lower half plane, and equation (4.10) can

be rearranged as

$$J(\alpha) = \gamma^{-1}\frac{d\tilde{\Psi}_+(\alpha,0)}{dy} + H_+(\alpha) = -D_-(\alpha) - H_-(\alpha) \quad (4.112)$$

This defines a function $\quad J(\alpha) \quad$ regular for $\quad \sigma > k_i \quad$ and also for

$\sigma < k_i\,ch\mu \quad$, and consequently $\quad J(\alpha) \quad$ is regular in

the whole $\quad \alpha \quad$-plane. The behavior of $\quad \Psi \quad$ near the edge (4.99)

yields

$$D_-(\alpha) \sim \alpha^{-1} \qquad \text{as} \quad \alpha \longrightarrow \infty \qquad (4.113)$$

Thus, $J(\alpha) \sim \alpha^{-1}$ as α tends to infinity, and we conclude from the Liouville theorem that $J(\alpha) \equiv 0$. Then $D_-(\alpha) = -H_-(\alpha)$ or

$$A(\alpha) = -\frac{1}{(2\pi)^{1/2}} \frac{k \, sh\mu}{(\alpha - kch\mu)(k^2 - k^2 ch^2\mu)^{1/2}} \qquad (4.114)$$

and $\Psi(x,y)$ may be found by taking the inverse transform of (4.104) with $A(\alpha)$ given by (4.114)

$$\Psi(x,y) = sgn(y)\frac{1}{2\pi i}\int_{-\infty+ia}^{+\infty+ia} \frac{e^{-i\alpha x - \gamma|y|}}{\alpha - kch\mu} \, d\alpha \qquad (4.115)$$

where a is chosen in the strip $k_i < a < k_i ch\mu$

As y enters in the integral in (4.115) through its absolute value, we shall only consider the region $y > 0$. As in section 4.2, we can formulate Ψ using closed contour integrals:

for $x < y$, $y > 0$

$$\Psi = \frac{1}{2\pi i}\int_{\bigcirc} \frac{e^{-i\alpha x - \gamma y}}{\alpha - kch\mu} \, d\alpha \qquad (4.116)$$

for $x > y$, $y > 0$

$$\Psi = \frac{1}{2\pi i}\int_{\bigtriangledown} \frac{e^{-i\alpha x - \gamma y}}{\alpha - kch\mu} \, d\alpha \qquad (4.117)$$

The integrand is analytic everywhere inside the contour of integration of (4.116) except at the pole $\alpha = kch\mu$. Thus, by the residue theorem

$$\Psi = e^{-ikxch\mu + ikysh\mu}$$

for $x < y$, $y > 0$ (4.118)

We have now to invert (4.115) or (4.117) in the region $x > y, y > 0$.

Inversion by the Convolution Theorem

We are going to apply the convolution theorem to expression (4.115). Using the methods of Appendix 4-A, it is easy to show that

$$f_1(x,y) = \frac{1}{2\pi} \int_{-\infty + ia}^{+\infty + ia} e^{-i\alpha x - \gamma y} \, d\alpha$$

$$= - ky \frac{J_1\left[k(x^2 - y^2)^{1/2}\right]}{(x^2 - y^2)^{1/2}} \qquad \text{for} \qquad x > y$$

$$= 0 \qquad \text{for} \qquad x < y \qquad (4.119)$$

The residue theorem yields

$$f_2(x,y) = \frac{1}{2\pi} \int_{-\infty + ia}^{+\infty + ia} \frac{e^{-i\alpha x}}{i(\alpha - kch\mu)} \, d\alpha$$

$$= e^{-ikxch\mu} \qquad \text{for } x > 0$$

$$= 0 \qquad \text{for } x < 0 \qquad (4.120)$$

Then

$$\Psi(x,y) = -ky \int_{x}^{\infty} d\sigma \, e^{-ik(x-\sigma)ch\mu} \frac{J_1\left[k(\sigma^2-y^2)^{1/2}\right]}{(\sigma^2-y^2)^{1/2}}$$

$$\text{for} \quad x > y \qquad (4.121)$$

This expression contains an infinite limit of integration and is therefore not well adapted to numerical computation. To obtain a better expression with finite limits we write $\Psi(x,y)$ as follows:

$$\Psi(x,y) = -ky \int_{y}^{\infty} d\sigma \, e^{-ik(x-\sigma)ch\mu} \frac{J_1\left[k(\sigma^2-y^2)^{1/2}\right]}{(\sigma^2-y^2)^{1/2}}$$

$$+ ky \int_{y}^{x} d\sigma \, e^{-ik(x-\sigma)ch\mu} \frac{J_1\left[k(\sigma^2-y^2)^{1/2}\right]}{(\sigma^2-y^2)^{1/2}}$$

$$= I_1 + I_2 \qquad (4.122)$$

Some algebra and formulas 2.13 (49) and 1.13 (54) of the Bateman Manuscript Project [4.3] yield the following expression

$$\Psi(x,y) = -e^{-ik(x-y)ch\mu} + e^{-ikxch\mu + ikysh\mu}$$

$$+ ky \int_{y}^{x} d\sigma \, e^{-ik(x-\sigma)ch\mu} \frac{J_1\left[k(\sigma^2-y^2)^{1/2}\right]}{(\sigma^2-y^2)^{1/2}} \qquad (4.123)$$

The second term has the form of a reflected wave; the other terms are hard to interpret in their present form. It is interesting to compute $\Psi(x,y)$ near the characteristic line $x = y$

$$\lim_{x \to y_+} \Psi(x,y) = -1 + \Psi_r(y_+, y) \tag{4.124}$$

Expression (4.118) shows that

$$\lim_{x \to y_-} \Psi(x,y) = \Psi_r(y_-, y) \tag{4.125}$$

and thus $\Psi(x,y)$ has a jump discontinuity across the characteristic line $x = y$

$$[\Psi]_{y_-}^{y_+} = -1 \tag{4.126}$$

This type of discontinuity is allowed because the type of the partial differential equation used in our mathematical model is purely hyperbolic. If viscous terms were added to this equation, this sharp discontinuity would be replaced by small zones of strong continuous change.

Inversion by Change of Integration Contour

The procedure is the same as in section 4.2. We therefore outline only the main steps. We work in region D_+ where $x > y$, $y \geqslant 0$ and define the set of polar hyperbolic coordinates

$$x = \eta \operatorname{ch} \xi \tag{4.127}$$

$$y = \eta \operatorname{sh} \xi \tag{4.128}$$

with

$$0 \leqslant \eta < \infty$$

$$0 \leqslant \xi < \infty$$

We start from expression (4.117); the integration contour in (4.117) is represented on fig. 4-9. We want to replace this contour ⌣ by the ellipse E defined by (4.52). The ellipse contains the branch points $-k$ and $+k$ which are the only singularities of the integrand of (4.117) inside the initial contour ⌣ .

When $\zeta > \mu$ the ellipse encloses the pole $\alpha = kch\mu$ which does not belong to the interior of the initial contour ⌣ and its contribution must be subtracted. We have

$$0 < \zeta < \mu$$

$$\Psi(x,y) = \frac{1}{2\pi i} \int_{E} \frac{e^{-i\alpha x - \gamma y}}{\alpha - kch\mu} \, d\alpha \qquad (4.129)$$

$$\mu < \zeta < \infty$$

$$\Psi(x,y) = e^{-ikx ch\mu + iky sh\mu}$$

$$+ \frac{1}{2\pi i} \int_{E} \frac{e^{-i\alpha x - \gamma y}}{\alpha - kch\mu} \, d\alpha \qquad (4.130)$$

The ellipse contribution may be evaluated as in section 4.2 and leads to the remarkable result

$$\Psi_E = -G(\zeta + \mu, \eta) - G(\zeta - \mu, \eta) \qquad (4.131)$$

where the function $G(\lambda, \eta)$ has been defined by (4.61) and certain of its properties summarized at the end of section 4.2, expressions (4.65) through (4.77).

Using the Heaviside step function we can assemble (4.129) and (4.130) into

$$\Psi = e^{-ikx ch\mu + iky sh\mu} h(\xi - \mu)$$
$$-G(\xi + \mu, \eta) - G(\xi - \mu, \eta) \qquad (4.132)$$

in region D_+.

Using expression (4.69) it is easy to show that Ψ is continuous across the line $\xi = \mu$. The Heaviside function jump is compensated by a jump in $G(\xi - \mu, \eta)$:

$$\Psi(\xi_+, \eta) = e^{-ik\eta} - G(2\mu, \eta) - \frac{1}{2} e^{-ik\eta}$$
$$\Psi(\xi_-, \eta) = -G(2\mu, \eta) + \frac{1}{2} e^{-ik\eta}$$

Thus,

$$\Psi(\xi_+, \eta) = \Psi(\xi_-, \eta) = \frac{1}{2} e^{-ik\eta} - G(2\mu, \eta) \qquad (4.133)$$

Expression (4.68) provides the limit of Ψ near the line $x = y$ in the region D_+

$$\lim_{x \to y_+} \Psi(x, y) = -1 - \Psi_r(y_+, y) \qquad (4.134)$$

We found this limit previously, expression (4.124), and we showed that $\Psi(x, y)$ had a jump discontinuity across the characteristic line $x = y$.

An asymptotic expression for Ψ_E may be found by using (4.70):

$$\Psi_E \sim \frac{\sqrt{sh\,\xi}}{(2\pi k\eta)^{1/2}} \left[\frac{e^{-ik\eta+i\pi/4}}{ch\,\xi + ch\,\mu} - \frac{e^{ik\eta-i\pi/4}}{ch\,\xi - ch\,\mu} \right]$$

$$+ O\left[\frac{1}{k\eta(ch(\xi-\mu)-1)} \right] \tag{4.135}$$

From (4.132) we can write the complete field in D_+ as a sum of a geometrical optics field

$$\Psi_{g.o.} = \Psi_i + \Psi_r\, h\,(\xi - \mu) \tag{4.136}$$

and the field Ψ_E of expression (4.131). We call Ψ_E diffracted wave because of its properties.

Then in D_+ we have

$$\Psi_d = \Psi_E\,(\xi, \mu) \tag{4.137}$$

while in D_-

$$\Psi_{g.o.} = \Psi_i\, h\,(\mu - |\xi|) \tag{4.138}$$

$$\Psi_d = -\Psi_E\,(|\xi|, \mu) \tag{4.139}$$

with these definitions

$$\Psi_t = \Psi_{g.o.} + \Psi_d \tag{4.140}$$

The form (4.140) is by now familiar, separating the complete field in a geometrical optics field and a diffracted wave compensating for the discontinuities of the geometrical optics field. The line $\xi = \mu$ boundary of the reflection region has a polar angle δ_+ determined by (4.87). The meaning of this expression was discussed in Chapter 3.

The geometrical optics field behaves like in the subsonic situation: it is the diffracted wave which, while present for the same physical reasons, propagates differently.

A region of complete silence appears under the half plane in R_- , while R_+ is a region of pure reflection; in both regions $\Psi_d = 0$. At the boundaries of these two regions, the characteristics originating at the half plane edge, the diffracted wave has a jump discontinuity. Near the downward characteristic the diffracted wave propagates only and the value of the field oscillates strongly, the number of oscillations increasing with the value of kr . The mathematical explanation lies in the fact that when λ becomes large $G(\lambda, \eta)$ is asymptotic to $(1/2) J_0(k\eta)$; then when η tends to 0 from some finite value, the Bessel function oscillates around zero. Diffraction patterns are shown on fig. 4-10 for several values of kr . They show all the properties described above and a general appearance different from the subsonic case diffractic patterns.

REFERENCES

4.1   Miles, J. W., _Potential Theory of Unsteady Supersonic Flow_, Cambridge University Press, Cambridge (1959).

4.2   Noble, B., _Methods Based on the Wiener-Hopf Technique_, Pergamon Press, New York (1958).

4.3   Bateman Manuscript Project, _Tables of Integral Transforms_, Vol. I, A. Erdelyi, Ed., McGraw-Hill, New York (1954).

4.4   Copson, E. T., _Asymptotic Expansions_, Cambridge University Press, Cambridge (1967).

APPENDIX 4-A

Inversion of $\quad I = \dfrac{1}{2\pi} \displaystyle\int_{-\infty+ia}^{+\infty+ia} \gamma^{-1} e^{\gamma|y|-i\alpha x} d\alpha$

To apply the convolution theorem to expression (4.46) we need

$$I = \frac{1}{2\pi} \int_{-\infty+ia}^{+\infty+ia} \gamma^{-1} e^{\gamma y - i\alpha x} d\alpha \qquad (4A.1)$$

where

$$\gamma = (k^2 - \alpha^2)^{1/2}$$

$$a < -k_i\, ch\,\mu < -k_i$$

When $\quad x > -y \ , \ y > 0 \quad$ we close the integration path by a circle $\Gamma_R \quad$ in the lower half plane. As $\quad \underset{\Gamma_R}{Max}\ \gamma^{-1} \quad$ tends to O as R tends to infinity, this circle does not give any contribution to the integral

$$I = \frac{1}{2\pi} \int_{\smile} \gamma^{-1} e^{\gamma y - i\alpha x} d\alpha \qquad (4A.2)$$

The integrand is analytic inside $\quad\smile\quad$ and thus $I = O$ for $x > -y$. When $x < -y \ , \ y > 0 \quad$ we close the integration contour in (A4.1) by a big circle in the upper half plane, whose contribution to the integral also vanishes

$$I = \frac{1}{2\pi} \int_{\triangle} \gamma^{-1} e^{\gamma y - i\alpha x} d\alpha \qquad (4A.3)$$

We define the set of hyperbolic coordinates

$$x = -\eta \, ch\, \xi$$
$$y = \eta \, sh\, \xi \qquad\qquad (4A.\,4)$$

with

$$0 \leqslant \xi < \infty$$
$$0 \leqslant \eta < \infty$$

and replace the contour ⌒ by the ellipse **E** defined by

$$\alpha = k\, ch(\xi - it) \qquad\qquad (4A.\,5)$$
$$-\pi < t \leqslant \pi$$

which contains all the singularities of the integrand in (4A. 3).

For $\xi > 0$ and t going from $-\pi$ to π, the ellipse is described in the clockwise direction. Introducing (4A. 5) in (4A. 3) we obtain

$$I = -\frac{1}{2\pi} \int_{-\pi}^{\pi} e^{+ik\eta cos t} \, dt = -J_0(k\eta) \qquad (4A.\,6)$$

and then

$$I = -J_0\left[k\,(x^2-y^2)^{1/2}\right] \qquad\qquad x < -|y|$$

$$= 0 \qquad\qquad x > -|y| \qquad (4A.\,7)$$

APPENDIX 4-B

Properties of the Function $G(\lambda, \eta)$

The function $G(\lambda, \eta)$ is defined by

$$G(\lambda, \eta) = \frac{1}{2\pi} \int_0^\pi e^{ik\eta\cos t} \frac{sh\lambda}{\cos t + ch\lambda} dt \qquad (4B.1)$$

and was seen to play a central role for both positive and negative flow directions. We give here the proofs of the Lemmas 1 - 7 of the end of section 4.2.

Lemma 1

$G(\lambda, \eta)$ is an odd function of λ

$$G(-\lambda, \eta) = - G(\lambda, \eta) \qquad (4B.2)$$

Proof. The integrand of (4B.1) is odd with respect to λ and so is $G(\lambda, \eta)$.

Lemma 2

The function $G(\lambda, \eta)$ converges uniformly for λ belonging to $[\lambda_0, +\infty)$ and η belonging to $[\eta_0, +\infty)$ where λ_0 and η_0 are arbitrarily small but different from zero.

Proof. To show that $G(\lambda, \eta)$ converges for any λ and η in the intervals given in the lemma, we write the following inequalities:

$$|G(\lambda,\eta)| \leqslant \frac{1}{2\pi} \int_0^\pi \left| e^{-ik\eta\cos\varphi} \frac{sh\lambda}{ch\lambda - \cos\varphi} \right| d\varphi$$

$$\leqslant \frac{1}{2\pi} \int_0^\pi \left| \frac{(sh\lambda/ch\lambda)}{1 - (\cos\varphi/ch\lambda)} \right| d\varphi$$

$$\leqslant \frac{1}{2\pi} \int_0^{\pi/2} \frac{d\varphi}{1 - (\cos\varphi/ch\lambda)} + \frac{1}{2\pi} \int_{\pi/2}^\pi d\varphi$$

$$\leqslant \frac{1}{2} \coth\lambda_0 + \frac{1}{4} \tag{4B.3}$$

This shows that for a given $\lambda_0 \neq 0$, $G(\lambda,\eta)$ is bounded and thus converges.

Lemma 3

The function $G(\lambda,\eta)$ converges uniformly to $(1/2) J_0(k\eta)$ when λ tends to infinity

$$\lim_{\lambda \to \infty} G(\lambda,\eta) = (1/2) J_0(k\eta) \tag{4B.4}$$

Proof. $J_0(k\eta)$ may be represented by the integral expression

$$J_0(k\eta) = \frac{1}{\pi} \int_0^\pi e^{ik\eta\cos t} dt \qquad (4B.5)$$

then

$$\left| G(\lambda,\eta) - (1/2) J_0(k\eta) \right| \leqslant \frac{1}{2\pi} \int_0^\pi \left| e^{ik\eta\cos t} \left(\frac{sh\lambda}{\cos t + ch\lambda} - 1 \right) \right| dt$$

$$\leqslant \frac{1}{2\pi} \int_0^\pi \left| \frac{ch\lambda - sh\lambda + \cos t}{ch\lambda + \cos t} \right| dt$$

$$\leqslant e^{-\lambda} k_1 \qquad (4B.6)$$

Thus,

$$\lim_{\lambda \to \infty} G(\lambda,\eta) = (1/2) J_0(k\eta)$$

uniformly with respect to η .

Lemma 4

      The function $G(\lambda,\eta)$ converges to $\frac{1}{2}$ when η tends to 0 and λ tends to infinity

$$\lim_{\lambda \to \infty, \eta \to 0} G(\lambda,\eta) = 1/2 \qquad (4B.7)$$

This is a direct consequence of Lemma 3.

Lemma 5

The function $G(\lambda, \eta)$ has a jump discontinuity at $\lambda = 0$.
When λ tends to 0 by superior values

$$\lim_{\lambda \to 0_+} G(\lambda, \eta) = \frac{1}{2} e^{-ik\eta} \tag{4B.8}$$

Proof. We decompose the interval $|0, \pi]$ in two parts

$$G(\lambda, \eta) = \frac{1}{2\pi} \int_0^\epsilon e^{-ik\eta \cos\varphi} \frac{\mathrm{sh}\,\lambda}{\mathrm{ch}\,\lambda - \cos\varphi} \, d\varphi$$

$$+ \frac{1}{2\pi} \int_\epsilon^\pi e^{-ik\eta\cos\varphi} \frac{\mathrm{sh}\,\lambda}{\mathrm{ch}\,\lambda - \cos\varphi} \, d\varphi$$

$$= I_1 + I_2 \tag{4B.9}$$

We apply to I_1 the mean value theorem

$$I_1 = \frac{1}{2\pi} \int_0^\epsilon e^{-ik\eta \cos\varphi_1} \frac{\mathrm{sh}\,\lambda}{\mathrm{ch}\,\lambda - \cos\varphi} \, d\varphi$$

with $0 < \varphi_1 < \epsilon$ and use the change of variable $\tau = \tan\dfrac{\varphi}{2}$ to get

$$I_1 = \frac{1}{\pi} e^{-ik\eta\cos\varphi_1} \tan^{-1}\left[\frac{\tan(\epsilon/2)}{\mathrm{th}\,(\lambda/2)}\right] \tag{4B.10}$$

Then

$$|I_2| \leqslant \frac{1}{2\pi} \int_{\epsilon}^{\pi} \left| \frac{sh\lambda}{ch\lambda - \cos\varphi} \right| d\varphi$$

$$\leqslant \frac{sh\lambda}{\epsilon^2} \tag{4B.11}$$

From (4B.10) and (4B.11) we conclude

$$\lim_{\substack{\lambda \to 0_+ \\ \epsilon \to 0}} I_1 = (1/2) e^{-ik\eta}$$

$$\lim_{\substack{\lambda \to 0_+ \\ \epsilon \to 0}} I_2 = 0$$

and thus

$$\lim_{\lambda \to 0_+} G(\lambda, \eta) = (1/2) e^{-ik\eta}$$

Lemma 6

When $k\eta(ch\lambda - 1) \gg 1$, $G(\lambda, \eta)$ has an asymptotic expansion of the form

$$G(\lambda, \eta) \sim \frac{1}{(8\pi k\eta)^{1/2}} \left[coth\frac{\lambda}{2} \; e^{-ik\eta + i\pi/4} \right.$$

$$\left. + th\frac{\lambda}{2} \; e^{ik\eta - i\pi/4} \right] + O\left[\frac{1}{k\eta(ch\lambda - 1)} \right] \tag{4B.12}$$

Proof. A simple application of the method of stationary phase

(Copson [4.4], p. 27) to expression (4B.1) whose stationary points are $t = 0$ and $t = \pi$ gives

$$G(\lambda, \eta) \sim \frac{1}{2\pi} \left(\frac{\pi}{2k\eta}\right)^{1/2} \frac{sh\lambda}{ch\lambda - 1} e^{-ik\eta + i\pi/4}$$

$$+ \frac{1}{2\pi} \left(\frac{\pi}{2k\eta}\right)^{1/2} \frac{sh\lambda}{ch\lambda + 1} e^{ik\eta - i\pi/4} + O\left(\frac{1}{k\eta}\right)$$

but does not yield the condition $k\eta(ch\lambda - 1) \gg 1$. To obtain this information we proceed as follows.

We multiply the definition of $G(\lambda, \eta)$ by $e^{ik\eta ch\lambda}$ and differentiate with respect to η

$$\frac{d}{d\eta} \left[G(\lambda, \eta) e^{ik\eta ch\lambda}\right] = \frac{ik}{2\pi} \int_0^\pi e^{ik\eta(cost + ch\lambda)} sh\lambda \, dt \qquad (4B.13)$$

The integral on the right hand side converges uniformly for $\lambda \in (0, +\infty)$ and $\eta \in (0, +\infty)$. According to Lemma 2, the integral defining $G(\lambda, \eta)$ also converges uniformly in the same intervals. The differentiation is thus justified.

Then (4B.13) yields

$$\frac{d}{d\eta} \left[G(\lambda, \eta) e^{ik\eta ch\lambda}\right] = \frac{ik sh\lambda}{2} e^{ik\eta ch\lambda} J_0(k\eta) \qquad (4B.14)$$

which, together with

$$\lim_{\eta \to \infty} G(\lambda, \eta) = 0 \qquad (4B.15)$$

gives

$$G(\lambda, \eta) = - \frac{ik\,sh\lambda}{2} e^{-ik\eta\,ch\lambda} \int_{\eta}^{\infty} e^{ik\sigma\,ch\lambda} J_0(k\eta)\,d\sigma \qquad (4B.16)$$

We now consider $k\eta$ sufficiently large and use for $J_0(k\sigma)$ its asymptotic expansion

$$J_0(k\sigma) \sim \left(\frac{2}{\pi k\sigma}\right)^{1/2} \cos(k\sigma - \pi/4) \qquad (4B.17)$$

Introduction of (4B.17) in (4B.16) and changes of variable of the form $v^2 = k\sigma(ch\lambda - 1)$ and $v^2 = k\sigma(ch\lambda + 1)$ yield

$$G(\lambda, \eta) \sim - \frac{i}{2} sh\lambda\, e^{-ik\eta\,ch\lambda} \left(\frac{2}{\pi}\right)^{1/2} \Bigg\{$$

$$(ch\lambda - 1)^{-1/2} \int_{[k\eta(ch\lambda-1)]^{1/2}}^{+\infty} e^{iv^2 + i\pi/4}\,dv$$

$$+ (ch\lambda + 1)^{-1/2} \int_{[k\eta(ch\lambda-1)]^{1/2}}^{+\infty} e^{iv^2 + i\pi/4}\,dv\Bigg\} + O(1/k\eta) \qquad (4B.18)$$

When $k\eta(ch\lambda - 1) \gg 1$ we can evaluate the two integrals by integration by parts, and this finally yields (4B.12).

Lemma 7

When $k\eta(ch\lambda - 1) \ll 1$ and $k\eta \gg 1$ an asymptotic expansion for $G(\lambda, \eta)$ is

$$G(\lambda, \eta) \sim \text{sgn}(\lambda) \, (1/2) \, e^{-ik\eta} + O\left\{[k\eta(\text{ch}\lambda - 1)]^{1/2}\right\}$$

$$+ \, O\left[(k\eta)^{-1/2}\right] \tag{4B.19}$$

Proof. We start from expression (4B.18) but now the first integral gives

$$\int_{[k\eta(\text{ch}\lambda-1)]^{1/2}}^{+\infty} e^{iv^2} dv = \frac{\pi^{1/2}}{2} e^{i\pi/4} + O\left\{[k\eta(\text{ch}\lambda-1)]^{1/2}\right\}$$
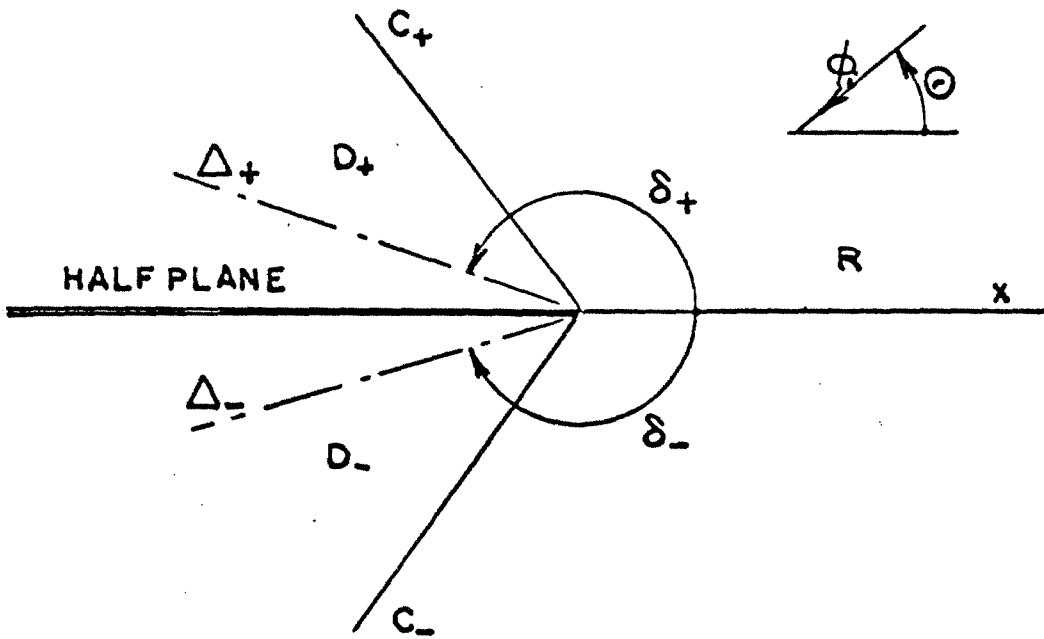
The asymptotic expansion (4B.19) follows immediately.

Fig. 4-1a.   Geometry of the problem, M < 0 .
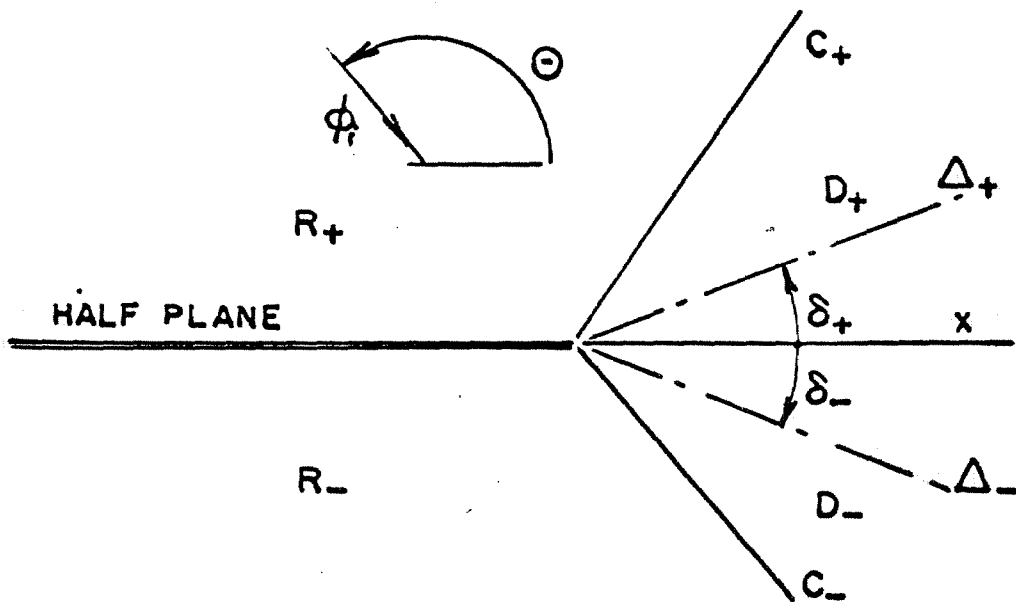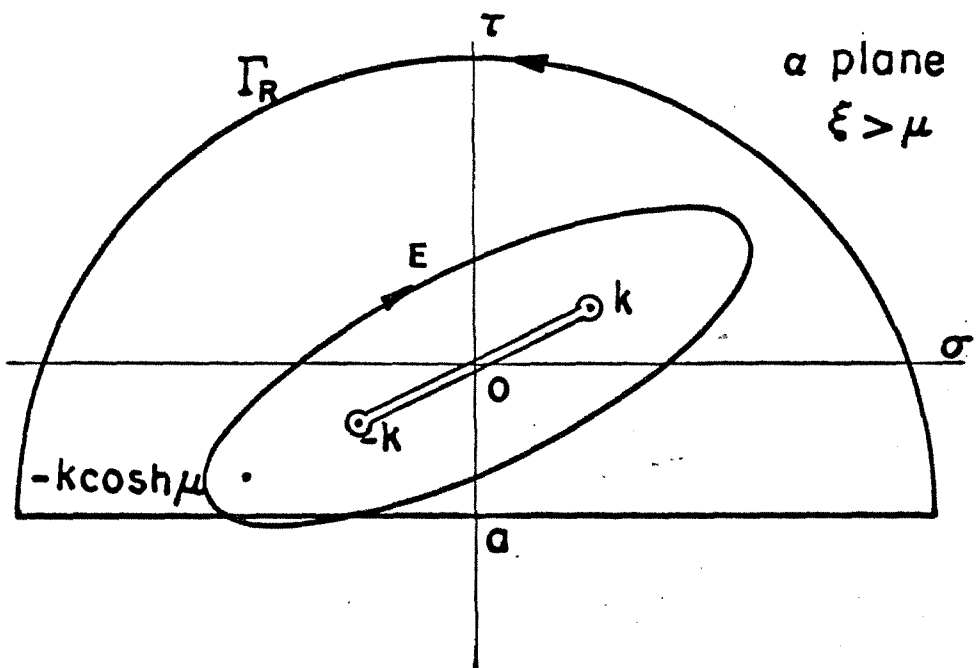

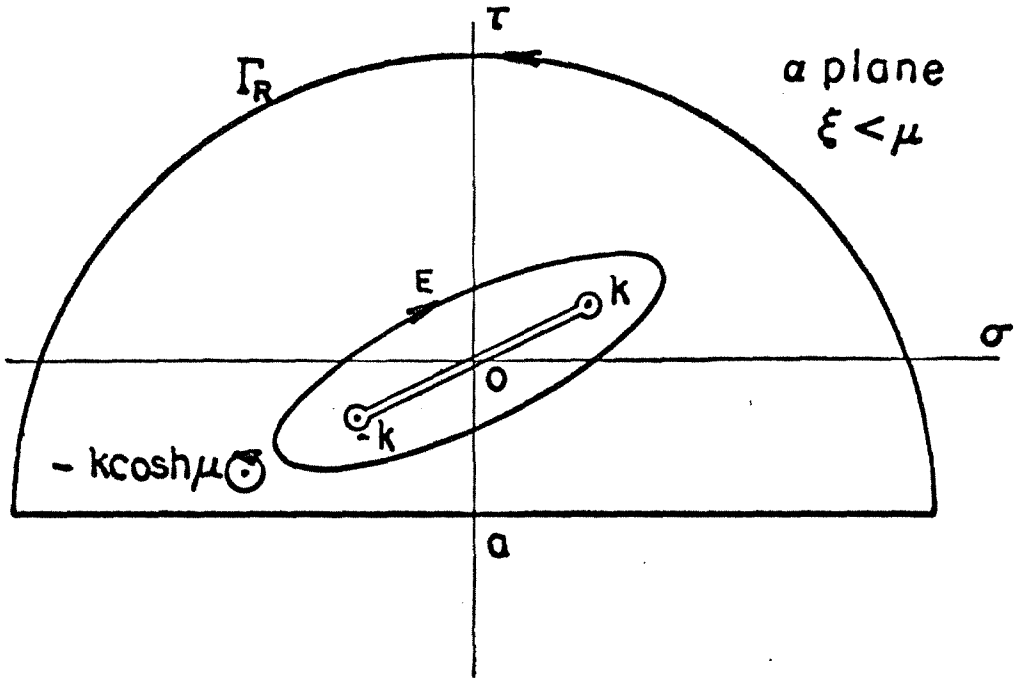Fig. 4-1b.   Geometry of the problem, M > 0 .

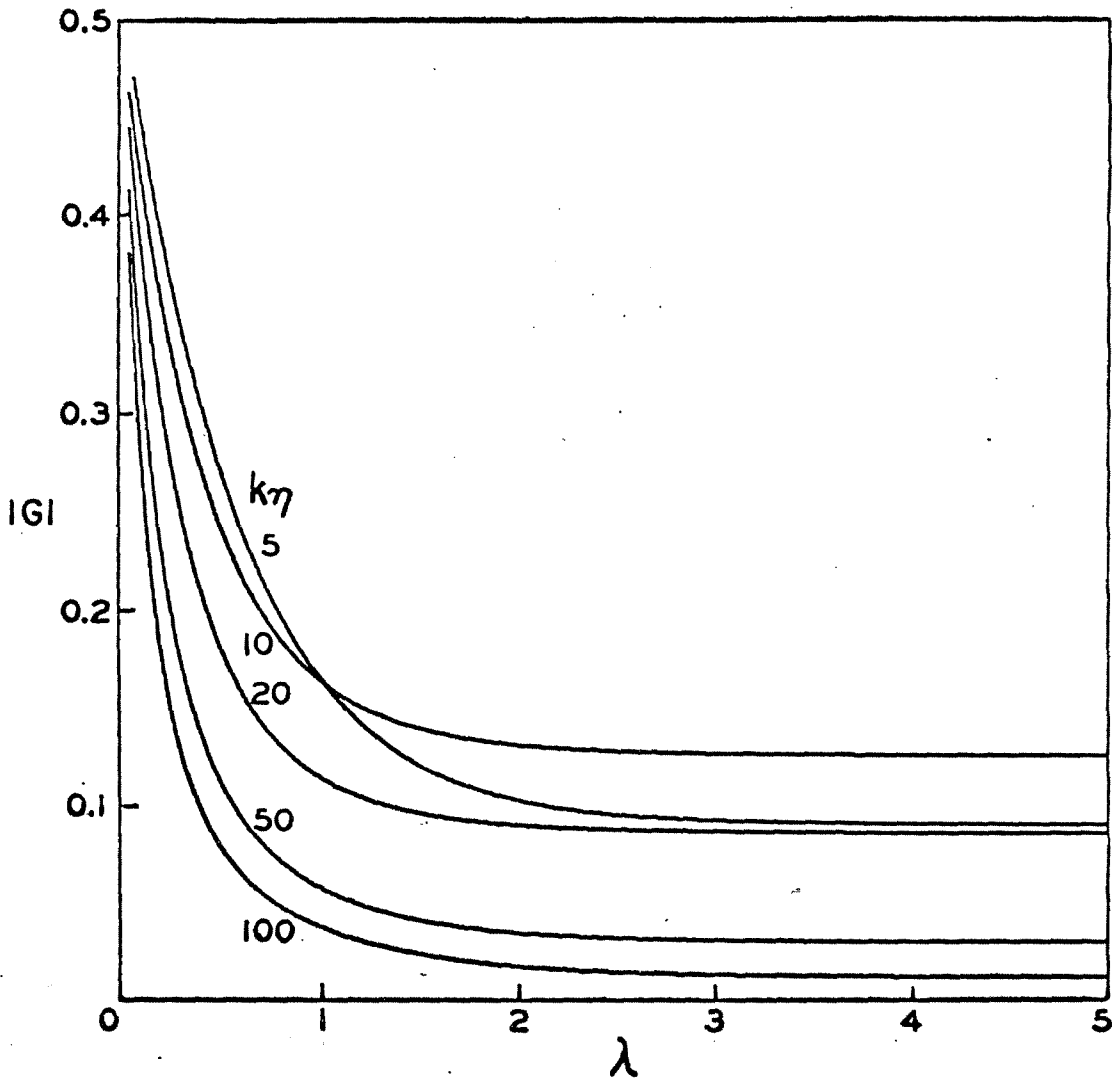Fig. 4-2.   Integration contours in the complex α plane for $M < 0$.

Fig. 4-3. Modulus of the function $G(\lambda, \eta)$

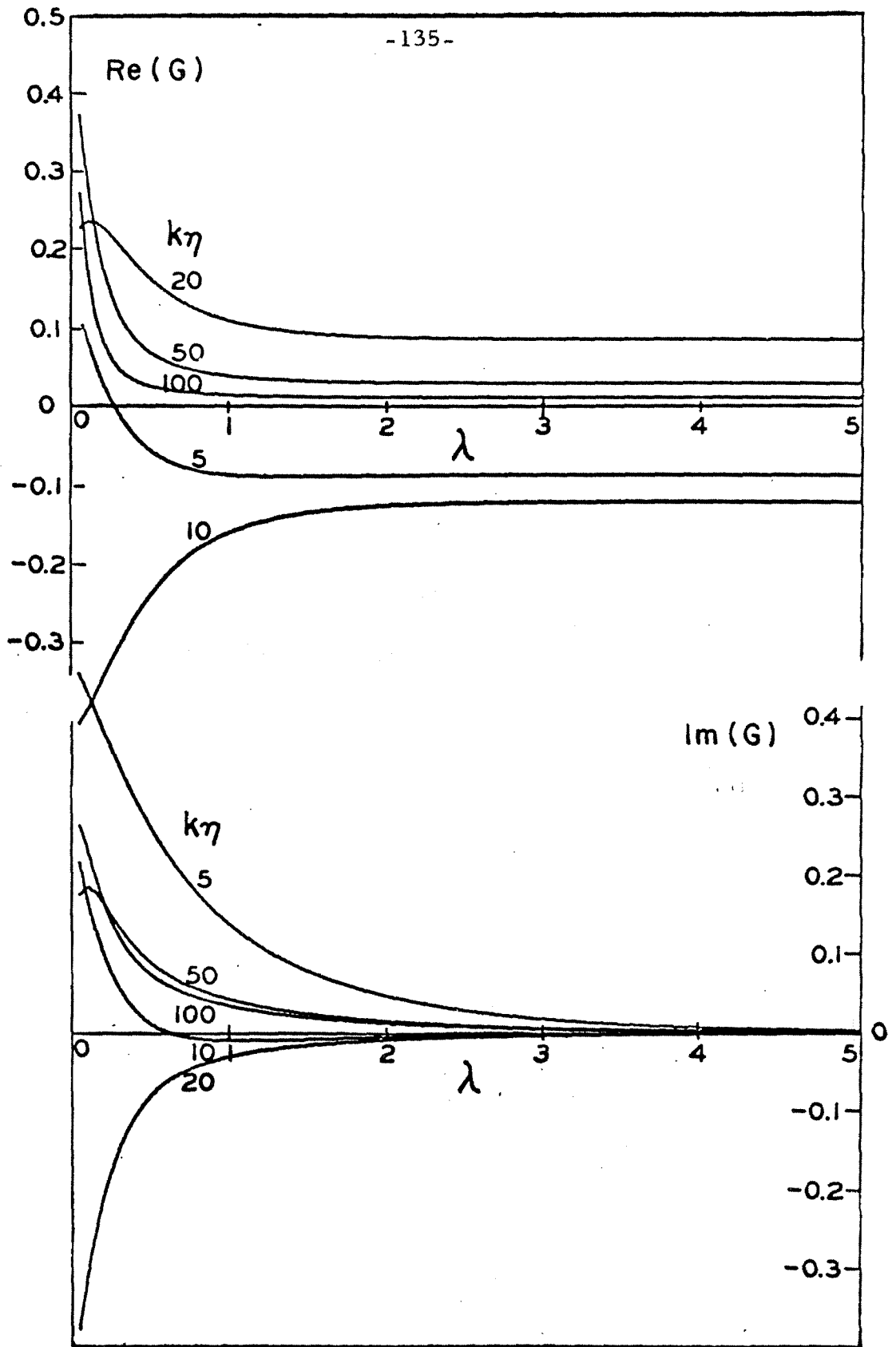$$G(\lambda, \eta) = \frac{1}{2\pi} \int_0^\pi e^{ik\eta \cos t} \frac{sh\lambda}{\cos t + ch\lambda} dt$$

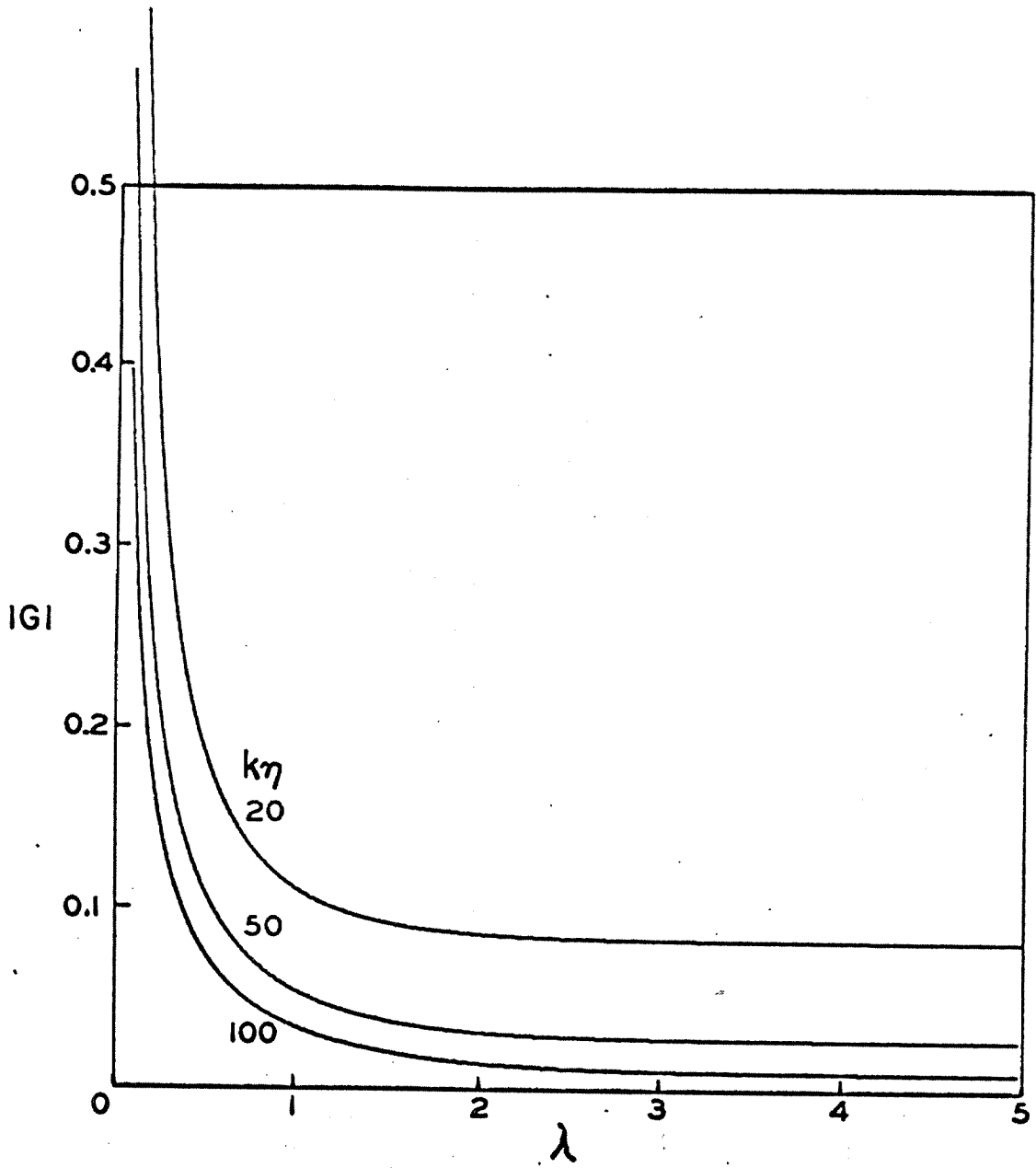Fig. 4-4. Real and imaginary parts of the function $G(\lambda, \eta)$

Fig. 4-5. Asymptotic expression (4.70) of $G(\lambda, \eta)$ for $k\rho(ch\lambda-1) \gg 1$
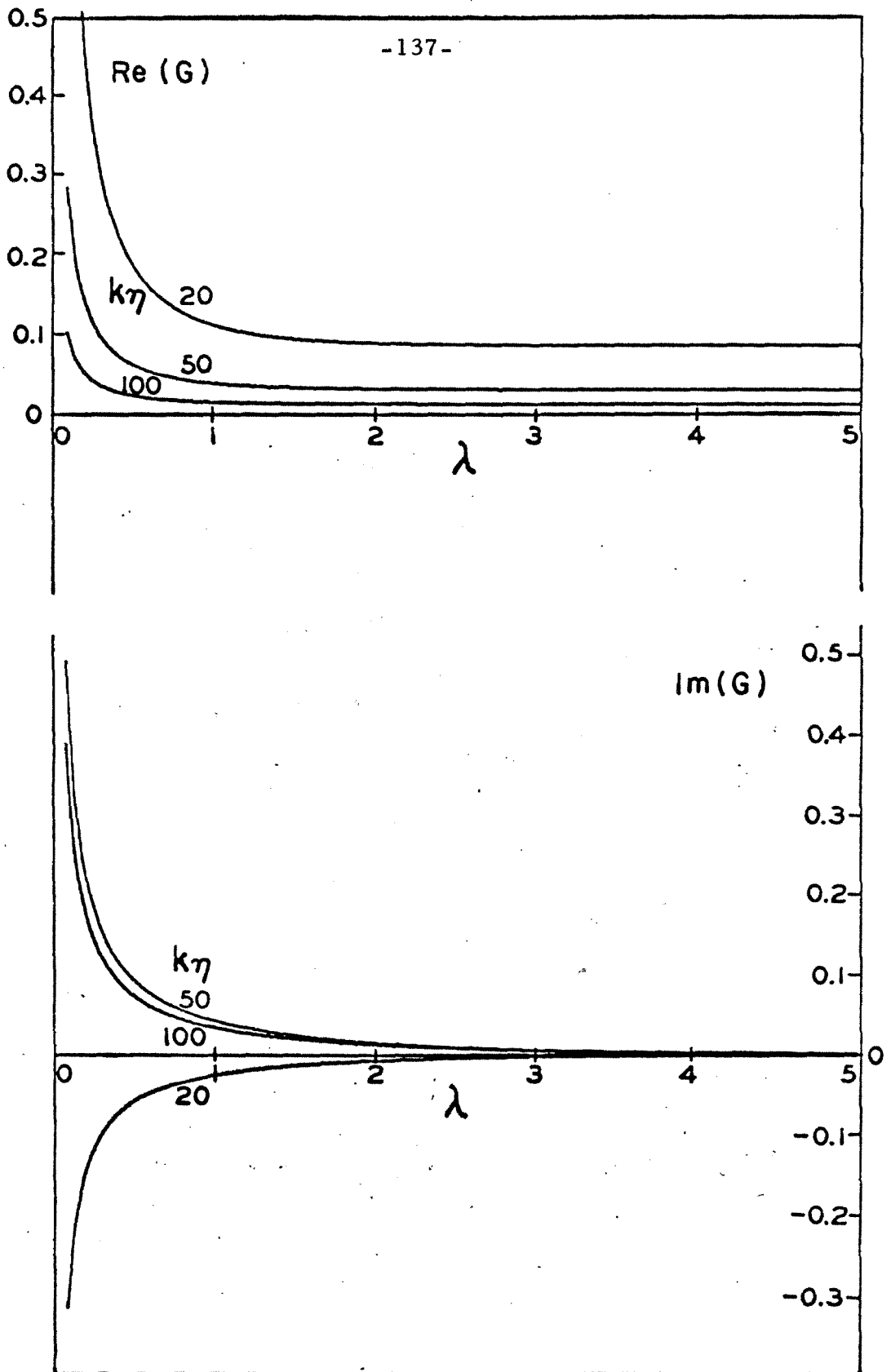
Fig. 4-6. Asymptotic expressions (4.70) of the real and imaginary parts of $G(\lambda, \eta)$ for $k\eta(ch-1) \gg 1$
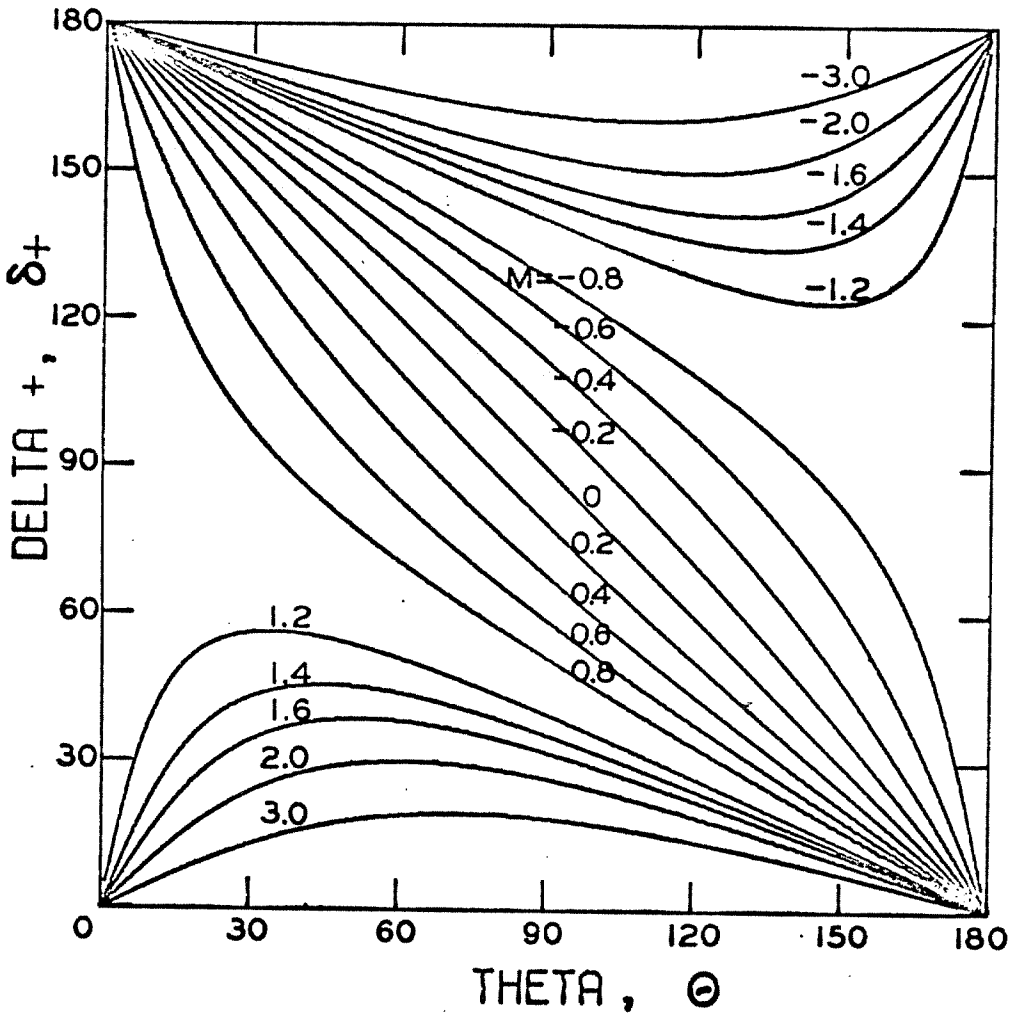
Fig. 4-7. Polar angle $\delta+$ defining the boundary of the reflection region. The boundary of the shadow region is at $\delta_- = -\delta_+$

Fig. 4-8a. Diffraction pattern of a plane wave impinging on a half plane in a supersonic moving medium, M = -1.2. The plane wave incidence angle $\Theta = 40^{\circ}$, kr = 30.

Fig. 4-8b. Diffraction pattern of a plane wave impinging on a half plane in a supersonic moving medium, M = -1.2. The plane wave incidence angle $\odot$ = 40°, kr = 40.
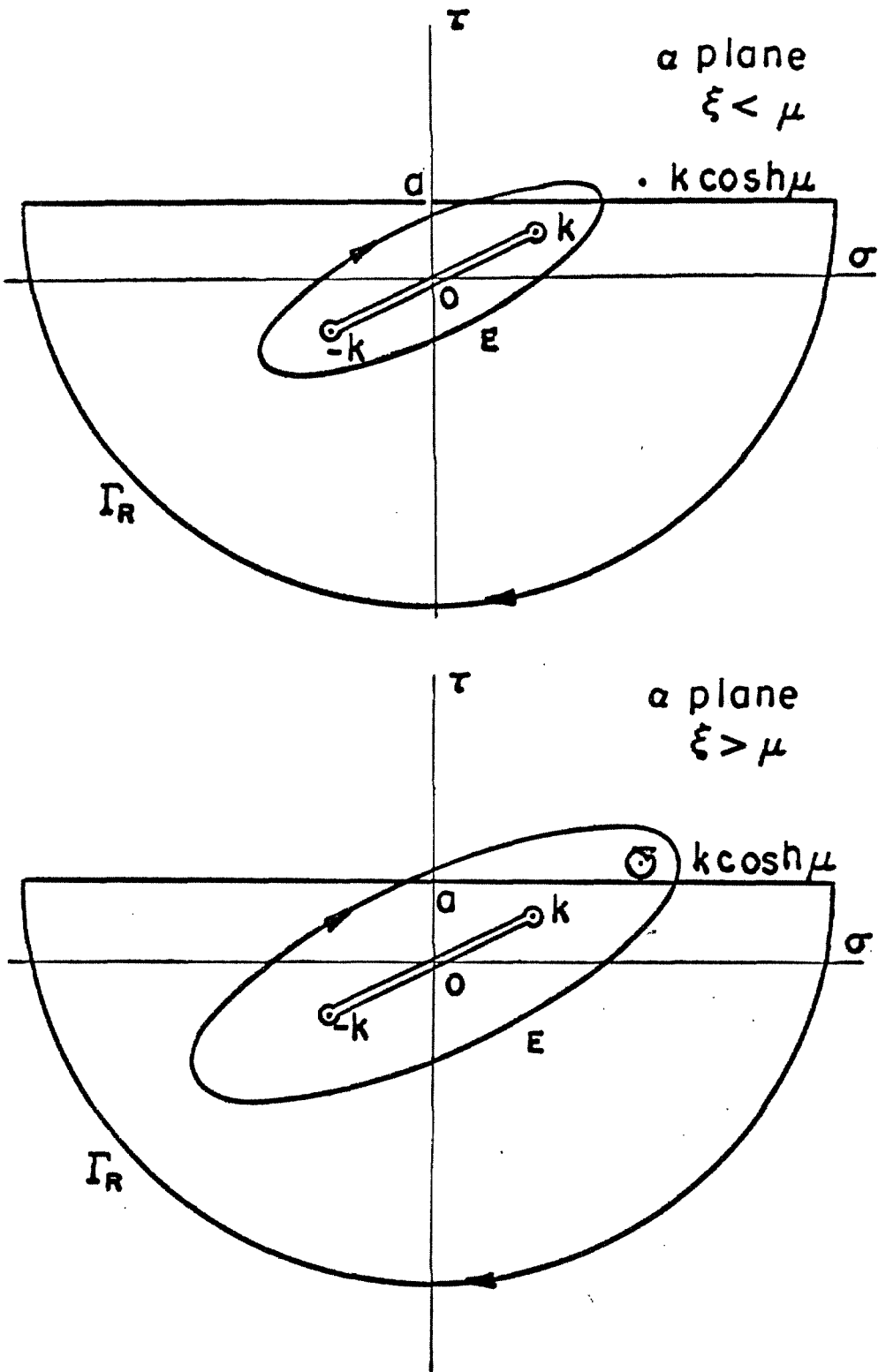
Fig. 4-9. Integration contours in the complex α plane for $M > 0$.
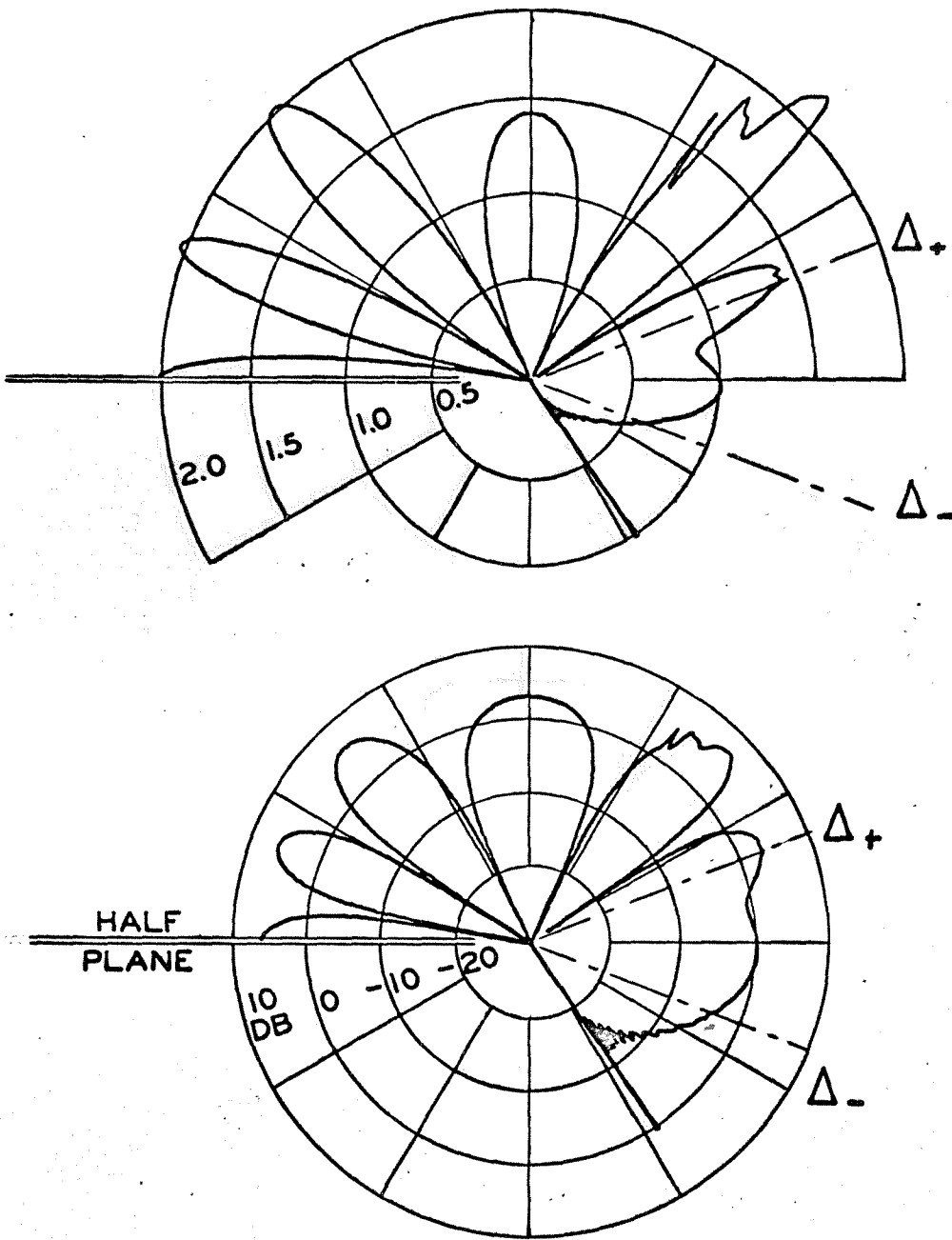
Fig. 4-10a. Diffraction pattern of a plane wave impinging on a half
plane in a supersonic moving medium, M = 1.2. The
plane wave incidence angle Θ = 130$^\sigma$, kr = 20.

Fig. 4-10b. Diffraction pattern of a plane wave impinging on a half
plane in a supersonic moving medium. M = 1.2. The
plane wave incidence angle Θ = 130°, kr = 30.

Fig. 4-10c. Diffraction pattern of a plane wave impinging on a half plane in a supersonic moving medium, $M = 1.2$. The plane wave incidence angle $\Theta = 130^\circ$, $kr = 40$.
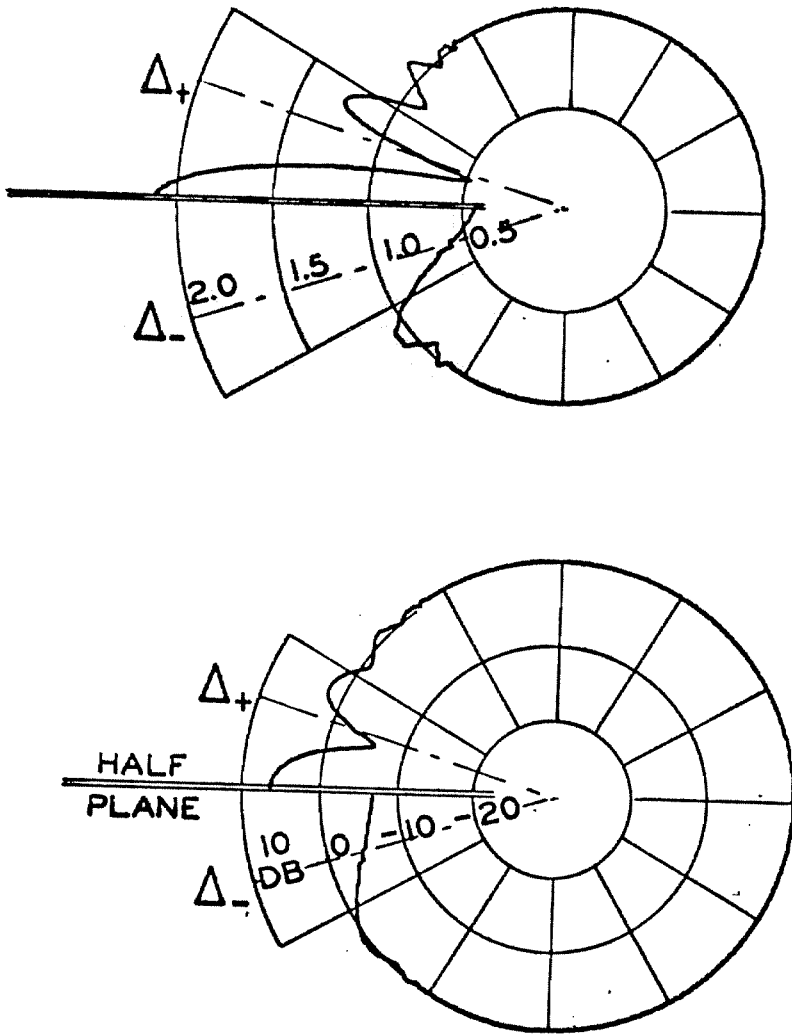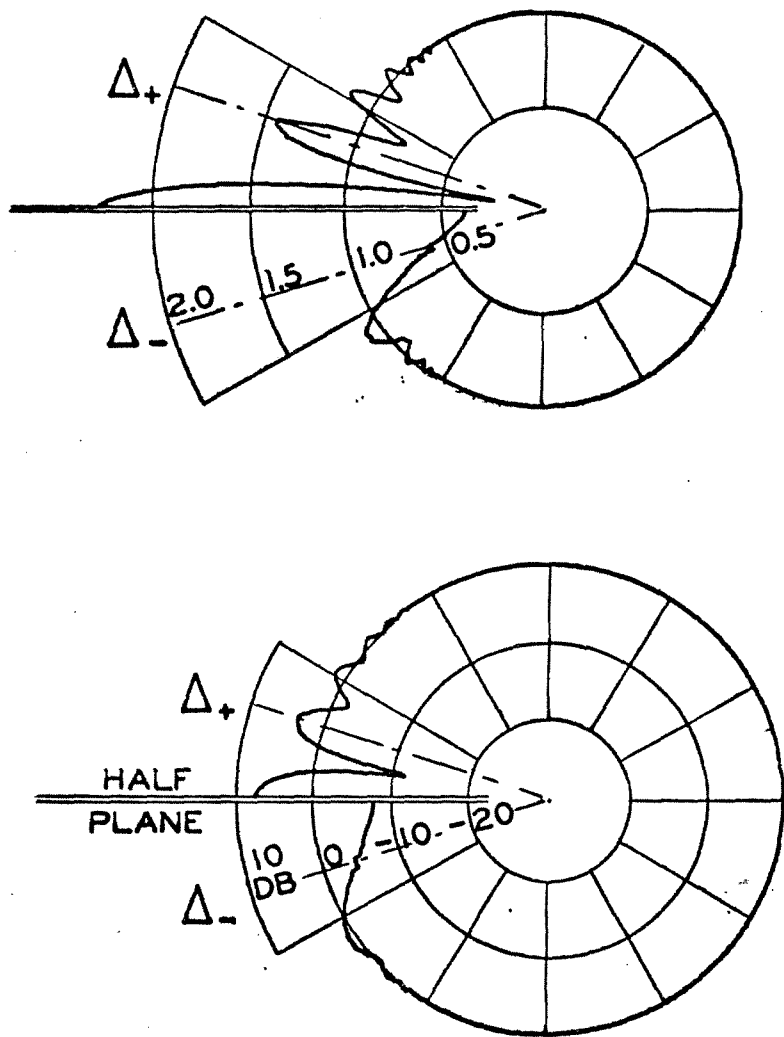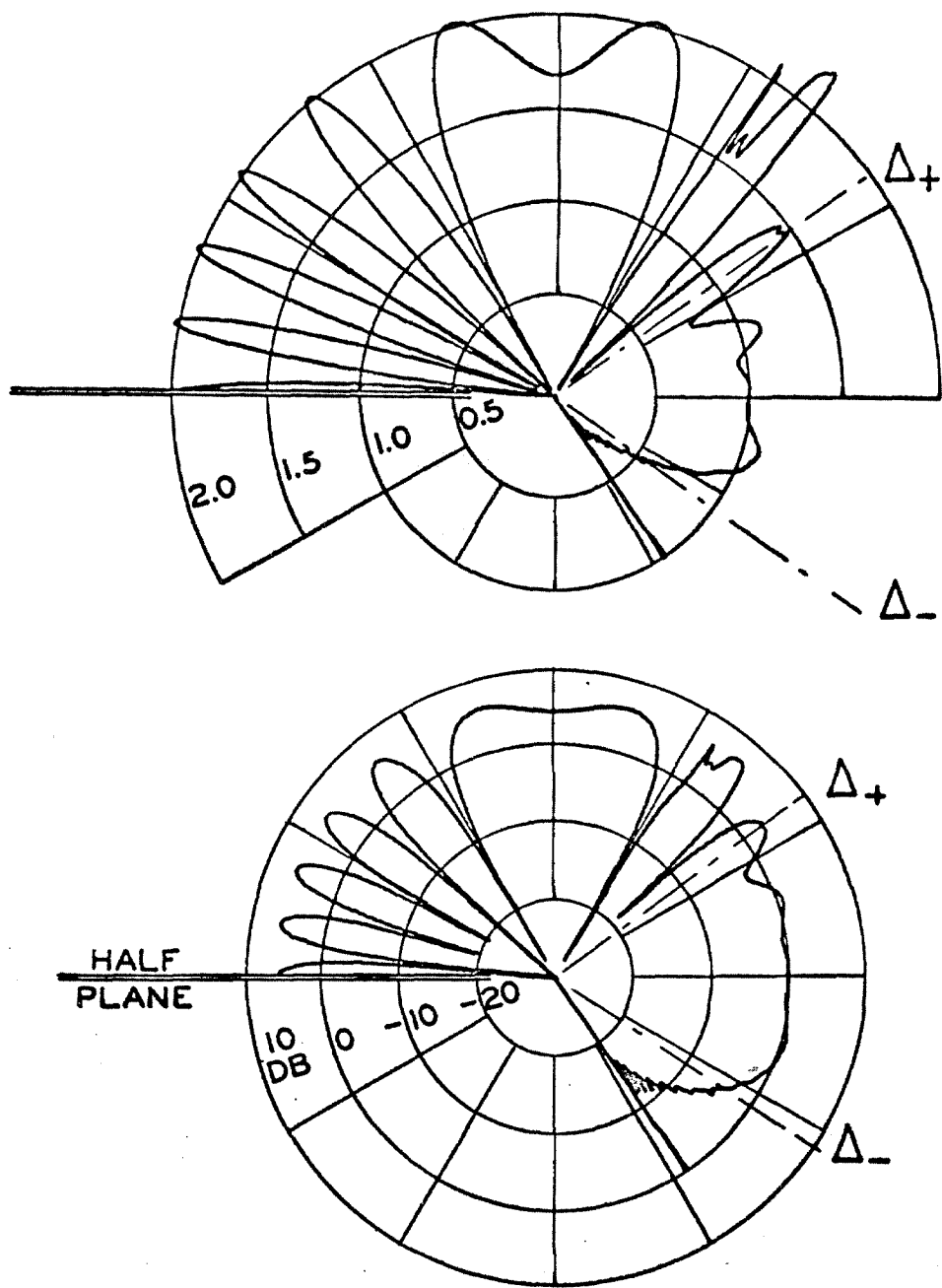
Fig. 4-10d. Diffraction pattern of a plane wave impinging on a half plane in a supersonic moving medium, $M = 1.2$. The plane wave incidence angle $\Theta = 100^b$, $kr = 20$.
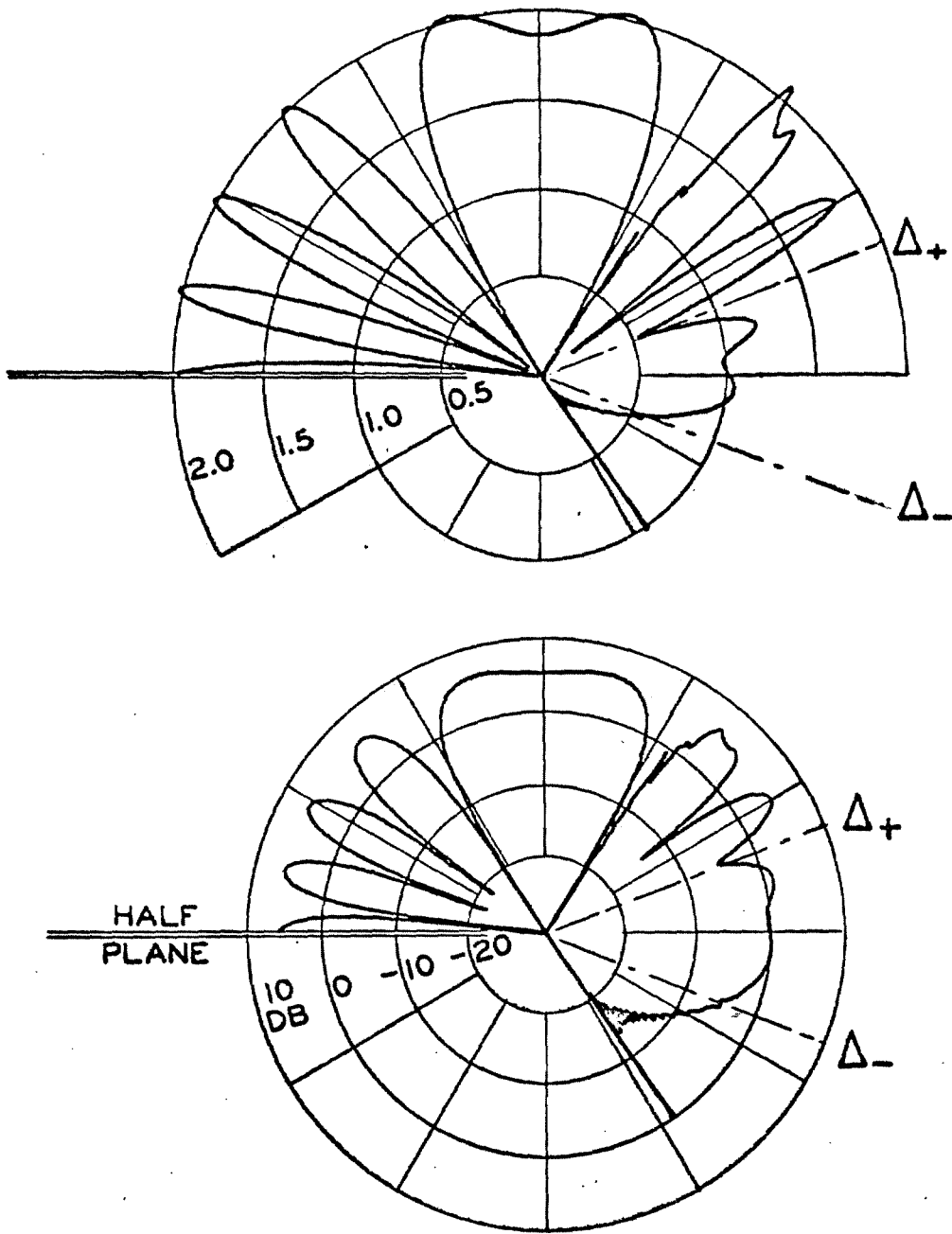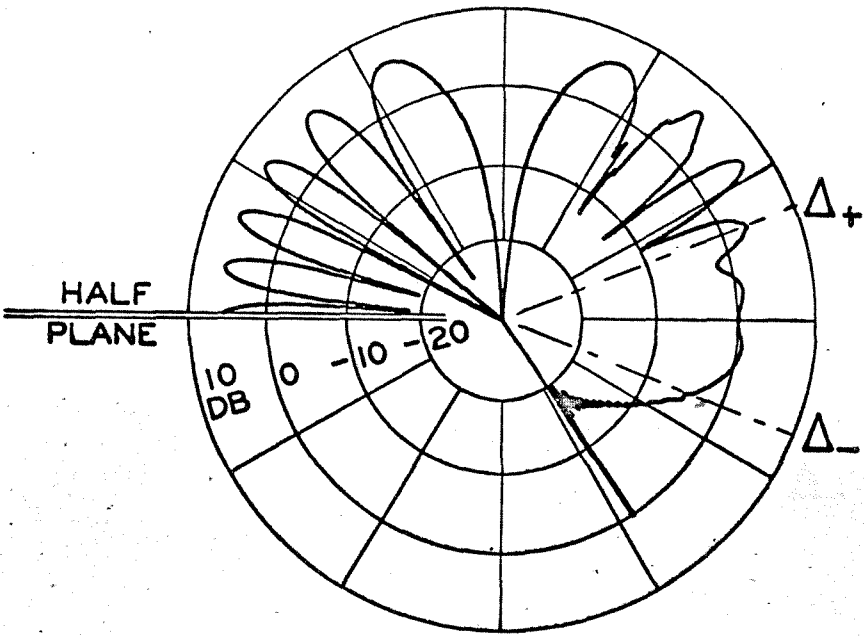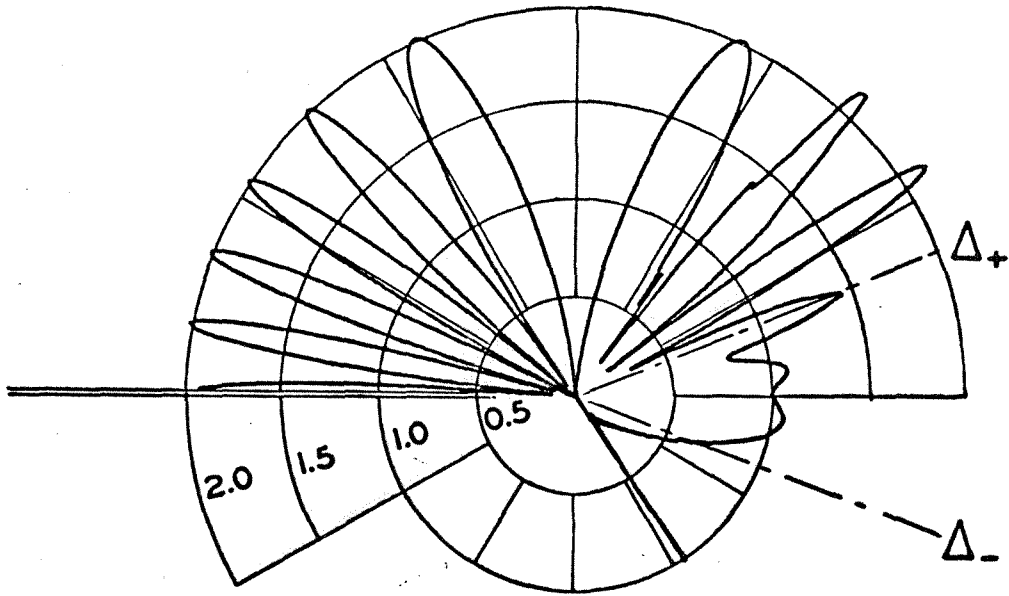
CHAPTER V

ACOUSTIC RADIATION FROM A TWO-DIMENSIONAL DUCT.
EFFECTS OF UNIFORM FLOW AND DUCT LINING.

5.1 INTRODUCTION

In the present high bypass-ratio turbofan engines the internal noise associated with the turbomachinery has become a major problem. The fan, which is the largest element, displaces the greatest amount of air and is most exposed to ground observation, is a strong noise generator. The noise produced consists of three types: broadband turbulence-generated noise, discrete tones generated by rotor blade passage and wake impingement on the stator vanes, multiple pure tones at lower frequencies associated with rotating shock patterns.

The discrete noise generation by axial compressors has been described by Tyler and Soffrin [5.1]. This noise is produced at the blade passage frequency and its harmonics and excites various propagating and attenuating duct modes. This discrete tone noise is prominent in present day engines with pressure levels reaching up to 160 db in the inlet duct and frequencies situated in the range 2000 to 7000 Hz of greatest sensitivity for the human ear (Marsh, et al. [5.2]).

Recently, Mather and Savidge [5.3] have suggested that what is considered as broadband noise might be identified, by a more detailed spectral analysis, as a series of discrete tones associated with the shaft rotation frequency and the stator guide vane number. They also show that these tones propagate like plane waves.

An important aspect of the transmission of sound generated by a turbofan is the radiation from the duct end section into the surrounding space.

The angular distribution of acoustic energy flow directly influences the sound pressure level at various positions with respect to

the aircraft and is of particular importance on the ground and on the sideline. In usual practice, the distribution patterns are computed by replacing the duct by an infinite wall with an aperture, neglecting the flow presence, and applying the Fraunhofer approximation of optics (such computations may be found, for instance, in reference [5.1]). These are strong assumptions and some doubt should be cast on the resulting radiation patterns and, in particular, on the predictions for the sideline radiation.

In the existing literature, the possibility of changing the radiation pattern by modifying the aperture field (i.e., by modifying the types of propagating modes) has received little attention. The problem of turbofan noise reduction is usually approached in two ways. In a first approach, a better aerodynamic design is sought which minimizes the noise generation by the fan. In a second approach, various acoustic devices, absorbing lining or resonator arrays, are inserted in the duct to attenuate the pressure modes before their radiation into the surrounding space.

Lowson [5.4] discusses the effect of the mode number on the radiation efficiency and angular distribution. Experimental results given by Copeland and Crigler [5.5] show reduced power and improved radiation patterns (less side radiation) for the lowest mode numbers.

While the attenuation properties of acoustical lining have been extensively studied, its effect on the external radiation also seems to be overlooked.

The purposes of this chapter are several. First we discuss

the validity of the approximations of the standard Fraunhofer computational scheme. For this we have developed in Appendix 5-A an exact solution by the Wiener Hopf technique, and in Appendix 5-B an approximate solution for the radiation problem for a simple duct made of two parallel semi-infinite plates. After comparing these solutions the effects of a parallel uniform gas flow are studied by using the simple transformation introduced in Chapter 3.

Finally, we discuss some aspects of the sound radiation from a duct with sound-absorbing lining or "soft walls." It is also shown that the same general technique may be used to solve the radiation problem in the presence of a uniform flow and absorbing walls. These results are of technological interest because they give an upper bound to the effects we can expect to obtain by installation of absorbing material on the duct walls.

5.2 ANALYSIS OF THE PROBLEM

Radiation Problem in a Stationary Medium

Consider a semi-infinite cylindrical duct parallel to the x-axis, its end section at $x = 0$, normal to the x-axis. Suppose for the moment that the duct has hard, or perfectly reflecting, walls.

Because the medium is stationary the pressure perturbation and velocity potential are proportional and may be used interchangeably to describe the boundary value problem. The problem will thus be stated in terms of a general potential ϕ^0.

All waves are considered steady with a time factor $\exp(-i\omega t)$ and satisfy the following boundary value problem:

$$\phi^0_{xx} + \phi^0_{yy} + \phi^0_{zz} + k^2 \phi^0 = 0 \qquad (5.1)$$

with $\quad k = \omega/c$

$$\frac{\partial \phi}{\partial n} = 0 \qquad \text{as the cylinder surface } D. \qquad (5.2)$$

The boundary condition expresses that the displacement vanishes at the hard wall. We decompose the complete field ϕ^0_t into an incoming wave ϕ^0_i travelling along the duct in the positive x direction and a field ϕ^0 induced by the incoming wave ϕ^0_i when it radiates from the duct end

$$\phi^0_t = \phi^0_i + \phi^0 \qquad (5.3)$$

The total field ϕ^0_t must satisfy one of the edge conditions:

$$\phi^0_t(x, R_+(\theta), \theta) - \phi^0_t(x, R_-(\theta), \theta) \sim x^{1/2} \qquad (5.4)$$

as $X \longrightarrow 0_-$ on the duct surface, or

$$\frac{\partial \phi_t^0}{\partial y} \sim x^{-1/2} \tag{5.5}$$

as $X \longrightarrow 0_+$ on the continuation of the duct.

The physical meaning of conditions (5.4) and (5.5) was discussed in Chapter 3.

In addition to (5.1) and (5.2), the induced potential ϕ^0 must satisfy Sommerfeld's radiation condition at infinity,

$$\lim_{r \to \infty} r \left(\frac{\partial \phi^0}{\partial n} - i k \phi^0 \right) = 0 \tag{5.6}$$

We suppose that some generating mechanism has excited one of the duct modes which propagates unattenuated in the positive X direction towards the duct end. This constitutes the incoming wave and the corresponding potential has the form

$$\phi_i^0 = e^{i k_x x} f(y, z) \tag{5.7}$$

This potential satisfies (5.1) and (5.2) and thus $f(y, z)$ is an eigenfunction of the problem

$$f_{yy} + f_{zz} + \mu^2 f = 0 \tag{5.8}$$

$$\frac{\partial f}{\partial n} = 0 \tag{5.9}$$

on the duct surface, with μ defined by

$$\mu^2 = k^2 - k_x^2 \tag{5.10}$$

Non-trivial solutions of the problem (5.8), (5.9) occur only for the eigenvalues μ_{mn} of μ. We wish to consider a propagating

mode as incoming wave, that is, a mode with a wave number real.

From (5.10),

$$k_x = k \left[1 - (\mu/k)^2 \right]^{1/2} \tag{5.11}$$

then k_x is real if $\mu^2 < k^2$. The factor $\left[1 - (\mu/k)^2 \right]^{1/2}$ appears very often and is therefore given a specific symbol

$$\eta = \left[1 - (\mu/k)^2 \right]^{1/2} \tag{5.12}$$

In order to discuss the effects of free stream flow and wall absorption we need a reliable computation scheme for radiation patterns in a stationary medium. Consider a duct formed by two parallel semi-infinite plates (Fig. 5-1); an exact solution for the radiation from this duct may be obtained utilizing the Wiener-Hopf technique (a good exposition may be found in Noble [5.6], pp. 105-110). This solution is arranged in computable form in Appendix 5-A.

Radiation problems are most generally solved by an approximate method developed in Appendix 5-B. In this method the duct is replaced by a plane screen with an aperture and the Fraunhofer approximation is used. This leads to a simple relation between the far field radiation and the Fourier transform of the field in the aperture, (5-B. 19) or (5-B.26). This method may therefore be applied to any cylindrical geometry for which the Wiener-Hopf solution is intractable. It also provides a useful tool for analytical study of the influence on the radiation pattern of a change in the aperture field.

Consider now an incoming wave of pressure amplitude A travelling in the duct of Fig. 5-1

$$p_i = A e^{ik_x x} \cos \mu_N (y - b) \tag{5.13}$$

where

$$\mu_N = N\pi / 2kb \tag{5.14}$$

and N is an integer less than $2kb/\pi$.

The pressure far field outside the duct has the form

$$p_t \sim A h(\theta; kb, N) (b/r)^{1/2} \tag{5.15}$$

We call the function $h(\theta; kb, N)$ the pressure angular distribution. The function h is dimensionless, of $O(1)$ and depends only on the reduced frequency $kb = \omega b/c$ and on the mode number N . (When a uniform flow is present h depends also on the Mach number M).

We also define

$$D(\theta; kb, N) = 20 \log_{10} h(\theta; kb, N) \tag{5.16}$$

the value of h in decibels.[*] The sound pressure level in the far field may then be obtained from (5.15),

---

[*]   We have taken some care in defining the angular distribution function, because this is not a standard quantity. As can be seen, $h(\theta; kb, N)$ conveys information on both amplitude and angular distribution and permits a direct computation of the SPL using relation (5.17).

The directivity index and directivity factor commonly used in acoustics (Beranek [5.7], p. 109) and taking the field of a unit source radiating in free space as a reference are more difficult to handle, and moreover the radiation of a unit source in free space has no physical meaning for the present application.

$$SPL = 20 \log_{10} P_t/P_{ref} \quad , \quad P_{ref} = 2 \cdot 10^{-5} N/m^2$$

or

$$SPL = 20 \log_{10} \hat{h}(\theta; kb, N) + 20 \log_{10} (A/P_{ref})$$
$$+ 20 \log_{10} (b/r)^{1/2}$$

thus

$$SPL = SPL(duct) + D(\theta; kb, N) + 10 \log_{10}(b/r) \qquad (5.17)$$

Using both exact and approximate techniques, $D(\theta; kb, N)$ has been calculated for several values of kb and N. A few typical patterns are shown on Figs. 5-2a-e, $M = 0$. The exact patterns appear on the left while the approximate patterns are on the right.

The patterns $D(\theta)$ obtained by the two methods are very similar both in amplitude and angular distribution. The largest differences occur near the normal to the duct axis. This is to be expected because the duct is replaced in the approximate method by an infinite screen that lies in this plane. The difference between exact and approximate pressure fields does not in general exceed 7 db. Despite the major assumptions it involves, the approximate solution is remarkably close to the exact solution. The approximate method may thus be used with confidence for cylindrical geometries for which the exact solution poses computational difficulties.

Radiation Problem for a Cylindrical Duct Immersed in a Subsonic Uniform Flow

It was noted in Chapter 3 that an essential difference exists between positive (exhaust) and negative (inlet) flow directions. In the first case the duct has a trailing edge, the Kutta-Joukowski condition applies, and the pressure is continuous across the duct continuation. In the second case the duct wall has a leading edge, and the velocity potential is continuous in the upstream region.

We proceed as in Chapter 3 by describing the general problem by using a function ϕ which represents the pressure perturbation p when $M > 0$ and the velocity potential φ when $M < 0$.

All the waves are now solutions of the convective wave equation

$$\phi_{xx}(1-M^2) + \phi_{yy} + \phi_{\zeta\zeta} + 2Mik\phi_x + k^2\phi = 0 \qquad (5.18)$$

and satisfy the no-displacement condition at the rigid wall

$$\frac{\partial \phi}{\partial n} = 0 \qquad (5.19)$$

Near the duct edge the complete potential ϕ_t satisfies one of the conditions (5.4) or (5.5). The induced potential ϕ must satisfy Sommerfeld's radiation condition (5.6) at infinity. The incoming wave potential ϕ_i has the form (5.7) where $f(y, \zeta)$ is an eigenfunction of the boundary value problem (5.8) (5.9), but in the present situation ϕ_i satisfies the convective wave equation and thus the expression for k_x is modified

$$k_x = \frac{k}{(1-M^2)} \left[1 - \left(\frac{\mu}{k}\right)^2 (1-M^2) \right]^{1/2} - \frac{kM}{(1-M^2)} \qquad (5.20)$$

Guided by Chapter 3 we define

$$k_x = k / (1-M^2)^{1/2} \qquad (5.21)$$

$$x_1 = x / (1-M^2)^{1/2} \qquad (5.22)$$

The incoming wave may then be written simply as

$$\phi_i = e^{-ik_1 M x_1} e^{ik_1 \eta_1 x_1} f(y,z) \qquad (5.23)$$

where the symbol η_1 designates the transformed η

$$\eta_1 = \left[1 - (\mu/k_1)^2 \right]^{1/2} \qquad (5.24)$$

Now define the new function ψ such that

$$\phi = e^{-ik_1 M x_1} \psi(x_1, y ; k_1, \mu) \qquad (5.25)$$

ψ is then a solution of the boundary value problem

$$\psi_{x_1 x_1} + \psi_{yy} + \psi_{zz} + k_1^2 \psi = 0 \qquad (5.26)$$

$$\partial \psi / \partial n = 0 \qquad (5.27)$$

on the duct surface. ψ_t satisfies one of the edge conditions (5.3) or (5.4) and ψ satisfies Sommerfeld's radiation condition (5.6).

The incoming wave potential ψ_i may be found from (5.23) and the definition (5.25)

$$\Psi_i = e^{ik_1 D_1 x_1} f(y, z) \tag{5.28}$$

This problem is completely identical to the problem for Φ^o stated by equations (5.1) - (5.6); thus,

$$\Psi = \Phi^o(x_1, y; k_1, \mu) \tag{5.29}$$

and then

$$\Phi_t(x, y; k, \mu, M) = e^{-ik_1 M x_1} \Phi_t^o(x_1; k_1, \mu) \tag{5.30}$$

The complete field corresponding to an incoming wave (k, μ) in the uniform flow case may be obtained from the complete field in the stationary case for an associated radiation problem for an incoming wave (k_1, μ) and a stretched x coordinate, x_1. This solution for the general potential Φ permits calculation of the pressure field.

When $1 > M \geqslant 0$ we have from the definition of Φ and (5.30),

$$P_t(x, y; k, M, \mu) = e^{-ik_1 M x_1} \Phi_t^o(x_1, y; k_1, \mu) \tag{5.31}$$

When $-1 < M \leqslant 0$, Φ represents the velocity potential φ and the perturbation pressure may be found through the relation

$$P_t = -\bar{\rho} \left(-i\omega \varphi_t + u \frac{\partial \varphi_t}{\partial x} \right) \tag{5.32}$$

which becomes

$$P_t = \frac{\bar{\rho} c i k_1}{(1 - M^2)^{1/2}} \left[\Phi_t^o + \frac{iM}{k_1} \frac{\partial \Phi_t^o}{\partial x_1} \right] \tag{5.33}$$

This is the pressure corresponding to a unit velocity potential incoming wave

$$\varphi_i = e^{-ik_1 Mx_1} e^{ik_1 \eta_1 x_1} f(y, z) \tag{5.34}$$

The associated incident pressure wave is

$$p_i = \frac{\bar{\rho} c i k_1}{(1-M^2)} (1 - M\eta_1) \varphi_i \tag{5.35}$$

The complete pressure field corresponding to a unit incident pressure wave is then

$$p_t = \frac{1}{1-M\eta_1} \left[\Phi_t^0 + \frac{iM}{k_1} \frac{\partial \Phi_t^0}{\partial x_1} \right] e^{-ik_1 Mx_1} \tag{5.36}$$

This expression contains both Φ_t^0 and $\partial \Phi_t^0 / \partial x_1$. To get a better idea of the effect of a negative Mach number (inlet situation) we may use the integral expression for Φ_t^0 for the special duct formed by two parallel semi-infinite plates.

The expression for Φ_t^0 in this case has the general form (Noble [5.6], expressions (3.34) or (3.37))

$$\Phi_t^0 = \int_{-\infty+ia}^{+\infty+ia} g(\alpha) e^{\gamma(b-|y|)-i\alpha x} d\alpha \tag{5.37}$$

where

$$\gamma = (\alpha^2 - k^2)^{1/2}, \quad Re(\gamma) > 0 \quad \text{for} \quad -k_i < \sigma < k_i$$

The application of (5.36) to (5.37) gives

$$p_t = \int_{-\infty+ia}^{+\infty+ia} g(\alpha_1) \frac{1+\alpha_1 M/k_1}{1-M\eta_1} e^{\gamma_1(b-|y|)-i\alpha_1 x_1} d\alpha_1 \qquad (5.38)$$

To obtain the far field pressure, the integral in (5.38) is evaluated using the saddle point method. The saddle point is at

$$\alpha_1 = -k_1 \cos\theta_1$$

and we may write

$$p_t = \frac{1-M\cos\theta_1}{1-M\eta_1} \phi_t^0(x_1, y; k_1, \mu) e^{-ik_1 M x_1} \qquad (5.39)$$

A comparison of (5.39) and (5.31) shows that when the Mach number is negative, the pressure field contains an additional factor

$$\frac{1-M\cos\theta_1}{1-M\eta_1} \qquad (5.40)$$

This factor is of order one, larger than one when

$$\theta_1 < \cos^{-1}\eta_1$$

We have derived previously expressions for the pressure field from which we can get relations for the angular distribution functions defined by (5.15).

In two dimensions, the far fields corresponding to incoming waves of amplitude A take the forms

for $M = 0$

$$p_t \sim A h_0(\theta; k, \mu)(b/r)^{1/2} \qquad (5.41)$$

for

$$p_t \sim A h(\theta; k, \mu, M)(b/r)^{1/2} \qquad (5.42)$$

When $1 > M \geqslant 0$ expression (5.31) leads to

$$r^{-1/2} h(\theta; k, \mu, M) = r_1^{-1/2} h_0(\theta; k_1, \mu) \tag{5.43}$$

where

$$r_1 = (x_1^2 + y^2)^{1/2}$$

or

$$r_1 = r\left(\frac{1 - M^2}{1 - M^2 \sin^2\theta}\right)^{1/2} \tag{5.44}$$

and

$$\tan\theta_1 = \frac{y}{x_1} = \frac{y}{x}(1 - M^2)^{1/2}$$

or

$$\tan\theta_1 = (1 - M^2)^{1/2} \tan\theta \tag{5.45}$$

then

$$h(\theta; k, \mu, M) = \left(\frac{1 - M^2}{1 - M^2 \sin^2\theta}\right)^{1/4} h_0(\theta_1; k_1, \mu) \tag{5.46}$$

When $-1 < M \leqslant 0$, expression (5.39) combined with (5.41) and (5.42) yields

$$h(\theta; k, \mu, M) = \left(\frac{1 - M^2}{1 - M^2 \sin^2\theta}\right)^{1/4} \frac{1 - M\cos\theta_1}{1 - M p_1} h(\theta_1; k_1, \mu) \tag{5.47}$$

For a three-dimensional space, the exponent 1/4 in (5.46) and (5.47) should be replaced by 1/2.

5.3 RESULTS

The method given above may be applied to any cylindrical duct.
We shall specialize it to study the radiation from the duct of Fig. 5-1
formed by two semi-infinite parallel plates. It would be more ap-
propriate to study the radiation from a duct of circular or annular
cross section since this would more closely represent an actual turbo-
fan. However, the exact Wiener-Hopf solution for such geometries
presents computational complexities, and actually the radiation pat-
terns are qualitatively similar to those from the two-plate duct (see
Tyler and Soffrin [5.1]).

Before starting our discussion, it is worth giving some of the
characteristics of the discrete tone noise generated by a typical turbo-
fan. Marsh, et al. [5.2] describe in detail the noise of a JT3D-3B
Pratt and Whitney engine. The JT3D develops a thrust of 18,000 lb.
at sea level on a standard day. Its bypass ratio is 1.4 to 1. The
sound pressure level reaches 150 to 160 db (620 to 2,000 N/m^2) in the
inlet and exhaust fan ducts. The fundamental frequencies are between
1800 and 3700 Hz. A complete noise spectrum may be found in [5.2],
Fig. 16.

The inlet duct diameter in the JT3D is about D = 50 inches.
For a frequency of 3000 Hz the parameter $kD/2$ which is similar to
kb (for the two parallel plate duct) is approximately 30.

Reference [5.2] does not provide any information concerning
the type of pressure mode which carries the acoustic energy. An up-
per bound for the mode number may be found by using the theory de-
veloped by Tyler and Soffrin [5.1] for the cutoff frequencies of duct

modes. Consider for instance that the inlet is a circular duct with hard walls. The eigenmodes for this duct have for expression

$$p_{mq}(r, \theta, t) = a_{mq} J_m(\mu_{mq} r) \cos(m\theta - \omega t) \qquad (5.48)$$

with

$$J'_m(\mu_{mq} D/2) = 0 \qquad (5.49)$$

q is the radial mode number and remains generally low. The integer m is the lobe number of the spinning pressure pattern which excites the mode (5.48). This number is related to the number of rotor blades B and guide vanes V by the relation

$$m = nB + lV \qquad , \qquad l = \ldots -1, 0, +1, \ldots$$

For a reduced frequency $kD/2 = 30$ the modes (5.48) will propagate without attenuation if $m \leqslant 20$. While there is no one-to-one correspondence between kb and $kD/2$ and between m and N, kb and N were chosen in the ranges discussed above.

We have calculated radiation patterns for multiple values of kb and N. Some typical patterns are shown on Fig. 5-2 a, b, c, d, e. The effect of the uniform flow has been included both for an inlet ($M < 0$) and exhaust ($M > 0$) situation. The basic radiation pattern ($M = 0$) is also given. When the reduced frequency kb is increased, the radiation pattern shows a larger number of lobes, a greater peak pressure, and the angular distribution is displaced towards the duct axis.

At constant frequency an increase in the mode number N re-

sults in a greater side radiation. A good discussion of the basic radiation patterns and their relation to the physical parameters of the fan (tip speed, blade and vane numbers) is given by Lowson [5.4]. The radiation efficiency and angular distribution are discussed, and it is concluded that it is desirable to have lower mode radiation for reduced power and improved angular distribution (less side line radiation).

The presence of a uniform flow has roughly the same effect as an increase in frequency. Most visible is an increase in the number of lobes, while the amplitude is mostly affected near the normal to the duct axis.

To see this more clearly, it is easy to obtain a full analytical expression for the angular distribution $h(\theta; k, \mu, M)$ by using the approximate method of Appendix 5-B. From (5-B.32), (5-B.33) or (5-B.34) expressions of the basic angular distribution h_0 and the relation between h and h_0 (5.30) for $M > 0$ or (5.38) for $M < 0$ we obtain h .

Consider, for example, N even and different from zero and M positive; then

$$h(\theta; k, \mu, M) = (2\pi)^{-1/2}(k_1 b)^{1/2} \eta_1$$

$$\left(\frac{1-M^2}{1-M^2 \sin^2\theta}\right)^{1/4} \left| \frac{(2/k_1 b)\sin\theta_1 \sin(k_1 b \sin\theta_1)}{(\mu_N|k_1)^2 - \sin^2\theta_1} \right| \tag{5.50}$$

We separate this expression into two factors. The first is the amplitude

$$Q = (2\pi)^{-1/2} (k_1 b)^{1/2} \eta_1 \left| \frac{1 - M^2}{1 - M^2 \sin^2\theta} \right|^{1/4} \tag{5.51}$$

The second is a normalized angular function

$$g(\theta) = \left| \frac{(2/k_1 b) \sin\theta_1 \sin(k_1 b \sin\theta_1)}{(\mu_N/k_1)^2 - \sin^2\theta_1} \right| \tag{5.52}$$

such that $\underset{\theta}{\text{Max}} \; g(\theta) = 1$. If we compare Q to Q_0 (corresponding to $M = 0$),

$$\frac{Q}{Q_0} = \frac{\eta_1}{\eta} \; (1 - M^2 \sin^2\theta)^{-1/4} \tag{5.53}$$

η_1 does not depend strongly on M , and thus Q shows a weak dependence on M and is most affected near $\theta = 90°$.

If we consider now expression (5.52) for $g(\theta)$ we see that the flow presence increases the reduced frequency from kb to $k_1 b$.

5.4 SEMI-INFINITE DUCT WITH ABSORBING WALLS

While the noise suppression properties of acoustic lining

set on the duct walls have been studied extensively, its effect on the

radiation pattern has been overlooked.

The introduction of acoustical lining in a duct replaces the no-

displacement condition of a perfectly reflecting wall by an impedance

relation between the pressure and normal velocity fluctuations.

If $Z_A = R_A + i X_A$ is the acoustic impedance of the

lining, its specific acoustic impedance ζ is the value of Z_A

normalized by the characteristic impedance of air

$$\zeta = Z_A / \rho c = (R_A / \rho c) + i (X_A / \rho c) \tag{5.54}$$

The specific admittance is defined by

$$\beta = 1/\zeta \tag{5.55}$$

The condition at the wall becomes, when the medium is not flowing,

$$\frac{\partial p}{\partial n} = i k \beta p \tag{5.56}$$

This condition changes the type of the duct propagating modes; a

change in the aperture field and in the radiated field results.

Another, more physical, description is as follows. The ab-

sorbing walls focus the acoustic energy towards the center of the

duct, while near the walls the energy is absorbed and the pressure

oscillations are small. The amplitude of the pressure field in the

aperture is decreased towards the edges. Such a decrease is equiva-

lent to a reduction of the aperture area and would result in a broader

main lobe in the radiation pattern and thus a lower directionality.

However, the decrease in pressure amplitude also produces a large

reduction in the side lobe amplitudes. Such phenomena are well known in the theory of aperture antennas (for instance, Collin [5.8], p. 76).

To show the effect of such a change of the aperture field we consider the ideal case of a perfectly absorbing wall ($\beta = \infty$ or $\zeta = 0$) where the perturbation pressure at the wall vanishes. We consider this situation for the duct of Fig. 5-1. The pressure amplitude for this case is given in Appendix 5-A, expressions (5-A.24) and (5-A.25) for a unit incoming duct mode

$$p_i = e^{ik_x x} \sin \mu_N (y - b) \tag{5.57}$$

where

$$\mu_N = N\pi / 2kb \tag{5.58}$$

A few radiation patterns for $N = 2$ are shown on the right side of Fig. 5-3a, b, c, d for this "soft wall" duct. On the left side, the radiation patterns for a hard wall duct are given for comparison.

The effect of a uniform medium flow has also been included without effort by applying the transformation of Section 5.2 (this is possible because the new condition at the wall $\phi = 0$ and the new edge condition $\phi(x, y, z) \longrightarrow C_1$ as $x \longrightarrow 0_+$ on the duct continuation do not essentially affect the method of Section 5.2).

The radiation patterns for the soft wall duct show a very weak side radiation (generally 20 db between the main lobe and the first side lobe); the main lobe as predicted is wider. For $N = 1$ (not shown), the main lobe is centered on the duct axis. The ratio between the far field pressures is given in Appendix 5-A, expression (5-A.38), which is reproduced below:

$$\sigma = \frac{(P_t)_{soft}}{(P_t)_{hard}} = (1/2)(N\pi/kb)(1+\eta)^{-1}\cot(\theta/2) \qquad (5.59)$$

The ratio σ is proportional to N/kb , thus sound absorbing walls are most effective for high frequency and low mode number duct waves. It is therefore advantageous to propagate the acoustic energy by lower order modes. The ratio σ is represented graphically on Fig. 5-4 for $N=1$ and $N=2$.

It is interesting at this point to make a small digression and compare the diffracted fields for a plane wave (k, Θ) incident on a hard and on a soft edge. The incident wave has a potential of the form

$$\phi_i = \exp(-ikx\cos\Theta - iky\sin\Theta) \qquad (5.60)$$

We give here only the asymptotic expressions for the diffracted fields valid for $kr \gg 1$ and θ far from $\Theta - \pi$ and $\pi - \Theta$.

The soft edge produces (Bowman and Senior [5.9])

$$\phi_{ds}^{\circ} \sim (2\pi kr)^{-1/2} \frac{2\cos\Theta/2\cos\theta/2}{\cos\theta + \cos\Theta} e^{ikr + i\pi/4} \qquad (5.61)$$

while the hard edge yields

$$\phi_{dH}^{\circ} \sim (2\pi kr)^{-1/2} \frac{2\sin\Theta/2\sin\theta/2}{\cos\theta + \cos\Theta} e^{ikr + i\pi/4} \qquad (5.62)$$

Then

$$\frac{\phi_{ds}^{\circ}}{\phi_{dH}^{\circ}} \sim \cot\Theta/2 \cot\theta/2 \qquad (5.63)$$

The diffracted field corresponding to a soft edge is more prominent in the forward direction; if the incidence angle is superior to $\pi/2$ the diffracted field is reduced by a factor $\cot \Theta/2$. A mode (k, N) in a duct may be represented as a combination of plane waves with an incidence angle given by

$$\Theta = \pi/2 + \cos^{-1}(N\pi/2kb) \tag{5.64}$$

(Morse and Ingard [5.10], p. 494).

Suppose $N\pi/2kb \ll 1$. Then

$$\cot \Theta/2 \simeq (1/2)(N\pi/2kb) \tag{5.65}$$

and

Expressions (5.63) and (5.59) are then identical. This simple computation shows how the acoustical characteristics of the region in the neighborhood of the edge (a few wavelengths) significantly modify the diffracted field.

Until now we have only considered ideally soft walls ($\zeta = 0$). This gave a qualitative picture of the influence of duct lining on the radiation pattern. It was seen that acoustical lining in an engine nacelle might significantly weaken the side radiation from the duct. As the engines of a commercial airplane remain nearly horizontal during takeoff, landing and flyby operations, the side radiation is important. It is difficult at this point to predict the change in ground noise for a real aircraft. A decrease in loudness would occur only if the radiation pattern for the basic duct without lining does not present a

prominent lobe near the duct axis. In any event, the reduction of side
radiation would cut by a factor of 1/3 to 2/3 the duration of maximum
loudness.

Finally, it is worth considering the extension of the method of
Section 5.2 to study the radiation from a duct with absorbing walls
(of finite impedance) in a uniformly moving medium. When there is
no flow, the boundary condition at the lining is

$$\frac{\partial p}{\partial n} = i k \beta p \tag{5.66}$$

where β is the material specific admittance. This new boundary
condition changes the eigenvalue problem (5.8), (5.9).

When the medium flows uniformly in the duct the condition at
the absorbing wall changes. At the present time there is some un-
certainty concerning the correct condition to apply.

If we assume continuity of displacement at the absorbing ma-
terial boundary as proposed by Ingard [5.11], i.e., if we suppose that
the specific impedance of the material represents the ratio of the
pressure to the time derivative of the displacement $\partial \xi / \partial t$,

$$\frac{p}{\partial \xi / \partial t} = \frac{\bar{\rho} c}{\beta} \tag{5.67}$$

Then the momentum equation in the n direction gives

$$\bar{\rho} \left(\frac{\partial}{\partial t} + u \frac{\partial}{\partial x} \right)^2 \xi = - \frac{\partial p}{\partial n} \tag{5.69}$$

and together with the definition (5.7) of the incoming mode, yields
the new boundary condition

$$\frac{\partial p}{\partial n} = ik\left(1 - M\frac{k_x}{k}\right)^2 \beta p \qquad (5.70)$$

If we suppose that the material impedance represents the ratio of the pressure to the normal velocity, we obtain

$$\frac{\partial p}{\partial n} = ik\left(1 - M\frac{k_x}{k}\right) \beta p \qquad (5.71)$$

In both expressions k_x has the form (5.19), but as it enters in the boundary conditions (5.70) or (5.71) it will be determined by an iterative process.

The eigenvalues μ_{mn} of the problem for f will be solution of a transcendental equation and will change when there is a uniform flow. Therefore, in addition to the transformation (5.20), (5.21) and (5.22), we must replace the admittance β for $M = 0$ by a new admittance β_1 to take the effect of the uniform flow on the absorbing material into account.

REFERENCES

5.1   Tyler, J.M., and Soffrin, T.G., "Axial Flow Compressor Noise Studies," SAE Trans., 70 (1962), p. 309.

5.2   Marsh, A.H., Elvas, I., Hoehne, J.C., and Frasca, R.L., "A Study of Turbofan Engine Compressor-Noise-Suppression Techniques," NASA CR-1056 (June 1968).

5.3   Mather, J.S.B., and Savidge, J., "New Observations on Tone Generation in Fans," J. Sound Vib., 16 (1971), pp. 407-418.

5.4   Lowson, M.V., "Theoretical Studies of Compressor Noise," NASA CR-1287 (March 1969).

5.5   Copeland, W.L. and Crigler, J.L., "Rotor-Stator Interaction Noise Studies of a Single Stage Axial-Flow Research Compressor," Paper presented at the 68th meeting, Acoustical Society of America, Austin, Texas (October 1964).

5.6   Noble, B., Methods Based on the Wiener Hopf Technique, Pergamon Press, New York (1958).

5.7   Beranek, L.L., Acoustics, McGraw-Hill, New York (1954).

5.8   Collin, R.E., "Radiation from Apertures," Antenna Theory, Part I, R.E. Collin and F.T. Zulker, Eds. McGraw Hill, New York (1969).

5.9   Bowman, J.J. and Senior, T.B.A., "The Half Plane," Electromagnetic and Acoustic Scattering by Simple Shapes, J.J. Bowman, T.B.A. Senior, and P.L.E. Uslenghi, Eds. North Holland Publishing Co., Wiley Interscience Division, Amsterdam-New York (1969).

5.10 Morse, P.M. and Ingard, K.U., Theoretical Acoustics, McGraw-Hill, New York (1968).

5.11 Ingard, K.U., "Influence of Fluid Motion Past a Plane Boundary on Sound Reflection, Absorption and Transmission," J. Acoust. Soc. Amer., 31 (1959), pp. 1035-1036.

5.12 Goodman, J., Introduction to Fourier Optics, McGraw-Hill, New York (1968).

5.13 Papoulis, A., Systems and Transforms with Applications in Optics, McGraw-Hill, New York (1968).

APPENDIX 5-A

Acoustic Radiation from a Duct Formed by Two

Semi-infinite Parallel Plates.   Exact Solution.

In this appendix we derive expressions for the amplitude of the far-field radiated pressure for a duct made of two semi-infinite parallel plates.   We start from the exact solution for the radiation problem obtained by the Wiener-Hopf technique and given in integral form by Noble [5.6], pp. 107-108.   The saddle point method is applied to the path integrals to obtain the far field pressure, and the functions $|L_+(\alpha)|$ and $|K_+(\alpha)|$ which arise in the final expressions are arranged in computable form.

The duct is represented on fig. 5-1 and the plates are supposed, for the moment, to be rigid, i.e., the displacement vanishes at the plates

$$\frac{\partial \phi_t^0}{\partial y}\bigg|_{y=\pm b} = 0 \qquad\qquad (5A\text{-}1)$$

for $x \leqslant 0$ on $y = \pm b$.

One progressive mode travels towards the open end of the duct

$$\phi_i^0 = \exp(i k_x x) \cos \mu_N (y - b) \qquad\qquad (5A\text{-}2)$$

where μ_N is one of the eigenvalues of the problem (5.8), (5.9) for the duct under consideration, $\mu_N = N\pi/2b$ and N is any integer less than $2bk/\pi$ so that

$$k_x = k = k\eta = k\left[1 - (\mu_N/k)^2\right]^{1/2} \qquad\qquad (5A\text{-}3)$$

is real.

The expressions for the complete field ϕ_t^o associated to the incident wave (5A-2) are given by Noble [5.6] and reproduced here for convenience. When N is even, ϕ_t^o is an even function of y

$$\phi_t^o = -\frac{ib}{2\pi}(k+k)L_-(-k)\int_{-\infty+ia}^{+\infty+ia}\frac{(\alpha+k)L_+(\alpha)}{\gamma(\alpha+k)}$$
$$\exp[\gamma(b-|y|)-i\alpha x]\,d\alpha \qquad (5A-4)$$

for $|y| \geq b$

When N is odd, ϕ_t^o is an odd function of y

$$\phi_t^o = \text{sgn}(y)\frac{1}{2\pi}(k+k)^{1/2}K_-(k)\int_{-\infty+ia}^{+\infty+ia}\frac{(\alpha+k)^{1/2}K_+(\alpha)}{\gamma(\alpha+k)}$$
$$\exp[\gamma(b-|y|)-i\alpha x]\,d\alpha \qquad (5A-5)$$

for $|y| \geq b$

where $\text{sgn}(y)$ is the sign of y .

The definitions of the various symbols used in the previous expressions are given in detail in ref. [5.6] and only summarized here.

The variable α is complex

$$\alpha = \sigma + i\tau \qquad (5A-6)$$

a small imaginary part is assigned to k

$$k = k_r + i k_i \quad , \quad k_i > 0$$

and γ is defined by

$$\gamma = (\alpha^2 - k^2)^{1/2} \qquad (5A-7)$$

and the branch of γ which is used is such that $\text{Re}(\gamma) \geq 0$ for α in the strip $-k_i \leq \tau \leq k_i$. A central step in the Wiener-Hopf technique is the decomposition of certain functions $L(\alpha)$ in a product $L(\alpha) = L_+(\alpha) L_-(\alpha)$, where $L_+(\alpha)$, $L_-(\alpha)$

are regular non-zero in the upper and lower half planes, respectively.

For the present problem the functions $L_\pm(\alpha)$, $K_\pm(\alpha)$ may be written as follows:

$$L_\pm(\alpha) = \exp\left[\mp X_2(\alpha) - T_\pm(\alpha)\right]\prod_{n=1}^{\infty}\left[(1-k^2 b_n^2)^{1/2} \mp i\alpha b_n\right] e^{\pm i\alpha b_n} \tag{5A-8}$$

$$K_\pm(\alpha) = \exp\left[\mp X_1(\alpha) - T_\pm(\alpha)\right]\prod_{n=1}^{\infty}\left[(1-k^2 b_{n-1/2})^{1/2} \mp i\alpha b_{n-1/2}\right] \tag{5A-9}$$
$$e^{\pm i\alpha b_{n-1/2}}$$

with

$$T_+(\alpha) = \pi^{-1} b \gamma \cos^{-1}(\alpha/k) \quad , \quad T_-(\alpha) = T_+(-\alpha) \tag{5A-10}$$

$$X_1(\alpha) = -i b\alpha \pi^{-1}\left[1 - c + \ln(\pi/2bk)\right] + (1/2)\alpha b \tag{5A-11}$$

$$X_2(\alpha) = -i b\alpha \pi^{-1}\left[1 - c + \ln(2\pi/bk)\right] + (1/2)\alpha b \tag{5A-12}$$

$$c = 0.5772$$

$$b_n = b/n\pi \tag{5A-13}$$

The expressions for $L_\pm(\alpha)$ and $K_\pm(\alpha)$ appear quite unwieldy, but we shall see that the pressure amplitude expressions contain only $|L_+(\alpha)|$ and $|K_+(\alpha)|$ which are considerably simpler.

The integrand in (5A-4) and (5A-5) seems to have a pole at $\alpha = -k = -k\eta$. Actually, $\alpha = -k\eta$ is also a simple zero of $L_+(\alpha)$

and $K_+(\alpha)$, and thus is only an apparent pole. To obtain the far field $|y| \geqslant b$ and $kr \rightarrow \infty$ we use the saddle point method. We consider now expression (5A-4) for N even and different from zero; the cases when N is odd or when the duct has soft walls may be treated in the same way, and only the final results are given at the end of this section.

The field Φ_t^o has the form

$$\Phi_t^o = \int_{-\infty+i\alpha}^{+\infty+i\alpha} g(\alpha)\, e^{f(\alpha)\, r}\, d\alpha \tag{5A-14}$$

where

$$x = r\cos\theta \quad , \quad y = r\sin\theta$$

$$g(\alpha) = -\frac{ib}{2\pi}\, (k+\kappa)\, L_-(-\kappa)\, \frac{(\alpha+\kappa)\, L_+(\alpha)}{\gamma\, (\alpha+\kappa)}\, e^{\gamma b} \tag{5A-15}$$

$$f(\alpha) = -\gamma|\sin\theta| - i\alpha\cos\theta \tag{5A-16}$$

The function $f(\alpha)$ may be developed in series around the saddle point α_o

$$f(\alpha) = f(\alpha_o) + (\alpha-\alpha_o)f'(\alpha_o) + \frac{1}{2}(\alpha-\alpha_o)^2 f''(\alpha_o)+\dots \tag{5A-17}$$

where α_o is a root of $f'(\alpha_o) = 0$ and is found to be

$$\alpha_o = -k\cos\theta$$

The far field for $kr \to \infty$ is then

$$\phi_t^o \simeq [2\pi/r|f''(\alpha_o)]^{1/2} g(\alpha_o) e^{f(\alpha_o)r - i\pi/4} \tag{5A-18}$$

or

$$\phi_t^o \simeq (2\pi)^{-1/2}(kb)^{1/2}(1+\eta) L_+(k) (1-\cos\theta)$$

$$\frac{L_+(-k\cos\theta)}{\eta - \cos\theta} e^{i(kr - kb\sin\theta - \pi/4)} (b/r)^{1/2} \tag{5A-19}$$

Then when N is even and different from zero

$$|\phi_t^o| \simeq (2\pi)^{-1/2}(kb)^{1/2}(1+\eta) |L_+(k\eta)| (1-\cos\theta)$$

$$|L_+(-k\cos\theta)/(\eta-\cos\theta)| (b/r)^{1/2} \tag{5A-20}$$

When N is equal to zero

$$|\phi_t^o| \simeq (2\pi)^{-1/2}(kb)^{1/2} 2 |L_+(k)||L_+(-k\cos\theta)| (b/r)^{1/2} \tag{5A-21}$$

When N is odd

$$|\phi_t^o| \simeq (2\pi)^{-1/2}(kb)^{-1/2}(1+\eta)^{1/2} |K_+(k\eta)| (1-\cos\theta)^{1/2}$$

$$|K_+(-k\cos\theta)/(\eta - \cos\theta)| (b/r)^{1/2} \tag{5A-22}$$

For a "soft" wall duct $\phi_t^o = 0$ on the plates and the incident wave has the form

$$\Phi_i^o = \exp(ik_x x)\sin\mu_N(y-b) \tag{5A-23}$$

with $\mu_N = N\pi/2b$ and N any integer less than $2kb/\pi$.

Applying the saddle point method to expressions (3.39) and (3.41) of ref. [5.6], we obtain for N even

$$|\Phi_t^o| \simeq (2\pi)^{1/2}(kb)^{-1/2}(N/4)\sin\theta$$

$$|L_+(k\eta)||L_+(-k\cos\theta)/(\eta-\cos\theta)|(b/r)^{1/2} \tag{5A-24}$$

and when N is odd

$$|\Phi_t^o| \simeq (2\pi)^{1/2}(kb)^{-1/2}(N/4)(1+\eta)^{-1/2}2^{1/2}\cos(\theta/2)$$

$$|k_+(k\eta)||k_+(-k\cos\theta)/(\eta-\cos\theta)|(b/r)^{1/2} \tag{5A-25}$$

To proceed we need practical expressions for $|L_+(\alpha)|$ and $|k_+(\alpha)|$. Computation of $|L_+(\alpha)|$ and $|k_+(\alpha)|$.

When the arbitrary imaginary part of k is set equal to zero,

$$k_i = 0$$

the arguments of $|L_+(\alpha)|$ and $|k_+(\alpha)|$ in the expressions for $|\Phi_t^o|$, are real. Then we see at once that

$$\text{Re}\{\chi_2(\alpha)\} = (1/2)\alpha b \tag{5A-26}$$

When $|\alpha| < k$ then γ is pure imaginary and consequently

$$Re\left\{T_+(\alpha)\right\} = 0 \tag{5A-27}$$

When $|\alpha| > k$, γ is real, but $\cos^{-1}(\alpha/k)$ is pure imaginary, and again (5A-27) is true. Thus, from (5A-8),

$$|L_+(\alpha)| = \exp(-\tfrac{1}{2}\alpha b) \prod_{n=1}^{\infty} | (1- k^2 b_n^2)^{1/2} - i\alpha b_n | \tag{5A-28}$$

We call J the integer part of kb/π

$$J < kb/\pi < J+1 \tag{5A-29}$$

For $1 \leqslant n \leqslant J$,

$$| (1- k^2 b_n^2)^{1/2} - i\alpha b_n | = kb_n | \mathcal{D}_n + \alpha/k | \tag{5A-30}$$

where

$$\mathcal{D}_n \equiv [1 - (n\pi/kb)^2]^{1/2} \tag{5A-31}$$

For $J < n < \infty$,

$$| (1- k^2 b_n^2)^{1/2} - i\alpha b_n | = [1 - (kb_n)^2(1- \alpha^2/k^2)]^{1/2} \tag{5A-32}$$

The infinite product of expression (5A-28) is composed of terms of two types, depending on the position of n with respect to J .

$$|L_+(\alpha)| = \exp(\tfrac{1}{2}\alpha b) \prod_{n=1}^{J} kb_n | \mathcal{D}_n + \alpha/k |$$
$$\prod_{n=J+1}^{\infty} [1 - (kb_n)^2(1-\alpha^2/k^2)]^{1/2} \tag{5A-33}$$

We also note that when $n = N/2$

$$\eta_n = \left[1 - (N\pi/2kb)^2\right]^{1/2} \equiv \eta \tag{5A-34}$$

and $|L_+(\alpha)|$ has a simple zero at $\alpha = -k\eta$ and then

$$|L_+(\alpha)/(\eta + \alpha/k)| = kb_{N/2} \exp(-\tfrac{1}{2}\alpha b)$$

$$\prod_{n=1, n\neq N/2}^{J} kb_n |\eta_n + \alpha/k| \prod_{n=J+1}^{\infty} \left[1 - (kb_n)^2(1 - \alpha^2/k^2)\right]^{1/2} \tag{5A-35}$$

The function $|K_+(\alpha)|$ may be arranged in a form similar to (5A-33) with J now defined as the integer part of $(kb/\pi) + 1/2$ or

$$2J - 1 < 2kb/\pi < 2J + 1 \tag{5A-36}$$

and replacing b_n by

$$b_{n-1/2} = \frac{kb}{(n-1/2)\pi} \tag{5A-37}$$

and η_n by

$$\eta_{n-1/2} = \left\{ 1 - \left[\frac{(n-1/2)\pi}{kb}\right]^2 \right\}^{1/2} \tag{5A-38}$$

Then

$$|K_+(\alpha)| = \exp\left(\tfrac{1}{2}\alpha b\right) \prod_{n=1}^{J} kb_{n-1/2} |\eta_{n-1/2} + \alpha/k|$$

$$\prod_{n=J+1}^{\infty} \left[1 - (kb_{n-1/2})^2(1 - \alpha^2/k^2)\right]^{1/2} \tag{5A-39}$$

Expressions (5A-33) and (5A-39) are well suited for numerical computation and also provide some qualitative information about $|\Phi_t^o|$. We consider again the N even case; then $|\Phi_t^o|$ vanishes when

$$\left| L_+ (-k\cos\theta)/(\eta - \cos\theta) \right| = 0 \tag{5A-40}$$

and from (5A-35) we see that this occurs when

$$\theta = \cos^{-1}(\eta_n) \qquad \text{for} \quad n = 1, 2 \ldots J, \quad n \neq N/2 \tag{5A-41}$$

Thus, the radiation pattern will be composed of J lobes in the angular interval $0 < \theta < \pi$. In the interval $\pi/2 < \theta < \pi$ the amplitude of the field $|\Phi_t^o|$ does not vanish, but decays exponentially on the same lobe.

Comparison of the Far Fields Corresponding to Hard and Soft Duct Walls.

From (5A-20) and (5A-24) or from (5A-22) and (5A-25) we deduce the ratio of the far fields for a given angular direction

$$G = \frac{|\Phi_t^o|_{soft}}{|\Phi_t^o|_{hard}} \approx (1/2)(N\pi/kb)(1+\eta)^{-1} \cot(\theta/2) \tag{5A-42}$$

This ratio is discussed in Section 5.4

APPENDIX 5-B

Acoustic Radiation from a Duct.

The Fraunhofer Approximation.

The usual procedure for computing the acoustic radiation from a duct is based on three major approximations.

1. The duct is replaced by an infinite plane screen with an aperture;

2. the aperture field and its normal derivative are assumed determined only by the duct outgoing waves;

3. the field at any point is computed by Kirchhoff's formula and the far field is obtained by applying the Fraunhofer approximation.

In this appendix we formalize this procedure to show how the approximations are introduced and also to derive an important formula relating the far field to the Fourier transform of the aperture field. This relation is well known in optics (Goodman [5.12], Papoulis [5.13]) and in antenna theory (Collin [5.8]), but is generally not recognized in acoustics. We give this relation in a form directly applicable to the acoustic radiation problems considered in Chapter 5.

In the first step the duct is replaced by an infinite screen with an aperture. This approximation will only be tested when we compare the exact solution to the present solution for a specific duct (Chapter 5). We note at this point that the field behind the duct aperture (for $\pi/2 < \theta < \pi$) cannot be computed.

Kirchhoff's formula is then used to compute the pressure at a point M_0 in a domain limited by the plane surface Σ_1 parallel to the screen and the large truncated sphere Σ_2 (fig. 5-5),

$$p(M_0) = \frac{1}{4\pi} \iint_{\Sigma_1+\Sigma_2} \left(\frac{\partial p}{\partial n} G - p \frac{\partial G}{\partial n}\right) d\sigma \qquad (5B-1)$$

where $\underset{\sim}{n}$ is the exterior unit normal and G is the Green's function in free space for the Helmholtz equation:

$$\nabla^2 G(\underset{\sim}{r_0}|\underset{\sim}{r_1}) + k^2 G(\underset{\sim}{r_0}|\underset{\sim}{r_1}) = -4\pi \delta(\underset{\sim}{r_0}-\underset{\sim}{r_1}) \qquad (5B-2)$$

$$G(\underset{\sim}{r_0}|\underset{\sim}{r_1}) = \frac{e^{ik|\underset{\sim}{r_0}-\underset{\sim}{r_1}|}}{|\underset{\sim}{r_0}-\underset{\sim}{r_1}|} \qquad (5B-3)$$

We then assume that the pressure field satisfies the Sommerfeld radiation condition at infinity

$$\lim_{R\to\infty} R\left(\frac{\partial p}{\partial n} - ikp\right) = 0 \qquad (5B-4)$$

so that (5B-1) becomes

$$p(M_0) = \frac{1}{4\pi} \iint_{\Sigma_1} \left(\frac{\partial p}{\partial n} G - p \frac{\partial G}{\partial n}\right) d\sigma \qquad (5B-5)$$

An expression containing only the pressure field derivative $\partial p/\partial n$ may be obtained by using the alternate Green's function whose normal derivative vanishes on Σ_1

$$\frac{\partial G_+}{\partial n}\bigg|_{\Sigma_1} = 0 \qquad (5B-6)$$

The Cartesian coordinates of M_0 are x_0, y_0, z_0, we call $\bar{M}_0(-x_0, y_0, z_0)$ the reflection of M_0. $M_1(x_1, y_1, z_1)$

is some arbitrary point.   Then the Green's function which satisfies

(5B-6) is

$$G_+(\underline{r}_0 \mid \underline{r}_1) = \frac{\exp(ikr_{01})}{r_{01}} + \frac{\exp(ik\overline{r}_{01})}{\overline{r}_{01}} \qquad (5B-7)$$

where

$$r_{01} = \left[(x_0 - x_1)^2 + (y_0 - y_1)^2 + (z_0 - z_1)^2 \right]^{1/2} \qquad (5B-8)$$

$$\overline{r}_{01} = \left[(x_0 + x_1)^2 + (y_0 - y_1)^2 + (z_0 - z_1)^2 \right]^{1/2} \qquad (5B-9)$$

On the surface Σ_1

$$\frac{\partial p}{\partial \underline{n}} = -\frac{\partial p}{\partial x} \qquad \text{and} \qquad G_+(\underline{r}_0 \mid \underline{r}_1) = 2\frac{e^{ikr_{01}}}{r_{01}}$$

where the point $M_1(\underline{r}_1)$ belongs now to Σ_1 .   Then (5B-5) be-

comes

$$p(M_0) = -\frac{1}{2\pi} \iint_{\Sigma_1} \frac{\partial p}{\partial x} \frac{e^{ikr_{01}}}{r_{01}} d\sigma \qquad (5B-10)$$

Consider now a duct travelling mode

$$p_i = \exp(ik_x x)\, f(y, z) \qquad (5B-11)$$

where $f(y, z)$ is an eigenfunction of the boundary value problem

$$f_{yy} + f_{zz} + \mu^2 f = 0 \qquad (5B-12)$$

$$B[f] = 0 \qquad (5B-13)$$

Expression (5B-13) represents some boundary condition taking gener-

ally the form of an impedance relation at the duct wall:

$$\frac{\partial f}{\partial \underline{n}} = i k \beta f$$

The wavenumber in the X direction, k_x, is given by

$$k_x = k \eta = k \left[1 - (\mu/k)^2 \right]^{1/2}$$

Then (5B-10) and (5B-11) yield

$$p(M_0) = -\frac{1}{2\pi} \iint_{\text{Aperture}} i k \eta \, f(y_1, z_1) \, \frac{e^{i k r_{01}}}{r_{01}} \, d\sigma \tag{5B-14}$$

The computation of $p(M_0)$ is greatly simplified by using the Fraunhofer approximation. We define

$$r_0 = \left(x_0^2 + y_0^2 + z_0^2 \right)^{1/2}$$

then

$$r_{01} = \left(r_0^2 - 2 y_0 y_1 - 2 z_0 z_1 + y_1^2 + z_1^2 \right)^{1/2} \tag{5B-15}$$

If the maximum diameter of the aperture $D = \max \left(y_1^2 + z_1^2 \right)^{1/2}$ is such that $k D^2 / r \ll 1$, we approximate r_{01} by

$$r_{01} \simeq r_0 - (y_0 y_1 + z_0 z_1)/r_0 \tag{5B-16}$$

and

$$p(M_0) \simeq -\frac{i k \eta}{2\pi r_0} e^{i k r_0} \iint_{\text{Aperture}} f(y_1, z_1)$$
$$\exp -i k \left(\frac{y_0}{r} y_1 + \frac{z_0}{r} z_1 \right) dy_1 \, dz_1 \tag{5B-17}$$

We define the Fourier transform of f

$$F(\mathcal{Y},\mathcal{Z}) = \frac{1}{(2\pi)^{1/2}} \iint_{\Sigma_1} f(y_1, z_1) \exp i(\mathcal{Y}y_1 + \mathcal{Z}z_1) dy_1 dz_1 \qquad (5B-18)$$

where $f(y_1, z_1)$ vanishes outside the aperture.

Then

$$p(M_0) \simeq -\frac{ik\rho}{(2\pi)^{1/2}} \frac{e^{ikr_0}}{r_0} F\left(-\frac{ky_0}{r_0}, -\frac{kz_0}{r_0}\right) \qquad (5B-19)$$

To obtain (5B-19) we supposed that the aperture did not have an infinite direction. We consider now an aperture infinite in the z direction and two-dimensional pressure modes travelling in the duct

$$p_i = \exp(ik_x x) f(y) \qquad (5B-20)$$

then

$$p(M_0) = -\frac{1}{2\pi} \int_{\text{Aperture}} ik\rho f(y_1) dy_1 \int_{-\infty}^{+\infty} \frac{e^{ikr_{01}}}{r_{01}} dz_1 \qquad (5B-21)$$

It is easy to show that

$$\int_{-\infty}^{+\infty} \frac{e^{ikr_{01}}}{r_{01}} dz_1 = \int_{-\infty}^{+\infty} e^{ik\ell cht} dt = \pi i H_0^1(k\ell) \qquad (5B-22)$$

where

$$\ell = \left[x_0^2 + (y_0 - y_1)^2\right]^{1/2} \qquad (5B-23)$$

To obtain the far field from (5B-21) we use the asymptotic expansion for H_0^1

$$H_0'(k\ell) \sim \left(\frac{2}{\pi k\ell}\right)^{1/2} e^{ik\ell - i\pi/4} \qquad (5B\text{-}24)$$

and the Fraunhofer approximation

$$\ell \simeq r_0 - y_0 y_1 / r_0 \qquad (5B\text{-}25)$$

Then

$$p(M_0) \simeq k^{1/2} \mathcal{D} \, r_0^{-1/2} e^{ikr_0 - i\pi/4} F(-k\sin\theta) \qquad (5B\text{-}26)$$

where

$$F(\mathcal{Z}) = \frac{1}{(2\pi)^{1/2}} \int_{\Sigma_1} f(y_1) \, e^{i\mathcal{Z}y_1} dy_1 \qquad (5B\text{-}27)$$

Application to Particular Duct Geometries

    1. Circular duct with hard walls. We define the polar co-ordinates for the aperture

$$y_1 = \rho \cos\varphi$$
$$\mathcal{Z}_1 = \rho \sin\varphi$$

The duct has a radius a; thus, $0 \leqslant \rho \leqslant a$.

    Then

$$f(y_1, \mathcal{Z}_1) = J_m\left(\beta_{mn} \rho/a\right) \begin{Bmatrix} \cos m\varphi \\ \sin m\varphi \end{Bmatrix} \qquad (5B\text{-}28)$$

where β_{mn} are the roots of the eigenvalue equation

$$J'_m (\beta mn) = 0$$

When $\quad n \neq 0$

$$|p(M_0)| \simeq (1/2) (ka)^2 \eta \, J_m(\beta mn) \, (a/r_0)$$

$$\left| \frac{\sin\theta \, [J_{m-1} (ka\sin\theta) - J_{m+1}(ka\sin\theta)]}{\beta^2_{mn} - (ka\sin\theta)^2} \right| \qquad (5B-29)$$

When $\quad m = 0, \; n = 0 \quad$ a plane wave propagates in the duct

$$f(y_1, z_1) = 1$$

and

$$|p(M_0)| \simeq (ka) (a/r_0) \left| \frac{J_1(ka\sin\theta)}{ka\sin\theta} \right| \qquad (5B-30)$$

2. Duct formed by two parallel semi-infinite hard plates. This duct is represented on fig. 5-1. The eigenfunctions are, in this case,

$$f(y_1) = \cos \mu_N (y_1 - b) \qquad (5B-31)$$

with

$$\mu_N = N\pi/2b \qquad , \quad N = 0, 1 \ldots < 2kb/\pi$$

When N is even and different from zero

$$|p(M_0)| \simeq (2\pi)^{-1/2} (kb)^{-1/2} 2\eta \, (b/r_0)^{1/2} \left| \frac{\sin\theta \, \sin(kb\sin\theta)}{(\mu_N/k)^2 - \sin^2\theta} \right| \qquad (5B-32)$$

When **N** is odd

$$|p(M_0)| \simeq (2\pi)^{-1/2} (kb)^{-1/2} 2\eta \, (b/r_0)^{1/2} \left| \frac{\sin\theta \, \cos(kb\sin\theta)}{(\mu_N/k)^2 - \sin^2\theta} \right| \qquad (5B-33)$$
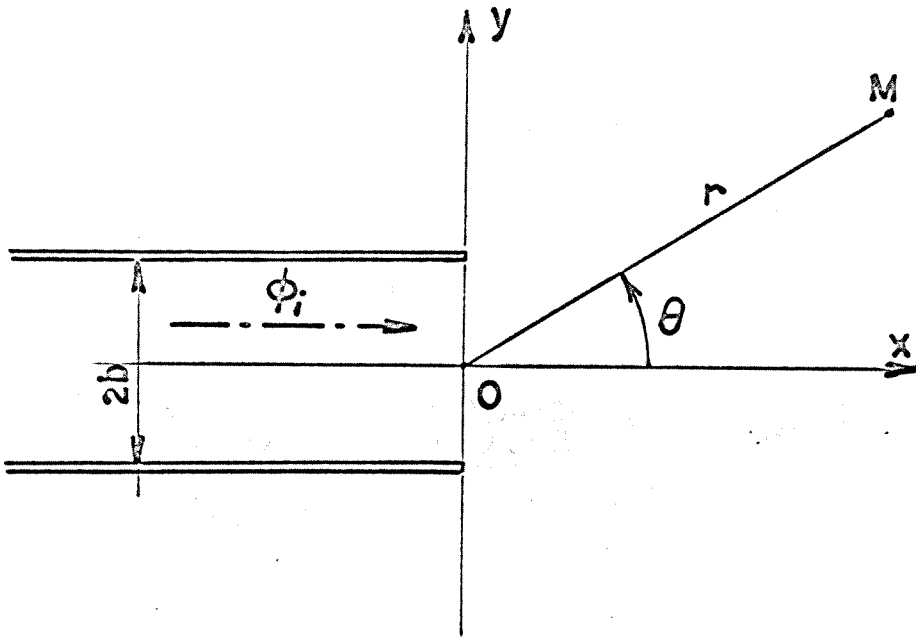
and when **N = 0**

$$|p(M_0)| \simeq (2\pi)^{-1/2} (kb)^{-1/2} 2 \, (b/r_0)^{1/2} \left| \frac{\sin(kb\sin\theta)}{\sin\theta} \right| \qquad (5B-34)$$

3. <u>Duct formed by two parallel semi-infinite soft plates.</u> The pressure perturbation vanishes at the duct walls; the eigenfunctions in this case are

$$f(y_1) = \sin \mu_N (y_1 - b) \qquad (5B-35)$$

with

$$\mu_N = N\pi/2b \quad , \quad N = 1, 2 \dots \; < \; 2kb/\pi$$

When **N** is even

$$|p(M_0)| \simeq (2\pi)^{-1/2} (kb)^{-1/2} 2\eta \, (b/r_0)^{1/2} \left| \frac{(\mu_N/k)\sin(kb\sin\theta)}{(\mu_N/k)^2 - \sin^2\theta} \right| \qquad (5B-36)$$

When **N** is odd

$$|p(M_0)| \simeq (2\pi)^{-1/2} (kb)^{-1/2} 2\eta \, (b/r_0)^{1/2} \left| \frac{(\mu_N/k)\cos(kb\sin\theta)}{(\mu_N/k)^2 - \sin^2\theta} \right| \qquad (5B-37)$$

Fig. 5-1. Geometry of the radiation problem for a duct formed by two semi-infinite parallel plates.
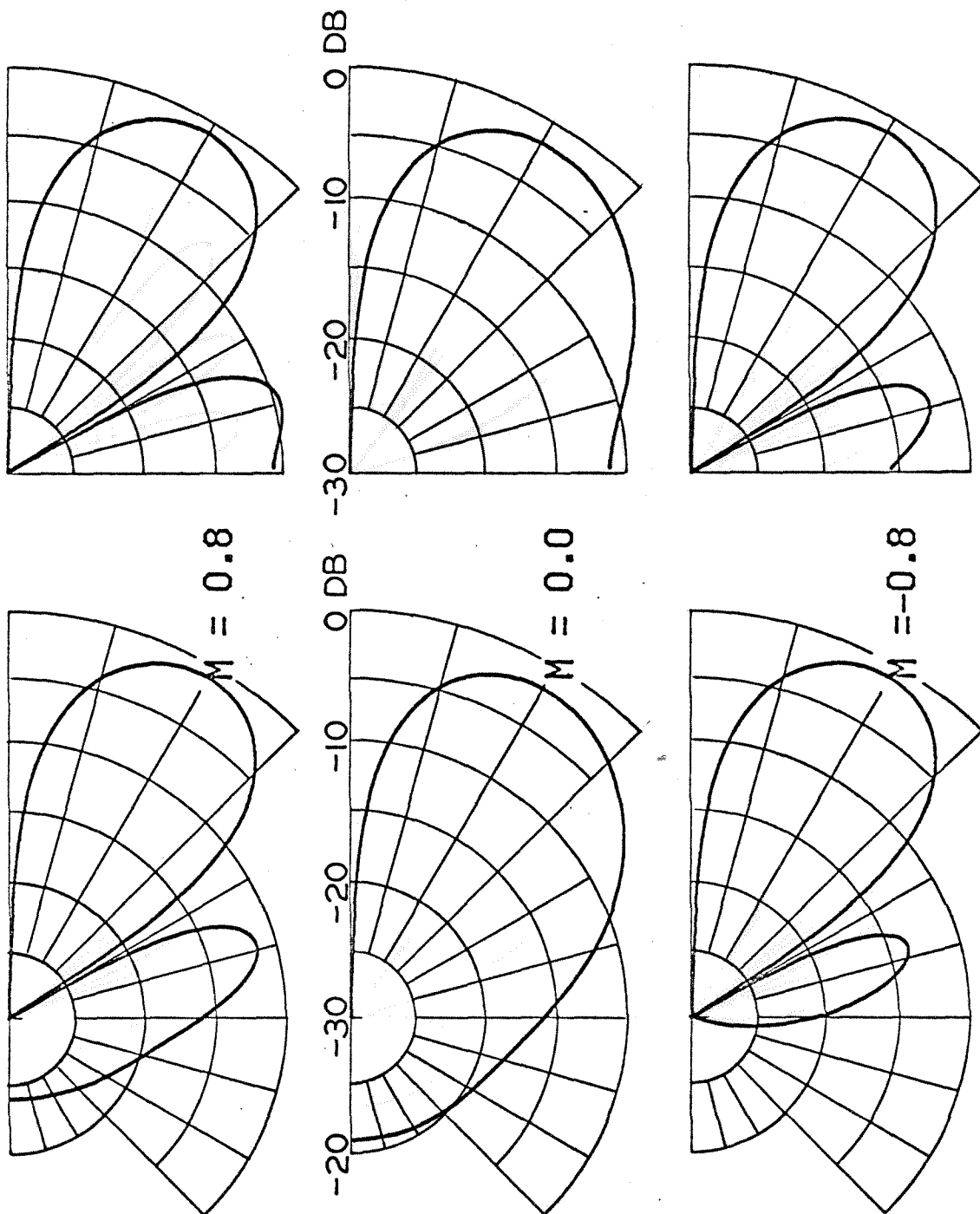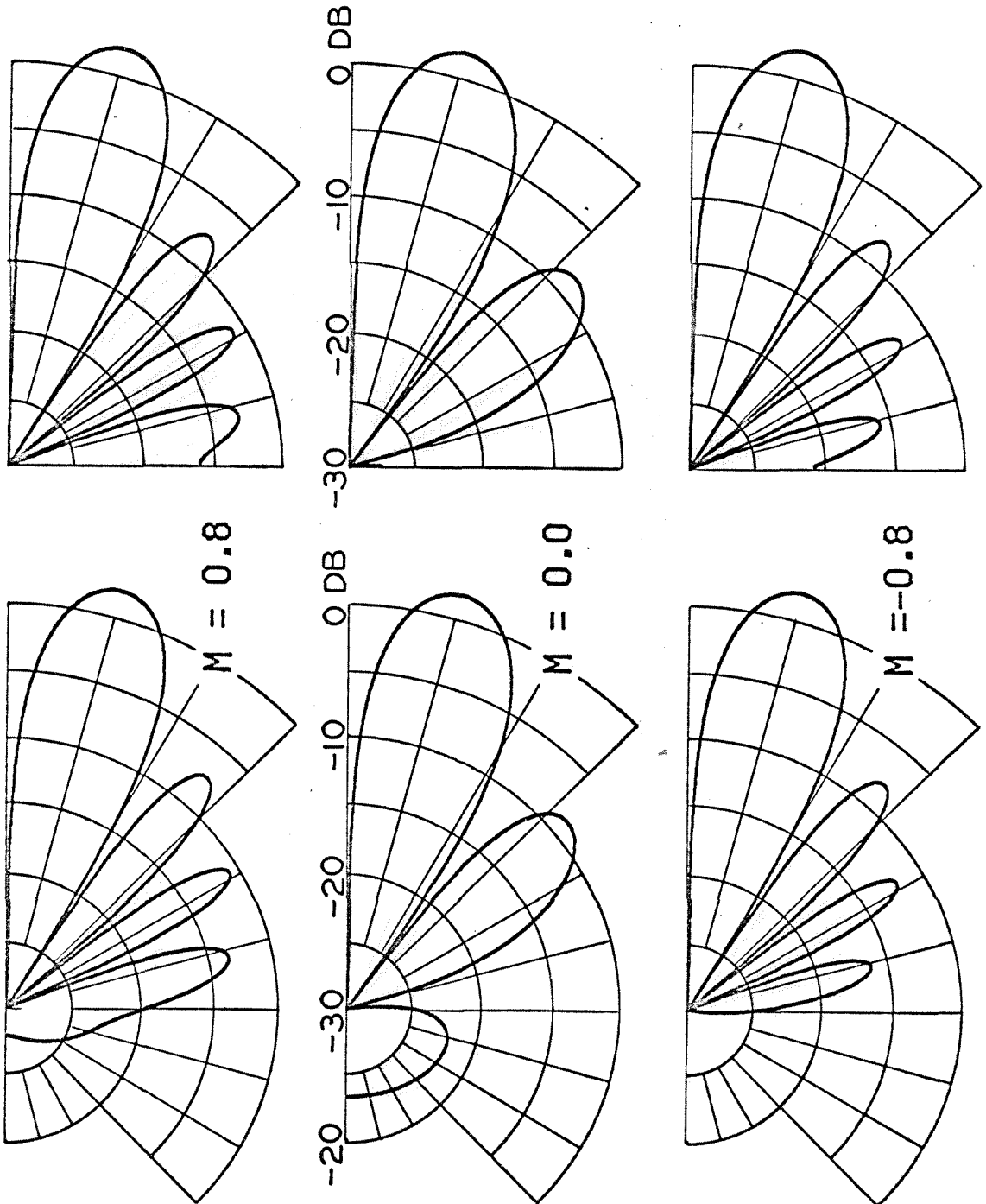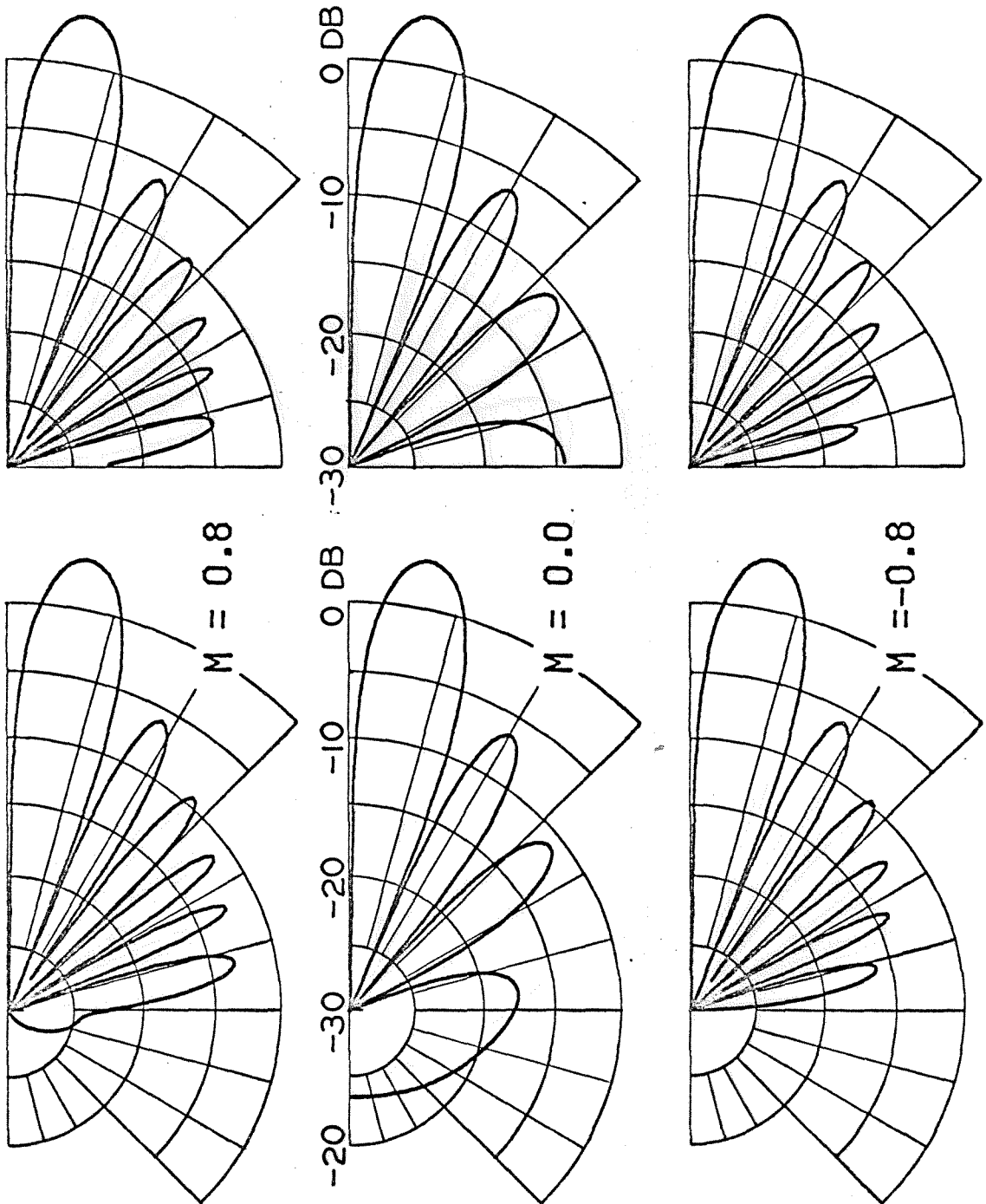
Fig. 5-2a. Radiation patterns $D(\theta; kb, N, M)$ for a duct formed by two semi-infinite parallel hard plates. The exact Wiener-Hopf solution is on the left; the approximate Fraunhofer solution is on the right. $kb = 4. N = 1$

Fig. 5-2b. Radiation patterns $D(\theta; kb, N, M)$ for a duct formed by two semi-infinite parallel hard plates. The exact Wiener-Hopf solution is on the left; the approximate Fraunhofer solution is on the right. $kb = 8$. $N = 1$.
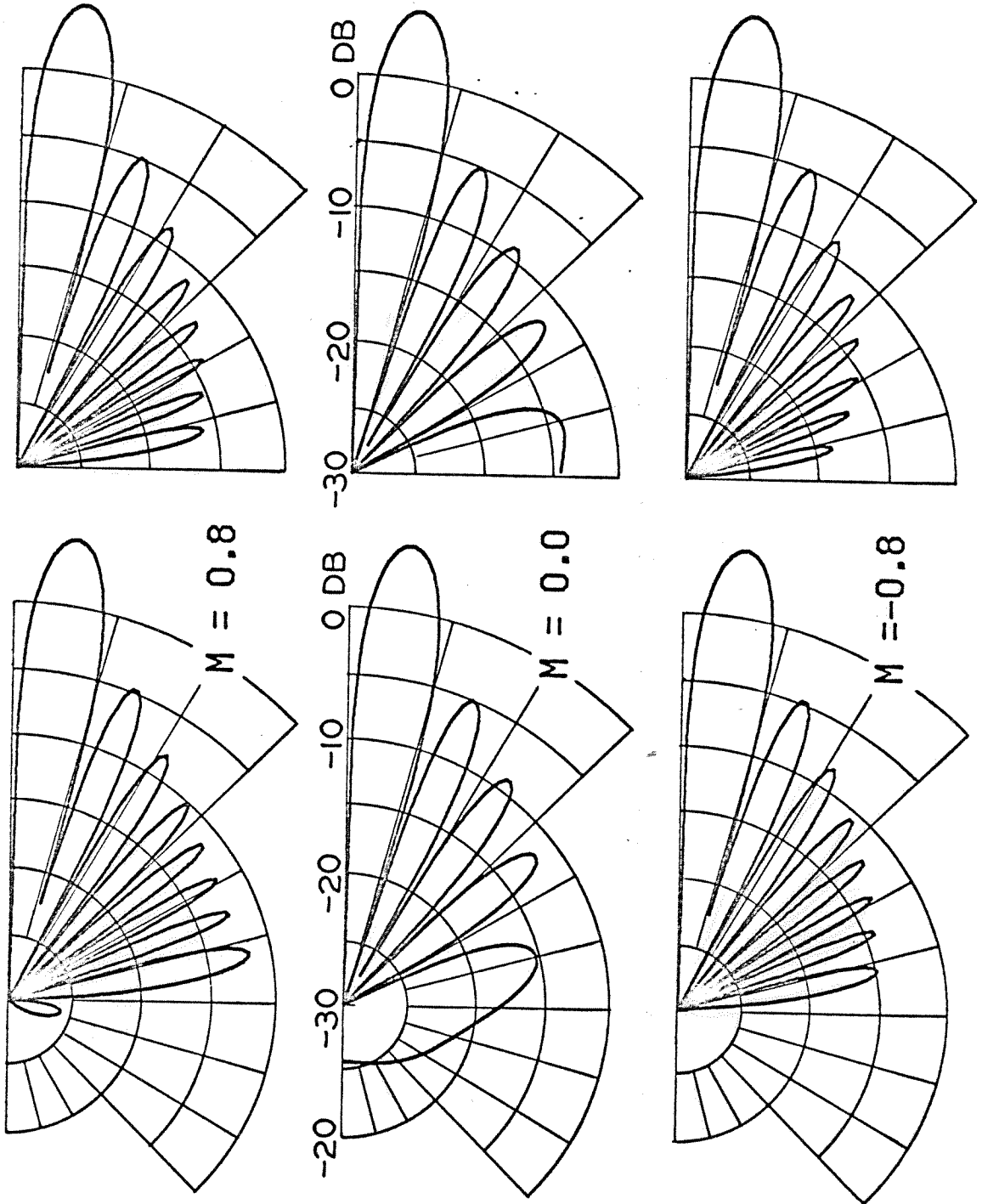
Fig. 5-2c. Radiation patterns $D(\theta; kb, N, M)$ for a duct formed by two semi-infinite parallel hard plates. The exact Wiener-Hopf solution is on the left; the approximate Fraunhofer solution is on the right. kb = 12. $N = 1$.

Fig. 5-2d. Radiation patterns $D(\theta; kb, N, M)$ for a duct formed by two semi-infinite parallel <u>hard</u> plates. The exact Wiener-Hopf solution is on the left; the approximate Fraunhofer solution is on the right. kb = 16. $N = 1$

Fig. 5-2e. Radiation patterns $D(\theta; kb, N, M)$ for a duct formed by two semi-infinite parallel <u>hard</u> plates. The exact Wiener-Hopf solution is on the left; the approximate Fraunhofer solution is on the right. $kb = 20$. $N = 1$.
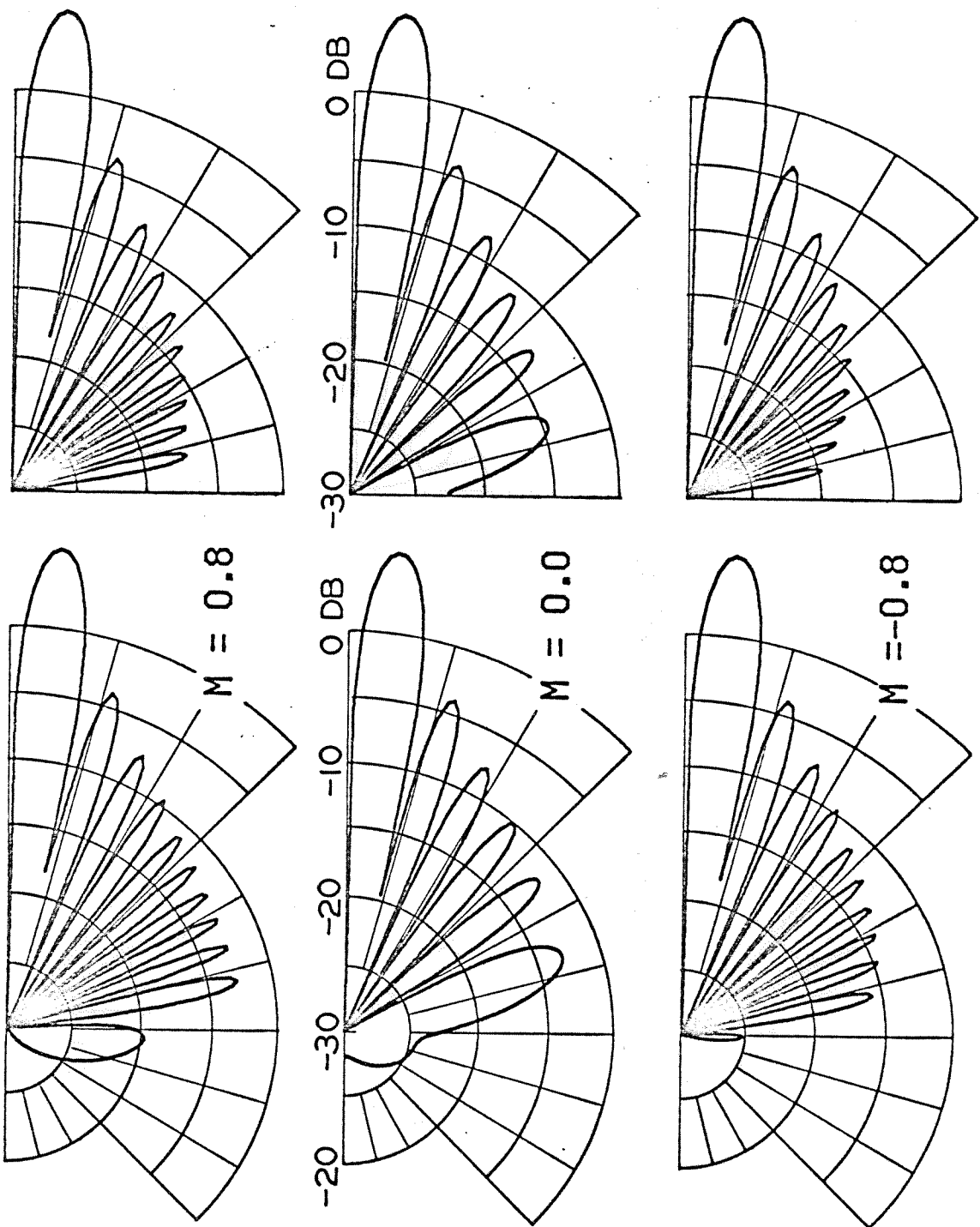
Fig. 5-3a. Radiation patterns $D(\theta; kb, N, M)$ for a duct formed by two semi-infinite parallel plates. Patterns corresponding to hard plates are on the left, while the patterns for soft plates are on the right. $kb = 8$. $N = 2$
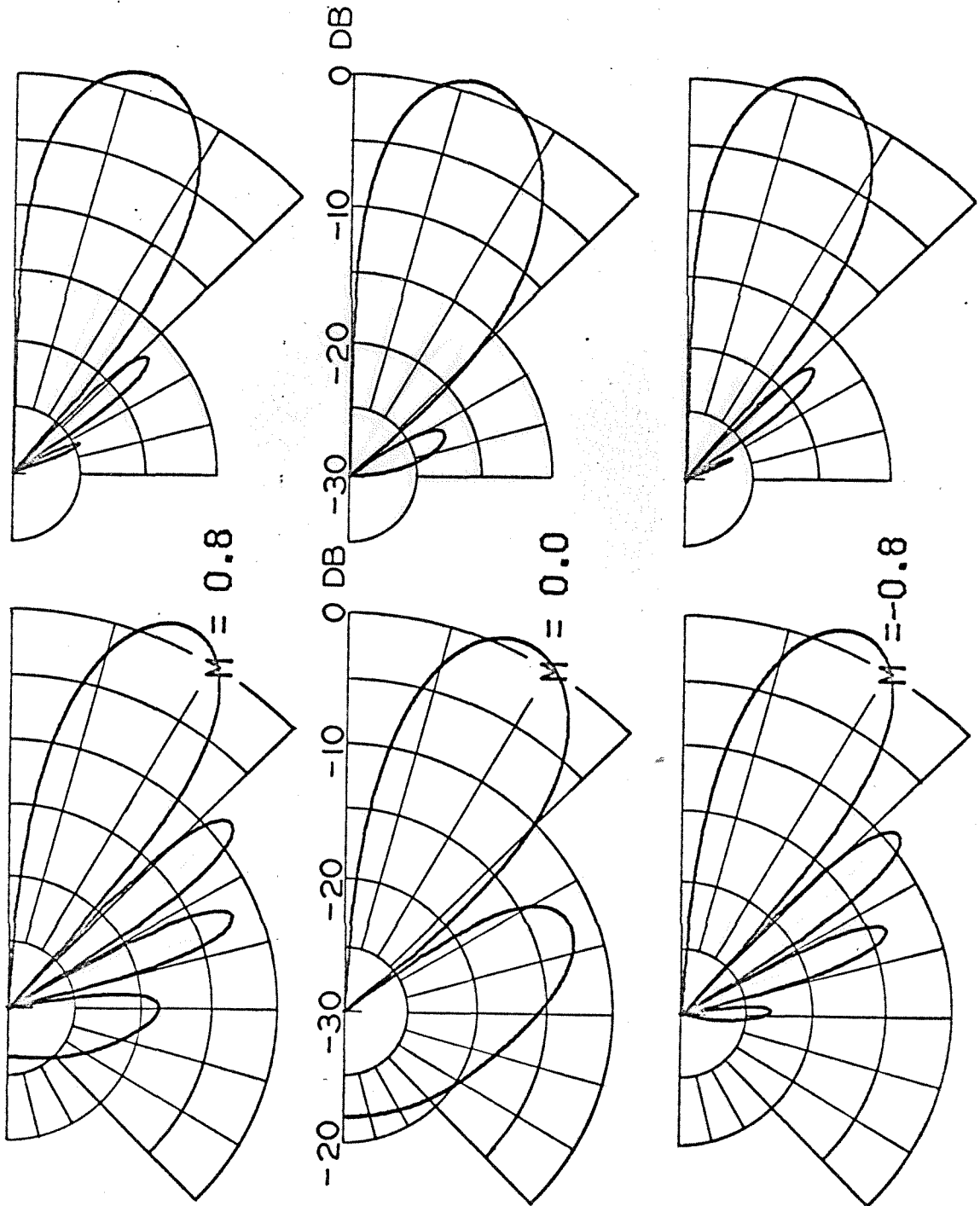
Fig. 5-3b. Radiation patterns $D(\theta; kb, N, M)$ for a duct formed by two semi-infinite parallel plates. Patterns corresponding to hard plates are on the left, while the patterns for soft plates are on the right. $= 12.$ **N = 2.**
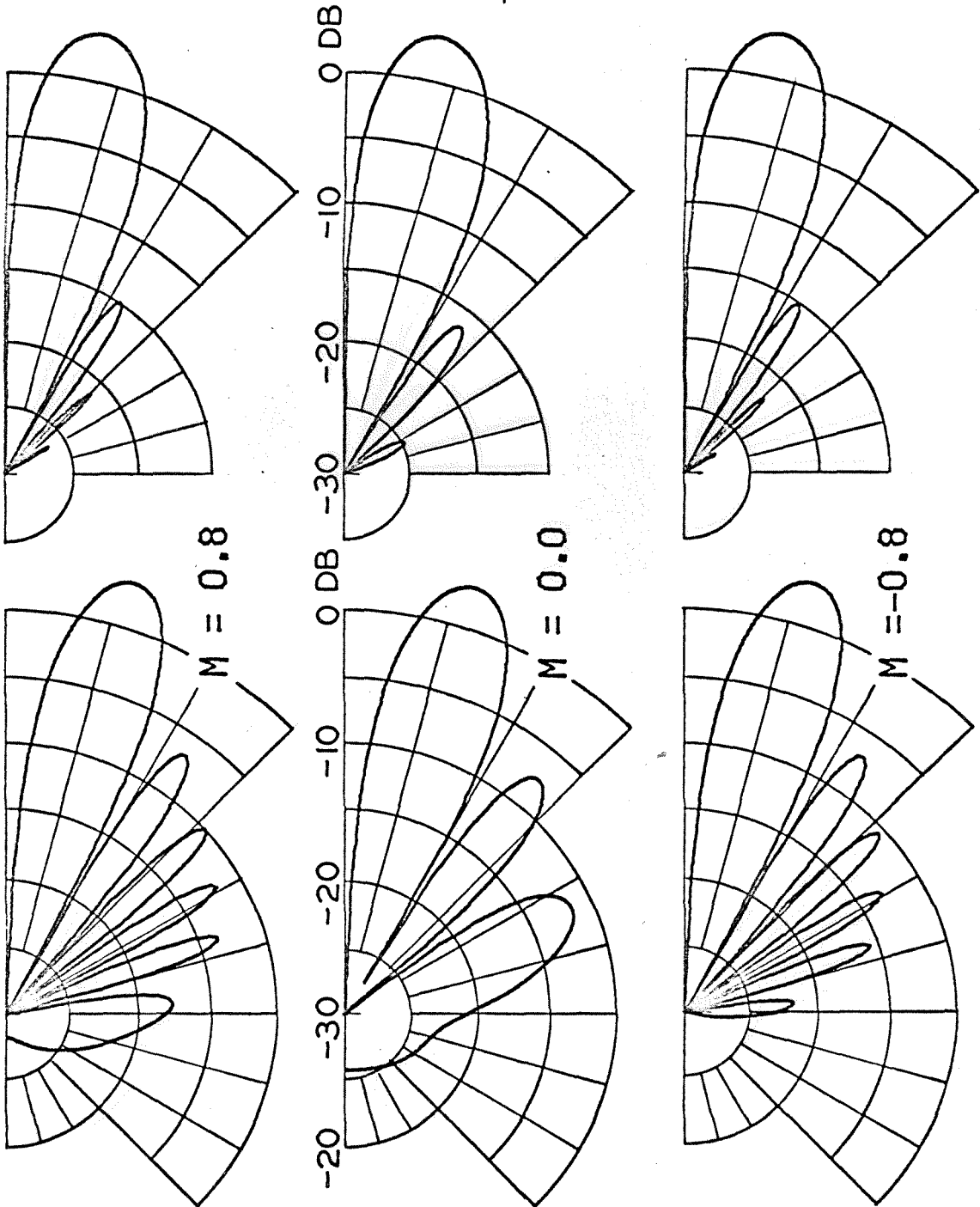
Fig. 5-3c. Radiation patterns $D(\Theta; kb, N, M)$ for a duct formed by two semi-infinite parallel plates. Patterns corresponding to hard plates are on the left, while the patterns for soft plates are on the right. kb = 16. $N = 2$.
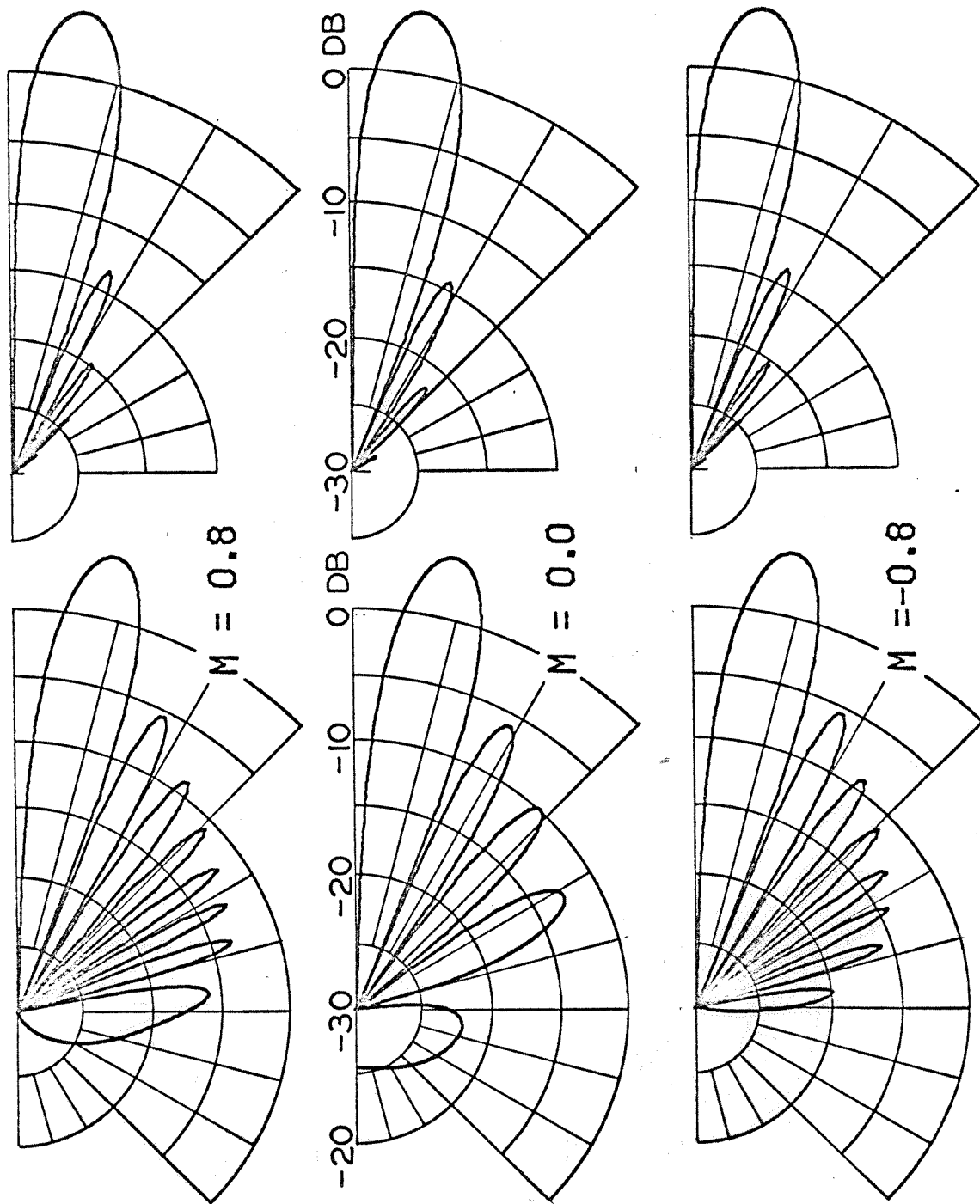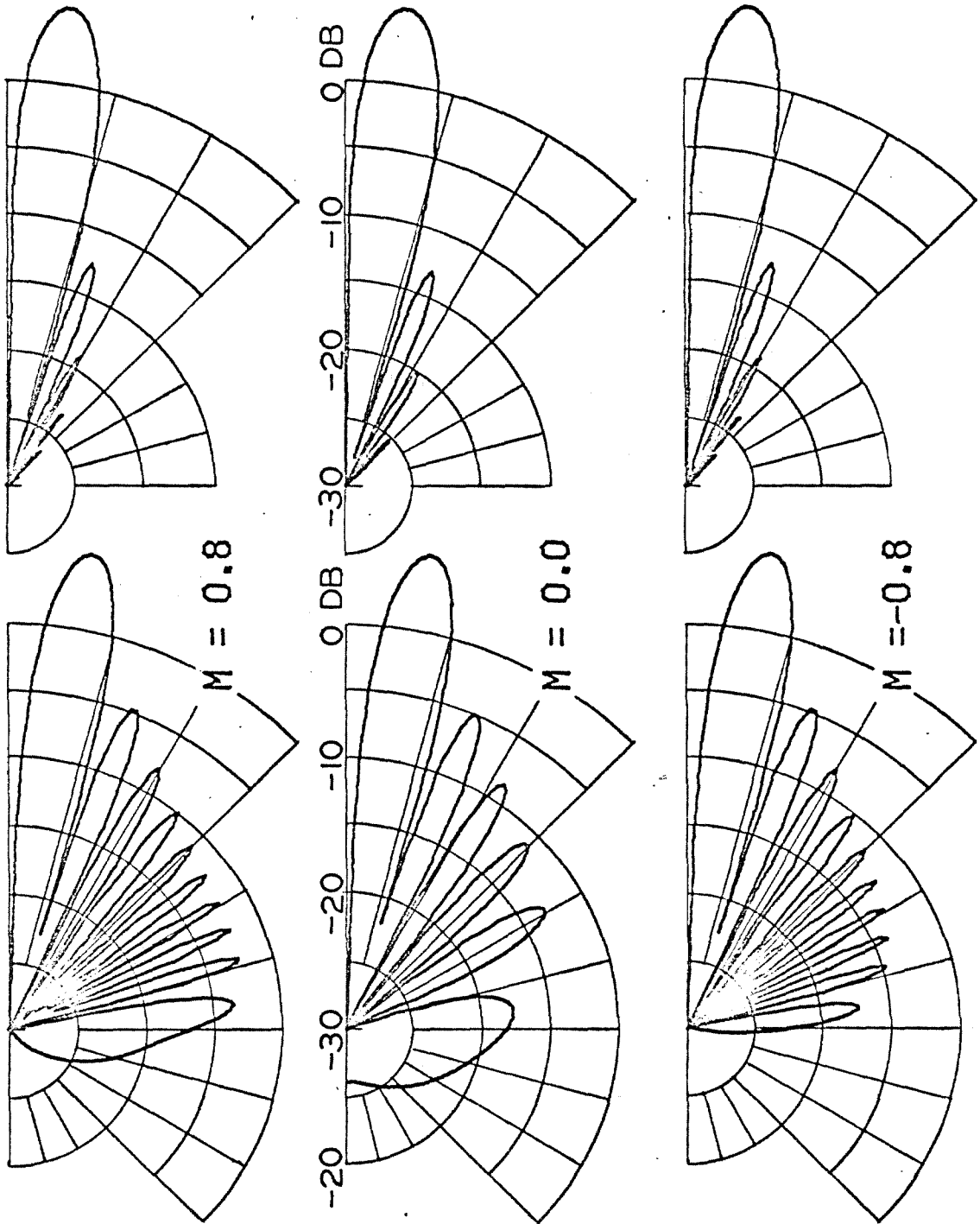
Fig. 5-3d. Radiation patterns $D(\theta; kb, N, M)$ for a duct formed by two semi-infinite parallel plates. Patterns corresponding to hard plates are on the left, while the patterns for soft plates are on the right. kb = 20. $N = 2$.
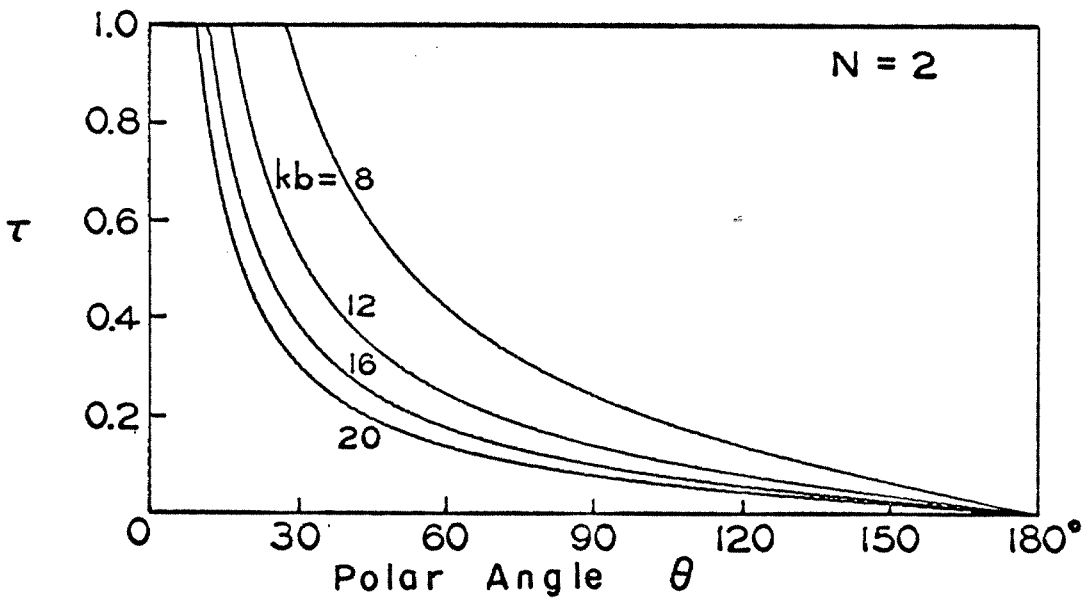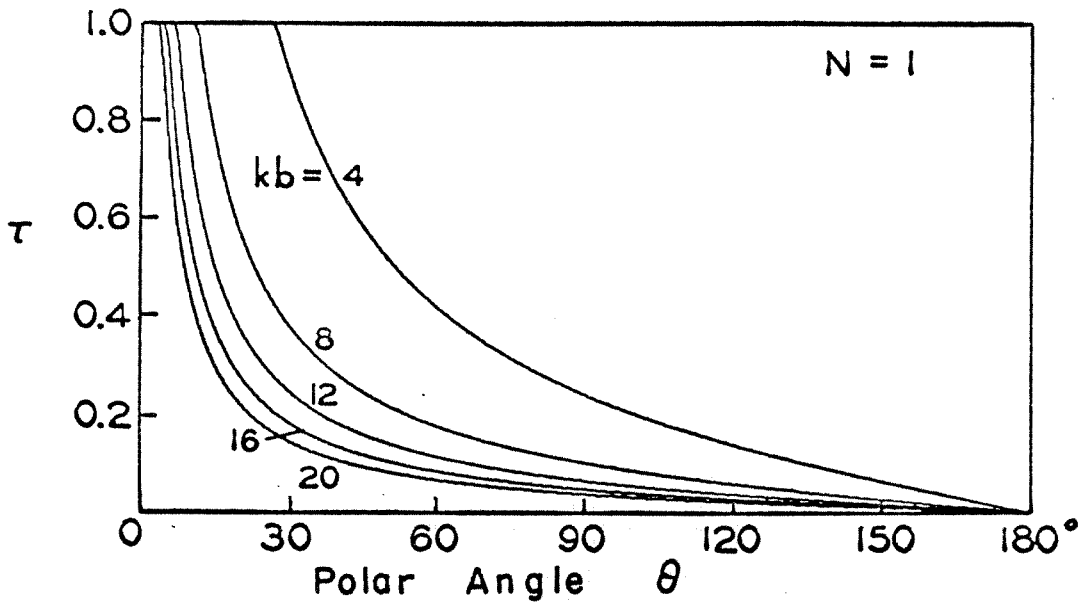
Fig. 5-4.   Ratio τ of the far field radiation corresponding to a soft wall duct to the far field for a hard wall duct. The duct is formed by two semi-infinite parallel plates.
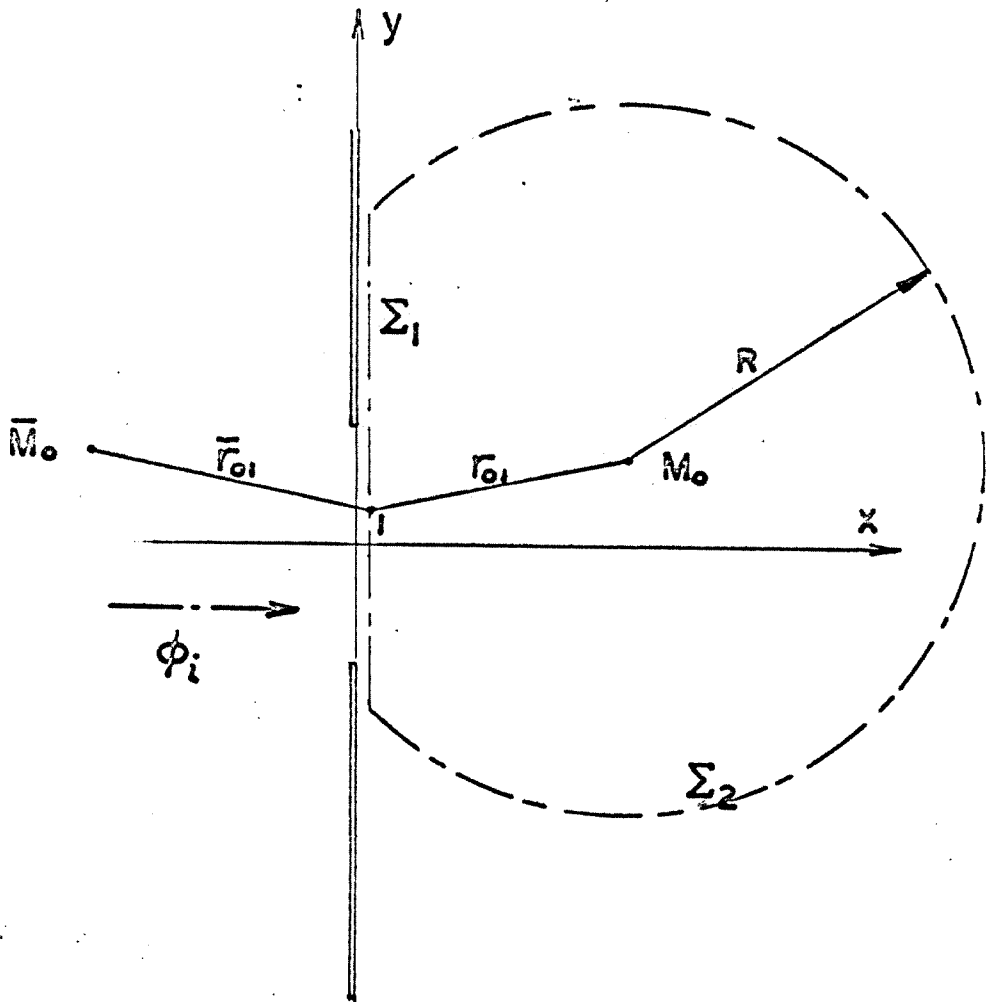
Fig. 5-5. Geometry of the approximate radiation problem.

CHAPTER VI

TRANSMISSION AND REFLECTION OF A PLANE ACOUSTIC WAVE

AT A COMPRESSOR BLADE ROW

6.1 INTRODUCTION

The axial turbomachinery in a turbofan engine generates acoustic pressure waves. These waves are transmitted and reflected by various blade rows (stator guide vanes, inlet guide vanes, other stages' blade rows), then propagate along the inlet and exhaust ducts and radiate from the end sections. In this chapter we study the transmission and reflection of a pressure wave by a single blade row. Our goal is to solve this problem utilizing the transformation developed in Chapter 3. This method is particularly suited to the present problem because it will provide relations between the basic transmission and reflection coefficients of the blade row in a stationary medium and the corresponding coefficients for the blade row immersed in a uniform flow. A clearer picture of the effect of the moving medium on the basic acoustical characteristics of the blade row will result.

We use a simple model developed by Kaji and Okazaki [6.1, 6.2] and by Mani and Horvay [6.3], where the blade row is represented as a linear two-dimensional cascade with thin non-cambered blades. The flow through the cascade is parallel to the blades, with a uniform Mach number M (for instance, the average between entrance and exit Mach numbers). The actual spinning pressure modes are represented in this model as plane waves incident on the blade row under various inclinations. The incidence angle is related to the propagation characteristics of the spinning mode.

Various techniques have been used to solve this problem. Kaji and Okazaki [6.1] based their analysis on the semiactuator description in which the blades are chosen of finite chord but infinitesi-

mal spacing. Only one transmitted wave propagating in the same direction as the incident wave and only one "specularly" reflected wave were considered. The blade row acts like a region of different impedance, with a unique propagation direction. Matching the pressure and mass flow on the blade row boundaries yields the transmission and reflection coefficients.

In a second paper [6.2], the effects of finite blade spacing were included. The incident wave induces a distribution of acoustic doublets on the blades. The distribution which cancels the normal velocity component on the blades is found and the pressure field can then be computed.

Mani and Horvay [6.3] treated two separate problems: an incidence problem where a plane wave impinges on an infinite set of semi-infinite blades, and an emission problem where the blade channel modes excited by the incident wave radiate at the open ends of a row of semi-infinite blades. The Wiener-Hopf technique yields the two solutions which are then combined to produce the transmission and reflection coefficients of the blade row. A basic assumption of this computation is that the blades are infinitely long, i.e., that the ratio of the blade chord to the wavelength ℓ/λ is large. Actually, Mani and Horvay showed that their solution yields results which compare well with those of Kaji and Okazaki [6.2], even when ℓ/λ is small.

Amiet [6.4] used the method of matched asymptotic expansions to compute the unsteady force distribution on the blades and the resulting pressure field. An inner incompressible flow satisfying the no-flow condition on the blades is matched to an outer flow governed

by the wave equation, using a small parameter proportional to the ratio of the chord length to the wavelength ℓ/λ . This method provides the flow-induced acoustic field, while the basic scattering characteristics of the blade row are neglected under the assumption $\ell/\lambda \ll 1$. The results obtained by Amiet [6.4] compare rather well with those of Kaji and Okazaki [6.1] for a Mach number around $M = 0.5$, but as the Mach number decreases, the transmission coefficient tends to unity while the reflection coefficient vanishes and the differences become more pronounced.

References [6.1] through [6.3] do not separate the effect of the uniform flow from the basic acoustic characteristics of the blade row, while the method used in reference [6.4] altogether neglects these characteristics and only provides the flow-induced acoustic field. In an actual turbofan, the ratio ℓ/λ is of order one and both fields flow induced, and scattered by the blade row must be accounted for.

It was shown in Chapter 3 that a class of acoustical boundary value problems in a subsonic medium could be solved by considering an associated problem in a stationary medium and applying a simple algebraic transformation. The Sommerfeld diffraction problem in a uniformly moving medium was solved in this way. The present problem where an infinite lattice of plates is immersed in a uniform flow has a very similar structure. In fact, the transformation immediately converts the convective wave equation into Helmholtz' equation and the boundary conditions on the blades into new boundary conditions for a problem in a stationary medium.

This would, at first glance, lead to the conclusion that the two problems in a moving and in a stationary medium are equivalent through the transformation and that the transmission and reflection coefficients may be directly obtained through the transformation. Unfortunately, this is not so. The difficulty lies in the fact that the uniform flow creates a fundamental difference between upstream and downstream regions.

In the upstream region, in front of the blade leading edges, the velocity potential φ is continuous. Downstream, the blade trailing edges produce vortex sheets, the velocity potential is discontinuous, but the pressure perturbation p is continuous. (A more extensive discussion may be found in Chapter 3.) To solve the difficulty we have adopted the following plan. We first describe in some detail the problem in a stationary medium ($M = 0$) in terms of a potential Φ representing the pressure or the velodity potential ($p = \bar{\rho} i \omega \varphi$). Then we deal with the case where the incident wave is downstream ($M > 0$). The problem is decomposed into an incidence problem (downstream) described in terms of the pressure and a radiation problem (upstream) described in terms of the velocity potential. The solutions are obtained by transforming the solutions of associated $M = 0$ problems. Simple relations for the transmission and reflection coefficients result. Finally, the case where the incident wave is upstream ($M < 0$) is briefly discussed.

6.2 TRANSMISSION AND REFLECTION AT A
BLADE ROW IN A STATIONARY MEDIUM

The geometry of the problem is shown on fig. 6-1. This problem is decomposed into an incidence and radiation problem following a procedure used by Mani and Horvay [6.3]. The incidence problem is shown on fig. 6-2. A plane wave is incident on a set of semi-infinite blades. The stagger angle is β, the distance between the blades d, the nth blade extends from $x = nd \tan \beta$ to $x = -\infty$. All waves are steady with a time factor $\exp(-i\omega t)$. The incident wave potential has the form

$$\phi_i = \exp(-ikx \cos \Theta_I - iky \sin \Theta_I) \tag{6.1}$$

$$k = \omega/c \tag{6.2}$$

The complete potential is as usual written as a sum of the incident wave potential and an induced potential

$$\phi_t = \phi_i + \phi \tag{6.3}$$

Equation (6.3) satisfies the Helmholtz equation, and consequently

$$\phi_{xx} + \phi_{yy} + k^2 \phi = 0 \tag{6.4}$$

On the blades the displacement vanishes

$$\frac{\partial \phi_t}{\partial y}\bigg|_{n\text{-th blade}} = 0 \qquad n = \ldots, -2, -1, 0, 1, \ldots \tag{6.5}$$

or

$$\frac{\partial \phi}{\partial y}\bigg|_{n\text{-th blade}} = ik \sin \Theta_I \exp(-ikx \cos \Theta_I - ikn d \sin \Theta_I) \tag{6.6}$$
$$n = \ldots, -2, -1, 0, 1, \ldots$$

We define the local set of coordinates originating at the nth blade edge:

$$x_n = x - nq \tag{6.7}$$

$$y_n = y - nd \tag{6.8}$$

with

$$q = d \tan \beta \tag{6.9}$$

The problems (6.1) through (6.6) may be solved by the Wiener-Hopf technique. The induced potential in the nth blade channel is related to the potential in the first channel by a simple phase relation

$$\Phi_n(x_n, y_n) = e^{-ikng} \Phi_0(x_n, y_n) \tag{6.10}$$

where

$$g = q \cos \Theta_I + d \sin \Theta_I \tag{6.11}$$

or

$$g = d \sin(\Theta_I + \beta) / \cos \beta \tag{6.12}$$

The potential in the first blade channel is a sum of modes propagating in the negative x -direction. The higher modes are exponentially attenuated; their contribution to the transmission is negligible if the blade channels are sufficiently long. The potential in the first blade channel (transmitted potential) has the form

$$\Phi_{trans} = \sum_{g=0}^{L} \sigma_0(g) e^{i\nu_g} e^{-ik\eta_g x} \cos(g \pi y / d) \tag{6.13}$$

where

$$\eta_\gamma = \left[1 - (\gamma\pi/kd)^2 \right]^{1/2} \tag{6.14}$$

The integer L is the greatest value of γ for which η_γ is real and the corresponding mode propagates unattenuated:

$$L < \frac{kd}{\pi} < L + 1 \tag{6.15}$$

$e^{i\nu_\gamma}$ is the transmission coefficient phase factor. $\tau_0(\gamma)$ is the modulus of the transmission coefficient

$$\tau_0(\gamma) = \tau_0(\gamma, \Theta_I, k ; \beta, d) \tag{6.16}$$

The blade row produces a reflected potential in the region $x' \geq 0$ which is a sum of plane waves. Again, we discard all the attenuated waves from this sum:

$$\phi_{refl} = \sum_{r=-N}^{S} R_0(r) e^{i\nu_r} e^{-ikx\cos\Theta_R - iky\sin\Theta_R} \tag{6.17}$$

Upper bounds for S and N are given in Appendix 6-A. It is shown that S is the largest integer contained in

$$\frac{1 + \sin(\Theta_I + \beta)}{2\cos\beta} \left(\frac{kd}{\pi}\right) \tag{6.18}$$

while N is the largest integer contained in

$$\frac{1 - \sin(\Theta_I + \beta)}{2\cos\beta} \left(\frac{kd}{\pi}\right) \tag{6.19}$$

$e^{i\nu_r}$ is the reflection coefficient phase factor. $R_0(r)$ is the modulus of the reflection coefficient and

$$R_0(r) = R_0(r, \Theta_I, k; \beta, d) \tag{6.20}$$

We now describe the radiation from the end of the blade channels.

We consider now a set of blades with stagger angle β extending

from $x = nd \tan\beta$ to $x = +\infty$ (fig. 6-3). The incident wave is one of the modes of the sum (6.13). In the first blade channel this wave has the form

$$\Phi_{inc} = e^{-ik\eta_\gamma x} \cos(\gamma \pi y/d) \tag{6.21}$$

This wave produces a radiated potential consisting of an infinity of plane waves. We discard the attenuated waves from this sum:

$$\Phi_{rad} = \sum_{r=-N}^{S} \epsilon_0(\gamma, r) e^{i\nu_\gamma r} e^{-ikx\cos\Theta_E - iky\sin\Theta_E} \tag{6.22}$$

The values of S and N are also determined by (6.18) and (6.19).

$\epsilon_0(\gamma, r)$ is the modulus of the radiation coefficient for the jth channel mode and the rth radiated plane wave.

We can now assemble expressions (6.13) and (6.22) to obtain the transmission coefficients

$$T_0(\gamma, r, \Theta_I, k; \beta, d) = \tau_0(\gamma, \Theta_I, k; \beta, d)\epsilon_0(\gamma, r) \tag{6.23}$$

There are $L+1$ blade channel modes and $N+S+1$ radiated

plane waves resulting in a matrix $(L+1) \times (N+S+1)$ of transmission coefficients. There are only $N+S+1$ reflection coefficients of the form (6.20).

The Wiener-Hopf technique also provides full expressions for T_o and R_o but they are not needed here. Our goal is to find relationships between T_o and R_o for the blade row in a stationary medium and T and R for the blade row in a moving medium, independent of the particular forms of T_o and R_o.

6.3 TRANSMISSION AND REFLECTION AT
A BLADE ROW IN UNIFORM FLOW

Consider an incident plane wave in the downstream region
($M > 0$). We describe this region in terms of the pressure. The
incident wave has now the form

$$p_i = \exp\left(-\frac{ikx\cos\Theta_I}{1-M\cos\Theta_I} - \frac{iky\sin\Theta_I}{1-M\cos\Theta_I}\right) \tag{6.24}$$

The complete pressure perturbation $p_t = p_i + p$ and con-
sequently p, the induced pressure perturbation, satisfy the
convective wave equation

$$p_{xx}(1-M^2) + p_{yy} + 2Mikp_x + k^2p = 0 \tag{6.25}$$

The displacement vanishes on the blade surfaces

$$\left.\frac{\partial p_t}{\partial y}\right|_{n\text{-th blade}} = 0 \qquad n = \ldots, -2, -1, 0, 1, \ldots \tag{6.26}$$

or

$$\left.\frac{\partial p}{\partial y}\right|_n = \frac{ik\sin\Theta_I}{1-M\cos\Theta_I}\exp\left(-\frac{ikx\cos\Theta_I}{1-M\cos\Theta_I} - \frac{iknd\sin\Theta_I}{1-M\cos\Theta_I}\right) \tag{6.27}$$

Guided by the results of Chapter 3, we introduce the following trans-
formation

$$k_1 = k/(1-M^2)^{1/2} \tag{6.28}$$

$$x_1 = x/(1-M^2)^{1/2} \tag{6.29}$$

$$\cos \Theta_I' = (\cos \Theta_I - M)/(1 - M\cos \Theta_I) \tag{6.30}$$

$$p = e^{-ik_1 M x_1} F(x_1, y; k, \Theta_I') \tag{6.31}$$

The boundary value problem for F is

$$F_{x_1 x_1} + F_{yy} + k_1^2 F = 0 \tag{6.32}$$

$$\frac{\partial F}{\partial y}\bigg|_{n\text{-th blade}} = i k_1 \sin \Theta_I' \exp(-ik_1 x_1 \cos \Theta_I')$$

$$\exp(-ik_1 n d \sin \Theta_I') \tag{6.33}$$

Thus,

$$F \equiv \Phi(x_1, y; \Theta_I', k_1, \beta_1, d) \tag{6.34}$$

where the new stagger angle β_1 is such that

$$\tan \beta_1 = \frac{q_1}{d} = \frac{q}{d(1-M^2)^{1/2}} \tag{6.35}$$

or

$$\tan \beta_1 = (1-M^2)^{-1/2} \tan \beta \tag{6.36}$$

From expressions (6.13), (6.31), and (6.34), we obtain the transmitted pressure in the first blade channel

$$P_{trans} = \sum_{\gamma=0}^{L} \sigma_0(\gamma, \Theta'_I, k_1; \beta_1, d)$$

$$e^{i\nu'_\gamma} e^{-ik_1\eta'_\gamma x_1 - ik_1 M x_1} \cos(\gamma \pi y/d) \tag{6.37}$$

where η'_γ represents the transformed η_γ

$$\eta'_\gamma = \left[1 - (\gamma\pi/k_1 d)^2 \right]^{1/2} \tag{6.38}$$

The reflected pressure field may be found from (6.17), (6.31), and (6.34)

$$P_{ref} = \sum_{r=-N}^{S} R_0(r, \Theta'_I, k_1; \beta_1, d)$$

$$e^{i\nu'_r} e^{-ik_1 x_1 \cos\Theta'_R - ik_1 y \sin\Theta'_R - ik_1 M x_1} \tag{6.39}$$

Θ'_R is the reflection angle in the associated problem for a stationary medium, and is related to the actual reflection angle by

$$\cos\Theta'_R = (\cos\Theta_R - M)/(1 - M\cos\Theta_R) \tag{6.40}$$

Consider now the radiation problem in the upstream region. We use the velocity potential φ to formulate this problem.

As an incident wave we take one of the modes from expression (6.37). In the first blade channel

$$\varphi_{inc} = e^{-ik_1 \eta'_j x_1 - i k_1 M x_1} \cos(j\pi y/d) \qquad (6.41)$$

We write the complete potential $\varphi_t = \varphi_i + \varphi$, where φ satisfies the convective wave equation

$$\varphi_{xx}(1-M^2) + \varphi_{yy} + 2Mik\varphi_x + k^2\varphi = 0 \qquad (6.42)$$

We use now the transformation (6.28), (6.29) and the function Ψ defined by

$$\varphi = e^{-ik_1 M x_1} \Psi(x_1, y; k_1, j) \qquad (6.43)$$

Then

$$\Psi_{inc} = e^{-ik_1 \eta'_j x_1} \cos(j\pi y/d) \qquad (6.44)$$

and

$$\Psi_{x_1 x_1} + \Psi_{yy} + k_1^2 \Psi = 0 \qquad (6.45)$$

The problem (6.44), (6.45) is identical to the problem (6.4), (6.21) for φ , and thus from (6.22) and (6.43) we get

$$\varphi_{rad} = \sum_{j=0}^{L} \epsilon_0(j, r) \, e^{i\nu'_j r} \, e^{-ik_1 M x_1} \, e^{-ik_1 x_1 \cos\Theta'_E - ik_1 y \sin\Theta'_E} \qquad (6.46)$$

Again, Θ'_E is related to the actual emission angle Θ_E by

$$\cos\Theta'_E = (\cos\Theta_E - M)|(1 - M\cos\Theta_E) \qquad (6.47)$$

From the velocity potential we compute the pressure by

$$p = \bar{\rho} c \left(i k \varphi - M \frac{\partial \varphi}{\partial x} \right) \tag{6.48}$$

or

$$p = \frac{\bar{\rho} c i k_1}{(1 - M^2)^{1/2}} \left(i k_1 \phi - M \frac{\partial \phi}{\partial x_1} \right) e^{-i k_1 M x_1} \tag{6.49}$$

For the incoming wave

$$p_{inc} = \frac{\bar{\rho} c i k_1}{(1 - M^2)^{1/2}} \left(1 + M \eta_j' \right) \varphi_{inc} \tag{6.50}$$

For the radiated waves

$$p_{rad} = \sum_{r = -N}^{S} \frac{\bar{\rho} c i k_1}{(1 - M^2)^{1/2}} \left(1 + M \cos \Theta_E' \right) \epsilon_0 (\mathcal{Y}, r)$$

$$e^{i \eta_j' r} e^{-i k_1 x_1 \cos \Theta_E' - i k_1 y \sin \Theta_E' - i k_1 M x_1} \tag{6.51}$$

and thus a unit incoming pressure wave produces

$$p_{rad} = \sum_{r = -N}^{S} \frac{1 + M \cos \Theta_E'}{1 + M \eta_j'} \epsilon_0 (\mathcal{Y}, r)$$

$$e^{i \eta_j' r} e^{-i k_1 x_1 \cos \Theta_E' - i k_1 y \sin \Theta_E' - i k_1 M x_1} \tag{6.52}$$

It is now possible to combine expressions (6.37) and (6.52) to

obtain the transmission coefficient for a blade row immersed in a uni-

form flow, the incident wave propagating downstream

$$T_1(\gamma, r, \Theta_I, k, M; \beta, d) =$$

$$\frac{1 + M\cos\Theta_E'}{1 + M\eta_\gamma'} \, \mathsf{E}_0(\gamma, r, k_1; \beta_1, d) \, \mathsf{G}_0(\gamma, \Theta_E', k_1; \beta_1, d) \quad (6.53)$$

and then from (6.23)

$$T(\gamma, r, \Theta_I, k, M; \beta, d) =$$

$$\frac{1 + M\cos\Theta_E'}{1 + M\eta_\gamma'} \, T_0(\gamma, r, \Theta_I', k_1; \beta_1, d) \quad (6.54)$$

The reflection coefficient is directly obtained from (6.39)

$$R(r, \Theta_I, k, M; \beta, d) = R_0(r, \Theta_I', k_1; \beta_1, d) \quad (6.55)$$

To obtain the simple results (6.54), (6.55), we had to assume that the blades were of infinite extent, i.e. ℓ/λ is large, so that upstream and downstream regions could be treated separately. Actually, the procedure used in the above derivation seems to yield good results even when ℓ/λ is less than one (Mani and Horvay [6.3]). In an actual fan or compressor $\ell/\lambda \sim 1$ and stagger angle and spacing are such that blade channels are physically existent. In view of all the other approximations used in the present model, the infinite extent assumption seems therefore reasonable.

When the incident wave is in the upstream region, i.e., the medium flows in the negative x direction ($M < 0$), we apply

the same techniques. The upstream region, where the incident wave propagates, is described in terms of the velocity potential, while the downstream region is described using the pressure perturbation, and the following expressions are obtained:

$$P_{trans} = \sum_{\gamma = 0}^{L} \frac{1 + M\eta'_{\gamma}}{1 + M\cos\Theta'_{I}} \, \overline{\zeta}_0(\gamma) \, e^{i\nu'_{\gamma}}$$
$$\exp(-ik_{\perp}\eta'_{\gamma} x_1 - ik_1 M x_1) \tag{6.56}$$

$$P_{ref} = \sum_{r = -N}^{S} \frac{1 + M\cos\Theta'_{R}}{1 + M\cos\Theta'_{I}} \, R_0(r) \, e^{i\nu'_{r}}$$
$$\exp(-ik_1 x_1 \cos\Theta'_{R} - ik_1 y \sin\Theta'_{R} - ik_1 M x_1) \tag{6.57}$$

$$P_{rad} = \sum_{r = -N}^{S} \epsilon_0(\gamma, r) \, e^{i\nu'_{r}}$$
$$\exp(-ik_1 x_1 \cos\Theta'_{R} - ik_1 y \sin\Theta'_{R} - ik_1 M x_1) \tag{6.58}$$

Then from (6.56) and (6.58) we obtain the transmission coefficients

$$T(\gamma, r, \Theta_I, k, M; \beta, d) =$$

$$\frac{1 + M\eta'_{\gamma}}{1 + M\cos\Theta'_{I}} \, T_0(\gamma, r, \Theta'_I, k_1; \beta_1, d) \tag{6.59}$$

and from (6.57) the reflection coefficients

$$R(r, \Theta_o, k, M; \beta, d) = \frac{1 + M\cos\Theta_R'}{1 + M\cos\Theta_I'} R_o(r, \Theta_I', k_1; \beta_1, d) \quad (6.60)$$

Under the assumptions used in the present mathematical model, expressions (6.54), (6.55), (6.59), (6.60) are completely general. They relate the acoustical characteristics of the blade row in a stationary medium to the characteristics of a blade row immersed in a uniform flow. The flow presence influences the transmission and reflection coefficients like an increase in frequency, from k to k_1, an increase in the stagger angle from β β_1, a change in the incidence angle from Θ_I to Θ_I' (when $M > 0$, then $\Theta_I' > \Theta_I$; when $M < 0$, then $\Theta_I' < \Theta_I$). Some multiplying factors also appear; their effect is more difficult to evaluate in the general case because they depend on the reflection and emission angles.

It is therefore useful to consider a specific situation where the expressions of T_o and R_o are known and study the effect of Mach number change on T and R.

Application of the Results

The semiactuator theory yields simple analytical expressions for the transmission and reflection coefficients T_o and R_o of a blade row in a stationary medium. Because the blade spacing in this theory is supposed infinitesimal, i.e., $d = 0$, only one "specularly" reflected wave ($r = 0$) and one transmitted wave ($r = 0$) exist. The transmitted wave propagates in the same di-

rection as the incident wave. The emission and reflection angles pertaining to the associated stationary medium problem are known.

Before we start to apply our results to this case, it is convenient to define the incidence angle α and the reflection angle δ with respect to the blade row normal direction x'. By looking at fig. 6-1 we see that

$$\alpha = \Theta_I + \beta \tag{6.61}$$

$$\delta = \Theta_R + \beta - \pi \tag{6.62}$$

For the semiactuator blade row in a stationary medium

$$\Theta'_E = \Theta'_I \tag{6.63}$$

$$\delta_1 = -\alpha_1 \tag{6.64}$$

or

$$\Theta'_R = \pi - \Theta'_I - 2\beta_1 \tag{6.65}$$

In the semiactuator theory, only one mode may propagate in the blade channels. Thus, $\gamma = 0$ and $\eta'_\gamma = 1$.

When the incident wave is downstream ($M > 0$), expressions (6.54) and (6.55) yield

$$T(\Theta_I, k, M; \beta, d) = \frac{1 + M\cos\Theta'_I}{1 + M} \, T_0(\Theta'_I, k_1; \beta_1, d) \tag{6.66}$$

and

$$R(\Theta, k, M; \beta, d) = R_0 (\Theta_{\perp}', k_1; \beta_1, d) \tag{6.67}$$

When the incident wave is upstream ($M < 0$) the expressions (6.59) and (6.60) give

$$T(\Theta_I, k, M; \beta, d) = \frac{1 + M}{1 + M \cos \Theta_I'} T_0 (\Theta_\perp', k_\perp; \beta_\perp, d) \tag{6.68}$$

and

$$R(\Theta_\perp, k, M; \beta, d) =$$

$$\frac{1 - M \cos(\Theta_I' + 2\beta_1)}{1 + M \cos \Theta_\perp'} R_0 (\Theta_\perp', k_1; \beta_1, d) \tag{6.69}$$

The expressions for T_0 and R_0 are developed in Appendix 6-B and reproduced here

$$T_0 = \left[1 + \frac{\sin^2 k\ell}{4} \left(\frac{\cos \alpha_1}{\cos \beta_1} - \frac{\cos \beta_1}{\cos \alpha_1} \right)^2 \right]^{-1/2} \tag{6.70}$$

$$R_0 = \left| \left(\frac{\cos \alpha_1}{\cos \beta_1} - \frac{\cos \beta_1}{\cos \alpha_1} \right) \frac{\sin k\ell}{2} \right| T_0 \tag{6.71}$$

It is interesting to write these expressions using the actual angles α and β . From (6.36) we deduce

$$\cos \beta_1 = \frac{(1-M^2)^{1/2} \cos \beta}{(1-M^2 \cos^2 \beta)^{1/2}} \qquad (6.72)$$

$$\sin \beta_1 = \frac{\sin \beta}{(1-M^2 \cos^2 \beta)^{1/2}} \qquad (6.73)$$

which, together with (6.30), produce

$$\cos \alpha_1 = \frac{(1-M^2)^{1/2}(\cos \alpha - M \cos \beta)}{(1-M \cos \Theta_1)(1-M^2 \cos^2 \beta)^{1/2}} \qquad (6.74)$$

Then

$$\frac{\cos \alpha_1}{\cos \beta_1} = \frac{\cos \alpha - M \cos \beta}{\cos \beta [1 - M \cos(\alpha - \beta)]} \qquad (6.75)$$

It is then easy to see that T vanishes and R becomes unity when

$$\alpha_1 = \pm \pi/2 \qquad \text{or} \qquad \cos \alpha = M \cos \beta \qquad (6.76)$$

and that R vanishes for $\cos \alpha_1 = \cos \beta_1$, or in terms of the actual angles

$$\cos \alpha - \cos \beta + M \cos \beta [\cos(\alpha - \beta) - 1] = 0 \qquad (6.77)$$

At $\alpha = \beta$, T is unity, while $R = 0$ and R will also

vanish for the second root of equation (6.77).

Kaji and Okazaki [6.1] have used the semiactuator theory to obtain directly the transmission and reflection coefficients of a blade row in a moving medium. All the features of T and R discussed above may also be found in reference [6.1] (for instance, equation (6.76), (6.77)). Plots of T and R obtained by the present method are almost identical to those given in [6.1], a few discrepancies occuring, for the case when the incident wave is upstream ($M < 0$), in the reflection coefficient R. Our R in this case is generally higher than R_{Kaji}. Reference [6.1] uses values of ℓ/λ of the order of $\frac{1}{2}$, while our theory is based on the assumption that ℓ/λ is large and thus would be expected to provide somewhat larger values for the reflection coefficient R. We give only two typical plots of T and R, fig. 6-4 for $M > 0$ and fig. 6-5 for $M < 0$. Other plots covering a large range of parameters may be found in reference [6.1].

Other applications of the general expressions (6.54), (6.55), (6.59), and (6.60) are conceivable. They could, for instance, be used to provide the transmission and reflection coefficients of a blade row in a steady flow from measurements of the stationary medium acoustical characteristics of the blade row. Such experiments in a stationary medium are, of course, much easier than in the presence of a steady flow.

REFERENCES

6.1 Kaji, S., and Okazaki, T., "Propagation of Sound Waves through a Blade Row. I. Analysis Based on the Semi-actuator Disk Theory," J. Sound Vib., 11 (1970), 339-353.

6.2 Kaji, S., and Okazaki, T., "Propagation of Sound Waves through a Blade Row. II. Analysis Based on the Acceleration Potential Method," J. Sound Vib., 11 (1970), 355-375.

6.3 Mani, R., and Horvay, G., "Sound Transmission through Blade Rows," J. Sound Vib., 12 (1970), 83-107.

6.4 Amiet, R.K., "Aerodynamic Sound Production and the Method of Matched Asymptotic Expansions," Ph.D. Thesis, Graduate School of Aerospace Engineering, Cornell University (1969).

APPENDIX 6-A

The Number of Reflected and Transmitted Waves

The reflected waves at a blade row in a stationary medium are of the form

$$\exp(-ikx\cos\Theta_R - iky\sin\Theta_R) \qquad (6A-1)$$

while the transmitted waves are proportional to

$$\exp(-ikx\cos\Theta_E - iky\sin\Theta_E) \qquad (6A-2)$$

It can be shown that the angles Θ_R and Θ_E are determined by the following set of equations:

$$\cos\Theta_R = \alpha_r^- \qquad (6A-3)$$

$$\sin\Theta_R = -\left[k^2 - (\alpha_r^-)^2\right]^{1/2} \qquad (6A-4)$$

$$\cos\Theta_E = \alpha_r^+ \qquad (6A-5)$$

$$\sin\Theta_E = \left[k^2 - (\alpha_r^+)^2\right]^{1/2} \qquad (6A-6)$$

where α_r^- and α_r^+ are the two roots of the second order equation

$$kg - \alpha q - 2\pi r = \pm d(k^2 - \alpha^2)^{1/2} \qquad (6A-7)$$

The canonical form of (6A-7) is

$$\alpha^2(q^2 + d^2) - 2\alpha q(kg - 2\pi r)$$
$$+ \left[(kg - 2\pi r)^2 - d^2 k^2\right] = 0 \qquad (6A-8)$$

with

$$q = d \tan \beta \tag{6A-9}$$

$$q = d \sin(\Theta_I + \beta) / \cos\beta \tag{6A-10}$$

The roots of equation (6A-8) are

$$\frac{\alpha_r^{\pm}}{k} = \sin\beta \cos\beta \left(\frac{q}{d} - \frac{2\pi r}{kd} \right)$$
$$\pm \cos\beta \left[1 - \left(\frac{q}{d} - \frac{2\pi r}{kd} \right)^2 \cos^2\beta \right]^{1/2} \tag{6A-11}$$

It can easily be shown that if α_r is real its extremum values are attained when

$$\frac{q}{d} - \frac{2\pi r}{kd} = \tan\beta \tag{6A-12}$$

then

$$\left(\frac{\alpha_r}{k} \right)_{\substack{Max \\ Min}} = \pm 1 \tag{6A-13}$$

Thus, if α_r is real, $|\alpha_r| \leqslant 1$, and the angles Θ_R, Θ_E determined by (6A-3) through (6A-6) are real, and consequently the plane waves (6A-1) and (6A-2) propagate unattenuated.

If α_r is complex the plane waves will be attenuated. The roots $\alpha_r^{\pm}$ will be real if the integer r satisfies the double inequality

$$-\left(\frac{1}{\cos\beta} - \frac{q}{d} \right) \frac{kd}{2\pi} \leqslant r \leqslant \left(\frac{1}{\cos\beta} + \frac{q}{d} \right) \frac{kd}{2\pi} \tag{6A-14}$$

We define the integers N and S by

$$N = \text{Integer part of } \left(\frac{1 - \sin(\Theta_I + \beta)}{2\cos\beta} \frac{kd}{\pi} \right) \qquad (6A-15)$$

$$S = \text{Integer part of } \left(\frac{1 + \sin(\Theta_I + \beta)}{2\cos\beta} \frac{kd}{\pi} \right) \qquad (6A-16)$$

then

$$-N \leqslant r \leqslant S \qquad (6A-17)$$

In actual fans the stagger angle β is generally less than 60°. Thus, an absolute upper bound for N and S is

$$\text{Max}(N, S) = \frac{2kd}{\pi} = \frac{4d}{\lambda} \qquad (6A-18)$$

For a particular engine like the Pratt and Whitney JT3D, $d/\lambda \sim 0.4$ for the fundamental frequency 3700 Hz and only the waves corresponding to $r = -1, 0, +1$ would propagate unattenuated.

The waves corresponding to $r = 0$ always propagate, the corresponding roots may be found using (6A-11)

$$\alpha_0^{\pm} = \sin\alpha\sin\beta \pm \cos\alpha\cos\beta \qquad (6A-19)$$

Thus,

$$\alpha_0^{+} = \cos(\alpha - \beta) = \cos\Theta_I \qquad (6A-20)$$

and

$$\Theta_E = \Theta_I \qquad (6A-21)$$

$$\alpha_o^- = -\cos(\alpha + \beta) = -\cos(\Theta_I + 2\beta) \qquad (6A-22)$$

and

$$\Theta_R = \pi - \Theta_I - 2\beta \qquad (6A-23)$$

The transmitted wave propagates in the same direction as the incident wave; the reflected wave propagates in the specular direction.

APPENDIX 6-B

Transmission and Reflection by a Blade Row

in a Stationary Medium

We use the semiactuator theory to obtain the transmission and reflection coefficients of a blade row in a stationary medium ($M = 0$). The blades have a finite chord ℓ but the spacing is assumed infinitesimal, i. e., the ratio d/λ is small. Consequently, only one-dimensional plane waves propagate in the blade row in a direction parallel to the blades (the X direction). The geometry of the problem is shown on fig. 6-1.

The transmission and reflection coefficients will be obtained by matching the pressure perturbations and $X'-$ direction displacements on the blade row boundaries. A plane wave is incident on the blade row in region I

$$p_i = \exp(-ikx\cos\Theta - iky\sin\Theta) \qquad (6B-1)$$

$$k = \omega/c \qquad (6B-2)$$

It is convenient to write this expression in terms of the Cartesian coordinates x', y' and the angle α

$$p_i = \exp(-ikx'\cos\alpha - iky'\sin\alpha) \qquad (6B-3)$$

It was shown in Appendix 6-A that when d/λ is small, only one reflected wave propagates in the specular direction

$$p_r = R\exp(-ikx'\cos\alpha_R - iky'\sin\alpha_R) \qquad (6B-4)$$

with

$$\alpha_R = \pi - \alpha \qquad (6B-5)$$

Then in region I

$$P_I = \exp(-ikx'\cos\alpha - iky'\sin\alpha)$$
$$+ R\ \exp(+ikx'\cos\alpha - iky'\sin\alpha) \qquad (6B-6)$$

Only one transmitted wave propagates in region III (d/λ is small),
in a direction parallel to that of the incident wave

$$P_{III} = T\ \exp(-ikx'\cos\alpha - iky'\sin\alpha) \qquad (6B-7)$$

In region II, one-dimensional plane waves propagate in the positive
or negative x directions. These waves have the same phase in the
y' direction as waves (6B-6) and (6B-7). Thus,

$$P_{II} = A\,e^{ikx - iky'\sin\alpha} + B\,e^{-ikx - iky'\sin\alpha} \qquad (6B-8)$$

and the associated velocity in the x direction is

$$w = \frac{1}{\rho i\omega}\frac{\partial P_{II}}{\partial x} \qquad (6B-9)$$

The matching relations at the blade row boundaries are
at $x' = 0$:

$$P_{II} = P_I \qquad (6B-10)$$

$$\left.\frac{\partial P_{II}}{\partial x}\right|_{x=0}\cos\beta = \left.\frac{\partial P_I}{\partial x'}\right|_{x'=0} \qquad (6B-11)$$

at $x' = -\ell$:

$$p_{II} = p_{III} \tag{6B-12}$$

$$\frac{\partial p_{II}}{\partial x}\Big|_{x=-\ell\cos\beta} \cos\beta = \frac{\partial p_{III}}{\partial x'}\Big|_{x'=-\ell\cos\beta} \tag{6B-13}$$

These four relations yield

$$A + B = 1 + R \tag{6B-14}$$

$$A - B = -\frac{\cos\alpha}{\cos\beta}(1-R) \tag{6B-15}$$

$$A e^{-ik\ell} + B e^{ik\ell} = T \tag{6B-16}$$

$$A e^{-ik\ell} - B e^{ik\ell} = -\frac{\cos\alpha}{\cos\beta} T \tag{6B-17}$$

and then

$$|T| = \left[1 + \frac{\sin^2 k\ell}{4}\left(\frac{\cos\alpha}{\cos\beta} - \frac{\cos\beta}{\cos\alpha}\right)^2\right]^{-1/2} \tag{6B-18}$$

$$|R| = \left|\left(\frac{\cos\alpha}{\cos\beta} - \frac{\cos\beta}{\cos\alpha}\right)\frac{\sin k\ell}{2}\right| |T| \tag{6B-19}$$
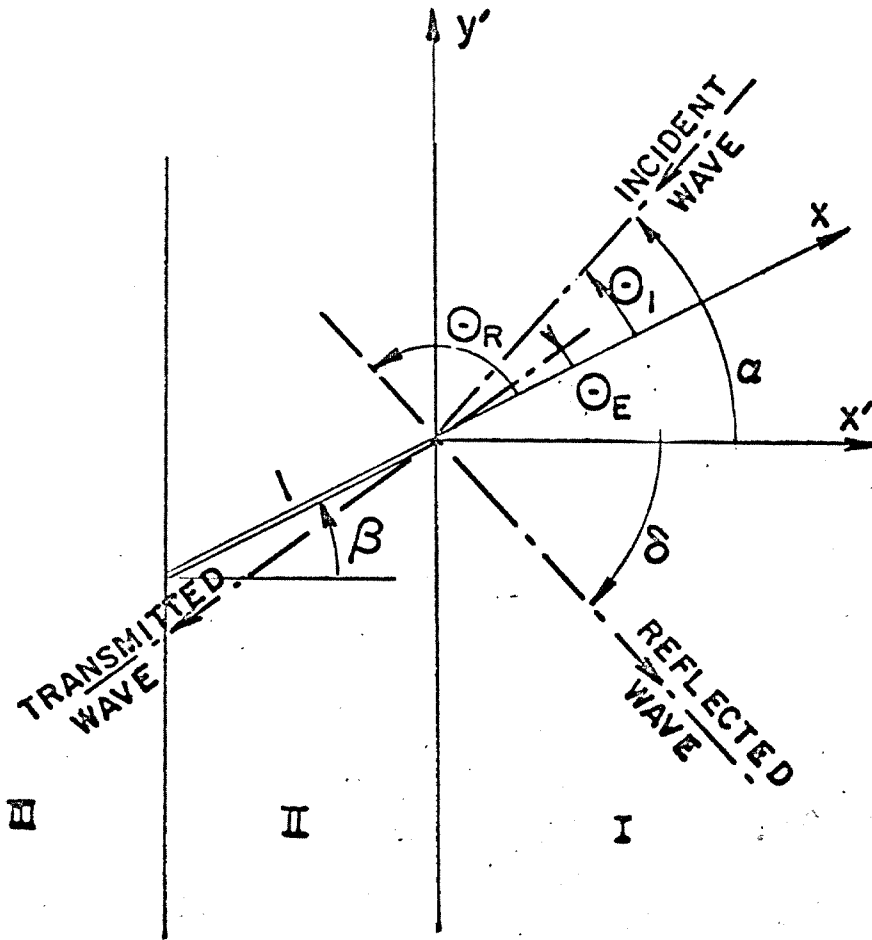
Fig. 6-1. Geometry of the Problem.
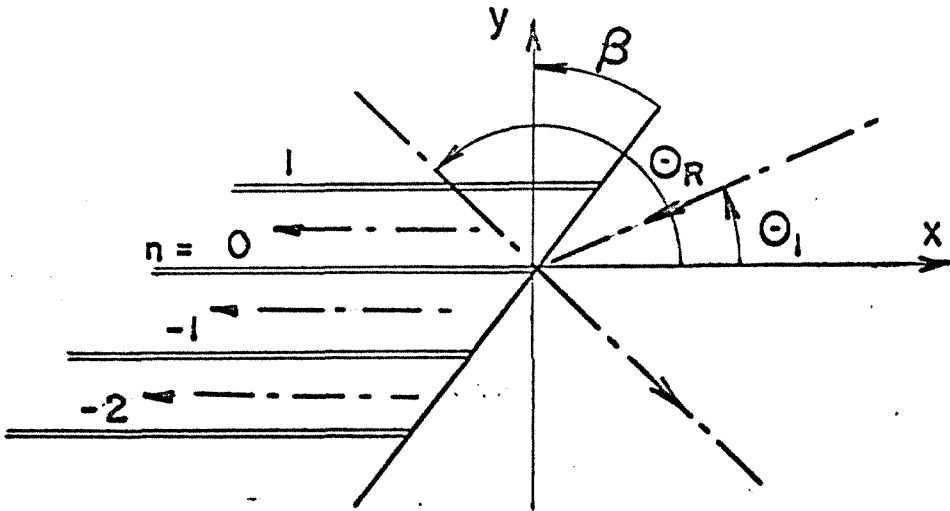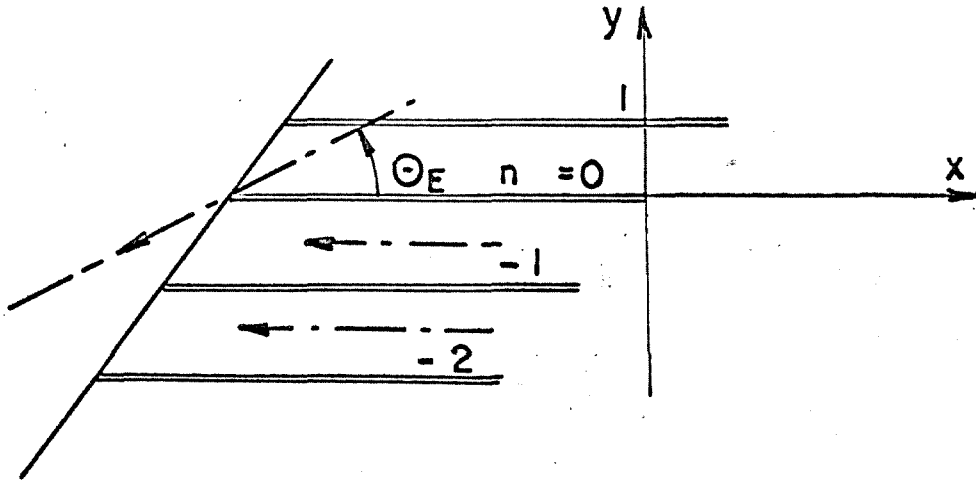
Fig. 6-2. Geometry of the Incidence Problem.
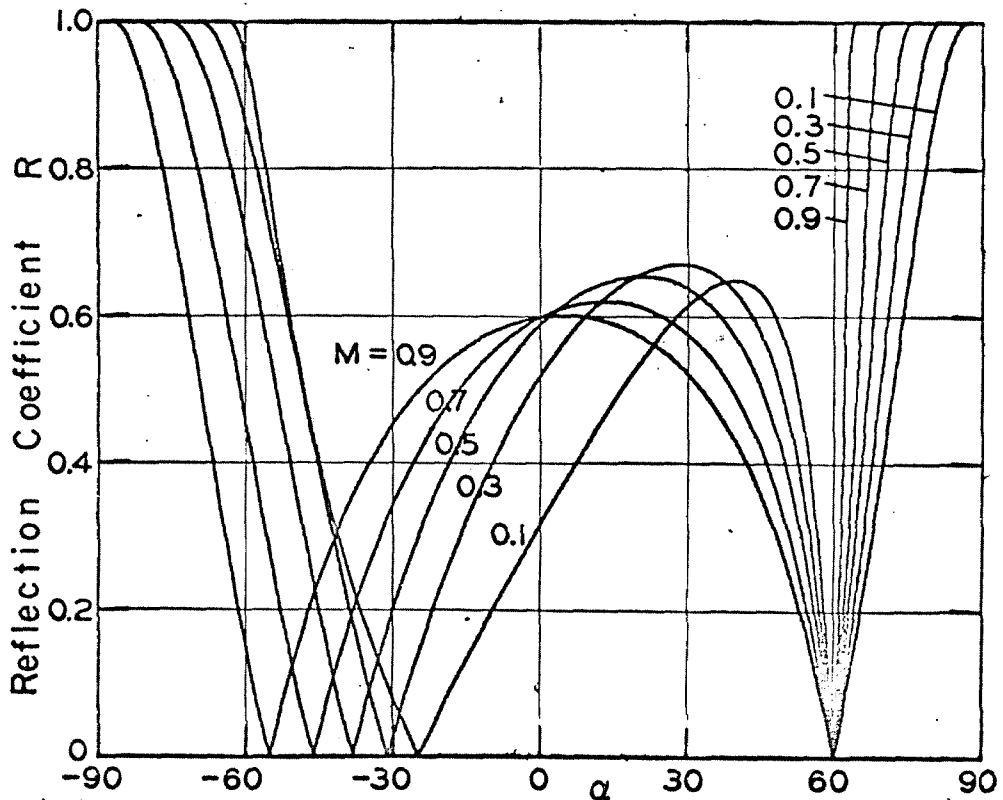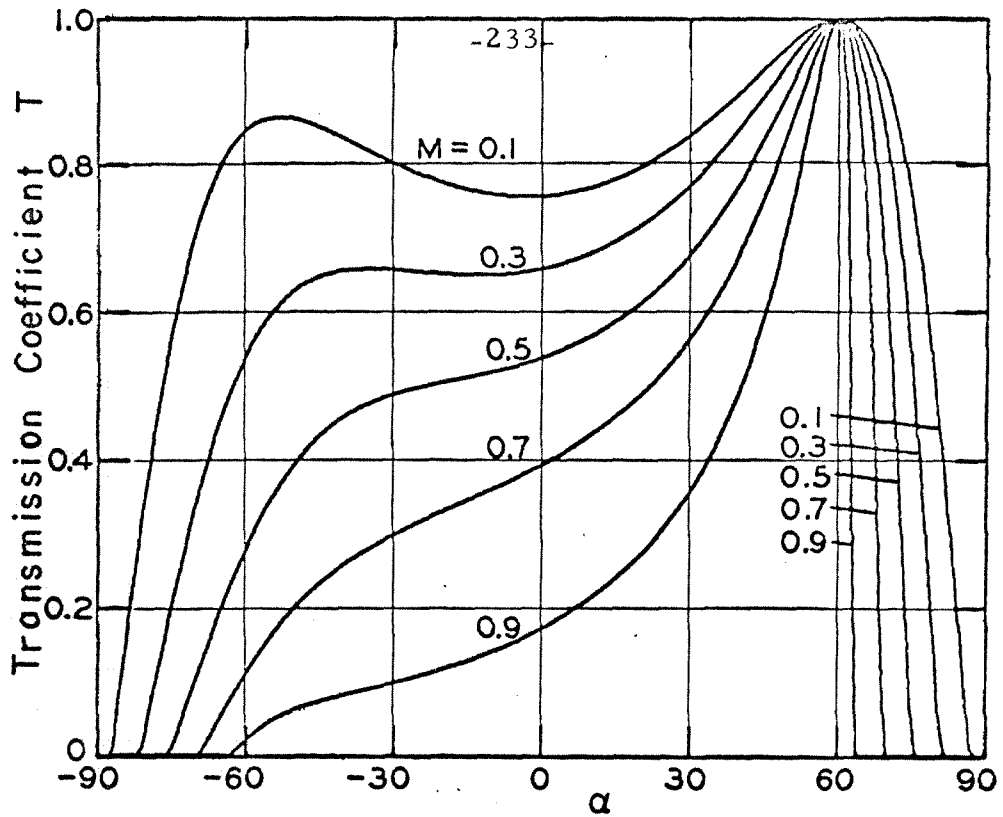

Fig. 6-3. Geometry of the Radiation Problem.

Fig. 6-4. Transmission and reflection of a plane wave incident on a blade row. The wave propagates upstream (M>0) in the direction α with respect to the blade row axis. $k\ell = \pi/2$, $\beta = 60°$.
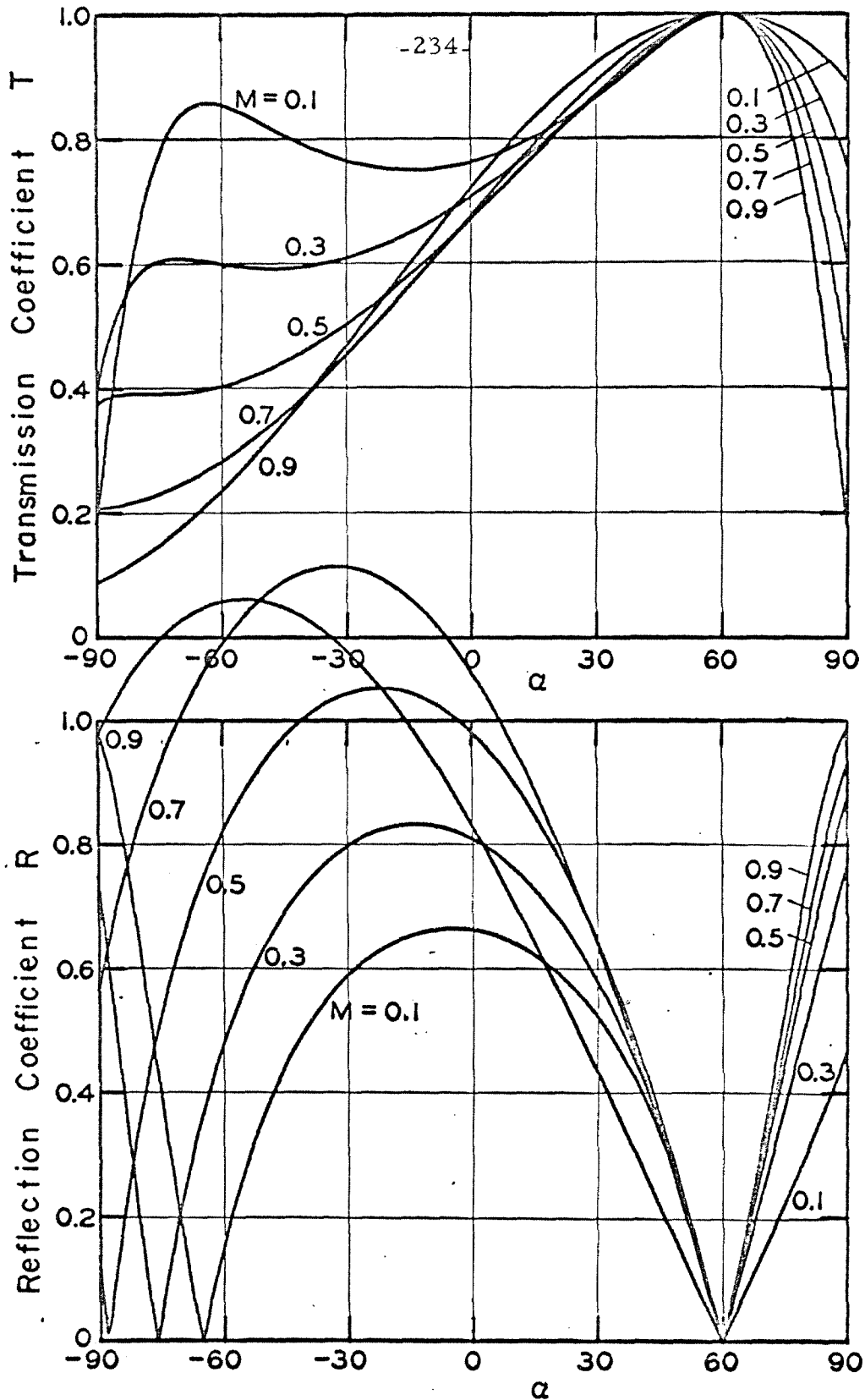
Fig. 6-5. Transmission and reflection of a plane wave incident on a
blade row. The wave propagates downstream (M<0) in the
direction α with respect to the blade row axis. $k\ell = \pi/2$,
$\beta = 60°$.